AD-A062 686 PRATT AND WHITNEY AIRCRAFT GROUP WEST PALM BEACH FL 6--ETC F/6 11/6
MANUFACTURING METHODS FOR PRODUCTION OF TITANIUM ALLOY COMPRESS--ETC(U)
FEB 77 F33615-72-C-1390

UNCLASSIFIED FR-7778 AFML-TR-77-10 NL

1 OF 2
AD
A062886

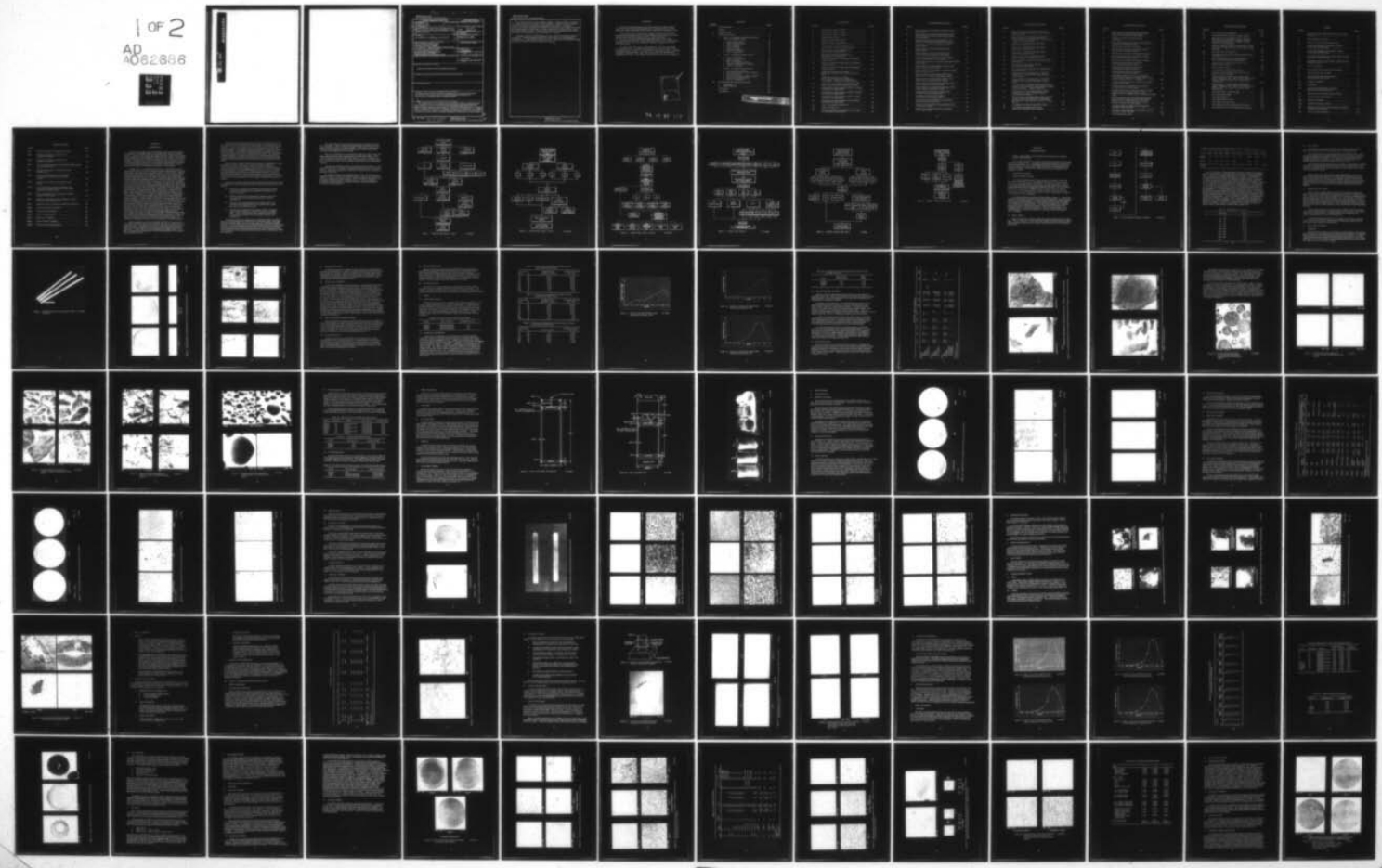

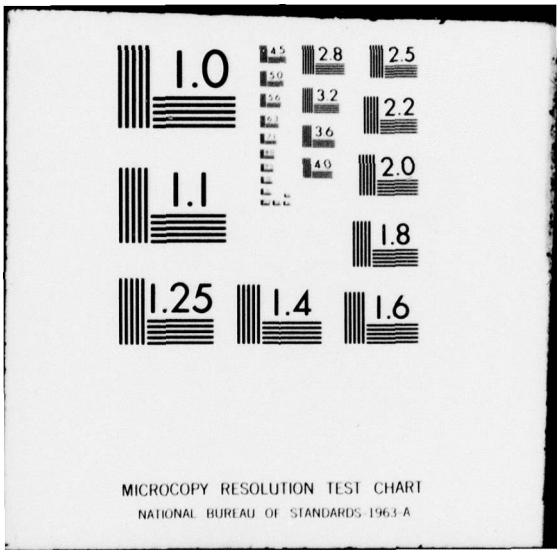
1.0
2.8
2.5
3.2
2.2
3.6
2.0
4.0
1.1
1.8
1.25
1.4
1.6
MICROCOPY RESOLUTION TEST CHART
NATIONAL BUREAU OF STANDARDS 1963-A

DDC FILE COPY

AD A062686

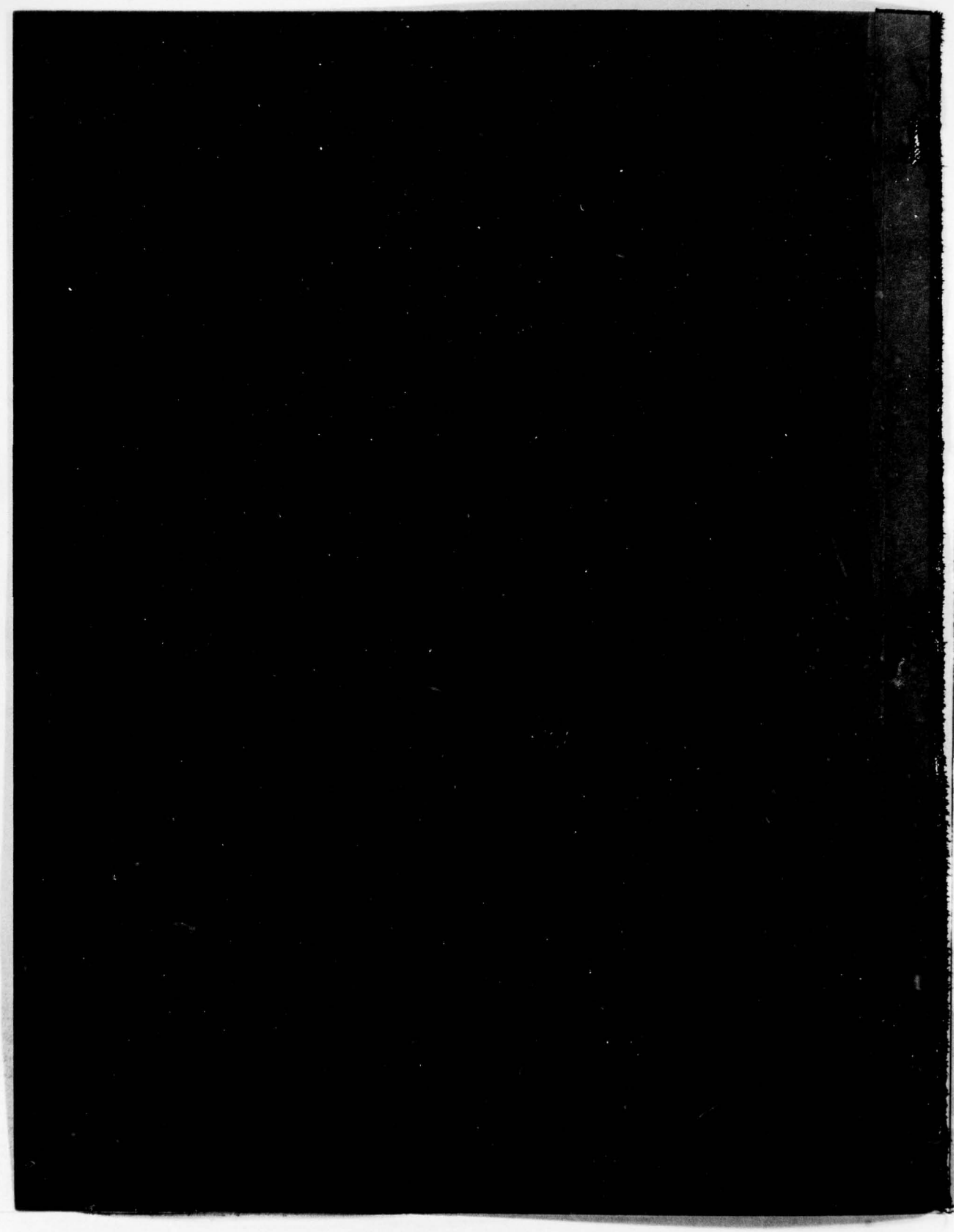

(9) Final rept. May 72 - Oct 76,

UNCLASSIFIED

SECURITY CLASSIFICATION OF THIS PAGE (When Data Entered)

(19) REPORT DOCUMENTATION PAGE		READ INSTRUCTIONS BEFORE COMPLETING FORM
1. REPORT NUMBER (18) AFML-TR-77-10	2. GOVT ACCESSION NO.	3. RECIPIENT'S CATALOG NUMBER
4. TITLE (and Subtitle) (6) MANUFACTURING METHODS FOR PRODUCTION OF TITANIUM ALLOY COMPRESSOR DISKS FROM POWDER BILLET		5. TYPE OF REPORT & PERIOD COVERED Final May 1972 - October 1976
		6. PERFORMING ORG. REPORT NUMBER (14) FR-7778
7. AUTHOR(s) (10) M. M./Allen, J. A./Miller, K. J./Larson		8. CONTRACT OR GRANT NUMBER(s) (15) F33615-72-C-1390
9. PERFORMING ORGANIZATION NAME AND ADDRESS Pratt & Whitney Aircraft Group Division of United Technologies Government Products Division P.O. Box 2691 West Palm Beach, Florida 33402		10. PROGRAM ELEMENT, PROJECT, TASK AREA & WORK UNIT NUMBERS
11. CONTROLLING OFFICE NAME AND ADDRESS Air Force Materials Laboratory Manufacturing Technology Division Air Force System Command Wright-Patterson Air Force Base, Ohio		12. REPORT DATE (11) February 1977
		13. NUMBER OF PAGES 167 (12) 167
14. MONITORING AGENCY NAME & ADDRESS (if different from Controlling Office)		15. SECURITY CLASS. (of this report) Unclassified
		15a. DECLASSIFICATION/DOWNGRADING SCHEDULE

16. DISTRIBUTION STATEMENT (of this Report)

Approved for public release; distribution unlimited

17. DISTRIBUTION STATEMENT (of the abstract entered in Block 20, if different from Report)

18. SUPPLEMENTARY NOTES

19. KEY WORDS (Continue on reverse side if necessary and identify by block number)

Titanium; Powder; Hydride-Dehydride; Rotating Electrode Process; Extrusion; Hot Isostatic Pressing Inclusions; Ferrofluid Cleaning; GATORIZED™; Microstructure; Ductility; Alpha; Transformed Beta

20. ABSTRACT (Continue on reverse side if necessary and identify by block number)

The original intent of the program was to establish methods of producing forged billet consolidated from Ti-6Al-2Sn-4Zr-6Mo alloy powder and forging billet into advanced engine compressor disks using the GATORIZING™ forging process. However, powder contamination problems necessitated a redirection of the program. The modified program included the evaluation of consolidation methods and quality control procedures. A partially successful method of cleaning contaminated titanium powder was developed.

DD FORM 1 JAN 73 1473 EDITION OF 1 NOV 65 IS OBSOLETE

392 887

UNCLASSIFIED

SECURITY CLASSIFICATION OF THIS PAGE (When Data Entered)

JDB

Clean titanium powder is not currently available. Methods capable of removing some contamination were evaluated. These methods are a possible remedy, but not a cure and may introduce additional contamination into the powder. Mechanical properties of extruded and forged Ti-6Al-2Sn-4Zr-6Mo powder billet compare favorably with conventionally processed billet receiving similar heat treatments with the exception of lower tensile ductility. Tentative powder and billet specifications were written and will be used until powder free of contamination is available.

Additional methods of producing titanium powder without contamination should be investigated. Cleaning techniques should not be used as part of a standard powder making process. A clean powder product must be developed before a production forging process can be optimized or parts tested in an engine.

FOREWORD

This Final Technical Report covers all work performed under Contract F33615-72-C-1390 "Manufacturing Methods for Production of Titanium Alloy Compressor Disks from Powder Billet" from 15 May 1972 to 30 September 1976.

This contract with the Government Products Division (formerly Florida Research and Development Center), Pratt & Whitney Aircraft, West Palm Beach, Florida was initially accomplished under the technical direction of Mr. Norman E. Klarquist, and the remaining effort under the direction of Mr. Carl Lombard, both of the Metals Processing Branch (LTM), Manufacturing Technology Division, Air Force Materials Laboratory, Wright-Patterson Air Force Base, Ohio.

Mr. Marvin M. Allen, Senior Program Manager, Materials Technology was responsible for the execution of the program. Mr. John A. Miller, Project Metallurgist and Mr. Kenneth J. Larson, Senior Metallurgist and Mrs. D. Sbriglia, Technician, contributed to the work. This report carries the internal P&WA designation of FR-7778. This technical report has been reviewed and is approved.

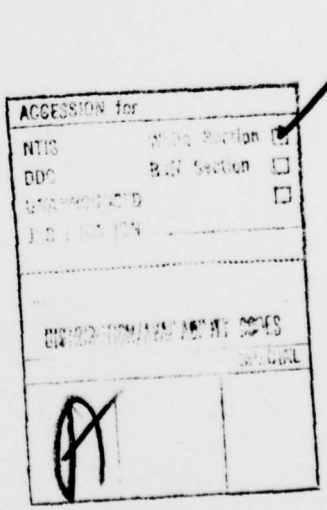

78 12 22 022

CONTENTS

SECTION		PAGE
	ILLUSTRATIONS	
	TABLES	
I	INTRODUCTION	1
II	PROGRAM DETAILS	10
	A. Task I - Processing, Evaluation and Selection of Powder Production Method	10
	1. Procurement of Powder	10
	2. Powder Characterization	13
	3. Billet Consolidation	32
	4. Billet Evaluation	36
	5. Forging Evaluation	45
	6. Defect Characterization	52
	7. Task I - Conclusions	57
	B. Task II - Consolidation Method Selection	58
	1. Powder Procurement	58
	2. Powder Characterization	61
	3. Billet Consolidation	65
	4. Billet and Forging Evaluations	72
	5. Additional Consolidation Evaluation	82
	6. Task II - Conclusions	102
	C. Task III - Ferrofluid Cleaning Process	102
	1. First Program Modification	102
	2. Laboratory Processed Powder Evaluation	106
	3. AVCO's Pilot Plant	115
	4. Pilot Plant Processed Powder Evaluation	119
	5. Second Program Modification	125
	6. Task III - Conclusions	150
III	CONCLUSIONS AND RECOMMENDATIONS	151
	A. Conclusions	151
	B. Recommendations	151
	APPENDIX A	153
	APPENDIX B	155

PRECEDING PAGE NOT FILMED BLANK

ILLUSTRATIONS

FIGURE		PAGE
1	Program Plan, Phase I, Task I	4
2	Program Plan, Phase I, Task II	5
3	Program Plan, Phase I, Task III	6
4	Program Plan, Phase II	7
5	Modified Program Plan Task II	8
6	Modified Program Plan Task III	9
7	Typical Hydride-Dehydride Flowsheet	11
8	Nonconsumable Cast Ti-6Al-2Sn-4Zr-6Mo	14
9	Macrostructure of Nonconsumable Cast Ti-6Al-2Sn-4Zr-6Mo Barstock	15
10	Microstructures of Nonconsumable Cast Ti-6Al-2Sn-4Zr-6Mo Barstock	16
11	TMCA Ti-6Al-2Sn-4Zr-6Mo Powder Distribution Frequency Curve	20
12	NUMEC Ti-6Al-2Sn-4Zr-6Mo Powder Distribution Frequency Curve	21
13	Nuclear Ti-6Al-2Sn-4Zr-6Mo Powder Distribution Frequency Curve	21
14	Typical Microstructure of -40 Mesh Ti-6Al-2Sn-4Zr-6Mo Powder As-Received From TMCA	24
15	Typical Microstructure of -40 Mesh Ti-6Al-2Sn-4Zr-6Mo Powder As-Received From NUMEC. Etchant: 1:1 Kroll's/Glycerine	25
16	Structure of Nuclear Metals Ti-6Al-2Sn-4Zr-6Mo Powder Showing Dendritic Solidification Pattern	26
17	Scanning Electron Micrographs of NUMEC -40 Mesh Ti-6Al-2Sn-4Zr-6Mo Powder	27
18	Scanning Electron Micrographs of NUMEC -40 Mesh Ti-6Al-2Sn-4Zr-6Mo Powder	28
19	Scanning Electron Micrographs of TMCA -40 Mesh Ti-6Al-2Sn-4Zr-6Mo Powder	29
20	Scanning Electron Micrographs of Nuclear Metals Ti-6Al-2Sn-4Zr-6Mo Powder	30
21	Task I, Hot Isostatic Pressing Can	33
22	Task I, Extrusion Can	34
23	As-Hot Isostatically Pressed Billets Showing Some Can Tapering and Nonuniformity	35

ILLUSTRATIONS (Continued)

FIGURE		PAGE
24	Macrostructures of Extruded Ti-6Al-2Sn-4Zr-6Mo Powder Billet	37
25	Microstructures of Extruded Ti-6Al-2Sn-4Zr-6Mo Powder Indicates the Beta Transus Was Exceeded During Extrusion	38
26	Microstructures of Heat-Treated (1670/1/ 1/AC + 1100/8/AC) Extruded Ti-6Al-2Sn-4Zr-6Mo Billets	39
27	Macrostructures of HIP Ti-6Al-2Sn-4Zr-6Mo Powder Billets	42
28	Microstructures of HIP Ti-6Al-2Sn-4Zr-6Mo Powder Billets	43
29	Microstructures of Heat-Treated (1670/1/AC + 1100/8/AC) HIP Ti-6Al-2Sn-4Zr-6Mo Billets	44
30	Fracture Surfaces of Tensile Specimens Showing Inclusions Responsible for Low Ductility	46
31	Typical Macrostructures of Forged Ti-6Al-2Sn-4Zr-6Mo Powder Billet	47
32	Microstructures of Ti-6Al-2Sn-4Zr-6Mo Extruded Powder Billets Forged at 1650°F	48
33	Microstructures of Ti-6Al-2Sn-4Zr-6Mo HIP Powder Billets Forged at 1650°F	49
34	Microstructures of Heat-Treated (1670°F/1/AC + 1100°F/8/AC), Forged Extruded Powder Billets	50
35	Microstructures of Heat-Treated (1670°F/1/AC + 1100°F/8/AC), Forged HIP Powder Billets	51
36	Nickel Inclusion in Failed Tensile Specimen of HIP Nuclear Metals Ti-6Al-2Sn-4Zr-6Mo	53
37	Nickel Inclusion in Failed Tensile Specimen of HIP Nuclear Metals Ti-6Al-2Sn-4Zr-6Mo	54
38	Inclusions Found in HIP Nuclear Metals REP Ti-6Al-2Sn-4Zr-6Mo Powder Billet	55
39	Inclusions Found in Hydride/Dehydride Ti-6Al-2Sn-4Zr-6Mo Powder Billet	56
40	Microstructure of Ti-6Al-2Sn-4Zr-6Mo Phase I, Tasks II and III REP Electrode	60
41	Schematic of Vacuum Hot-Pressing Setup Used For Tasks II and III Studies	62
42	Typical As-Compacted Vacuum Hot Pressing of Ti-6Al-2Sn-4Zr-6Mo	62

ILLUSTRATIONS (Continued)

FIGURE		PAGE
43	Macrostructures of Ti-6Al-2Sn-4Zr-6Mo REP Powder Pressings (1650°F and 14.8 ksi) of Powder Lots from Task II	63
44	Microstructures of Ti-6Al-2Sn-4Zr-6Mo REP Powder Vacuum Hot Pressings (1650°F and 14.8 ksi) of Powder Lots from Task II	64
45	Task II, Lot 1 Ti-6Al-2Sn-4Zr-6Mo Powder Distribution Frequency Curve	66
46	Task II, Lot 2 Ti-6Al-2Sn-4Zr-6Mo Powder Distribution Frequency Curve	66
47	Task II, Lot 3 Ti-6Al-2Sn-4Zr-6Mo Powder Distribution Frequency Curve	67
48	Task II, Lots 2 and 3 Ti-6Al-2Sn-4Zr-6Mo Powder Distribution Frequency Curve	67
49	Typical "Hollows" Present in Ti-6Al-2Sn-4Zr-6Mo REP Powder	70
50	Macroetched Slices from As-Extruded Ti-6Al-2Sn-4Zr-6Mo Billet	74
51	Microstructures of Extrusions Near Edge (Top) and at Center (Bottom)	75
52	Microstructure of Extrusions After a 1670(1)AC + 1100(8)AC Heat Treatment Near Edge (Top) and Center (Bottom)	76
53	Microstructures of Extrusions After a 1670(1)AC + 1100(8)AC Heat Treatment (Structures Taken at Center)	78
54	Fracture Surfaces of Tensile Specimens Taken From Extruded (1500 and 1550°F), Forged (1650°F) and Heat-Treated [1670(1)AC + 1000(8)AC] Material	79
55	Microstructure of As-Forged Pancakes (1650°F) Consisting of Very Fine, Equiaxed Alpha in a Transformed Beta Matrix	80
56	Macrostructure of As-Hipped Billets (Note: Porosity Present in 1500, 1550, and 1600°F Compactions; Stain in 1500°F Billet Indicates Presence of Canning Material)	83
57	As-Hipped Ti-6Al-2Sn-4Zr-6Mo REP Powder	84
58	Hot Isostatically Pressed Billet After a 1670/1/AC + 1100/8/AC Heat Treatment	85

ILLUSTRATIONS (Continued)

FIGURE		PAGE
59	Microstructure of Hot Isostatically Pressed and Forged (1650°F), and Heat-Treated (1670/1/AC + 1100/8/AC) Ti-6Al-2Sn-4Zr-6Mo Powder	86
60	Modified Extrusion Can Used for Task II Extrusions	88
61	Macro and Microstructure of As-Extruded (1550°F) Ti-6Al-2Sn-4Zr-6Mo REP Powder	90
62	Microstructures of 1550°F Extrusion	91
63	Macro and Microstructure of As-Hipped (1675°F) Ti-6Al-2Sn-4Zr-6Mo REP Powder	93
64	Microstructures of 1675°F Hot Isostatic Pressing	94
65	Macro and Microstructure of As-Hipped (1800°F) Ti-6Al-2Sn-4Zr-6Mo REP Powder	95
66	Microstructures of 1800°F Hot Isostatic Pressing	96
67	Typical Inclusions Found in Consolidated Ti-6Al-2Sn-4Zr-6Mo REP Powder	98
68	Typical Inclusions Found in Consolidated Ti-6Al-2Sn-4Zr-6Mo REP Powder	99
69	Typical Inclusions Found in Consolidated Ti-6Al-2Sn-4Zr-6Mo REP Powder	100
70	Typical Microstructure of Ferro-Fluid Cleaned Ti 6246 Powder Vacuum Hot Pressed at 1700°F/15 ksi and Heat Treated 1670/1/AC + 1100/8/AC	105
71	Vacuum Hot Pressing of Lab-Processed Ferro-Fluid Cleaned Ti 6246 Powder	107
72	Forged Vacuum Hot Pressing of Lab-Processed Ferrofluid Cleaned Ti 6246 Powder	109
73	Microstructural Review of Extruded (1500°F); Forged (1650°F) and Heat Treated (1670°F/1 hr/AC + 1100°F/8 hr/AC) Ferrofluid Cleaned Ti-6Al-2Sn-4Zr-6Mo Powder	111
74	Microstructural Review of Hot Isostatically Pressed (1675°F/15 ksi); Forged (1650°F) and Heat Treated (1670°F/1 hr/AC + 1100°F/8 hr/AC) Ferrofluid Cleaned Ti-6Al-2Sn-4Zr-6Mo Powder	114
75	Conceptual Design Ferrofluid Particle Separation Vessel for AVCO Pilot Plant	116
76	Ferrofluid Density Separation Electromagnet in AVCO Pilot Plant, During Assembly	117
77	Particle Separation Vessel	117

ILLUSTRATIONS (Continued)

FIGURE		PAGE
78	Wash Column Cleaning Approach	118
79	Ferrofluid-Cleaned Ti 6246 REP Powder Task III	121
80	Microstructure of VHP (1650°F/15 ksi - Top) and VHP Plus 50% Forged (1650°F - Bottom) Ferrofluid Cleaned Ti 6246 Powder After a 1670°F/1/AC and 1100°F/8/AC Heat Treatment	122
81	Inclusions Found on Tensile Fracture Surfaces of VHP and Forged Ferrofluid Cleaned Ti 6246 Powder Tensile Specimens	123
82	Full-Scale Task III Extrusion Can	124
83	Macroslices of Full-Scale Extrusion Showing Porosity and Small Cracks	126
84	Macro and Microstructure of Extruded (1600°F) Ti-6Al-2Sn-4Zr-6Mo REP Cleaned Powder	129
85	Microstructure of Heat Treated (1670°F/1/AC + 1100°F/8/AC) Extrusion	130
86	Subscale Disk Preforms	132
87	Cross Sections of Subscale Disk Forging	133
88	Diagram for Test Specimens Machined from 8-in. Diameter Pancake Forgings	135
89	Microstructures of Heat-Treated Forgings (Top - 1690°F/2/Rapid Air Cool + 1525°F/2/AC + 1100°F/8/AC) (Bottom - 1720°F/2/Furnace Cool to 1500°F/2/AC + 1100°F/8/AC)	136
90	Microstructures of Heat-Treated Forgings (Top - 1690°F/2/Rapid Air Cool + 1525°F/2/AC + 1100°F/8/AC) (Bottom - 1720°F/2/Furnace Cool to 1500°F/2/AC + 1100°F/8/AC)	137
91	PWA 1220 Ultimate Tensile Strength	141
92	PWA 1220 Yield Strength	141
93	PWA 1220 Elongation	142
94	PWA 1220 Reduction in Area	142
95	PWA 1220 0.2 Percent Creep	143
96	PWA 1220 RT Low-Cycle Fatigue (Strain Control)	146
97	PWA 1220 500°F Low-Cycle Fatigue (Strain Control)	146

TABLES

TABLE		PAGE
I	Chemical Analysis of Ingot Material Prior to Powder Conversion	12
II	Numec Blend Sieve Analysis	12
III	Inclusion Count of Vacuum Hot Pressings	18
IV	Particle Size Distribution for TMCA -40 Mesh Ti-6Al-2Sn-4Zr-6Mo Powder	19
V	Particle Size Distribution for NUMEC -40 Mesh Ti-6Al-2Sn-4Zr-6Mo Powder	19
VI	Particle Size Distribution For Nuclear Metals -35 Mesh Ti-6Al-2Sn-4Zr-6Mo Powder	19
VII	Distribution Values of Characteristic Particle Size (X_c) and Shape Factor (N)	22
VIII	Task I Chemistries	23
IX	Bulk Density of Ti-6Al-2Sn-4Zr-6Mo Powders	31
X	Particle Density Measurements	31
XI	BET Specific Surface Measurements on Ti-6Al-2Sn-4Zr-6Mo Powder	31
XII	Mechanical Properties	41
XIII	Chemistries	59
XIV	Particle-Size Distributions of -35 Mesh REP Ti-6Al-2Sn-4Zr-6Mo Powder	68
XV	Bulk Density of Ti-6Al-2Sn-4Zr-6Mo Powders	69
XVI	Particle Density Measurements	69
XVII	Mechanical Properties	77
XVIII	Interstitial Chemistry Analysis	81
XIX	Mechanical Properties of Task II Additional Pancakes (1670(1)AC plus 1100(8)AC)	92
XX	Inclusion Analysis Summary	101

TABLES (Continued)

TABLE		PAGE
XXI	Chemical Analysis of Vacuum Hot Pressing	104
XXII	Mechanical Properties of 1700°F/15 ksi Vacuum Hot Pressing	106
XXIII	Mechanical Properties of 1650°F/15 ksi Vacuum Hot Pressing	106
XXIV	Task III Chemistry Analysis of Ferrofluid Cleaned Powder (Ti-6Al-2Sn-4Zr-6Mo)	110
XXV	Mechanical Properties of Ferrofluid Cleaned Ti-6246 Powder	112
XXVI	Particle Size Distributions of 35 Mesh REP Ti-6Al-2Sn-4Zr-6Mo Ferrofluid Cleaned Powder	120
XXVII	Chemistry of Ferrofluid Cleaned REP Ti-6246 Powder	120
XXVIII	Room Temperature Tensile Test Results From Consolidated Ferrofluid Cleaned Ti 6246 Powder (1670°F/1/AC+1100°F/8/AC)	122
XXIX	Room Temperature Tensile Properties of PS 140 Cleaned Ti 6246 Powder	127
XXX	Mechanical Properties of Task III Extrusion (1600°F) [1670°F(1)AC plus 1100°F/8/AC]	128
XXXI	Interstitial and Iron Analysis of Large-Scale Extrusion	131
XXXII	Pancake Processing Parameters	134
XXXIII	Task III Tensile Properties	139
XXXIV	Task III Creep Properties	144
XXXV	Task III LCF Properties	145
XXXVI	Task III Fracture Toughness	148
XXXVII	Task III RT Notch Stress Rupture	149

SECTION I

INTRODUCTION

A new era in jet engine materials technology began a few years ago with the introduction of high Mach number, supersonic cruise engines of military aircraft. Because of the stringent operating temperature requirements imposed on the components of these engines for extended periods of time, the workhorse titanium alloys used in prior subsonic engines, such as Ti-6Al-4V alloy, were marginal. Responding to the need for new titanium alloy compositions capable of operation at higher temperatures, the titanium-producing industry developed several promising compositions, one of which was Ti-8Al-1Mo-1V, which is used both in the Mach 3+ J58 engine and the Mach 2+ TF30 engines.

In 1969, the Air Force Materials Laboratory, recognizing the need for titanium alloys with even greater strength-to-weight ratios and higher operating temperature capability for more advanced engines, contracted Pratt & Whitney Aircraft (Contract F33615-68-C-1226) to screen several developmental alloy compositions produced by the United States and British titanium industries to determine those most attractive for further evaluation. Ingot casting, billet conversion, engine disk forging procedures, and heat treatments were established by Pratt & Whitney Aircraft under this contract for one of the most promising of the alloys, Ti-6Al-2Sn-4Zr-6Mo. Based upon the results of the work on this contract, this alloy, with its outstanding strength-to-weight ratio, was selected for extensive use in the advanced high thrust-to-weight F100/F401 engines under development by Pratt & Whitney Aircraft. Specifically, fan disks, high compressor disks, and high compressor blades and vanes are being made of the alloy. Once this selection of Ti-6Al-2Sn-4Zr-6Mo alloy was made, Pratt & Whitney Aircraft undertook a very large development effort involving all facets of processing, including ingot solidification, billet conversion, disk forging, and heat treatment, to evolve optimum processing for the various classes of engine components. Simultaneously, studies for correlating microstructure with mechanical properties were carried on, leading to (1) the establishment of unprecedented billet microstructural standards, which are now used by billet suppliers and disk forgers for assuring a high quality disk product, and (2) the realization that metallographic examination could be used as an effective nondestructive quality control tool to qualitatively assess selected mechanical properties, as well as the uniformity of processing of disks. Pratt & Whitney Aircraft has, under Air Force Materials Laboratory sponsorship (Contract F33615-71-C-1569), developed a metallographic control method involving an automatic electro-optical scanning system, which can analyze, classify, and store information from photomicrographic negatives prepared from structural replicas of selected locations of Ti-6Al-2Sn-4Zr-6Mo disk forgings. This method holds significant promise for more reliable and less costly inspection.

High strength alloys, such as Ti-6Al-2Sn-4Zr-6Mo, are more heavily alloyed than the weaker alloys of the Ti-6Al-4V class and are, therefore, more segregation prone. Segregation inherent in the ingot sizes required to make engine hardware is detrimental to the level and reproducibility of mechanical properties. Because disks of advanced high thrust-to-weight engines are so thin in cross section, the importance of minimizing segregation to the greatest degree possible is obvious.

The powder metallurgy approach is, therefore, the logical route for the development of advanced engine disks of high strength, segregation-prone titanium alloys. In the case of powder made from molten metal, individual powder particles consist of small amounts of metal and solidification is rapid; thus, thermal gradients are minimized and microsegregation is confined to individual powder particles. In the hydride-dehydride process, segregated areas can be no larger than the size of the crushed hydrided particles. The consolidation of powder particles into a billet of suitable size for forging engine hardware, therefore, produces a product that has a uniform structure devoid of the type of gross macrosegregation that is associated with large conventionally melted ingots.

Extensive work in powder characterization, powder consolidation, forging procedures, and heat treatment has resulted in subscale pancakes of Ti-6Al-2Sn-4Zr-6Mo, which exhibit an improved level and uniformity of mechanical properties over conventionally melted material. The Pratt & Whitney Aircraft-developed GATORIZING™ forging process has been used to produce subscale powder pancake forgings of Ti-6Al-2Sn-4Zr-6Mo alloy, as well as subscale pancake and full-scale engine disk forgings of conventionally melted Ti-6Al-2Sn-4Zr-6Mo alloy. These GATORIZED™ forgings possess a uniformity of structure that is not possible to achieve utilizing conventional forging techniques.

Benefits to be obtained for high strength Ti-6Al-2Sn-4Zr-6Mo alloy through the utilization of powder metallurgy and the GATORIZING forging process are as follows:

- Alleviation of segregation, affording product integrity through improved mechanical property capability and uniformity as a result of the powder
- Structural uniformity and unrestricted, uniform metal movement (low flow stress and lack of die chill) as a result of GATORIZING
- Reduced cross-sectional thickness of forgings without prior machining will respond better to heat treatment due to close tolerance of GATORIZING process
- Reduced engine component costs through reduction of forging input weight and associated reduction of final part machining costs. Fewer rejections due to poor quality and less expensive inspection costs due to microstructural controls on the finished part.

The original intent of the program was to establish methods of producing forged billet consolidated from Ti-6Al-2Sn-4Zr-6Mo alloy powder and forging billet into advanced engine compressor disks using the GATORIZING forging process. The original program was structured to demonstrate the reproducibility of processes used in producing the powder billets and to establish preliminary material specifications, process specifications, and quality control procedures for the processes. Cost analyses of these procedures were an integral part of the entire program.

The original program was divided into two phases as illustrated in Figures 1 through 4. Phase I involved the production and evaluation of subscale disks produced by powder metallurgy methods. In this phase, emphasis was placed on powder production method selection, billet consolidation method selection, and forging parameter selection.

Phase II was to include (1) the production of full-scale engine compressor disks using the optimum processing sequence developed from Phase I, and (2) the evaluation of the disks produced in spin tests, low-cycle fatigue tests, and by mechanical property cut-up. Finally, the economics of producing these disks were to be analyzed, and preliminary material and process specifications prepared.

A powder contamination problem was identified during the Phase I, Task I material evaluations. The powder contamination problem became paramount in Phase I, Task II and necessitated a redirection of program effort resulting in a program modification.

The modified program was divided into three tasks. The first task was identical to Phase I, Task I of the original program. Flow charts for Tasks II and III are presented in Figures 5 and 6. Task II included the evaluation of consolidation methods and quality control procedures. Task III evaluated the ferrofluid cleaning technique as a possible method of cleaning contaminated Ti-6Al-2Sn-4Zr-6Mo powders.

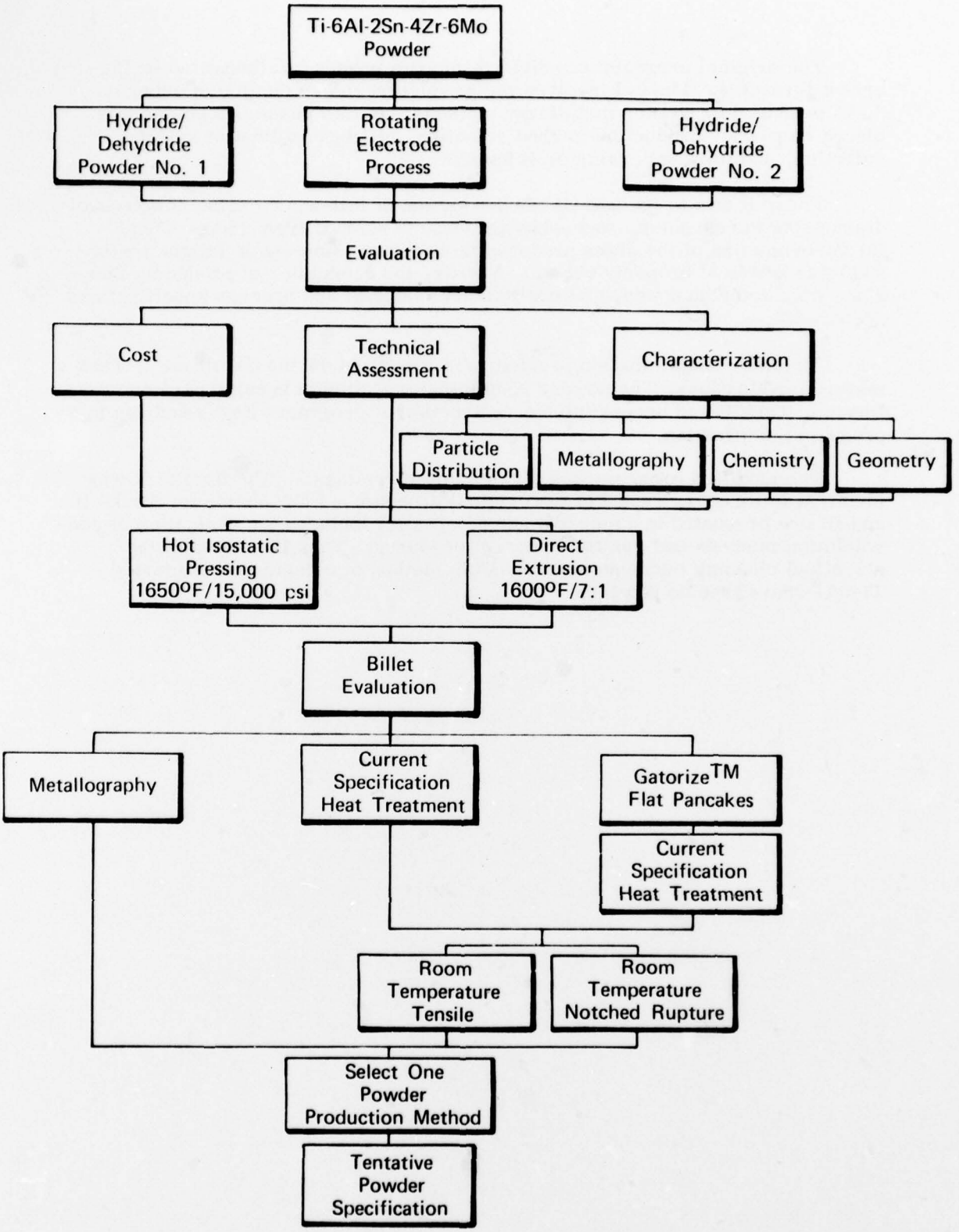

Figure 1. Program Plan, Phase I, Task I FD 65125C

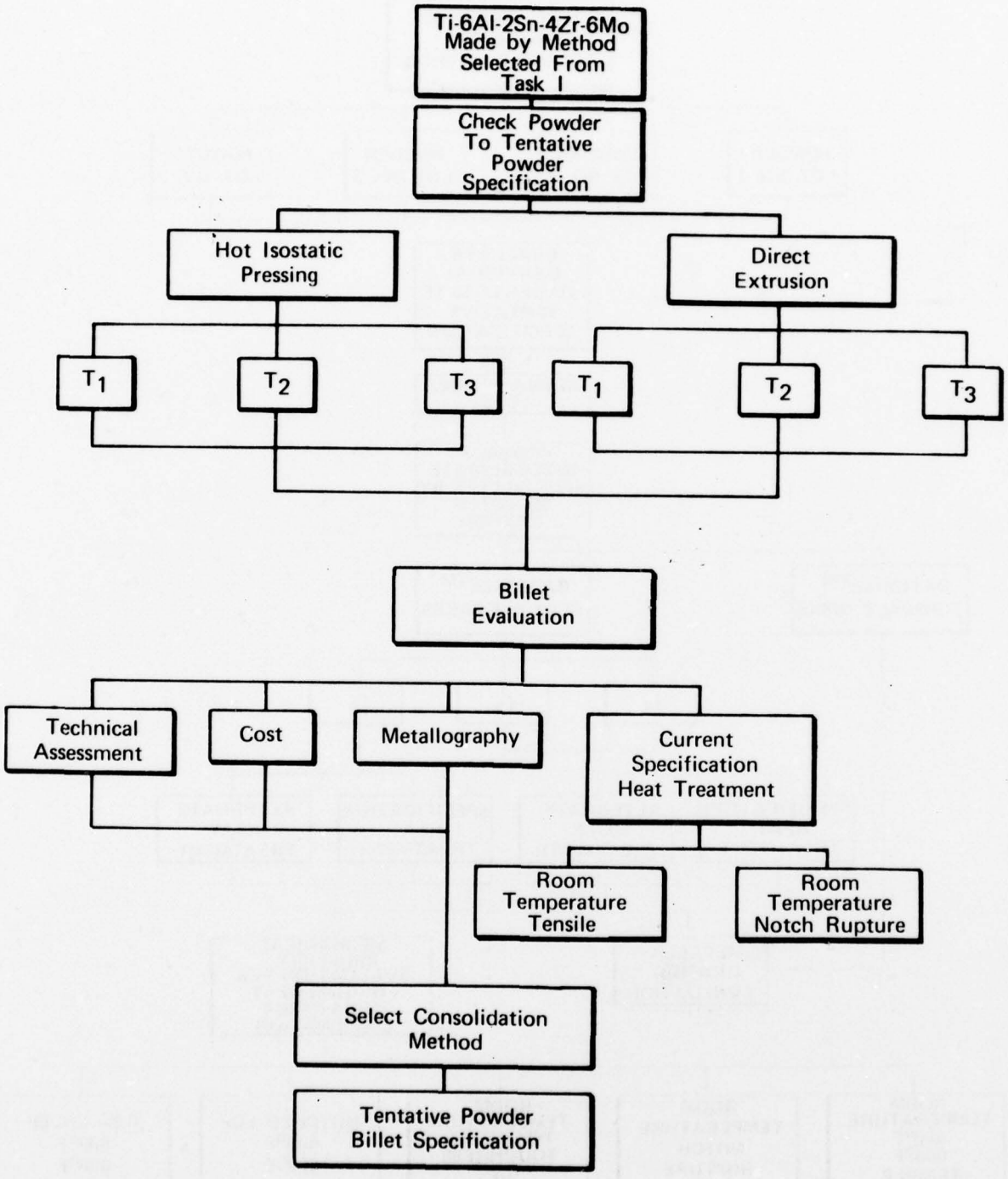

Figure 2. Program Plan, Phase I, Task II FD 56648B

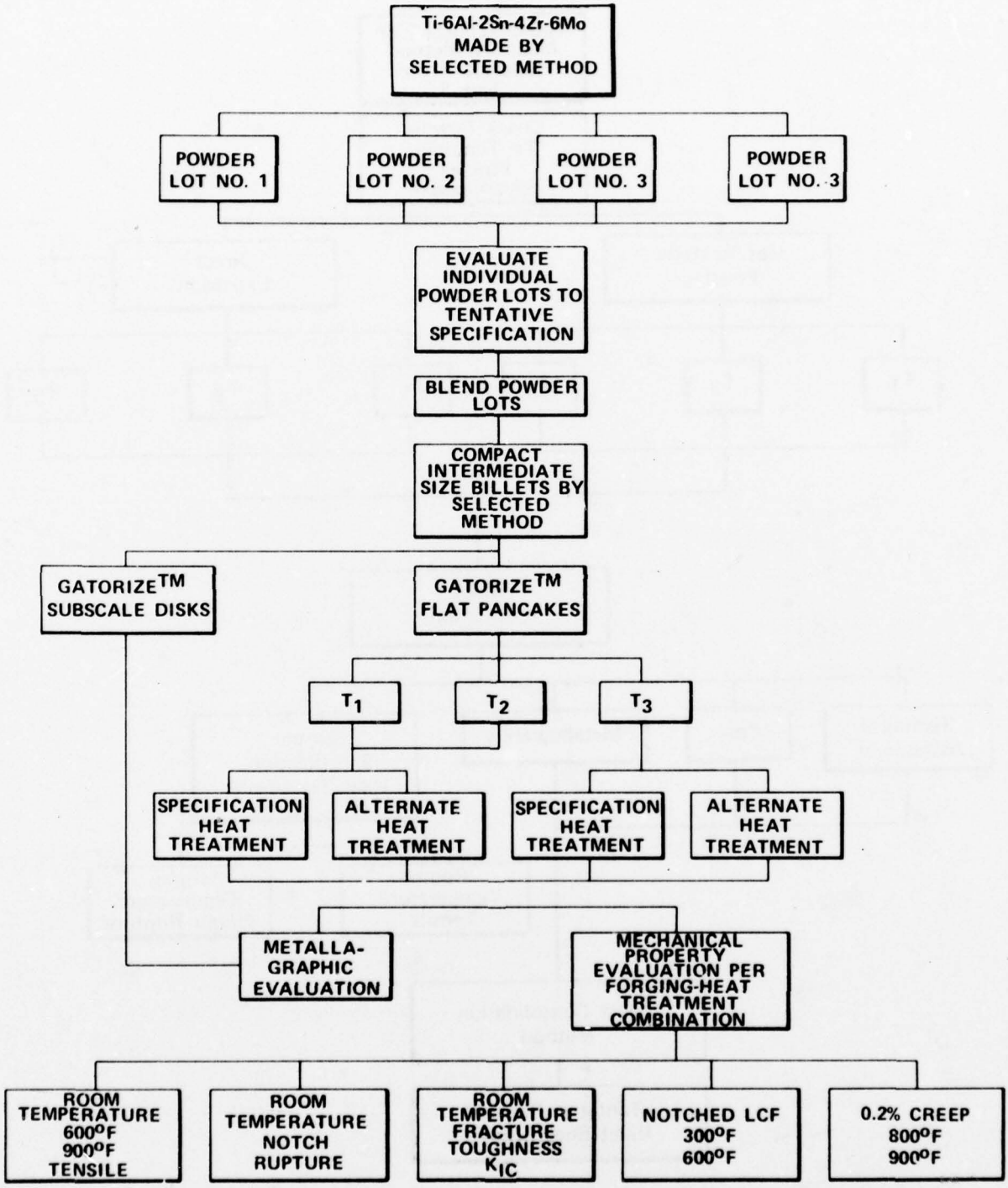

Figure 3. Program Plan, Phase I, Task III FD 56649A

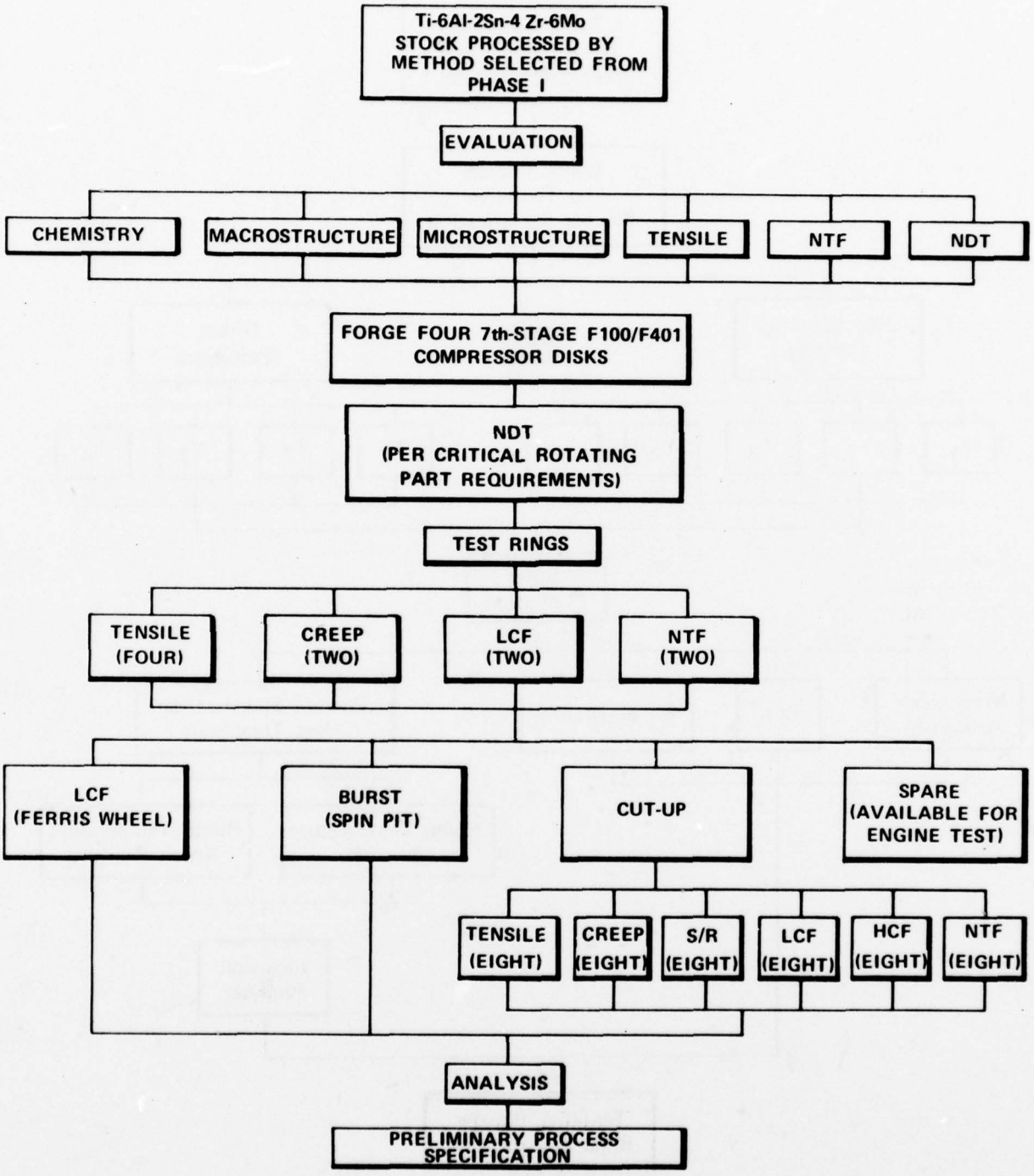

Figure 4. Program Plan, Phase II FD 56650A

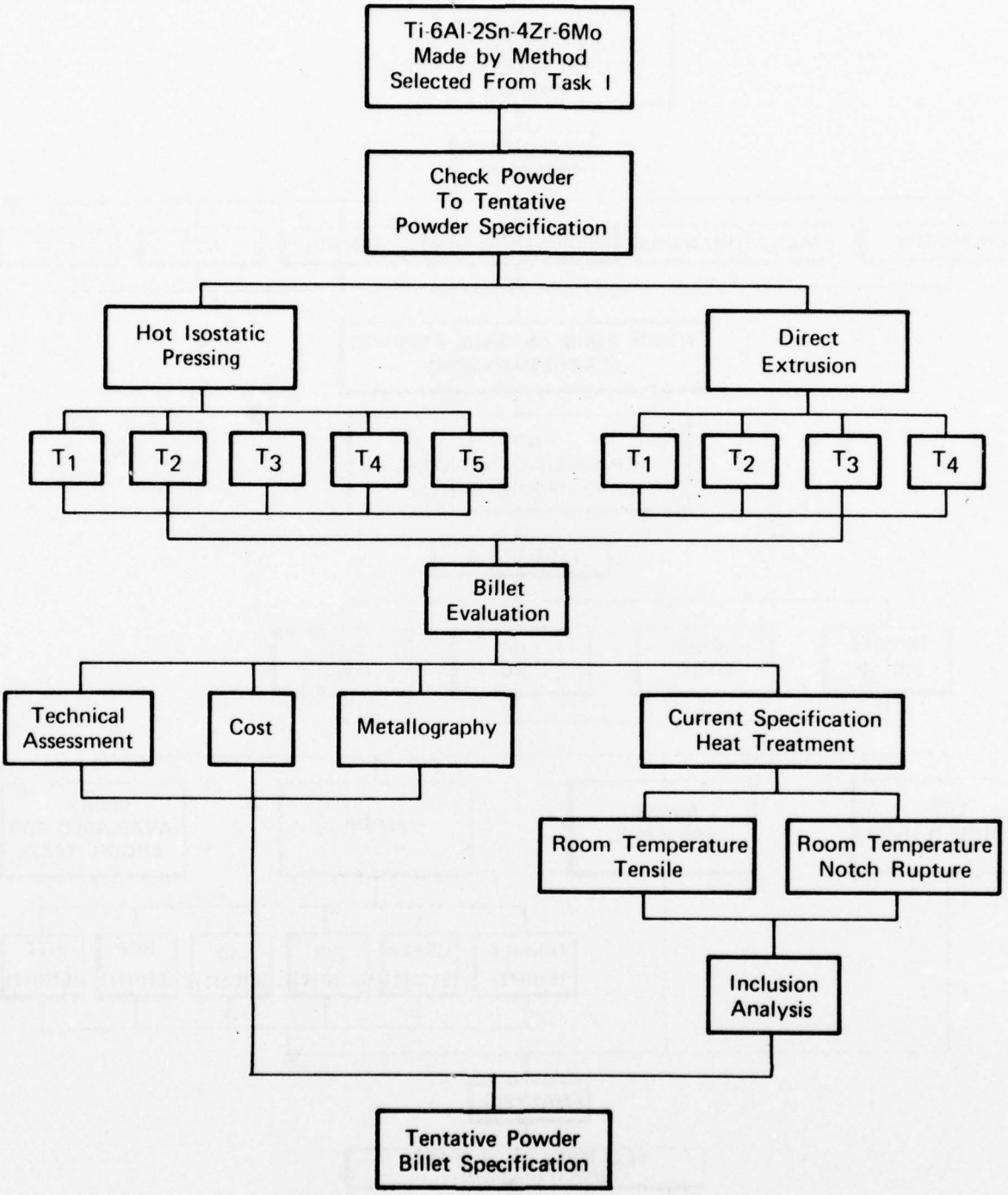

Figure 5. Modified Program Plan Task II FD 98365

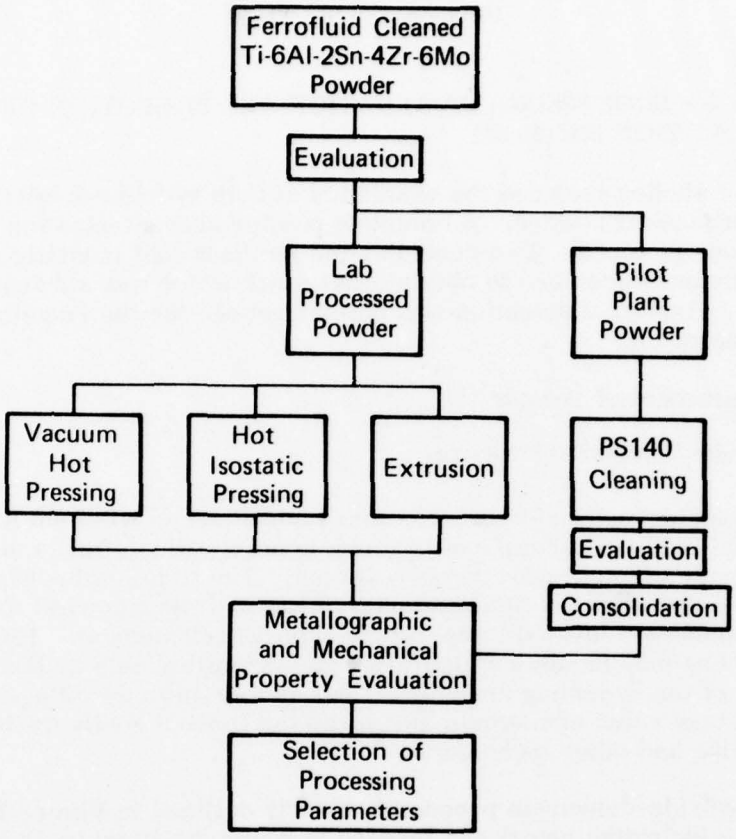

Figure 6. Modified Program Plan Task III FD 98364

SECTION II

PROGRAM DETAILS

A. TASK I - PROCESSING, EVALUATION AND SELECTION OF POWDER PRODUCTION METHOD

Task I studies included the evaluation of both hydride-dehydride and rotating electrode processed powder. A complete powder characterization was performed on the various powders. Two consolidation methods (hot isostatic pressing and direct extrusion) were used to obtain billet stock which was subsequently forged and tested. Finally, a selection of a powder source for the remainder of the program was made.

1. Procurement of Powder

a. Hydride-Dehydride Process

The hydride-dehydride process takes advantage of titanium's affinity for hydrogen and the brittle nature of titanium hydride, which forms upon cooling from an elevated temperature heat treatment. The titanium hydrogen reaction is reversible and allows a final material of low hydrogen content to be obtained through subsequent elevated temperature exposure in vacuum. The feed material for the process may be any configuration and is limited only by the physical dimensions of the hydriding chamber. This is a definite advantage due to the minor monetary value of titanium scrap and the limited configurations amenable to chip milling and other techniques.

The hydride-dehydride process is briefly outlined in Figure 7. The process consists of a hydriding retort and furnace in which the titanium is heated and maintained in a hydrogen atmosphere. A brittle titanium hydride forms upon cooling. Large chunks of titanium hydride are broken down to the desired size of powder by a crushing and screening process. The material is prepared for a dehydrogenation procedure in which the hydrogen is removed from the powder in an evacuated chamber at elevated temperature. After the "sintered cake" of dehydrided powder is broken up, the powder is screened, cleaned and analyzed prior to shipping.

(1) Numec Powder

Numec obtained Ti-6Al-2Sn-4Zr-6Mo ingot from the RMI Company at Niles, Ohio. The 8-in. diameter, 112-lb ingot (heat X-22081) was double-vacuum melted. RMI's chemical analysis is given in Table I and fully meets PWA 1216 chemistry specification.

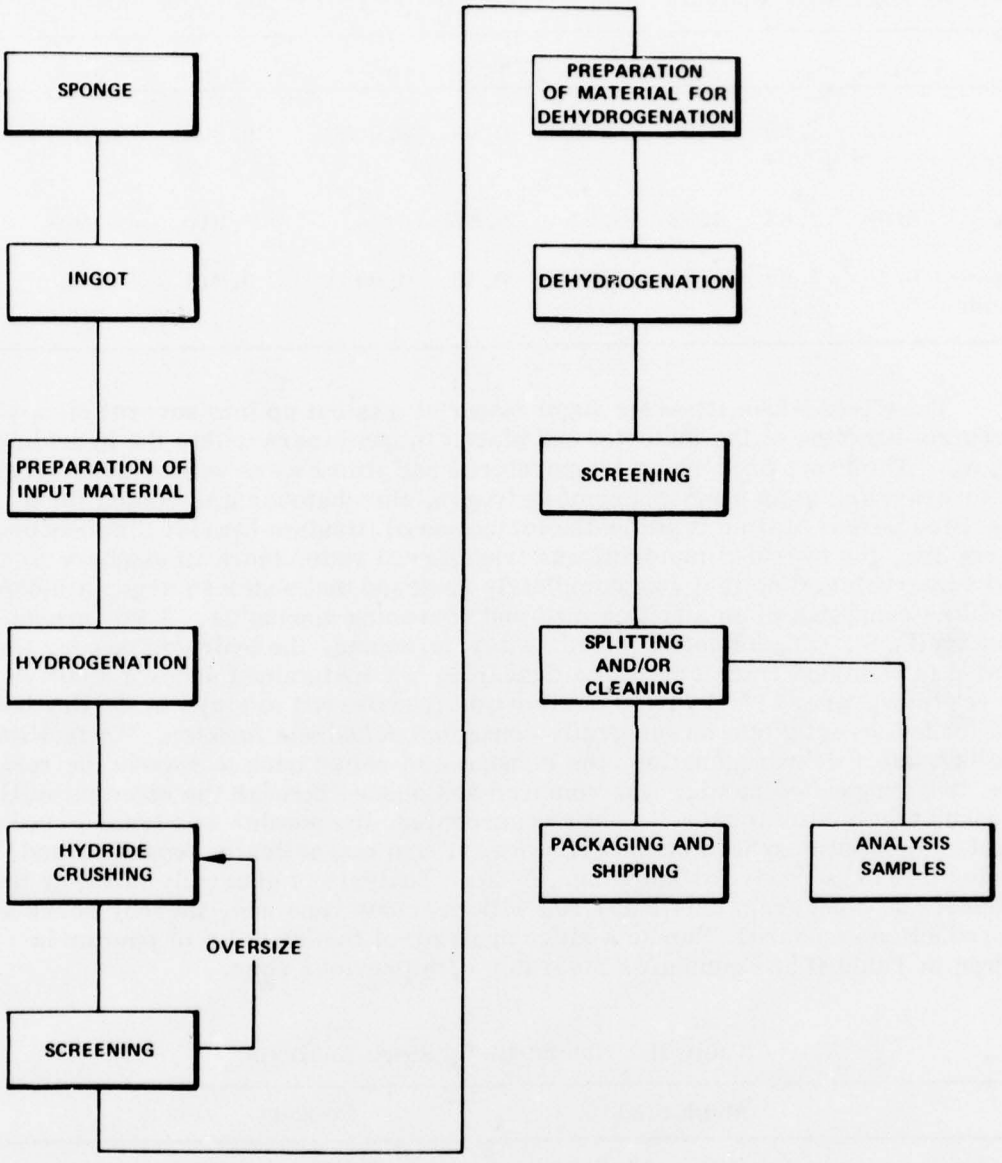

Figure 7. Typical Hydride-Dehydride Flowsheet FD 65863A

Table I. Chemical Analysis of Ingot Material Prior to Powder Conversion

	Al	Sn	Zr	Mo	Fe	H	N	O_2	C
RMI (Numec)	6.20	2.00	3.90	6.40	0.05	0.0052	0.006	0.079	0.01
TMCA	6.00	2.03	4.02	5.97	0.076	-	0.010	0.078	-
Teledyne-Titanium	6.20	2.08	4.12	6.01	0.10	0.0084	0.011	0.10	0.020

The Ti-6Al-2Sn-4Zr-6Mo ingot material was cut up into several pieces to facilitate handling of the material and placed in containers within the hydriding retort. The exact processing temperatures and times were vendor proprietary. After hydriding in an atmosphere of hydrogen, the chamber was cooled for a specified period of time to allow the formation of titanium hydride. Subsequent to cooling, the hydrided material was transferred under inert atmosphere to a hydride crushing line that was completely enclosed and under an argon atmosphere. The line consisted of an attrition mill and screening apparatus. A jaw crusher was available, but was not required. After screening, the hydrided powder was sealed in cans and transferred to a dehydride box maintained under a positive inert atmosphere. The hydried powder was transferred to trays in the dry box and loaded directly into an integrally connected dehydride furnace. To facilitate cooling, after dehydrogenation, the furnace was rolled back to expose the retort. The dehydrogenated powder was removed and passed through the attrition mill to breakup the "sintered cake." After rescreening, the powder was transferred to another inert atmosphere chamber, where it was magnetically separated and loaded into cans ready for shipping. A sieve analysis is generally made by the producer to compare a particular run with previous runs and, thereby serve as a production standard. Numec's sieve analysis of the 50-lb lot of powder is shown in Table II and compares favorably with previous runs.

Table II. Numec Blend Sieve Analysis

Mesh Size		Percent
	+40	Trace
-40	+50	11.48
-50	+60	19.20
-60	+80	26.84
-80	+100	12.53
-100	+140	11.71
-140	+200	9.84
-200	+270	3.91
-270	+325	1.05
-325		3.44

(2) TMCA Powder

TMCA double-vacuum melted a 100-lb, 8-in. diameter ingot (V-4773). Ingot chemistry is given in Table I along with other vendor chemistries.

TMCA ingot material was cleaned and placed in a hydriding retort. After the hydrogen going into the hydriding chamber, the system was leak-checked and brought up to approximately 1550°F. The chamber was maintained at this temperature for an hour. Following a 24 hour cooling cycle, the chamber was opened and the hydrided material transferred to a jaw crusher.

Material was broken down further in a roll crusher. The amount of crushing necessary was dependent upon the completeness of the hydriding process. Subsequent to screening, the material was cleaned to remove possible contamination from the crushing operations.

Cleaned powder was transferred to a dehydriding chamber, where it was evacuated and maintained at approximately 1300°F until the desired out-gassing level, established by prior experience, was obtained. Upon removal from the chamber, the compacts were screened to the desired mesh size. The -40 mesh screened powder was split before analysis to ensure a uniform and representative sample. The powder was then placed in plastic bags and filled with argon for shipment.

b. Rotating Electrode Process

Nuclear metal's rotating electrode process (REP) results in a spherical powder rather than the angular powder resulting from the hydride-dehydride process. Starting stock may be either wrought or cast, but must be machined (turned) into electrodes sized to fit in Nuclear's powder rig. The electrode is rotated at high speed (approximately 10,000-15,000 rpm) in a helium atmosphere, while the end of the electrode is exposed to an arc maintained between the titanium electrode and a stationary tungsten tipped electrode. The resulting arc-melted metal flies off the ends of the bar as small droplets, which freeze in flight as spherical powder particles.

The electrode material was cast by Teledyne Titanium in their nonconsumable vacuum-melting facility. The ingot was cast in a 5-in. diameter steel mold, rolled down at Teledyne Allvac to an approximate 2.5-in. diameter, and finally centerless ground to 2.500 ±0.003 diameter.

A structural investigation of the 2.5-in. diameter bars (Figures 8 through 10) revealed a microstructure consisting of fine Widmanstatten alpha typical of material hot worked entirely in the beta field.

2. Powder Characterization

a. Background

Characterization analyses were performed on all the powders. The hydride-dehydride powders were manufactured by Titanium Metals Corporation of American (TMCA) and Nuclear Materials and Equipment Corporation (NUMEC). Teledyne Titanium supplied Nuclear Metals with nonconsumable cast ingot for their rotating electrodes. Several of the characterization studies performed are used as screening evaluations in the metal powder industry.

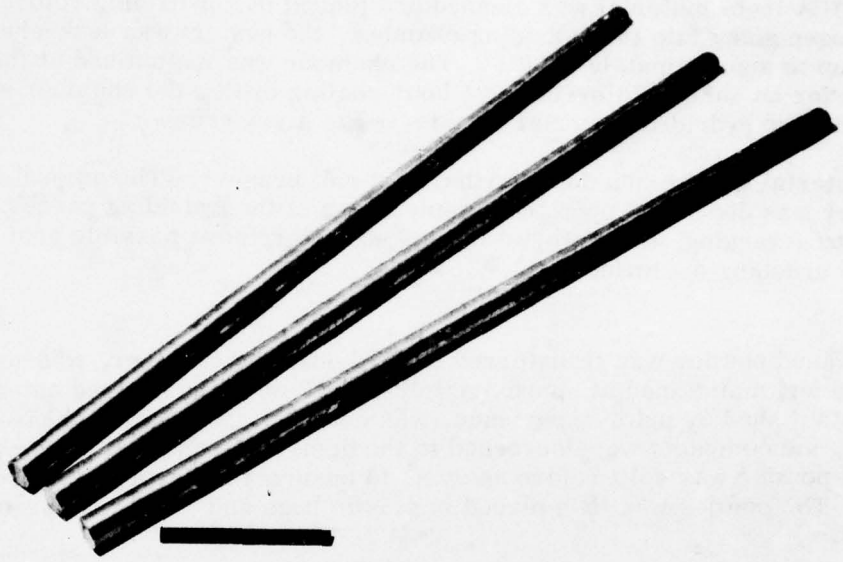

Figure 8. Nonconsumable Cast Ti-6Al-2Sn-4Zr-6Mo Barstock FE 121801

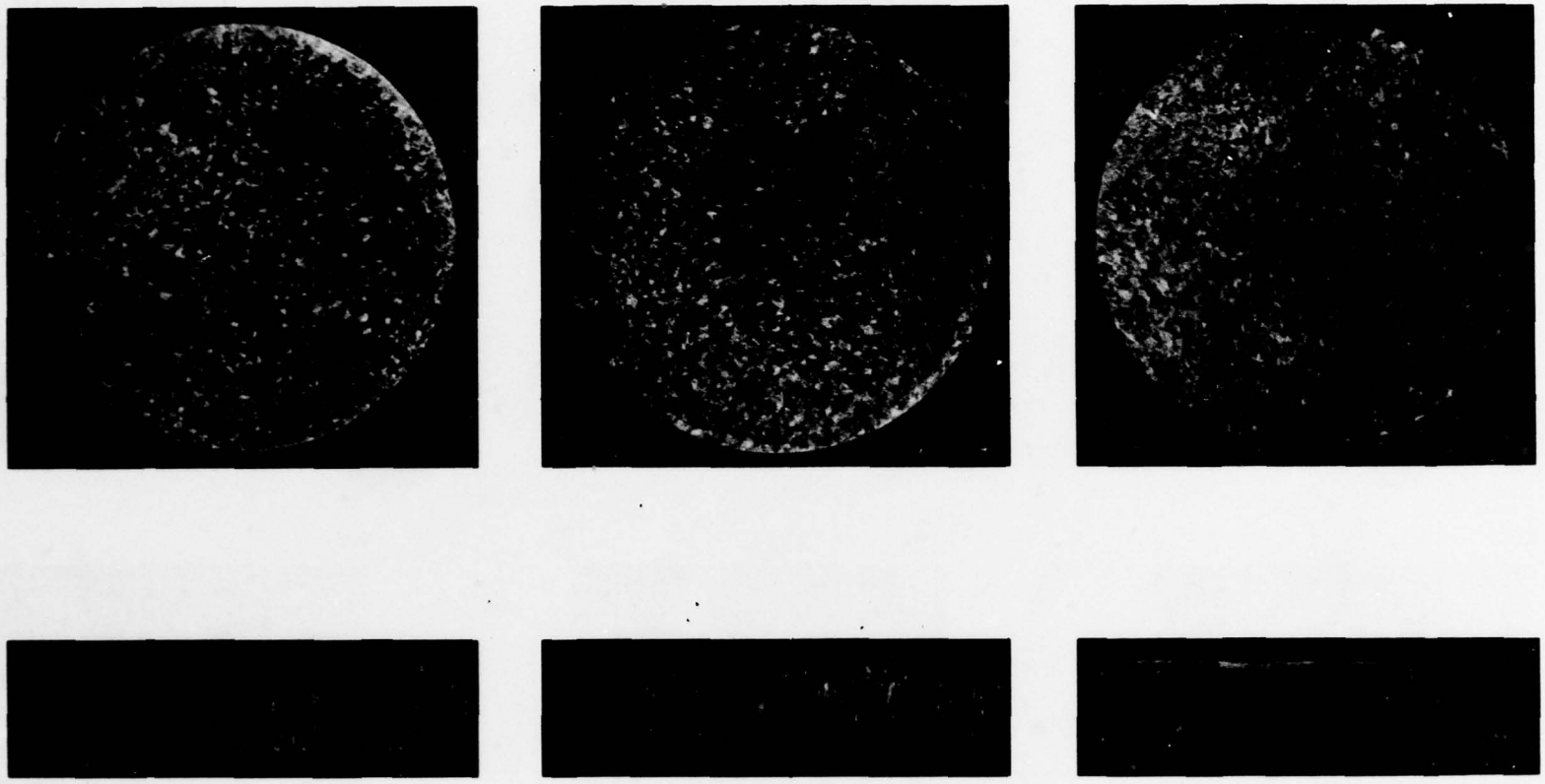

Figure 9. Macrostructure of Nonconsumable Cast Ti-6Al-2Sn-4Zr-6Mo Barstock

FD 65126

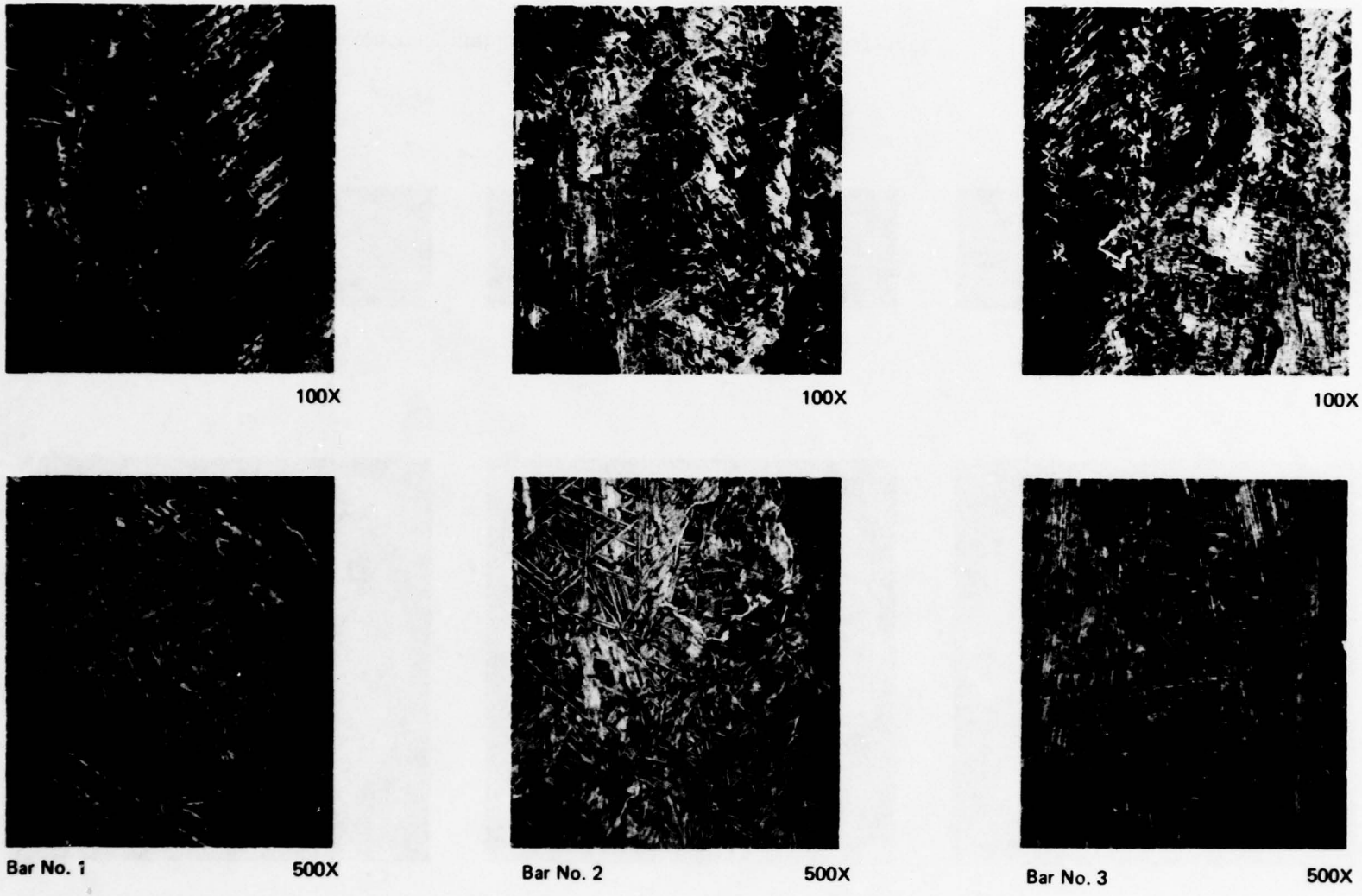

Figure 10. Microstructures of Nonconsumable Cast Ti-6Al-2Sn-4Zr-6Mo Barstock

FD 65127

(1) Vacuum Hot Pressing

Vacuum hot pressing of a randomly selected sample is a practice used to determine the cleanliness of a powder. An anodic etch inspection of hot-pressed powder indicates a powder's purity and freedom from inclusions and/or microsegregation, which may be carried over from the ingot. Metallographic review of hot-pressed compactions provides an indication of microstructural changes to be expected from consolidation processes.

(2) Particle Size Distribution

Particle size distribution analysis provides a common denominator for the comparison of powders produced by various sources. Distribution frequency curves can be plotted showing the percent of powder retained on the screen as a function of mesh size. A general equation of the form $Y = 1-\exp-(X-Xo/Xc)^N$ can be used to describe the sigmoidal curve plotting the mesh size distribution in a cumulative fashion, i.e., the percent of the sample that is less than the stated size. In this equation, Y is the fraction of the powder sample that is less than any given mesh size, X. The parameter X_O is the value of X at a value of $Y = 0$ ($X_O = 0$ for powder mesh size distributions), and X_C is called the characteristic mesh size. This corresponds to the value of X at which $Y = 0.632\ (1-1/e)$, and serves to fix the position of the curve along the X axis. The shape of the curve is governed by the factor N, which for a normal Gaussian distribution of particle size is 3.44. Distribution values of X_C and N are determined by converting the basic equation to one of the form $\ln \ln 1/1-Y = N \ln X - N \ln X_C$, and performing a least squares analysis to obtain the slope and intercept of the resulting straight line. In addition to providing flow parameter information, this analysis aids in comparing the powders from various sources as well as the reproducibility of particle distribution.

(3) Bulk and Interstitial Chemistry Analysis

Bulk and interstitial chemistry analysis of powders provides a method of assessing the ability of a powder facility to produce powder free from undesirable and/or uncontrolled interstitial and impurity elements. Interstitial analysis becomes increasingly important as the mesh size decreases because of the high surface-to-volume ratio of the finer mesh sizes. Finer particles are more prone to adsorbed gas. The absence of contamination in the finer mesh size powder is indicative of the control and quality of the process.

(4) Structural Analysis

Scanning electron microscopy (SEM) is used to characterize surface morphology and area of powder particles. The information can be used to determine surface to volume ratios and surface structure effects on consolidation. Characterization of individual particles is possible due to the excellent depth of field obtainable by scanning electron microscopes in comparison with other conventional metallographic techniques.

(5) Density Measurements

Apparent density measurements per ASTM B212-48 are necessary to determine the approximate yield to be expected from a consolidation sequence and to compare the packing characteristics of different types of powder. Particle densities per ASTM B328-60 determines the degree of hollows that may exist in the powder. Bulk density measurements are made at rest and in the vibrated condition to indicate the ability of powder to be compacted. The information is used to determine yields from additional processing.

(6) BET Measurements

BET surface area measurements were performed on all of the powders. The specific surface is defined as the ratio of the surface area to mass. This analysis, in general, measures the extent of surface roughness, and, in effect, evaluates the material's propensity for adsorbing gas during subsequent processing.

b. Results

(1) Vacuum Hot Pressing

Hot pressings were made in a columbium die capable of yielding a 1-in. diameter cylinder approximately 3/4 in. long. The powder was cold compacted at room temperature prior to compaction at 1650°F under a vacuum (10^{-5} atm). An inclusion count was performed on the hot pressings subsequent to blue etch anodizing. The results are presented in table III. The inclusion count of TMCA powder was an order of magnitude greater than the other powders. Alpha-stabilized flecks about 1/64 in. in diameter comprised the majority of TMCA inclusions.

Table III. Inclusion Count of Vacuum Hot Pressings

Vendor	Type of Powder	Inclusions Per $in.^2$
Nuclear	Rotating Electrode	2.3
NUMEC	Hydride/Dehydride	2.3
TMCA	Hydride/Dehydride	23.4

(2) Particle Size Distributions

Particle size distributions were determined by screening a 100-gram sample for 15 min on a vibratory platform using 8-in. diameter Tyler series screens per ASTM designation B-414-66. Results of the particle size distribution measurements are tabulated in Tables IV through VI and frequency distribution curves are shown in Figures 11 through 13. Distribution values of X_c and N are shown in Table VII. Figure 11 indicates a significantly skewed distribution for TMCA powder. The NUMEC powder (Figure 12) exhibited a more uniform distribution and Nuclear Powder (Figure 13) exhibited an almost normal Gaussian distribution (shape factor of 3.44). Although the characteristic mesh size was virtually the same for all the powders, the shape factor and distribution farequency curves indicated that the TMCA powder contained the largest fraction of fine powder.

Table IV. Particle Size Distribution for TMCA -40 Mesh Ti-6Al-2Sn-4Zr-6Mo Powder

Screen Size Mesh	Screen Size μ	Weight-Percent Retained on Screen	Cumulative Percent Less Than
45	354	12.53	100.00
60	250	24.63	87.47
80	177	17.86	62.84
120	125	14.44	44.98
170	88	9.62	30.54
230	62	6.08	20.94
325	44	8.09	14.84
400	37	4.04	6.75
PAN	<37	2.71	2.71

Table V. Particle Size Distribution for NUMEC -40 Mesh Ti-6Al-2Sn-4Zr-6Mo Powder

Screen Size Mesh	Screen Size μ	Weight-Percent Retained on Screen	Cumulative Percent Less Than
45	354	3.56	100.00
60	250	27.87	96.44
80	177	25.72	68.57
120	125	19.04	42.85
170	88	11.77	23.81
230	62	6.57	12.04
325	44	2.94	5.47
400	37	0.74	2.53
PAN	<37	1.79	1.79

Table VI. Particle Size Distribution For Nuclear Metals -35 Mesh Ti-6Al-2Sn-4Zr-6Mo Powder

Screen Size Mesh	Screen Size μ	Percent Retained	Cumulative Percent Less Than
45	354	4.58	99.99
60	250	21.37	95.41
80	177	31.22	74.04
120	125	25.43	42.82
170	88	10.74	17.39
230	62	4.50	6.65

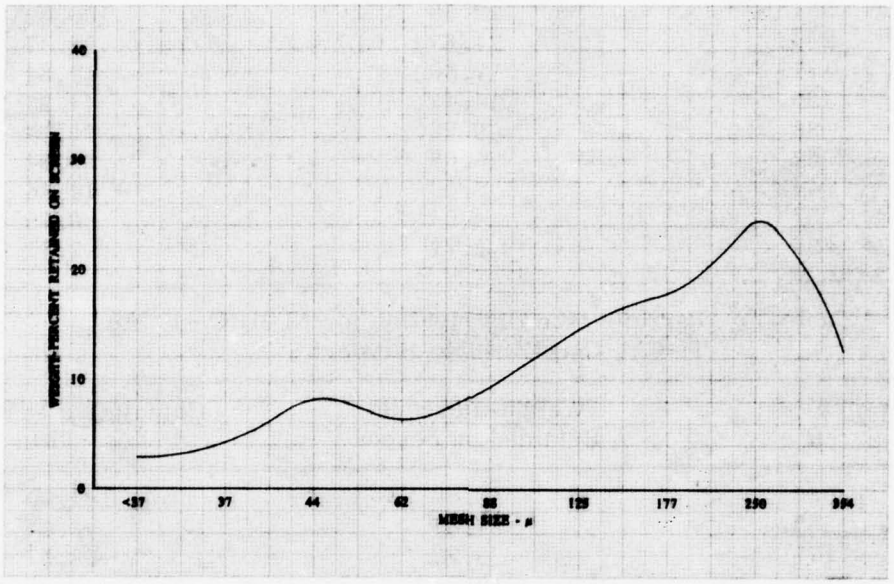

Figure 11. TMCA Ti-6Al-2Sn-4Zr-6Mo Powder Distribution Frequency Curve DF 94629

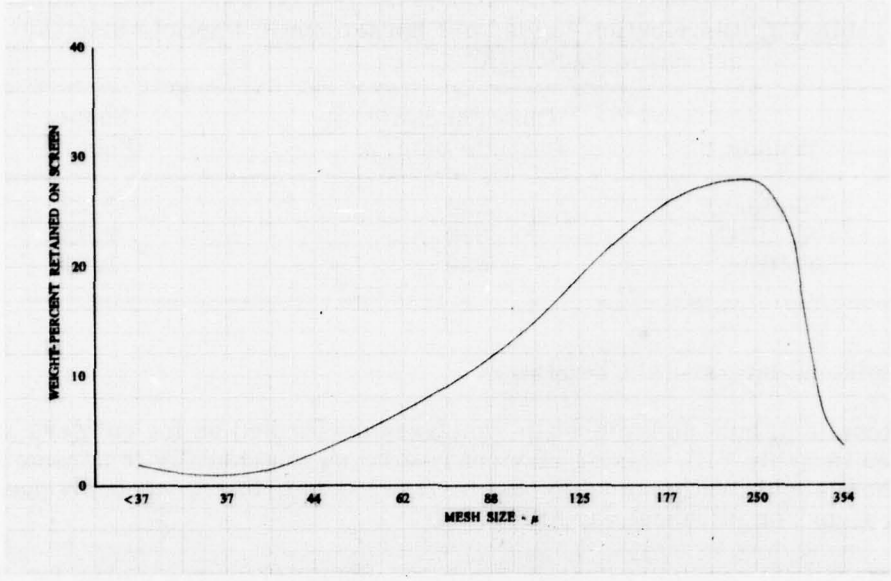

Figure 12. NUMEC Ti-6Al-2Sn-4Zr-6Mo Powder Distribution Frequency Curve DF 94628

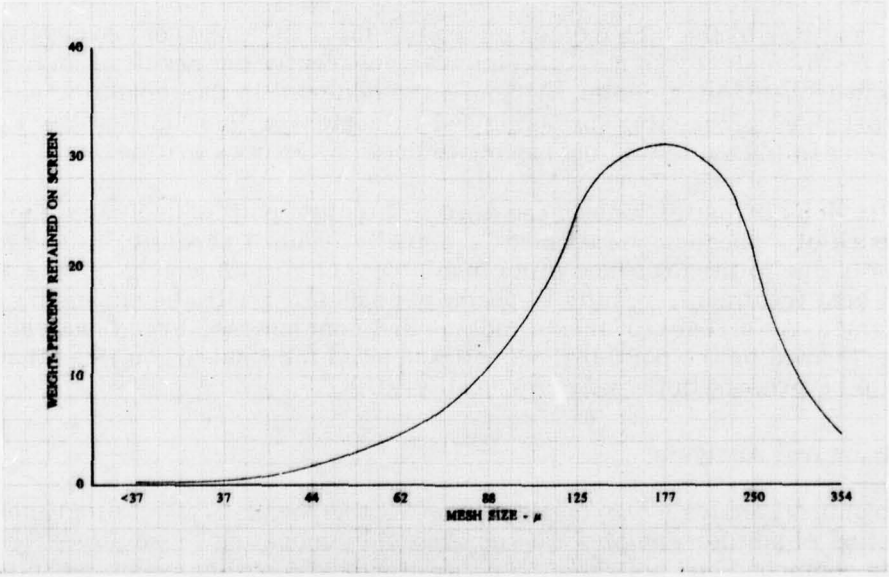

Figure 13. Nuclear Ti-6Al-2Sn-4Zr-6Mo Powder Distribution Frequency Curve DF 94630

Table VII. Distribution Values of Characteristic Particle Size (X_c) and Shape Factor (N)

Vendor	Characteristic Particle Size, μ	Shape Factor
Nuclear	224	3.22
NUMEC	226	2.12
TMCA	230	1.69

(3) Bulk and Interstitial Chemistry

Results of bulk and interstitial analyses performed on the powders are tabulated in Table VIII. Major element results were generally in agreement with ingot chemistry. While some disparities were noted, this is probably due to analytical and/or intraheat variations.

Interstitial results indicated a rather substantial oxygen pickup for the hydride/dehydride-processed material. This was particularly true of the TMCA powder, which was not all-inertly processed. The REP-processed powder, on the other hand, showed an apparent drop in oxygen content. This anomalous behavior was probably due to experimental scatter. However, Nuclear Metals personnel have indicated this occurrence has been noted in several instances and may, in fact, be related to the nature of the REP process.

In addition to the high oxygen content of the TMCA powder, excessively high hydrogen content was noted. This was apparently the result of an inadequate dehydrogenization cycle. Although the material in this condition underwent subsequent processing (pressing and extrusion) without difficulty, a vacuum-annealing cycle was necessary to drive off excess hydrogen.

Previous investigations in the area of titanium powder indicated the occurrence of a phenomenon termed "thermally induced porosity." It is felt that this is due to the presence of an insoluble gas (argon) which, upon subsequent heat treatment, results in porosity associated with the expansion in gas volume. As a result of these findings and conclusions, argon analyses were performed on the powders. Results showed minimal argon (less than 1 ppm) to be present in the powders (Table VIII).

(4) Structural Analysis

Structural analysis was conducted on all the powders. Metallographic examination of powder samples was conducted by mounting loose powder in epoxy mounting compound and polishing by using standard metallographic techniques applicable to titanium. Polished specimens were etched in a 50-50 mixture of Kroll's reagent and glycerine. Photomicrographs at 100X and 500X are shown in Figures 14 and 15.

Table VIII. Task I Chemistries

	Al	Sn	Zr	Mo	Fe	H, ppm	N, ppm	O, ppm		C, ppm	Ar, ppm
Nuclear											
Ingot	6.20	2.08	4.12	6.01	<0.1	84	110	1,000		200	
Powder	5.9	2.2	4.3	5.8	-	46	40	850		180	0.7
As-HIP'D	-	-	-	-	-	90	10	580	1200*	-	
As-Extruded	-	-	-	-	-	80	80	1,210		-	
NUMEC											
Ingot	6.20	2.00	3.90	6.40	.05	52	60	790		100	
Powder	6.00	2.0	3.9	6.0	-	79	100	1,300		157	0.3
As-HIP'D	-	-	-	-	-	100	60	2,110		-	
As-Extruded	-	-	-	-	-	160	110	1,940		-	
TMCA											
Ingot	6.00	2.03	4.02	5.97	.076	-	100	780		-	
Powder	6.00	2.20	4.0	5.80	-	670	120	2,050		77	<0.2
As-HIP'D	-	-	-	-	-	-	-	-		-	
+ VAC Anneal	-	-	-	-	-	220	50	2,120		-	
As-Extruded	-	-	-	-	-	560	190	2,290		-	
+ VAC Anneal	-	-	-	-	-	190	170	2,300		-	

*Chemistry rechecked

EX 1954-3
MICRO NO. AF-1 100X

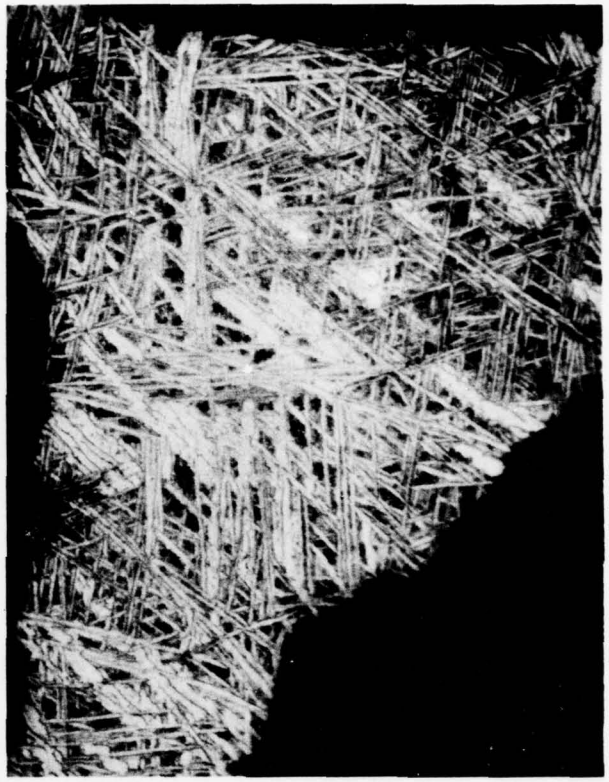

EX 1954-5
MICRO NO. AF-1 500X

NOTE:
SECONDARY FRACTURING OF PARTICLES IN LEFT PHOTO. ETCHANT: 1:1 KROLLS/GLYCERINE

Figure 14. Typical Microstructure of -40 Mesh Ti-6Al-2Sn-4Zr-6Mo Powder As-Received From TMCA. FD 65883

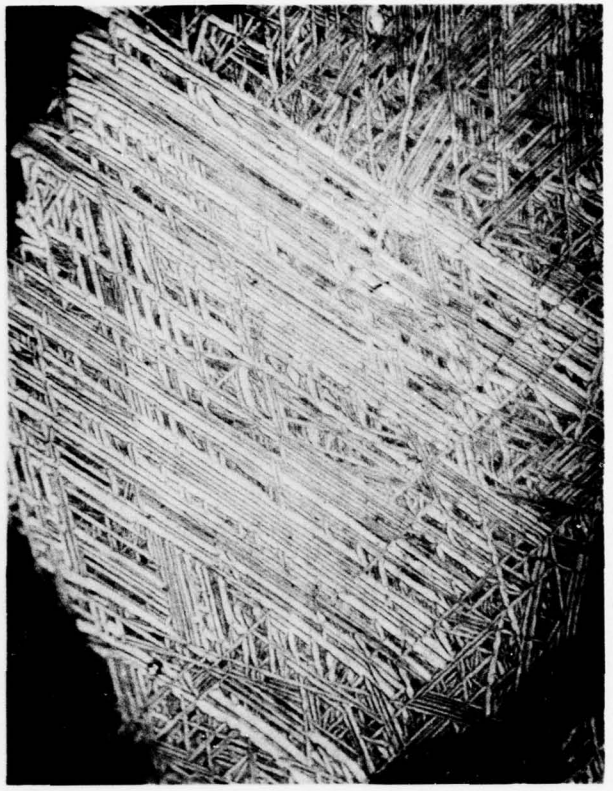

Figure 15. Typical Microstructure of -40 Mesh Ti-6Al-2Sn-4Zr-6Mo Powder As-Received From NUMEC. FD 65882
Etchant: 1:1 Kroll's/Glycerine

The hydride-dehydride powders showed an erratic response to the etchant, with some particles showing typical Widmanstatten structures, while others were rather amorphous in appearance at 100X. The 500X photomicrographs revealed on alpha platelet morphology indicative of the input material. Cross-sectional metallographic examination, of the Nuclear Metals' powder (Figure 16) shows the dendritic solidification pattern of the individual powder particles, plus some evidence of microshrinkage.

Scanning electron micrographs of the NUMEC powder sample are shown in Figures 17 and 18. Secondary particle cracking appears evident in the SEM micrographs. A large number of fine particles adhere to the coarse angular powder particles, which comprise the bulk of the sample. Micrographs of TMCA -40 Mesh powder (Figure 19) were very similar in appearance to NUMEC powder. Nuclear Metals' rotating electrode process (REP) powder shows the powder to be generally spherical, with very smooth surfaces. Few agglomerated secondary particles were noted, and only occasional elliptical-shaped particles were observed (Figure 20).

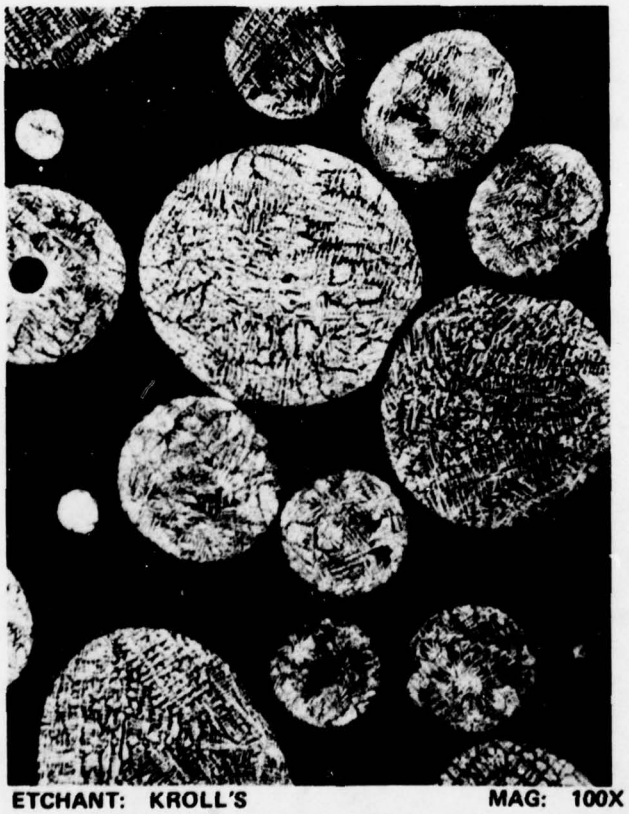

Figure 16. Structure of Nuclear Metals Ti-6Al-2Sn-4Zr-6Mo Powder Showing Dendritic Solidification Pattern FD 66995

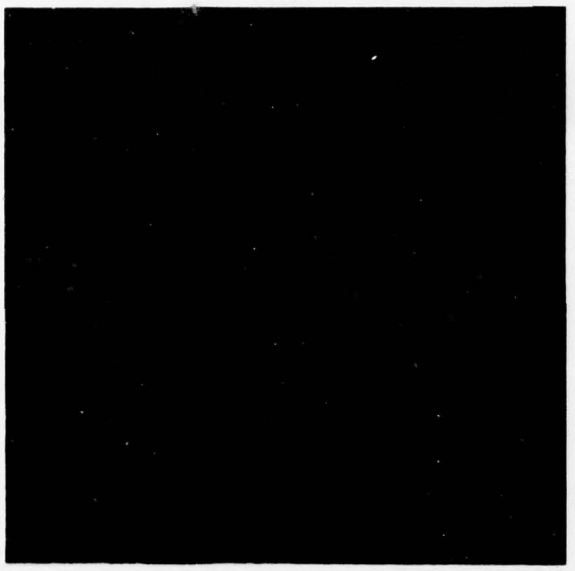

FAL 728044 MAG: 410X

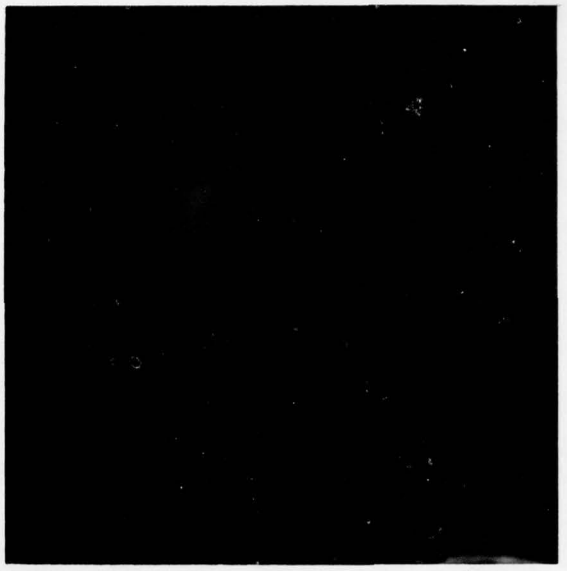

FAL 728048 MAG: 850X

FAL 728047 MAG: 170X

FAL 728045 MAG: 850X

Figure 17. Scanning Electron Micrographs of NUMEC -40 Mesh Ti-6Al-2Sn-4Zr-6Mo Powder FD 65880

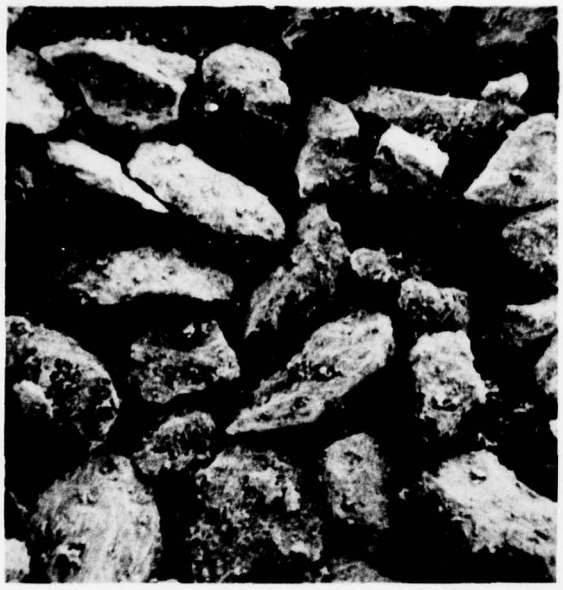

FDL 728041 MAG: 41X

FAL 728042 MAG: 115X

FAL 728043 MAG: 161X

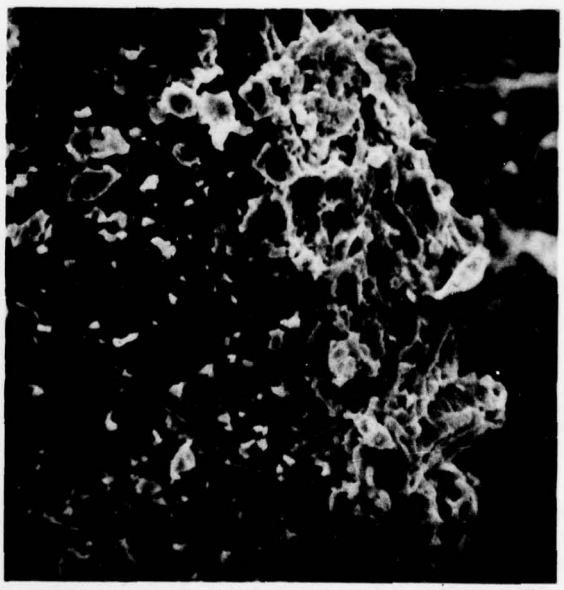

FAL 728046 MAG: 850X

Figure 18. Scanning Electron Micrographs of NUMEC -40 Mesh Ti-6Al-2Sn-4Zr-6Mo Powder FD 65881

40X FE 728049

80X FE 7280411

405X FE 7280412

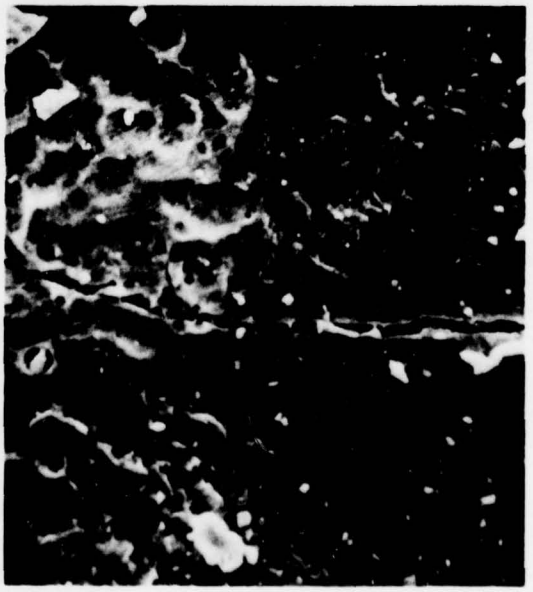

850X FE 7280413

Figure 19. Scanning Electron Micrographs of TMCA -40 Mesh Ti-6Al-2Sn-4Zr-6Mo Powder FD 64428

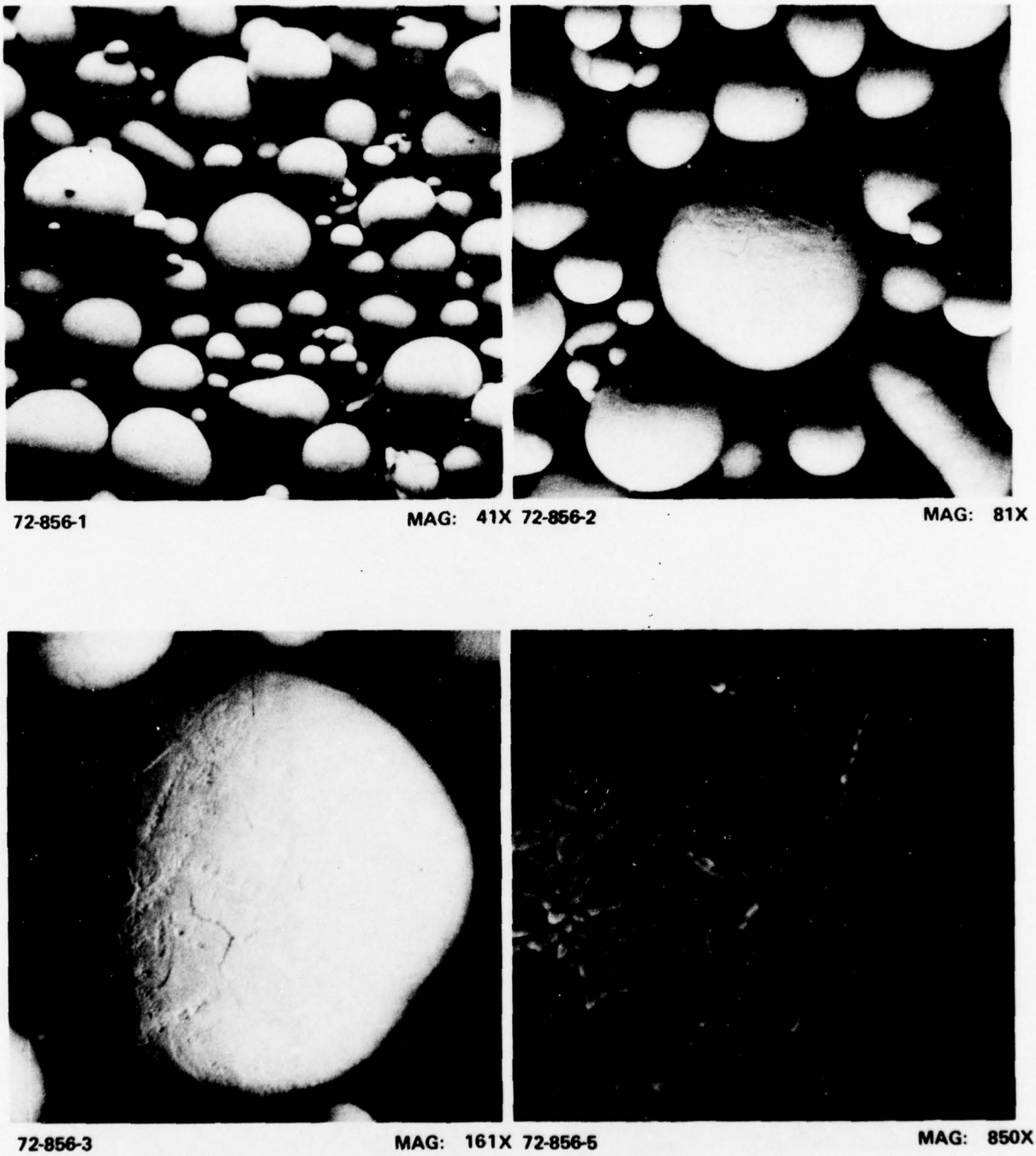

Figure 20. Scanning Electron Micrographs of Nuclear Metals Ti-6Al-2Sn-4Zr-6Mo Powder FD 66996

(5) Density Measurements

Bulk densities were measured in accordance with ASTM Procedure B212-48. One sample was taken under static conditions and a second after the apparatus had been vibrated to measure "tap density." Results of the bulk density measurements are summarized in Table IX. The slightly higher density of TMCA over NUMEC powder can be attributed to the higher fraction of fines in the TMCA product. The percentages of theoretical density were typical of either REP (Nuclear) or hydride-dehydride (NUMEC and TMCA) powder. The results indicate that better packing densities are obtainable with spherical particles.

Particle density measurements were performed on the powder according to ASTM designation B328-60. Results are shown in Table X. The values are in good agreement with prior measurements made on Ti-6Al-2Sn-4Zr-6Mo alloy.

Table IX. Bulk Density of Ti-6Al-2Sn-4Zr-6Mo Powders

Vendor	Mesh Size	Method	Bulk Density	% of Theoretical
Nuclear	-35	Measured at Rest	0.103 lb/in^3	61.3
Nuclear	-35	Vibrated	0.111 lb/in^3	66.0
NUMEC	-40	Measured at Rest	0.071 lb/in^3	41.9
NUMEC	-40	Vibrated	0.086 lb/in^3	51.2
TMCA	-40	Measured at Rest	0.076 lb/in^3	45.3
TMCA	-40	Vibrated	0.097 lb/in^3	57.9

Table X. Particle Density Measurements

Vendor	Density, g/cc	Density, lb/in^3
Nuclear	4.62	0.168
NUMEC	4.70	0.171
TMCA	4.62	0.168

(6) BET Measurements

Results of the BET surface area measurements are presented in Table XI. The values reflect the lower degree of surface roughness, plus the absence of a -325 mesh fraction in the REP powder. The higher value for TMCA, compared to NUMEC, reflects the greater percentage of fines in the TMCA powder.

Table XI. BET Specific Surface Measurements on Ti-6Al-2Sn-4Zr-6Mo Powder

Vendor	Type of Powder	Surface Area/Mass
Nuclear	REP	0.087 m^2/gm
NUMEC	Hydride-Dehydride	0.119 m^2/gm
TMCA	Hydride-Dehydride	0.169 m^2/gm

3. Billet Consolidation

The necessity for special precautions and procedures in the preparation and the canning of nickel-base alloy powders is an established fact. The necessity for all-inert processing of titanium alloys has not been fully evaluated. Although all-inert processing was not used in the production of all the titanium powders under evaluation or in the canning procedures, exposures to possible adverse conditions were minimized.

a. Can Design

The basic can design selected has been proved successful in the processing of nickel-base superalloy powders. The interior of the can was modified to permit the use of special can-filling procedures. The extrusion and HIP cans were machined from mild steel tubing and billet stock. The evacuation tubes were stainless steel.

b. Can Preparation

In fabricating the containers, end caps and weld rings were welded onto the cans, as shown in Figures 21 and 22. After welding, the cans were cleaned and leak checked. Nicrobraze 10 was placed around the perimeter of the braze cover and on top of the weld ring. Powder was poured into the cans, and then the can and powder were placed inside a vacuum-induction melting furnace. The powder was vacuum-out-gassed about 8 hr at less than 1μ prior to heating. The powder was then heated until the braze began to flow and then the braze cover was lowered into place and brazed onto the weld ring. Following the brazing operation, the head plug was welded in place. After leak checking, the space above the brazed cover was evacuated and sealed.

c. Extrusion

Three mild steel cans filled with Ti-6Al-2Sn-4Zr-6Mo powder were extruded at RMI, Ashtabula, Ohio. All cans were placed in 1-in. thick graphite containers (to prevent excessive scaling) before being placed in a furnace and soaked for 8 hr at 1650°F, prior to extrusion. The material was extruded from a 6-1/8-in. diameter liner through a 2.4-in. diameter orifice die, with a 60-deg included angle (a reduction ratio of 6.3:1).

Average upset pressures of 1054 tons (extrusion constant = 19.1 tons/in.^{2}) and average run pressures of 925 tons (16.8 tons/in.^{2}) were required. Approximately 30% of the maximum press capacity was used. Extrusion lengths correspond closely with powder packing densities.

d. Hot Isostatic Pressing

Three filled and evacuated cans were hot isostatically pressed by Crucible Materials Research Center. Silica sand was poured into a 7-1/2-in. diameter can. The sealed cans were placed inside the larger can and surrounded with additional silica. Application of a warm vacuum on the can compacted the silica and demoisturized the can. After sealing the large can and heating it to 1650°F, it was placed in an autoclave and a pressure of 15,000 psi was applied. Nonuniformity of the HIP'd cans (Figure 23) may be partially attributed to a nonuniform packing of the silica powder in the large can.

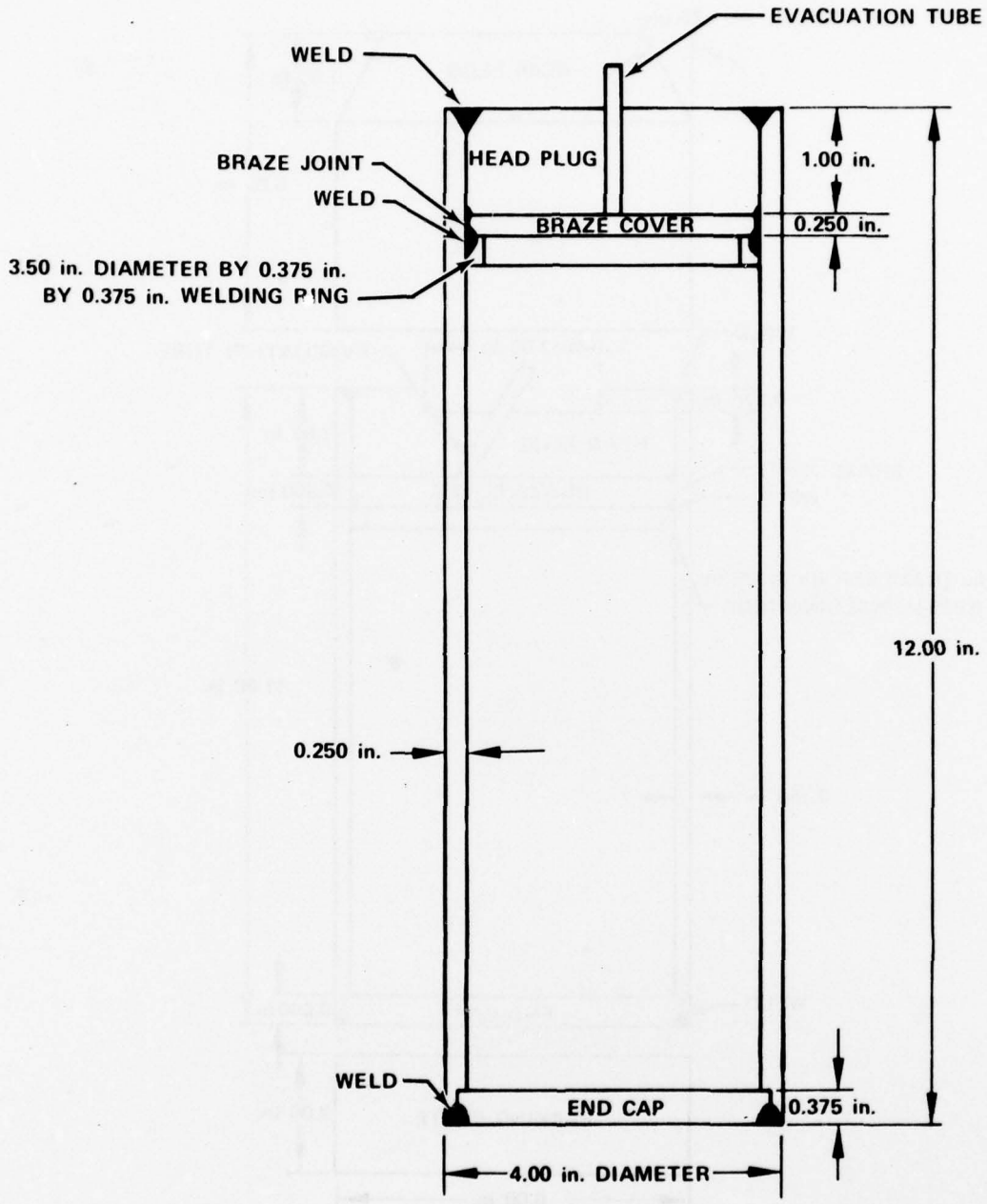

Figure 21. Task I, Hot Isostatic Pressing Can FD 66997

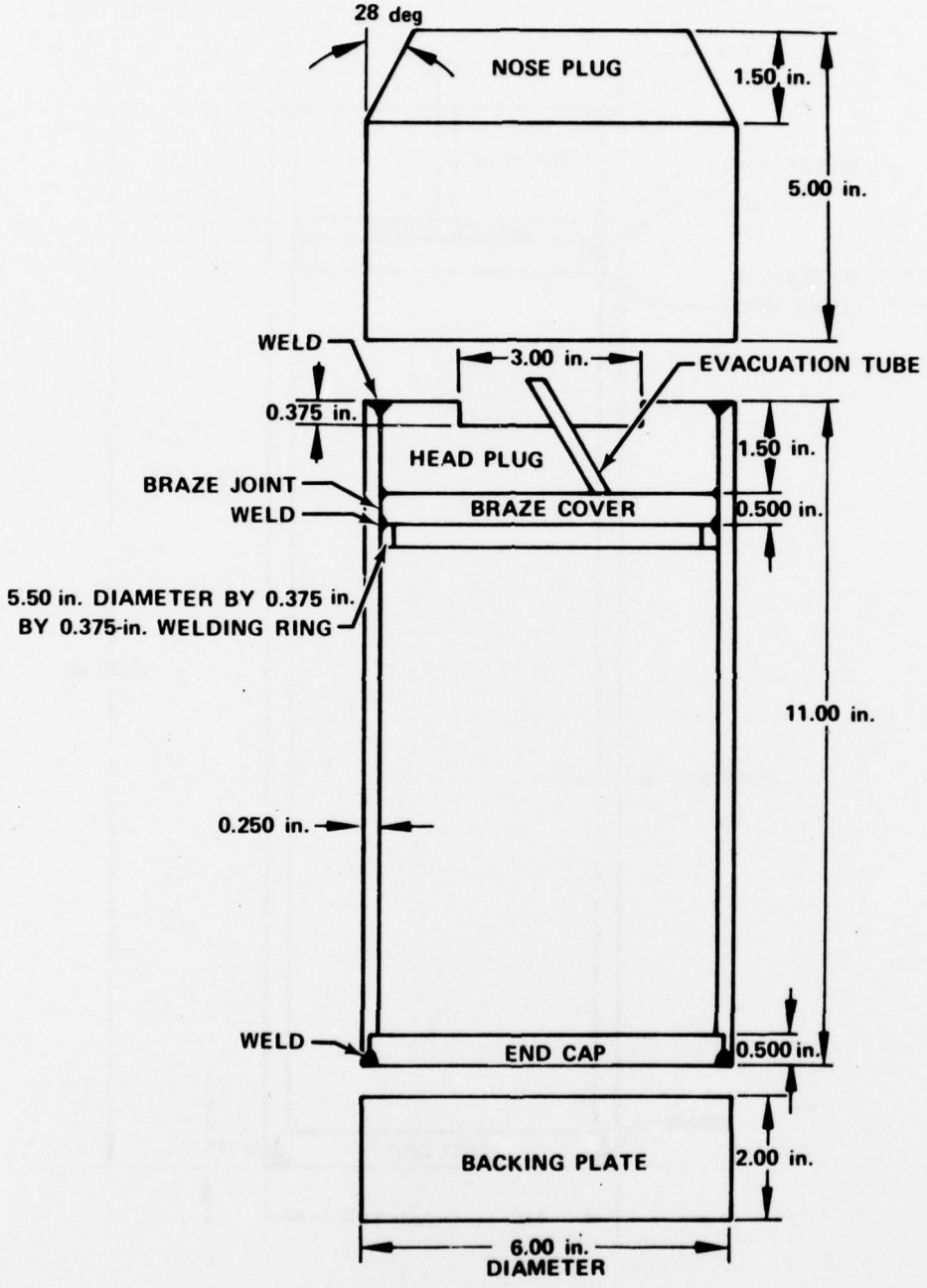

Figure 22. Task I, Extrusion Can FD 66998

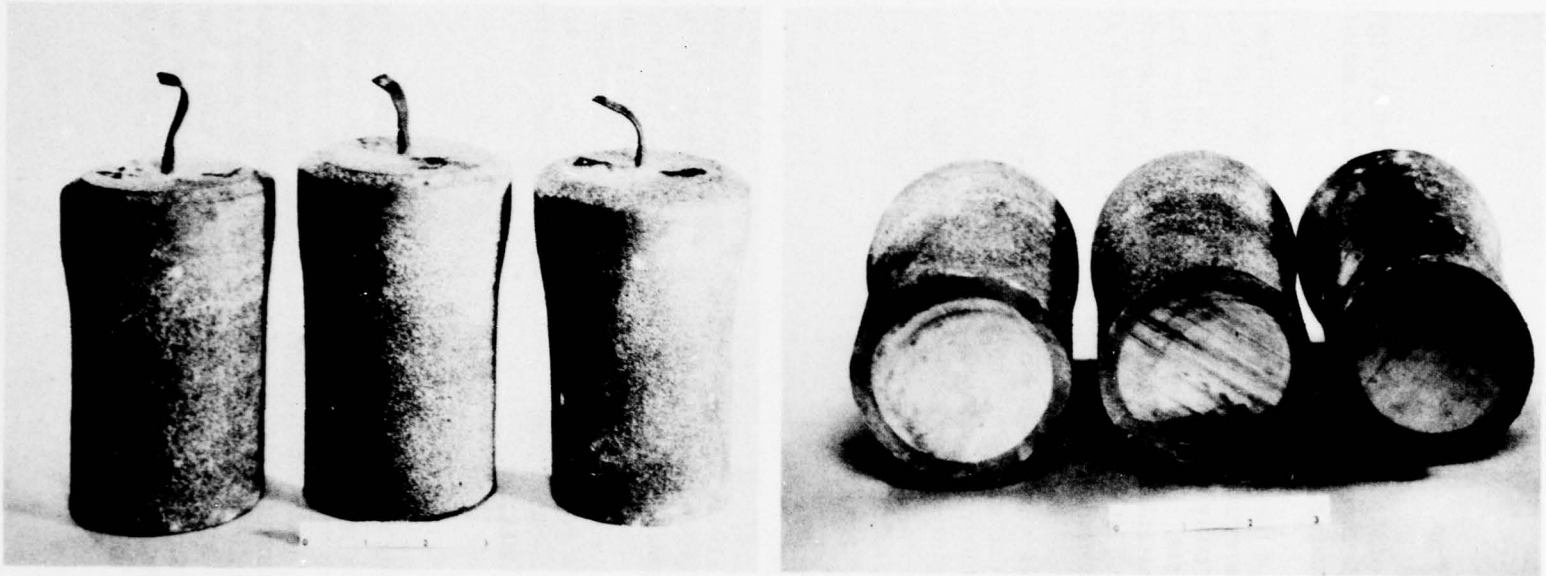

Figure 23. As-Hot Isostatically Pressed Billets Showing Some Can Tapering and Nonuniformity FD 69990

4. Billet Evaluation

a. Direct Extrusion

(1) Structural Evaluation

Macrostructures of the extruded material are shown in Figure 24. A fine, uniform macrostructure was evidenced. The NUMEC material exhibited a noticeable surface-to-center variation.

Microstructures of the extruded material indicated that the beta transus was exceeded during the extrusion operation (Figure 25). Adiabatic heating during extrusion was apparently sufficient to result in the fine transformed beta structure in all the billets. Slightly coarser secondary alpha platelets and grain boundary alpha were present in the Nuclear and NUMEC materials. The absence of these qualities in the TMCA material was, again, probably a result of the excessively high hydrogen content.

Microstructures (Figure 26) of the heat-treated (1670/1/AC+1100/8/AC) extruded powders were indicative of a material that experienced temperatures above the beta transus during extrusion. The transformed structure was similar to the as-extruded structure, with some coarsening of alpha platelets occurring during heat treatment. Based on the contractor's previous experience, a 1670°F/1/AC+1100°F/8/AC heat treatment was selected as the baseline heat treatment for the entire program.

(2) Interstitial Chemistry

Quantitative interstitial analyses of the extruded powder materials are given in Table VIII. Oxygen results showed about a 300- to 600-ppm oxygen and a slight ($\sim$50 ppm) nitrogen increase in all the materials. This increase was indicative of the "pickup" resulting from shipping and handling prior to outgassing and can sealing procedures that preceded the extrusion operation. As previously noted, the incomplete dehydrogenization of the TMCA material was evidenced in the extruded product. Subsequent vacuum annealing reduced the hydrogen level from 560 ppm to 190 ppm.

(3) Sonic Inspection

All extruded billets were machined to right cylinders approximately 10 in. long. Surfaces were either surface or centerless ground or lathe turned. The sonic inspection equipment consisted of a basic research-type water tank with an automatic billet indexing/rotation and traversing pickup. A curved 1/4- by 3/4-in. type SIL Automated Industries pipe transducer was used because scans were made axially with the billets rotated at the termination of every traverse. An Alden Recorder (Model 311DA) was used in conjunction with a Sperry UM721 Reflectscope in recording each sonic inspection. Billets were inspected at a sensitivity capable of detecting a No. 2 flat bottom hole (.03125 inch diameter). No defects were found in the extruded billets.

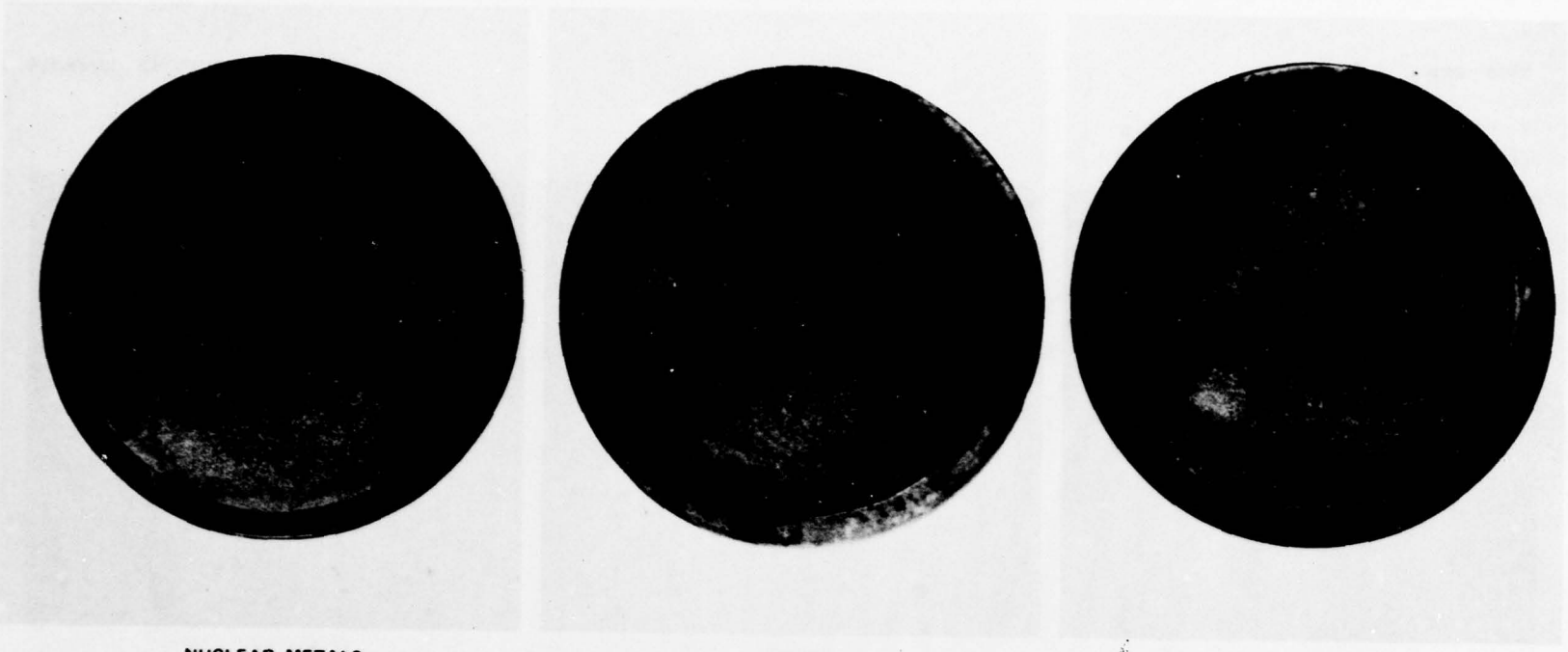

Figure 24. Macrostructures of Extruded Ti-6Al-2Sn-4Zr-6Mo Powder Billet

FD 69997

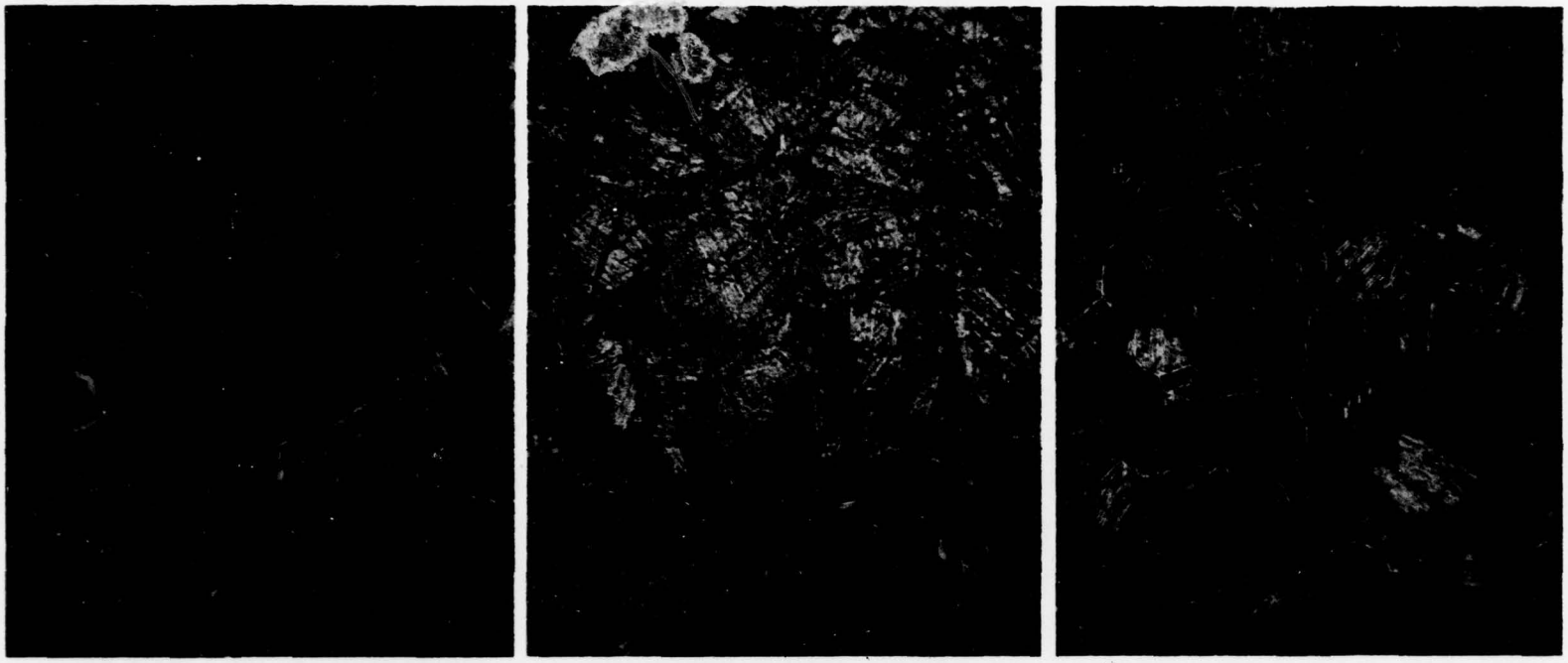

NUCLEAR METALS TMCA NUMEC

ETCHANT: KROLL'S

MAG: 400X

Figure 25. Microstructures of Extruded Ti-6Al-2Sn-4Zr-6Mo Powder Indicates the Beta Transus Was Exceeded During Extrusion FD 69998

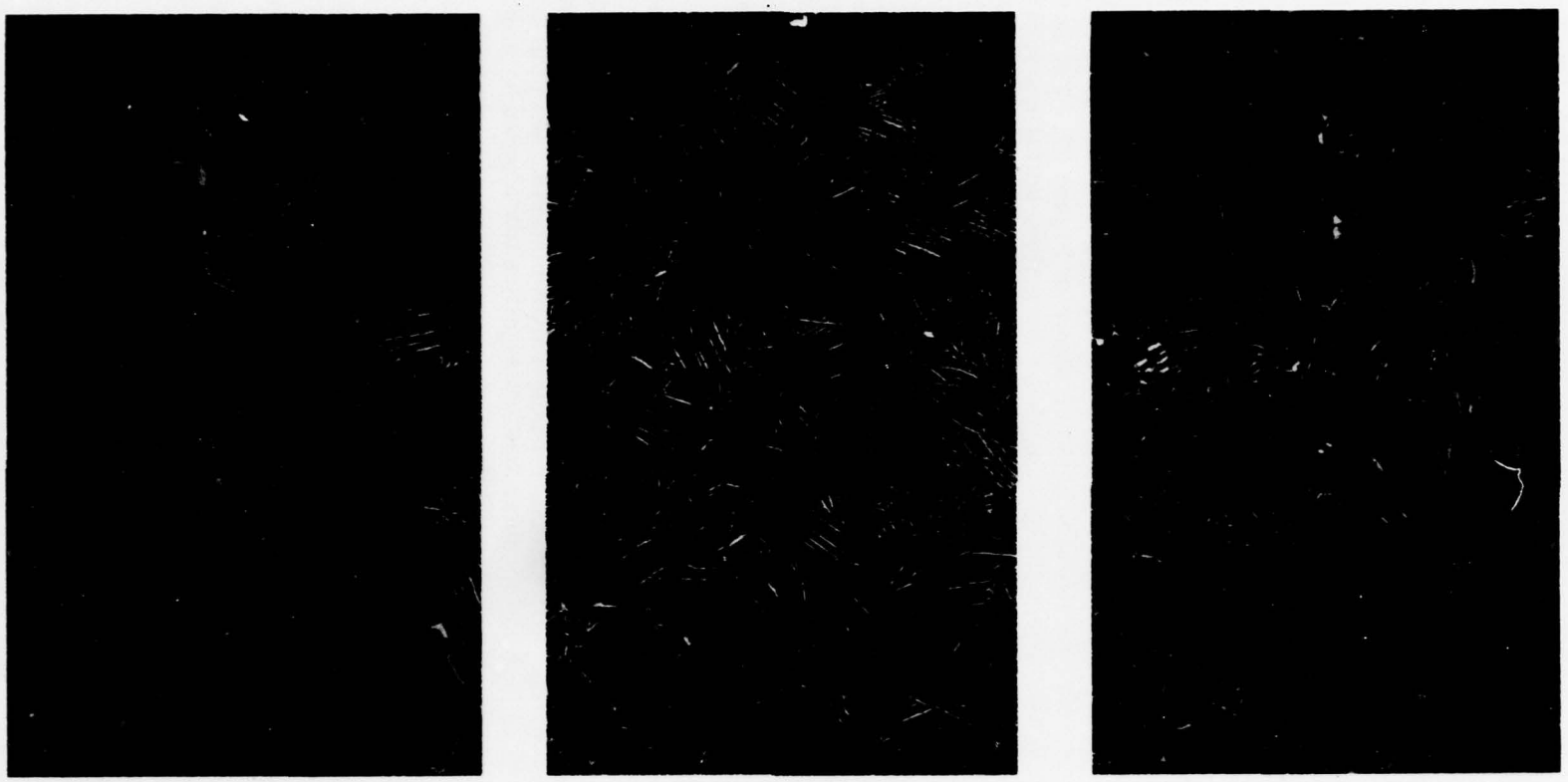

Figure 26. Microstructures of Heat-Treated (1670/1/1/AC + 1100/8/AC) Extruded Ti-6Al-2Sn-4Zr-6Mo Billets

FD 72611

(4) Mechanical Properties

The extruded billets were given a 1670/1/AC+1100/8/AC heat treatment. Tensile and room temperature notched stress-rupture testing was conducted on the heat-treated materials. Results are listed in Table XII.

The variation in yield strengths were influenced by the varying interstitial levels. Nuclear Metals material had the lowest yield and interstitial levels; the converse was true for the TMCA material. The excessive number of inclusions in the TMCA material accounted for the clearly inferior ductility.

b. Hot Isostatic Pressing

(1) Structural Evaluation

Macrostructures of as-HIP'd billets are shown in Figure 27. The compacted powder from all three sources exhibited a very fine, uniform structure. The NUMEC material showed a slight surface-to-center variation in structure, most likely due to surface chilling during the pressing cycle. Closer examination of the macro slices revealed the presence of inclusions.

Typical microstructures of the HIP billets are shown in Figure 28. The Nuclear Metals and NUMEC materials consisted of coarse alpha platelets in a transformed beta matrix. This structure was typical of what would be expected from the HIP cycle (i.e., 1650°F plus slow cool). The TMCA material exhibited a much finer acicular alpha structure. Unlike the Nuclear and NUMEC materials, platelet coarsening did not occur. This was a result of the excessively high hydrogen content (670 ppm).

The microstructures after heat treatment (1670/1/AC + 1100/8/AC) are shown in Figure 29. The Nuclear and NUMEC structures were "broken-up" significantly as a result of the heat treatment. The structures of both consisted of 30 to 40% primary alpha (some equiaxed, predominantly elongated) in a fine transformed beta matrix. The structure of the TMCA material, with the exception of the removal of hydride needles, was not significantly altered by either the vacuum anneal or full heat treatment.

(2) Interstitial Chemistry

Quantitative interstitial analyses of the HIP material are given in Table VIII. These results show the relative oxygen pickup of the powder during subsequent processing. Nuclear and TMCA materials showed little, if any, increase in oxygen. The NUMEC material did show a rather substantial oxygen pickup which could have resulted from a can leak prior to consolidation. A decrease in hydrogen content (220 vs 670) in the TMCA material as a result of the vacuum annealing cycle was noted.

Changes in hydrogen and nitrogen contents were also seen in the HIP material as compared to the powder and ingot chemistries. These changes were within desired limits for this alloy and were probably due to analytical variances.

Table XII. Mechanical Properties*

Vendor	Material Condition	Tensile				RT Notched Stress-Rupture		
		.2 Y.S.	UTS	El	RA	Failure Stress	Total Time	Time at Failure Load
Nuclear	HIP	157.7	173.0	2.1	2.2	180	30.2	.2
		159.4	178.0	0.87	2.9	170	21.2	1.2
NUMEC	HIP	-	168.2	0.1	nil	150	(Failed on Loading)	
		163.4	179.8	3.4	4.6	150		
TMCA	HIP	-	139.4	nil	nil	150	(Failed on Loading)	
		-	171.9	nil	nil	150		
Nuclear	Extruded	159.4	177.9	12.8	23.2	225	68.9	3
		157.7	176.3	13.1	20.1	215	68.9	3
NUMEC	Extruded	166.1	186.7	10.4	23.9	225	78.7	4.5
		168.3	184.5	7.6	19.1	225	85.7	11.7
TMCA	Extruded	177.1	188.9	1.7	2.9	235	124.5	6.2
		173.3	186.3	1.0	2.1	150	(Failed on Loading)	
Nuclear	HIP + Forge	-	179.9	nil	nil	230	30	0
		(1) 165.0	169.2	1.0	3.5	230	30	0
NUMEC	HIP + Forge	195.4	196.4	1.0	3.2	170	2.7	2.7
TMCA	HIP + Forge	172.1	191.7	4.0	10.1	220	25.2	0.2
Nuclear	Extruded + Forge	-	49.7	-	-	230	30.0	0
		(1) 173.0	181.3	11.0	29.3	230	30.0	0
NUMEC	Extruded + Forge	188.3	192.3	1.0	1.0	230	30.0	0
		(1) 173.1	183.1	3.5	6.3			
TMCA	Extruded + Forge	-	130.8	<1.0	-	250	45.4	0

*1670/1/AC+1100/8/AC unless otherwise noted
(1) 1700/1/AC+1100/8/AC

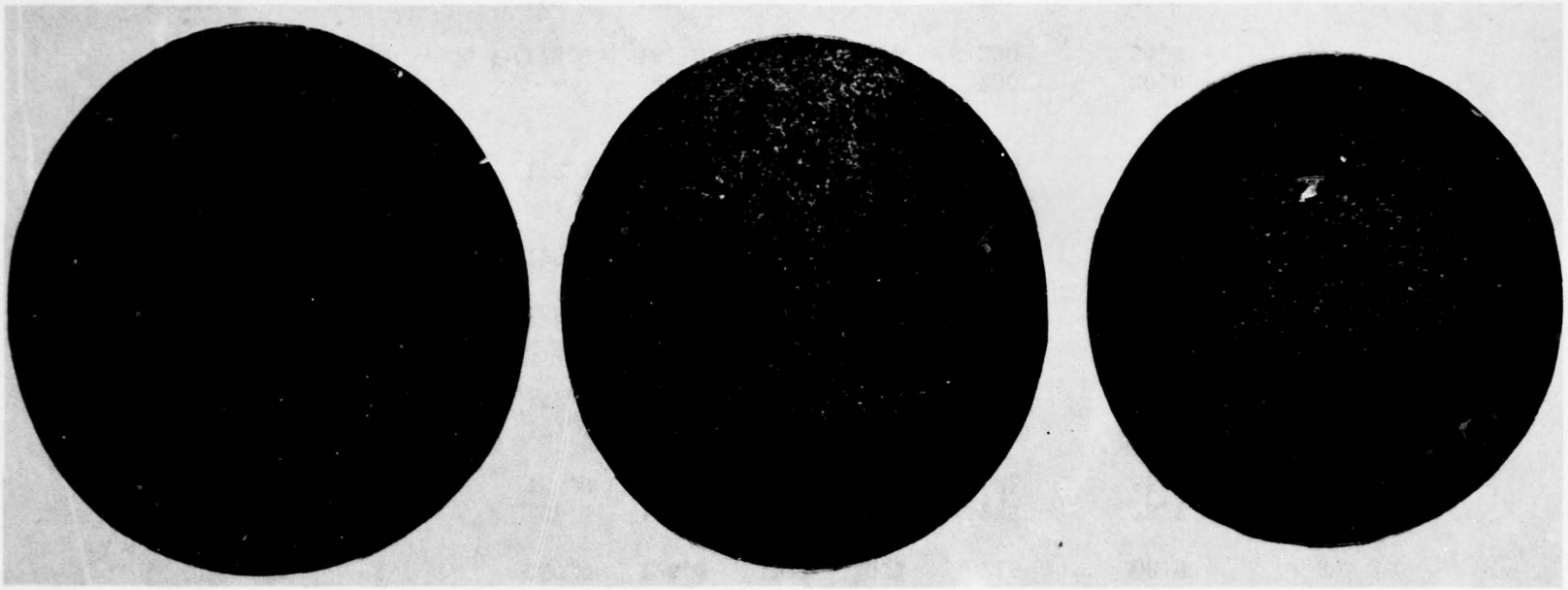

NUCLEAR METALS TMCA NUMEC

ETCHANT: KROLL'S MAG: 1¼X

Figure 27. Macrostructures of HIP Ti-6Al-2Sn-4Zr-6Mo Powder Billets FD 69991

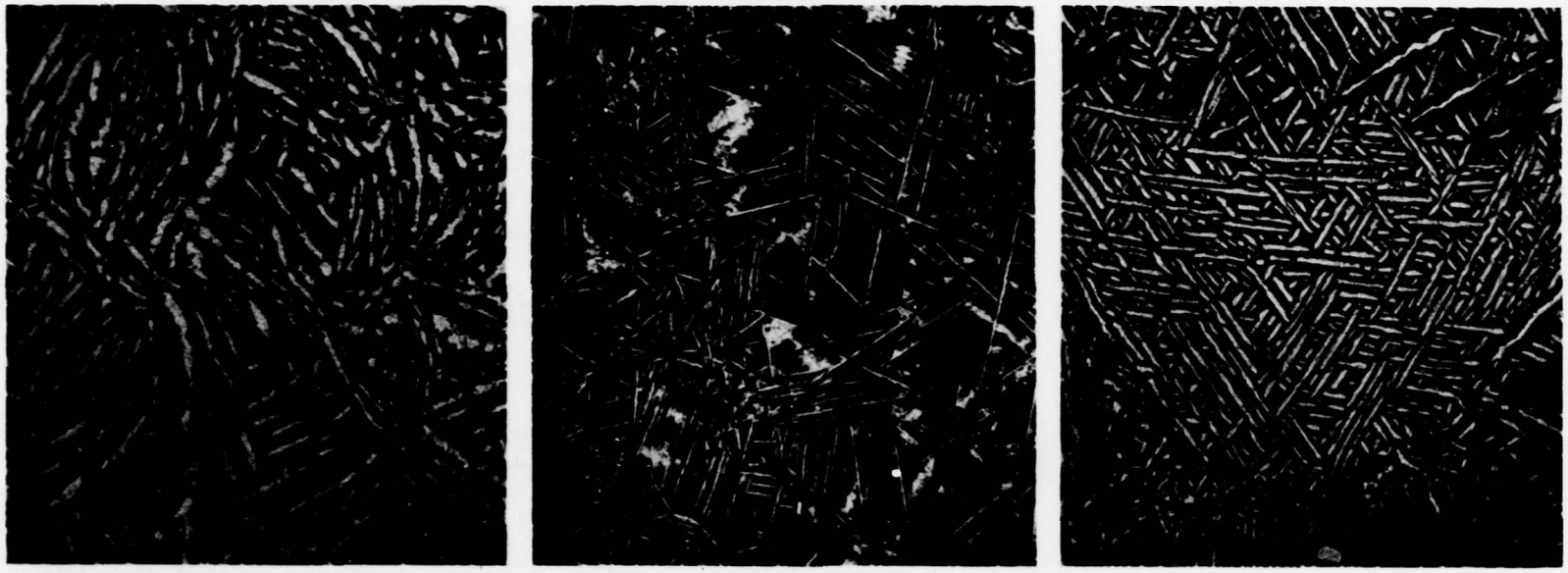

Figure 28. Microstructures of HIP Ti-6Al-2Sn-4Zr-6Mo Powder Billets

FD 69992

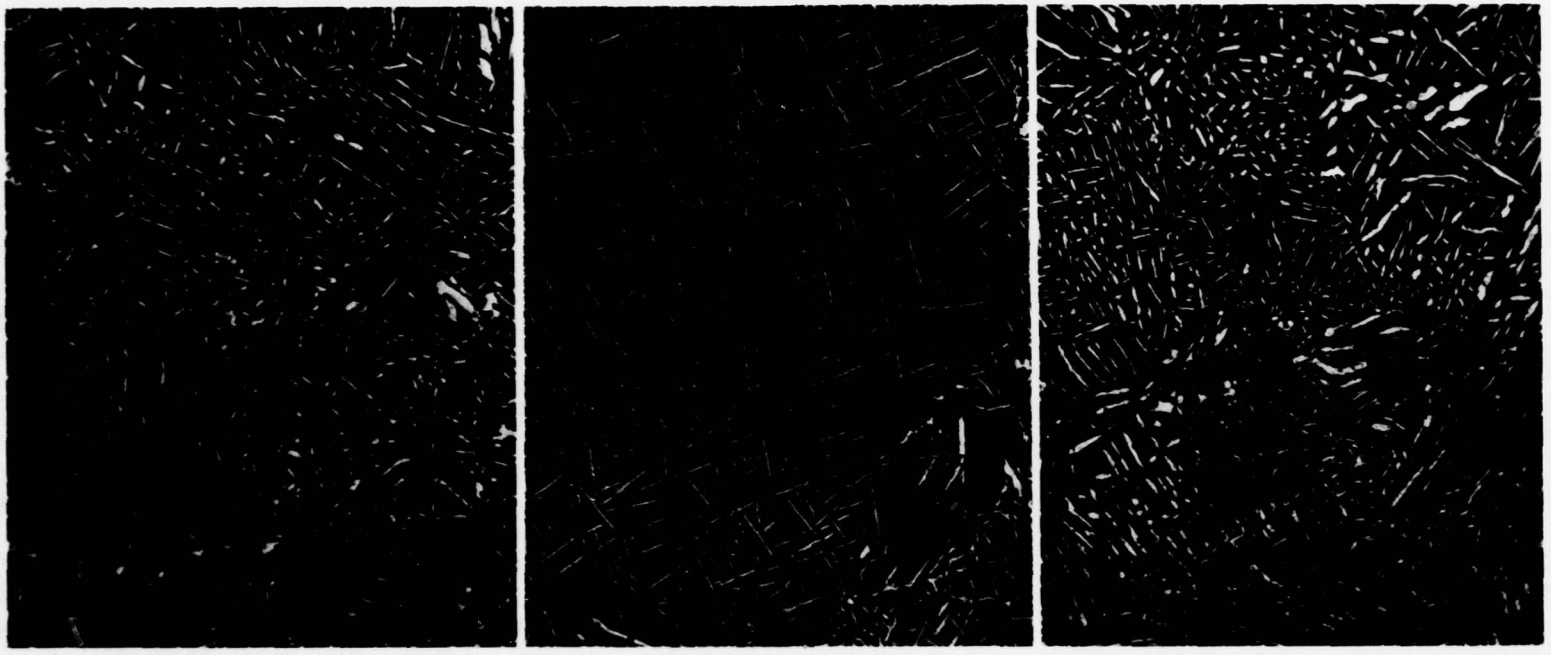

Figure 29. Microstructures of Heat-Treated (1670/1/AC + 1100/8/AC) HIP Ti-6Al-2Sn-4Zr-6Mo Billets FD 71077

(3) Sonic Inspection

The same equipment and procedures used for analyzing the extruded billets were used to examine the HIP billets. All HIP billets were free of noticeable defects, however, the sensitivity of the equipment was not adequate to reveal the small inclusions present in the material.

(4) Mechanical Properties

Tensile and room temperature notch stress-rupture specimens were machined from all the HIP billets after a 1670/1/AC + 1100/8/AC heat treatment. Results are summarized in Table XII.

The testing dramatically pointed out the detrimental effect of inclusions on high strength titanium alloys. All fractures (both in tensile and stress-rupture testing) were found to originate from inclusions (Figure 30). The fracture progressed from the inclusion in a brittle manner, resulting in poor ductility and, in some cases, an absence of yielding.

The Nuclear Metals material exhibited the most encouraging results, with some tensile ductility and nearly acceptable stress-rupture properties. On the other hand, the TMCA material, with its high inclusion content, showed a complete absence of ductility and yielding.

A plausible explanation for the lower ductility exhibited by the HIP material is the presence of a greater effective defect size. Experience with deliberately doped titanium powder has shown that extrusion results in elongation of the inclusions. Upon testing in the longitudinal direction, the effective defect size would be greatest in the HIP material.

5. Forging Evaluation

Forging multiples measuring 4.1 in. long and 1.75 in. in diameter were machined from both the extruded and HIP'ed billets. All the multiples were forged at 1650°F. The finished pancake size measured approximately 1/2-in. thick by 5 in. in diameter (an 88% reduction).

a. Structural Evaluation

Macrostructures of the forged material (either HIP or extruded), were typical of that shown in Figure 31. All forgings exhibited an extremely fine, uniform, and, hence, somewhat featureless macrostructural appearance.

With the exception of the TMCA HIP material, which was forged in the high hydrogen condition, microstructural observations reinforced the macrostructural findings (Figures 32 and 33). All of the forgings, with the aforementioned exception, had a uniformally fine dispersion of primary alpha. The HIP material showed a tendency for the persistence of more elongated alpha, whereas the extruded material was predominantly equiaxed.

Microstructures of heat treated (1670/1/AC+1100/8/AC) forgings are shown in Figures 34 and 35. The heat treated structures were extremely uniform and fine grained. Again, the extruded material exhibited a tendency for a more equiaxed form of primary alpha.

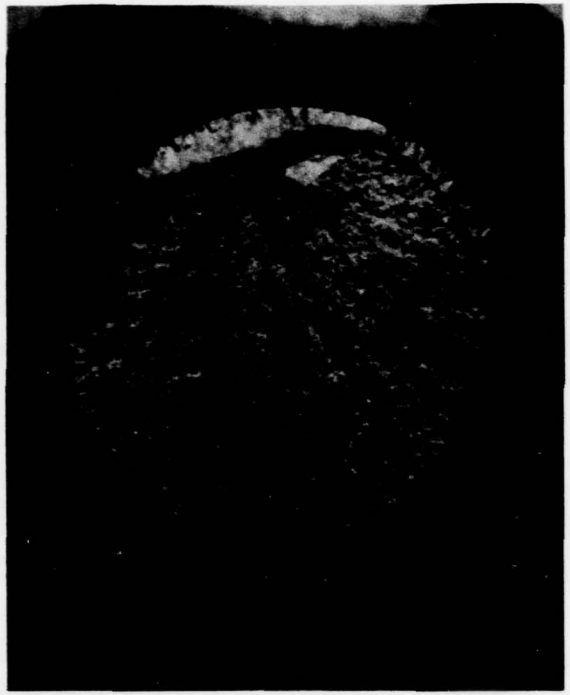

NUCLEAR METALS

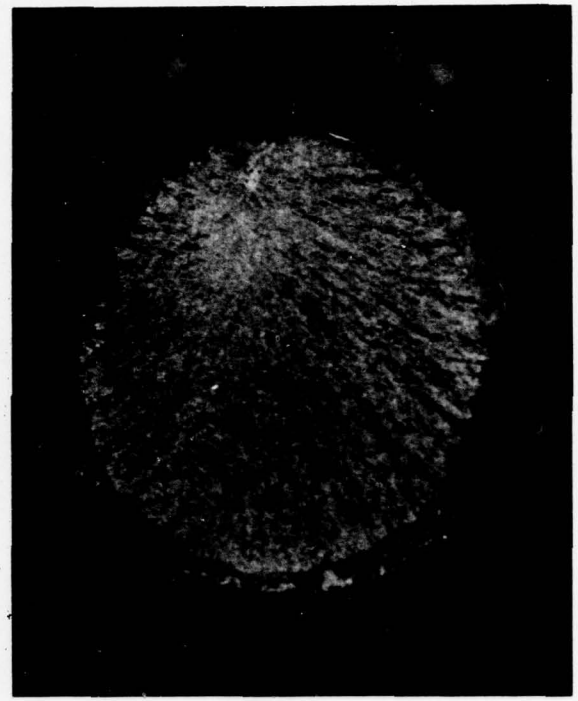

NUMEC

ETCHANT: KROLL'S

MAG: 10X

Figure 30. Fracture Surfaces of Tensile Specimens Showing Inclusions Responsible for Low Ductility FD 69996

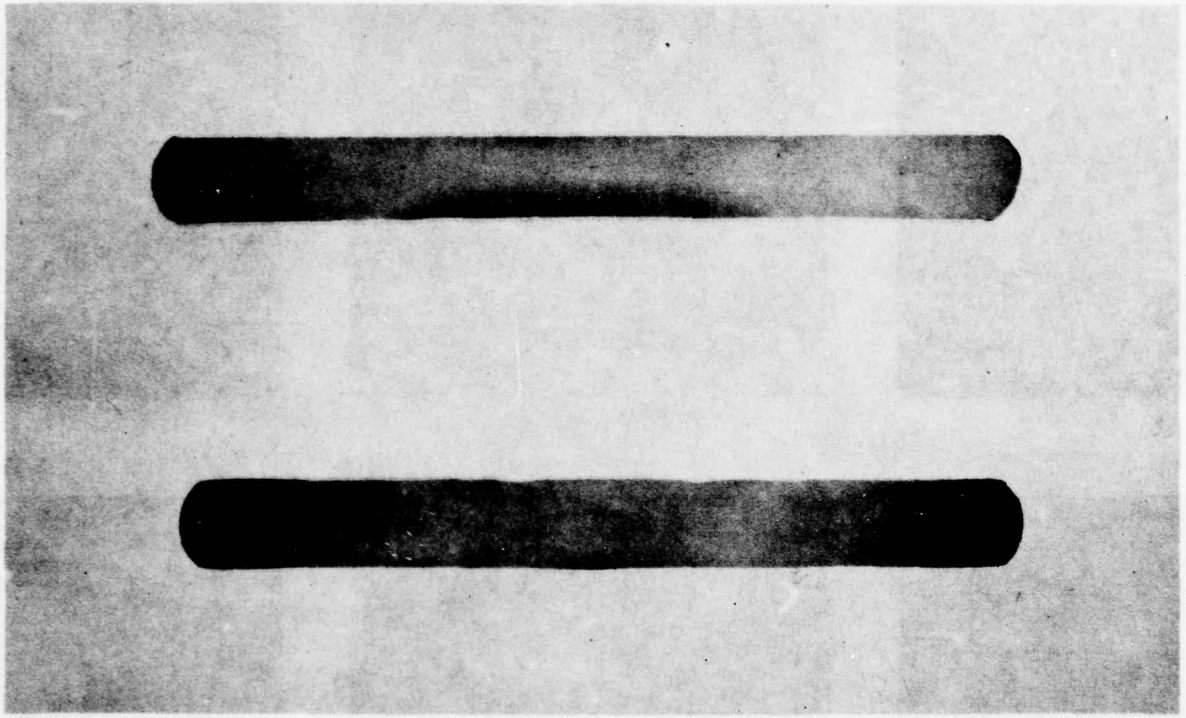

Figure 31. Typical Macrostructures of Forged Ti-6Al-2Sn-4Zr-6Mo Powder Billet FD 72613

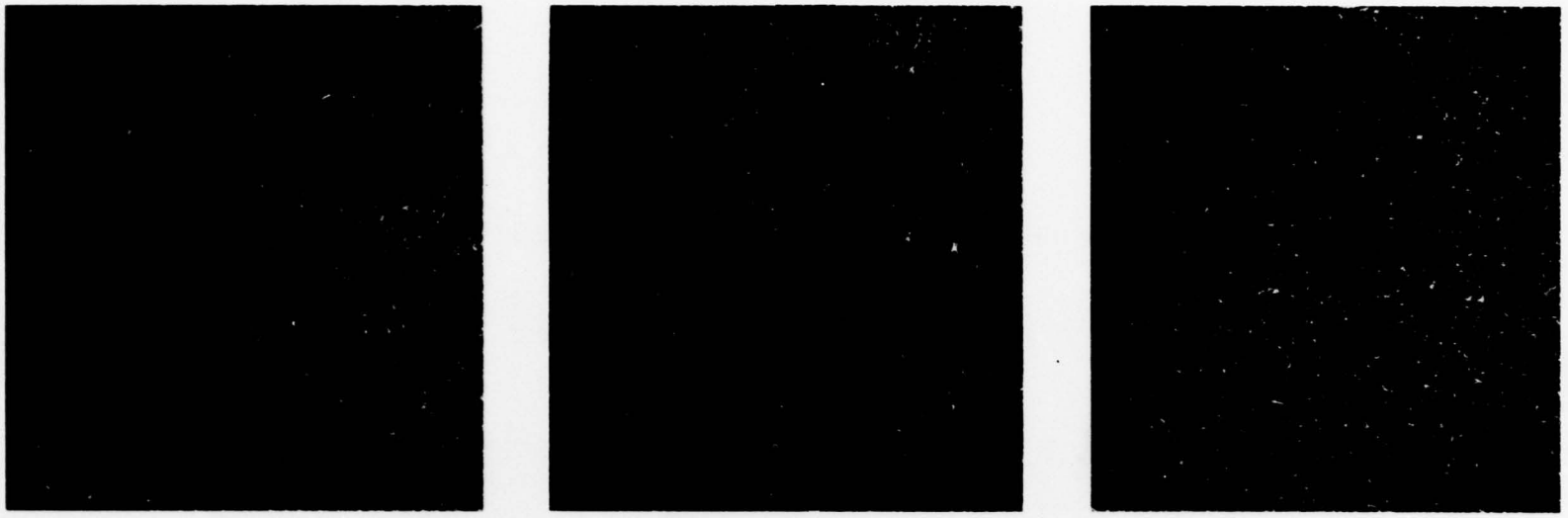

ETCHANT: KROLL'S

MAG: 100X

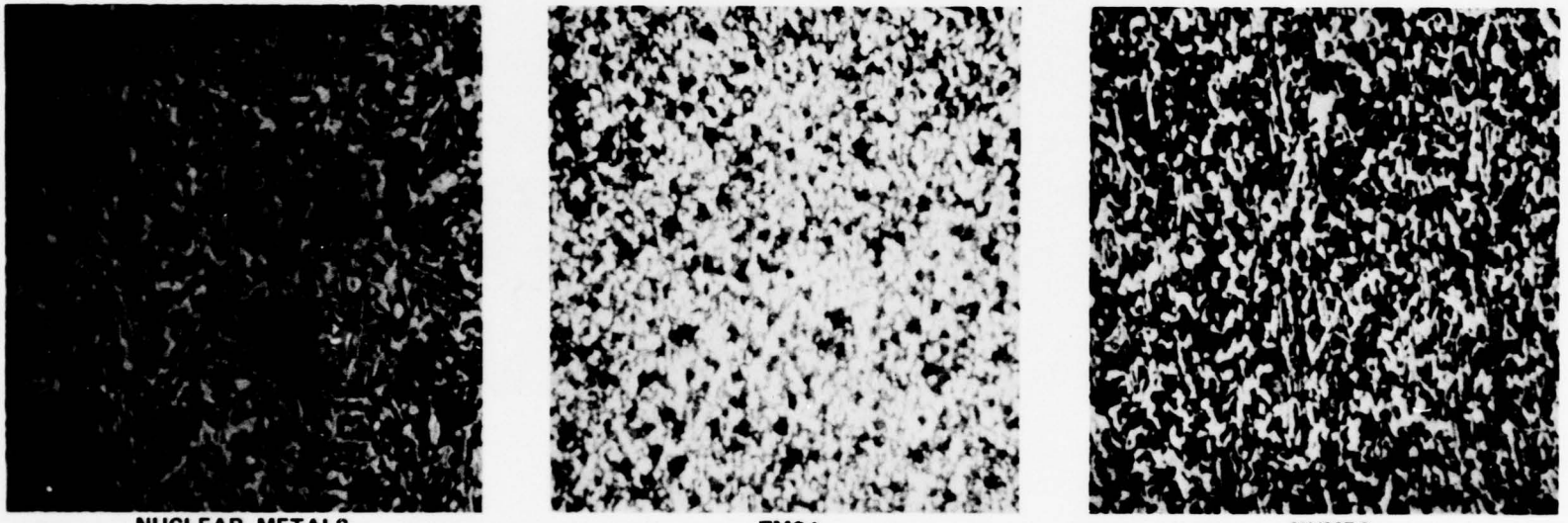

NUCLEAR METALS

TMCA

NUMEC

ETCHANT: KROLL'S

MAG: 500X

Figure 32. Microstructures of Ti-6Al-2Sn-4Zr-6Mo Extruded Powder Billets Forged at 1650°F

FD 69999

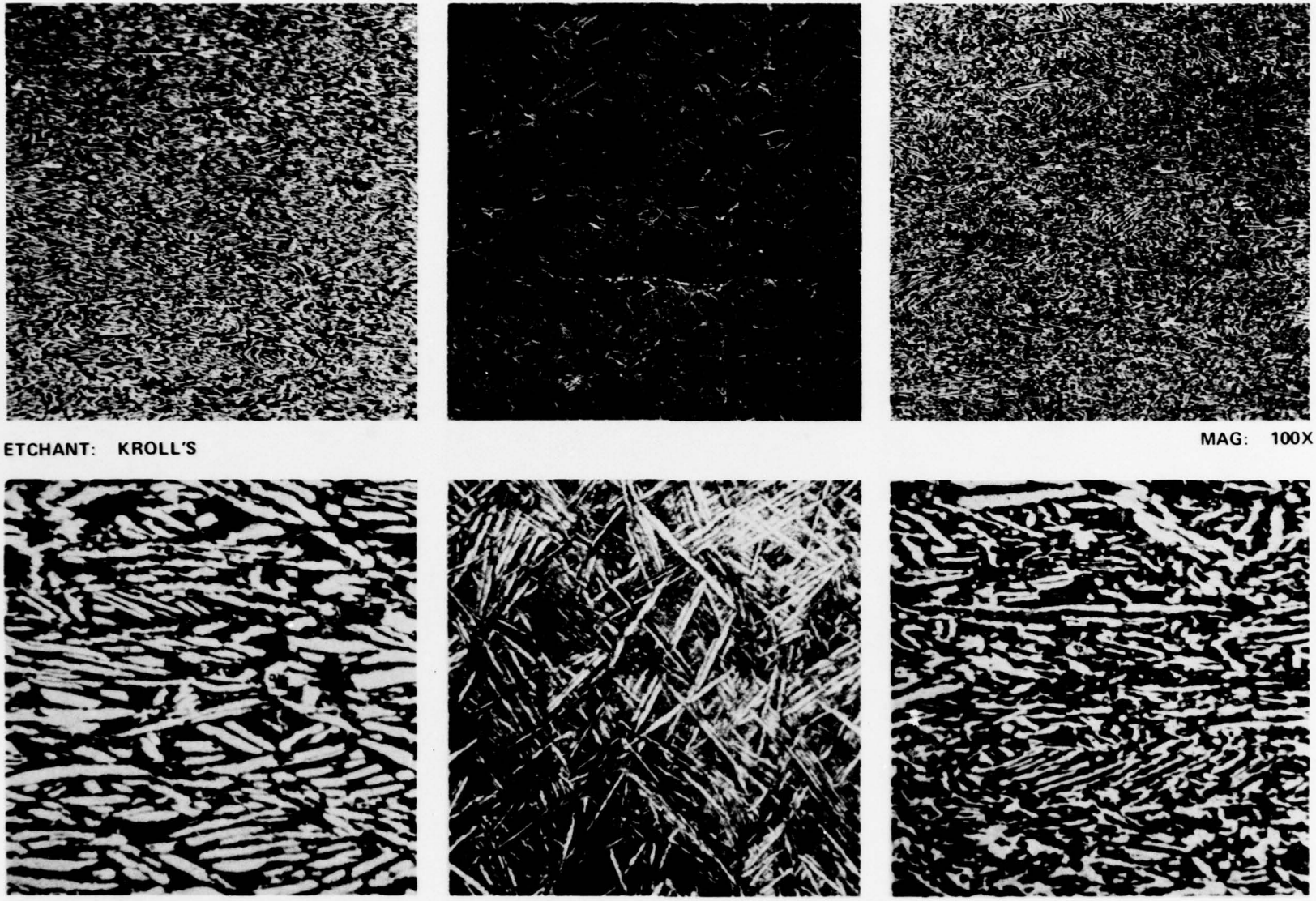

Figure 33. Microstructures of Ti-6Al-2Sn-4Zr-6Mo HIP Powder Billets Forged at 1650°F FD 69994

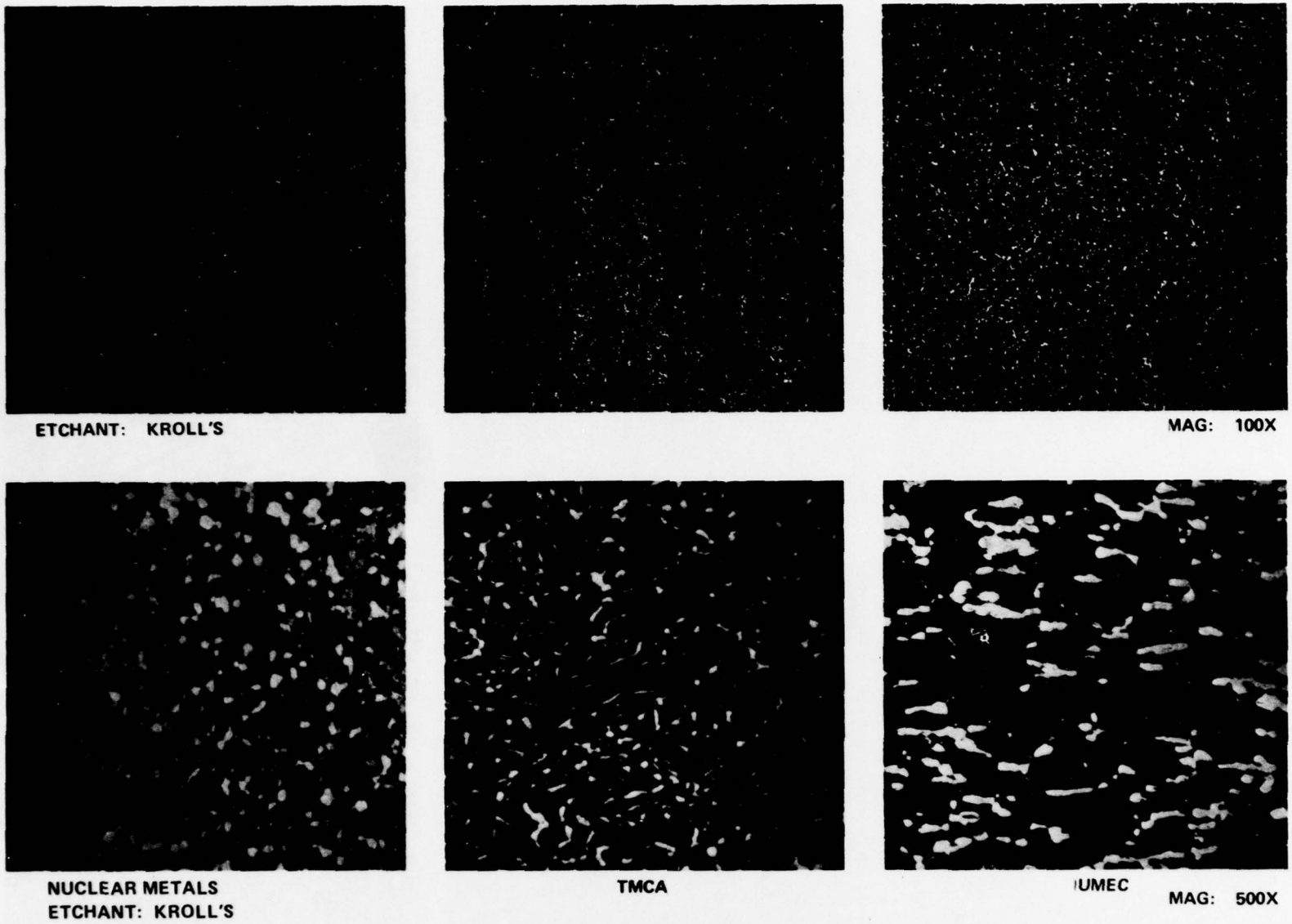

Figure 34. Microstructures of Heat-Treated (1670°F/1/AC + 1100°F/8/AC), Forged Extruded Powder Billets FD 70267

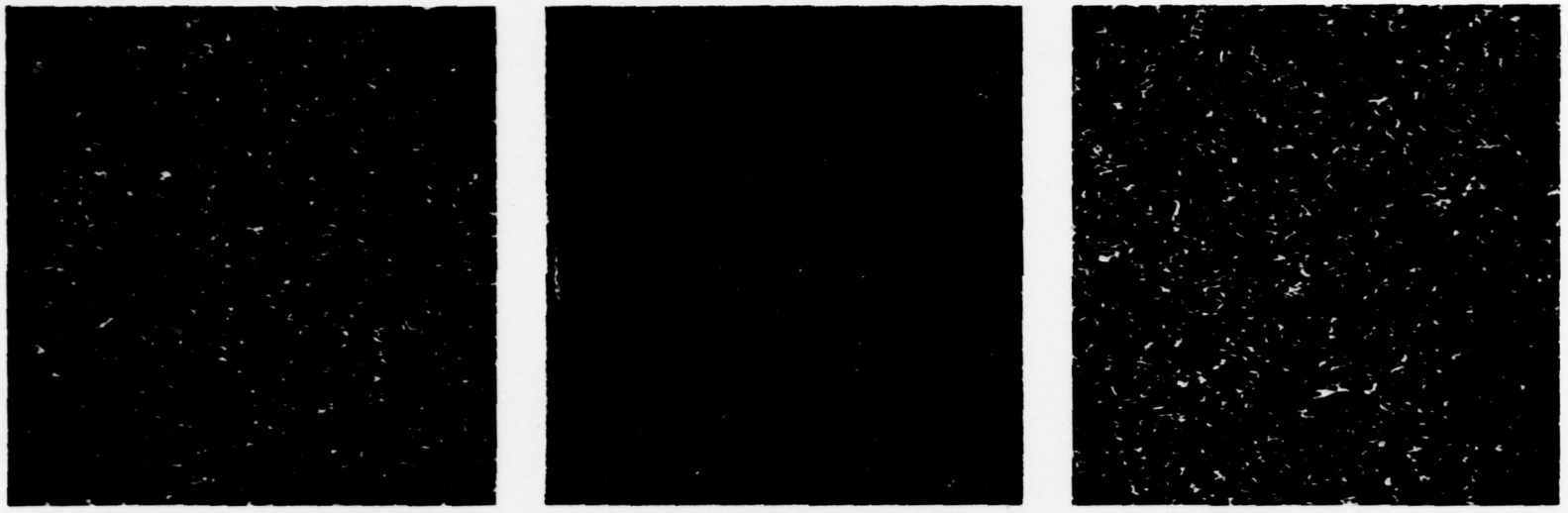

ETCHANT: KROLL'S

MAG: 100X

NUCLEAR METALS

TMCA

NUMEC

ETCHANT: KROLL'S

MAG: 500X

Figure 35. Microstructures of Heat-Treated (1670°F/1/AC + 1100°F/8/AC), Forged HIP Powder Billets FD 69995

b. Mechanical Properties

All forged pancakes were given a 1670/1/AC+1100/8/AC heat treatment prior to room temperature tensile and notch stress-rupture testing. Test results are given in Table XII.

As with previous testing, all tensile failures originated from inclusions within the specimens. The thin cross section of the pancake forgings apparently resulted in a rapid cooling rate, with resultant higher tensile and yield strengths. This accounted for part of the absence of ductility, but not to the extent observed. One encouraging result was obtained with the extruded and forged material from Nuclear Metals, viz., good strength and ductility.

Notch stress-rupture results were quite good for all of the forged materials and were fully acceptable to current specifications.

6. Defect Characterization

As noted previously in this report, inclusions were present in the powder material from all three material sources. Although the extent and nature of these inclusions varied among the sources, their presence in the material resulted in equally catastrophic effects on tensile ductility. To identify these inclusions so that their source could be identified and eliminated, extensive electron backscatter and microprobe work was performed.

a. *REP Powder*

Several inclusions in the Nuclear Metals powder were found to contain nickel and chromium. One inclusion was identified as being similar in composition to the base alloy. The nickel and chromium inclusions (which were most predominant) were apparently nickel-base alloy powder particles, which were not completely eliminated from the chamber prior to processing the titanium powder (Figures 36, 37, and 38).

b. Hydride/Dehydride Powder

(1) TMCA

A significant number of alpha-stabilized regions were observed in the TMCA billet. Microprobe analysis verified these areas to be high in Ti, Al, and Sn and low in Mo and Zr, indicating the presence of another alloy. Other inclusions were shown to consist of Fe, Co, and Cr. The iron and chromium inclusions were probably due to erosion of the crushing equipment (Figure 39).

(2) NUMEC

Electron backscatter and microprobe analysis of several NUMEC inclusions showed high titanium and tin and low zirconium, molybdenum and aluminum. This, again, indicated the presence of another alloy. A silicon inclusion was also found in the NUMEC material (Figure 39). The silicon inclusion may have been introduced during the canning procedure.

MAG: 50X

A. NICKEL INCLUSION (ARROW)

MAG: 280X

B. ELECTRON BACKSCATTER MICROGRAPH INDICATING PRESENCE OF ELEMENTS WITH LARGER ATOMIC NUMBERS THAN THE MATRIX

MAG: 280X

C. TITANIUM MICROGRAPH

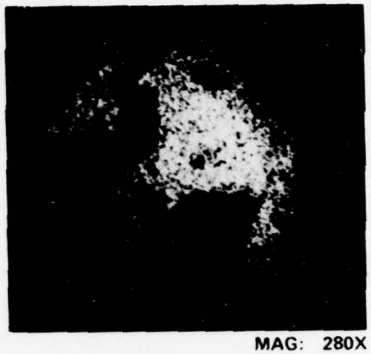

MAG: 280X

D. NICKEL MICROGRAPH

Figure 36. Nickel Inclusion in Failed Tensile Specimen of HIP Nuclear Metals Ti-6Al-2Sn-4Zr-6Mo FD 73071

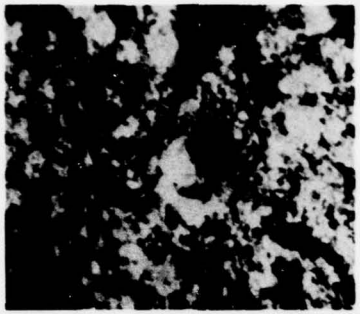

MAG: 50X

A. NICKEL INCLUSION (ARROW)

MAG: 260X

B. ELECTRON BACKSCATTER MICROGRAPH INDICATING PRESENCE OF ELEMENTS WITH LARGER ATOMIC NUMBERS THAN THE MATRIX

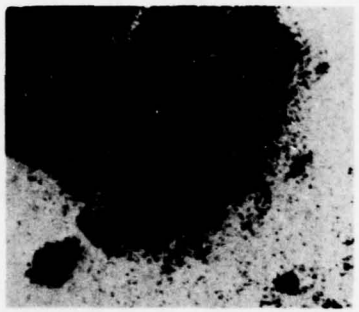

MAG: 260X

C. TITANIUM MICROGRAPH

MAG: 260X

D. NICKEL MICROGRAPH

Figure 37. Nickel Inclusion in Failed Tensile Specimen of HIP Nuclear Metals Ti-6Al-2Sn-4Zr-6Mo FD 73072

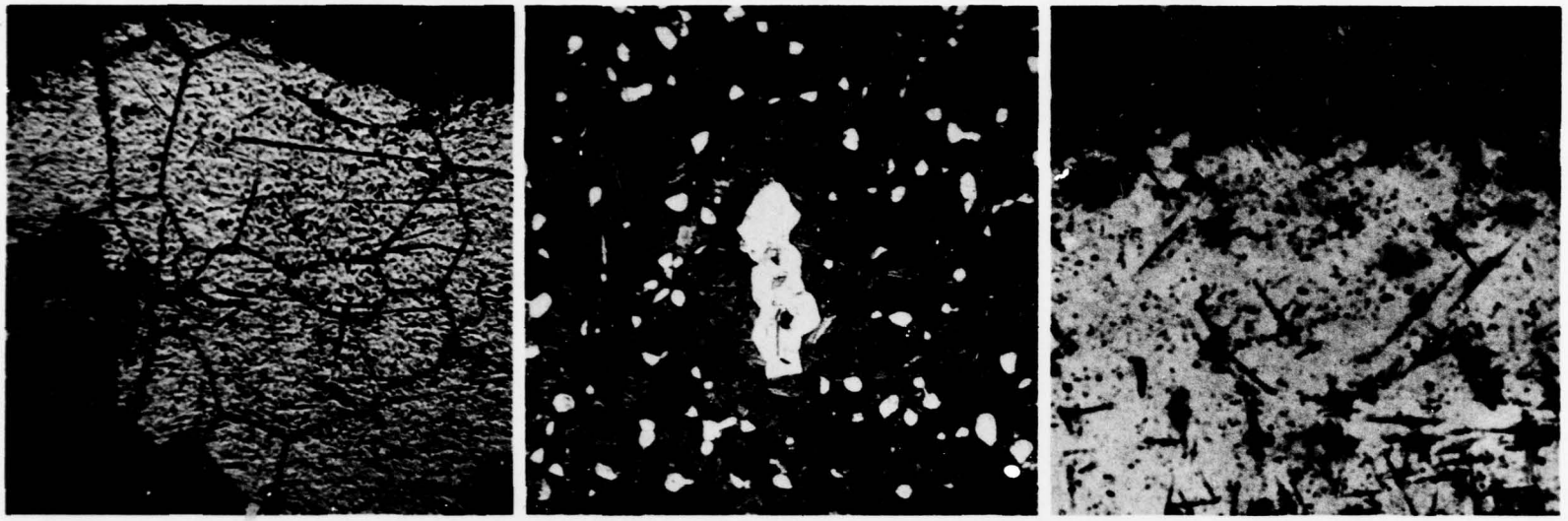

ETCHANT: KROLL'S

MAG: 500X

Figure 38. Inclusions Found in HIP Nuclear Metals REP Ti-6Al-2Sn-4Zr-6Mo Powder Billet FD 71076

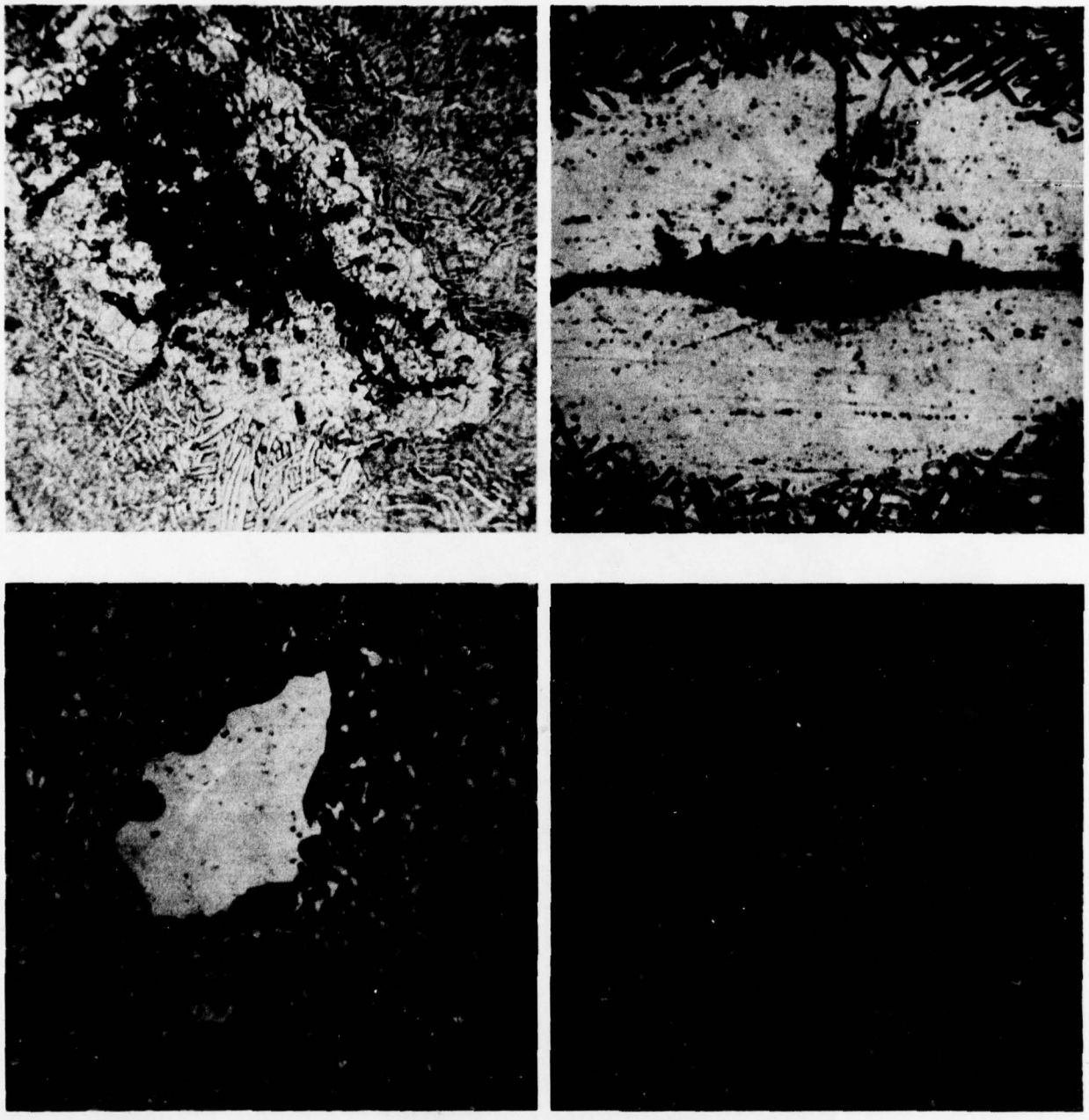

Figure 39. Inclusions Found in Hydride/Dehydride Ti-6Al-2Sn-4Zr-6Mo Powder Billet FD 71079

7. Task I - Conclusions

a. General

1. The presence of inclusions in high strength powder titanium alloys results in (1) severe degradation in mechanical property levels or, (2) minimal ductility in the consolidated product. Brittle fracture and, in some cases, premature failure prior to yielding are found to occur due to the presence of relatively small inclusions. Therefore, these inclusions, regardless of their nature, must be eliminated if the titanium alloy powder product is to be successfully used.

2. Inert handling (Nuclear and NUMEC) of titanium powder results in significantly lower interstitial "pickup". The interstitial content is also related to the particle distribution and specific surface. Nuclear Metals powder has the lowest percentage of fine particles, lowest specific surface, is handled all-inertly, and results in consolidated material with a negligible oxygen increase. This implies that more stringent handling procedures are required with hydride/dehydride powder because of its characteristically higher specific surface.

3. Both hot isostatic pressing and direct extrusion have been demonstrated to be viable means of consolidating titanium powder alloys to theoretical density.

b. Selection of Powder Source

In accordance with the program plan, one powder source was selected for producing all the powder material for the duration of the program. Based on Task I results, Nuclear Metals was chosen as the powder source. The reasons for their selection were as follows:

1. Significantly lower interstitial levels

- Lower percentage of fine particles
- Lower specific surface
- All inert handling.

2. Nature of inclusions

Primarily nickel-base powder alloys that can be eliminated by isolating a special unit for production of titanium alloys only or by using more stringent cleaning procedures that would include the running of several "wash heats" through the unit prior to collection of final product.

3. Higher Bulk Density

This will result in a higher yield (and, hence, lower cost) in the production of forging billet.

4. Mechanical Properties

While being strongly influenced by the presence of inclusions, the ductility of the Nuclear Metals powder was typically higher than either of the hydride/dehydride powders.

5. Structural Uniformity

Unlike the hydride/dehydride process in which the structure of the starting material is retained, the REP powder will always result in a fine cast structure that is independent of the input material. Hence, possible changes in consolidation variables to compensate for varying powder structure, which could be associated with the hydride/dehydride product would not be required.

c. Tentative Powder Specification

Based on the completed characterization of the hydride/dehydride and rotating electrode processed powder, a tentative Ti-6Al-2Sn-4Zr-6Mo powder specification was prepared. (See Appendix A.) The composition requirements are basically the same as those of the wrought Ti-6246 alloy and are required to ensure desirable properties in the finished product. Particle size distribution is also important because it is instrumental in controlling the resulting interstitial level of the consolidated powder. No acceptance limits have been established for the remainder of the proposed specification due to the present lack of sufficient experience.

B. TASK II - CONSOLIDATION METHOD SELECTION

1. Powder Procurement

a. Raw Material Procurement

Nuclear Metals, West Concord, Massachusetts, procured 1300 lb of 8-in. diameter billet stock from TMCA (heat number N-1507). Ingot chemistry (Table XIII) was found to be within acceptable limits. Sufficient billet material was ordered to produce the required quantity of powder for the remainder of the program. The 8-in. diameter billet was converted to approximately 2.75-in. round corner square (RCS) by Armstrong Metals, Readville, Massachusetts. Conversion of the ingot was performed above the beta transus to facilitate workability. The 2.75 RCS was turned to 2.50 in. diameter and cut into 10-in. long electrodes by Nuclear Metals. Typical electrode microstructure (Figure 40) consisted of acicular alpha, typical of beta-processed material.

Table XIII. Chemistries

	Al	Sn	Zr	Mo	Fe	H	N	O	C	Ar
Task I										
Ingot (Tel-Ti)	6.20	2.08	4.12	6.01	<0.1	0.0084	0.0110	0.100	0.020	
REP Powder	5.90	2.20	4.30	5.80		0.0046	0.0040	0.085	0.018	0.7
Tasks II and III										
Ingot (TMCA)	6.20	2.00	4.30	6.00	0.07	0.0090	0.0050	0.080	0.026	
Lot 1	6.10	1.70*	3.55	6.25	0.07	0.0067	0.0275	0.077	<0.010	0.3
Lot 2	6.05	1.70*	3.55	5.95	0.07	0.0078	0.0060	0.084	0.010	0.1
Lot 3	6.00	1.70*	3.55	6.10	0.07	0.0098	0.0040	0.086	<0.010	0.3
Blended Lots (2 and 3)	6.00	1.70*	3.55	5.95	0.07	0.0066	0.0032	0.080	<0.010	1.0
P&WA™ Specification Range	5.50 to 6.50	1.75 to 2.25	3.50 to 4.50	5.50 to 6.50	0.15 Maximum	0.015 Maximum	0.04 Maximum	0.15 Maximum	0.04 Maximum	

*Rechecked and found to be 2.28 weight-percent for each lot

100X

500X

Figure 40. Microstructure of Ti-6Al-2Sn-4Zr-6Mo Phase I, Tasks II and III REP Electrode FD 75591

b. Production of Powder

Several precautions were taken by Nuclear Metals to ensure high-quality powder. These included, but were not limited to, the following:

1. Several wash heats of Ti-6Al-4V were run through the equipment prior to running the Ti-6Al-2Sn-4Zr 6 Mo alloy.

2. An extensive cleaning was performed on the powder-making equipment prior to conversion of the electrodes to powder.

3. A fresh tungsten "stinger" was used for each electrode to eliminate possible tungsten contamination due to erosion.

4. The powder-making chamber was brushed down after each 100-lb lot.

5. All powder handling was conducted in a special titanium powder room to prevent possible cross contamination with nuclear processed nickel and steel alloys handled within the plant.

6. Screening was conducted using a new set of screens.

7. Powder was run under a plate magnet to remove possible iron-bearing inclusions.

Three 100-lb lots of powder were produced by Nuclear Metals. Lot 1 was used for Task II evaluations and Lots 2 and 3 were used for Task III.

2. Powder Characterization

Prior to blending, each lot of powder was initially passed through a 16:1 sample reducer, followed by a 2:1 sample reducer. The resulting powder samples were divided; half were retained by Nuclear Metals and the other half were shipped to P&WA for characterization. After the initial lot sampling, powder lots 2 and 3 were blended together and the blend processed through the same sampling sequence described above.

a. Vacuum Hot Pressing

A schematic of the vacuum hot pressing setup is shown in Figure 41 and a typical as-compacted pressing is shown in Figure 42. The ring around the top is the result of machining the punch from the sides of the can. Four (3 lots plus blend) vacuum hot pressings (VHP) were made. All the pressings were performed at 1650°F and 14.8 ksi. The load was applied for 2 hr, except for the first pressing, which had to be aborted after 10 minutes due to equipment hydraulic problems.

Macro- and microstructural analyses (Figures 43 and 44 showed that a fully compacted material resulted from the vacuum hot-pressing parameters (including the 10-min cycle). Blue-etch anodizing of each VHP did not reveal any inclusions.

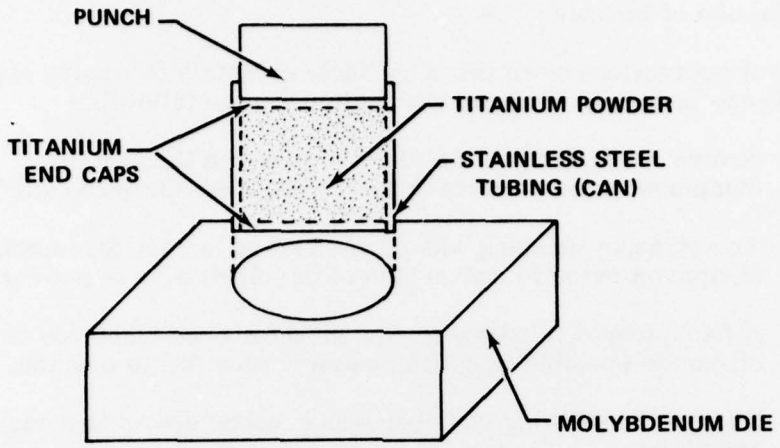

Figure 41. Schematic of Vacuum Hot-Pressing Setup Used for Tasks II and III Studies FD 75592

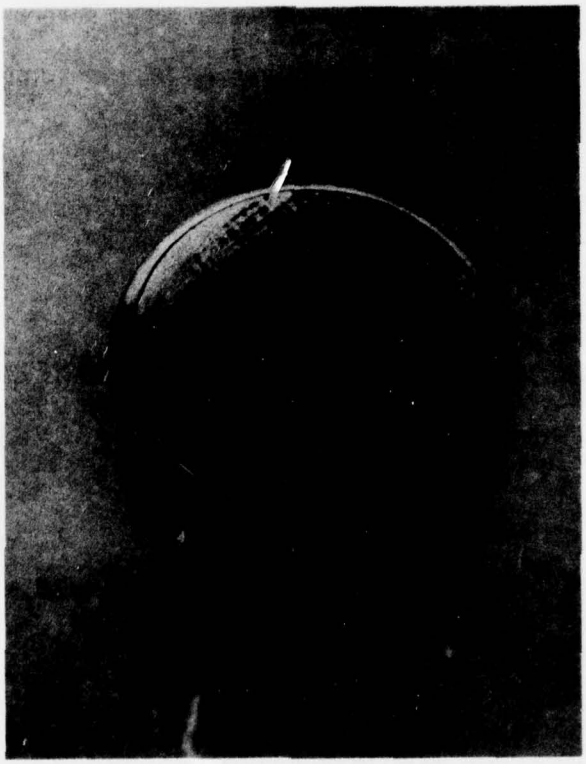

Figure 42. Typical As-Compacted Vacuum Hot Pressing of Ti-6Al-2Sn-4Zr-6Mo FD 75593

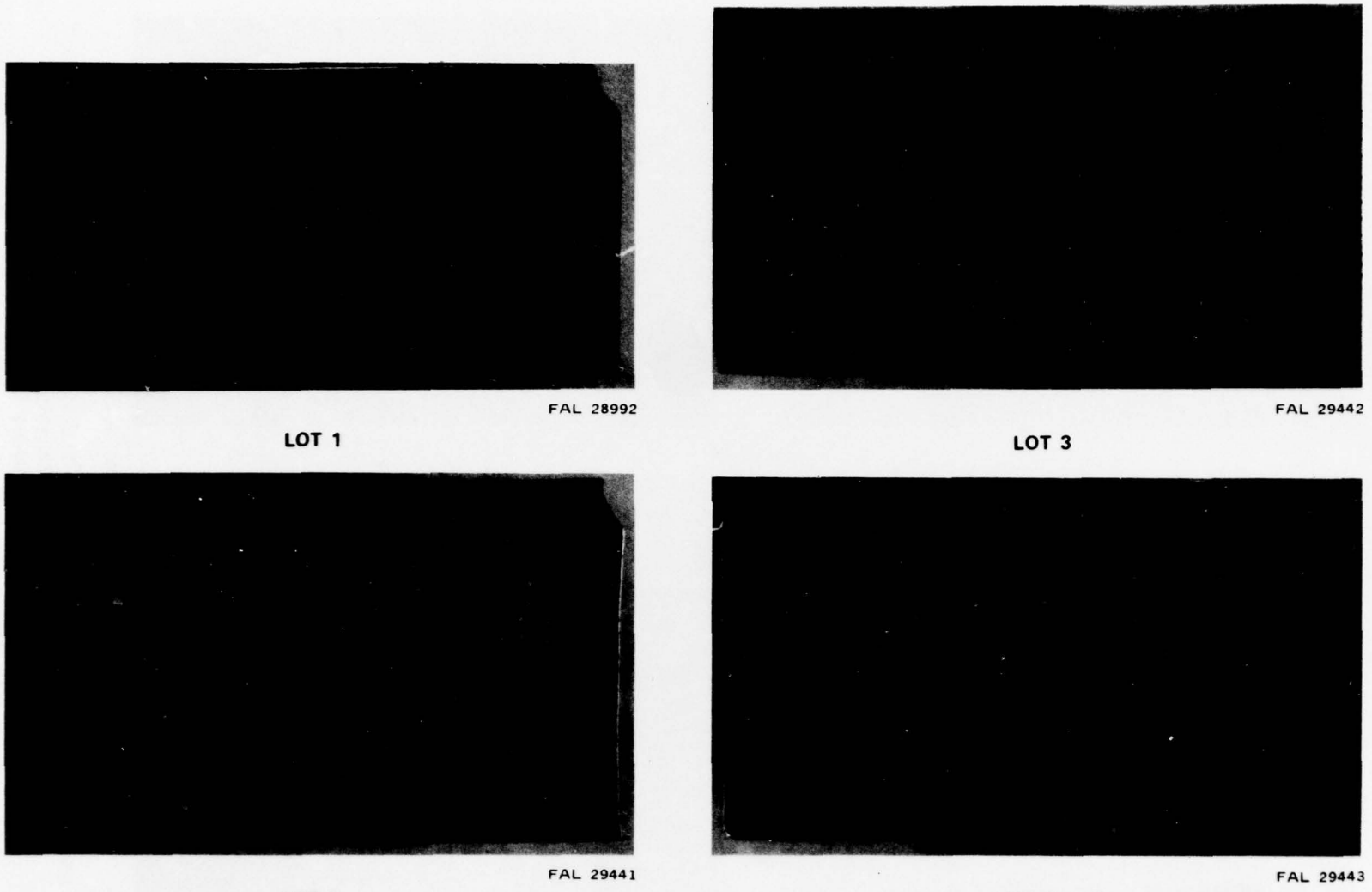

Figure 43. Macrostructures of Ti-6Al-2Sn-4Zr-6Mo REP Powder Pressings (1650°F and 14.8 ksi) of Powder Lots from Task II FD 75594

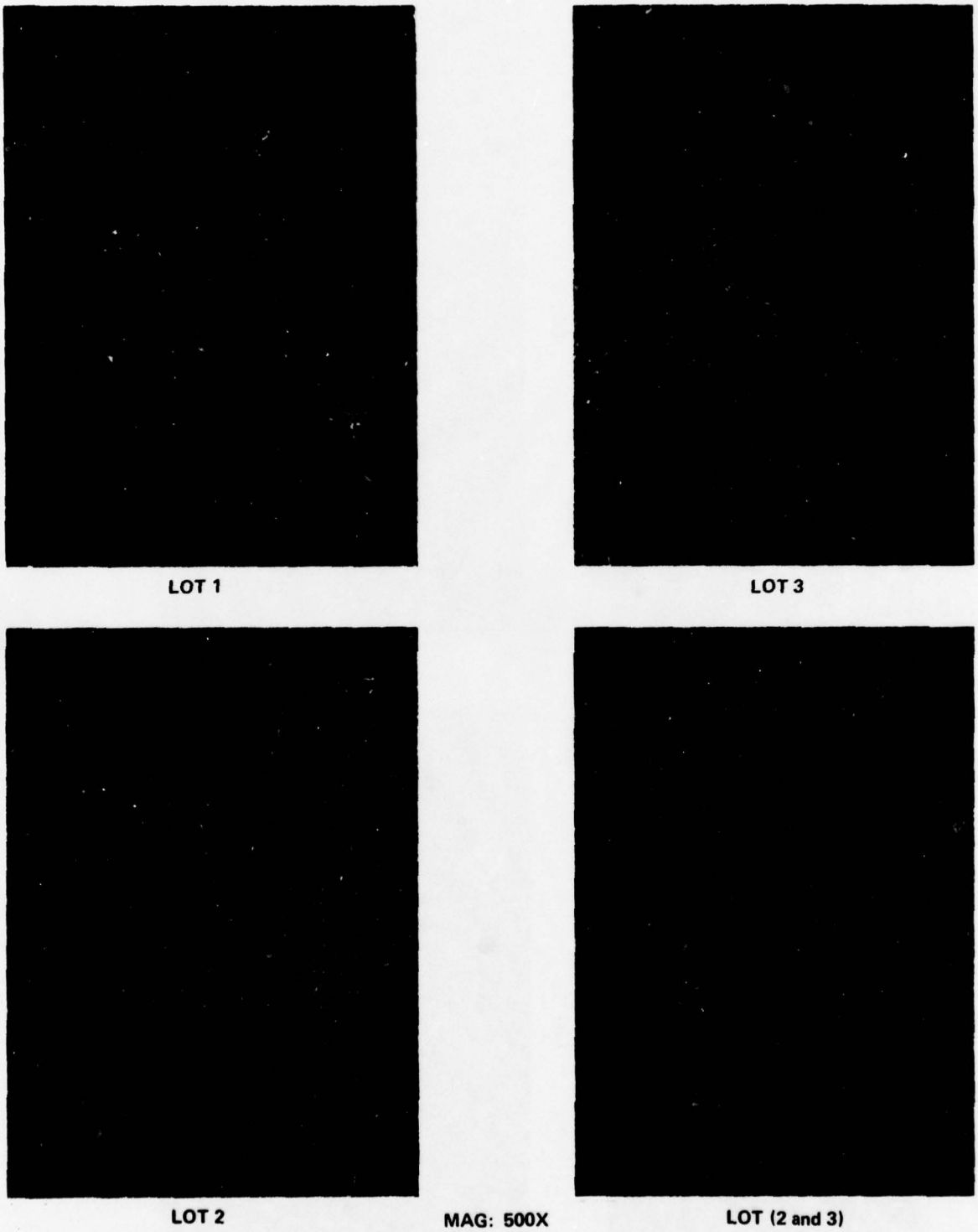

Figure 44. Microstructures of Ti-6Al-2Sn-4Zr-6Mo REP Powder Vacuum Hot Pressings (1650°F and 14.8 ksi) of Powder Lots from Task II FD 75595

b. Particle-Size Distribution

The particle-size distribution was conducted in accordance with ASTM B-214-64, viz., by screening a 100g sample on a vibrating platform in 8-in. diameter US Standard Series screens for 15 min. Results are shown in Table XIV and are plotted in Figures 45 through 48. Lot-to-lot particle distributions were similar and consistent with the analysis on the original Task I 50-lb lot of REP powder (Table XIV and Figure 13). The above analysis verified the repeatibility and consistency of Nuclear Metals process.

c. Bulk and Interstitial Chemistry Analysis

Results of bulk and interstitial analyses performed on the powders are tablulated in Table XIII. Interstitial analyses indicated that no interstitial pickup occurred during the conversion of billet to powder and confirms results obtained in Task I.

Tin measurements made by atomic absorption techniques fell below the P&WA specification range. Rechecking by wet chemistry techniques resulted in a value of 2.28 weight-percent, which fell within the acceptable range. The variation in Zr chemistries between the ingot and powder lots was attributed to analytical measurement variations. Comparison of the interstitial nitrogen content measured for Lot 1 powder and the remaining lots indicated a probable measurement error. No other significant variations were observed in either the bulk or interstitial analyses of the various powder lots. Argon analyses were performed by Gollob Analytical Service Corporation, New Jersey. Argon content was within the desired 1 ppm limit.

d. Density Measurements

Bulk and particle density measurements are presented in Tables XV and XVI. Bulk densities were comparable to Task I results. Particle densities, however, were somewhat lower (0.164 lb/in^3). Variations were not attributed to chemistry because the chemistries of Task I powder were nearly identical to Task II powder. Measurement errors may have contributed to the variation. The pyncnometer used to measure the densities did not have temperature control or evaporation control, which could have resulted in a lower than theoretical density measurement. Metallography confirmed the presence of "hollows" (Figure 49) which may have contributed to the lower particle density measurements.

3. Billet Consolidation

a. Can Design

The basic can design selected had proved successful in the processing of nickel-base superalloy powders. The interior of the can was modified to permit the use of special can-filling-procedures. Extrusion and HIP cans were machined from mild steel tubing, boiler plate, and billet stock. Evacuation tubes were made from stainless-steel tubing. The can designs for Task II consolidations were identical to Task I design.

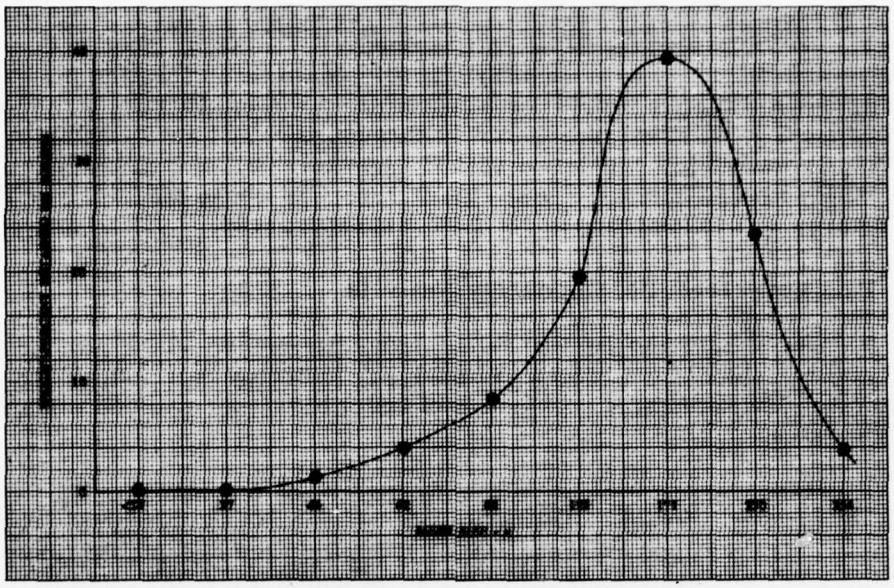

Figure 45. Task II, Lot 1 Ti-6Al-2Sn-4Zr-6Mo Powder Distribution Frequency Curve DF 97624

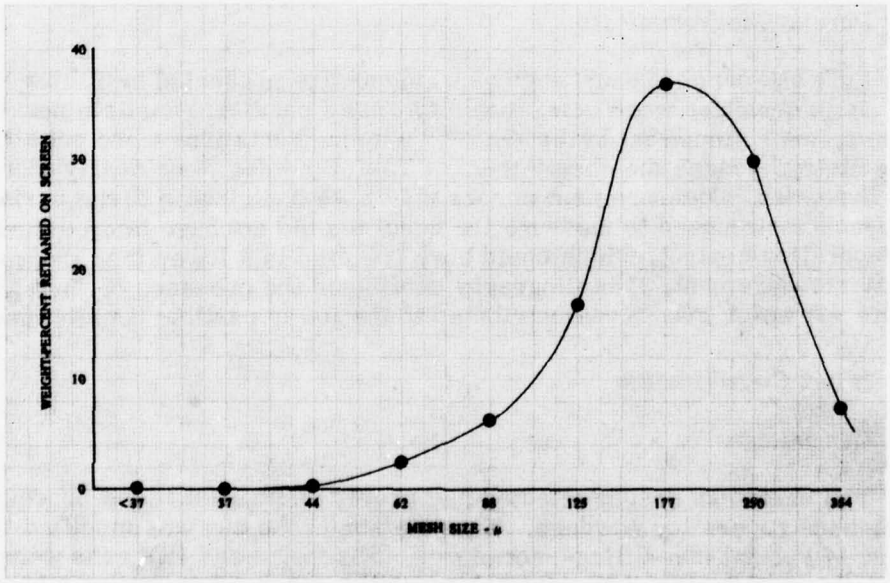

Figure 46. Task II, Lot 2 Ti-6Al-2Sn-4Zr-6Mo Powder Distribution Frequency Curve DF 97625

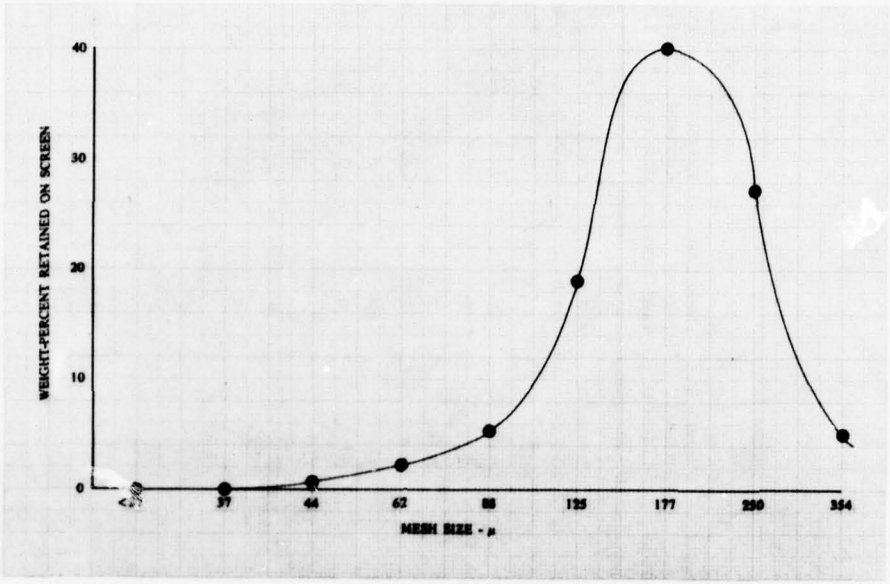

Figure 47. Task II, Lot 3 Ti-6Al-2Sn-4Zr-6Mo Powder Distribution Frequency Curve DF 97626

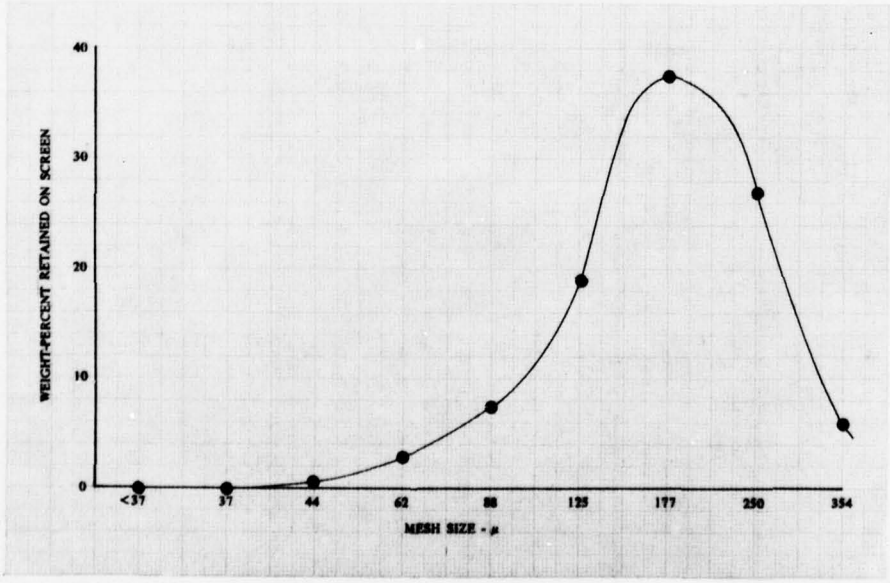

Figure 48. Task II, Lots 2 and 3 Ti-6Al-2Sn-4Zr-6Mo Powder Distribution Frequency Curve DF 97627

Table XIV. Particle-Size Distributions of -35 Mesh REP Ti-6Al-2Sn-4Zr-6Mo Powder

Screen Size		Task I		Lot 1		Lot 2		Lot 3		Lot (2 + 3)	
Mesh	μin.	Weight - % Retained on Screen	Cumulative Percent Less Than	Weight - % Retained on Screen	Cumulative Percent Less Than	Weight - % Retained on Screen	Cumulative Percent Less Than	Weight - % Retained on Screen	Cumulative Percent Less Than	Weight - % Retained on Screen	Cumulative Percent Less Than
45	354	4.58	99.99	3.8	100	7.5	100	5.1	100	5.9	100
60	250	21.37	95.41	23.4	96.2	29.9	92.5	27.4	94.9	26.8	94.1
80	177	31.22	74.04	39.3	72.8	36.9	62.6	40.7	67.5	37.6	67.3
120	125	25.43	42.82	19.6	33.5	16.8	25.7	19.0	26.8	18.9	29.7
170	88	10.74	17.39	8.3	13.9	6.1	8.9	5.2	7.8	7.5	10.8
230	62	4.50	6.65	4.0	5.6	2.5	2.8	2.10	2.6	2.8	3.3
325	44	1.87	2.50	1.4	1.6	0.2	0.3	0.5	0.5	0.5	0.5
400	37	0.19	0.28	0.1	0.2	0	0.1	0	0	0	0
PAN	<37	0.09	0.09	0.1	0.1	0.1	0.1	0	0	0	0

Table XV. Bulk Density of Ti-6Al-2Sn-4Zr-6Mo Powders

Lot No.	Mesh Size	Method	Bulk Density g/cc	Bulk Density lb/in^3	Percent of Theoretical
1	-35	Measured at Rest	2.88	0.104	61.9
1	-35	Vibrated	3.11	0.112	66.7
2	-35	Measured at Rest	2.84	0.103	61.3
2	-35	Vibrated	3.10	0.112	66.7
3	-35	Measured at Rest	2.76	0.100	59.5
3	-35	Vibrated	3.01	0.109	64.9
2 and 3	-35	Measured at Rest	2.82	0.102	60.7
2 and 3	-35	Vibrated	3.05	0.110	65.5
Average	-35	Measured at Rest	2.82	0.102	60.9
Average	-35	Vibrated	3.07	0.111	66.0
Task I	-35	Measured at Rest	2.85	0.103	61.3
		Vibrated	3.08	0.111	66.0

Table XVI. Particle Density Measurements

Lot No.	Density, g/cc	Density, lb/in^3
1	4.48	0.162
2	4.69	0.170
3	4.47	0.162
2 and 3	4.49	0.162
Average	4.53	0.164
Task I	4.62	0.168

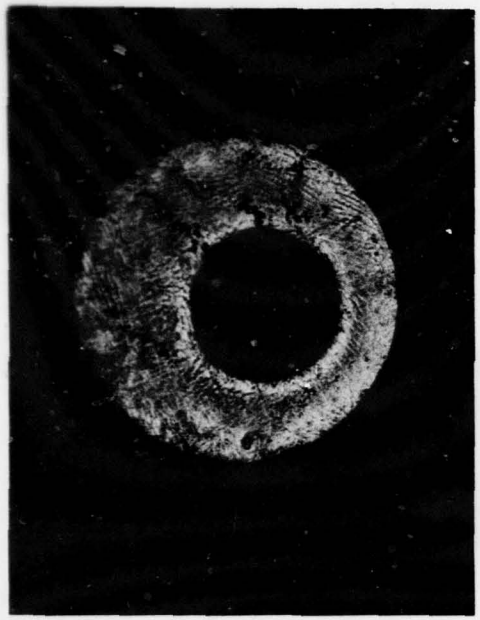
MAX: 250X

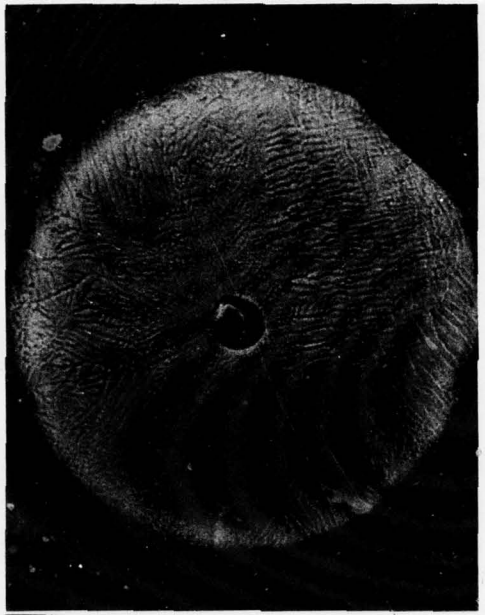
MAX: 250X

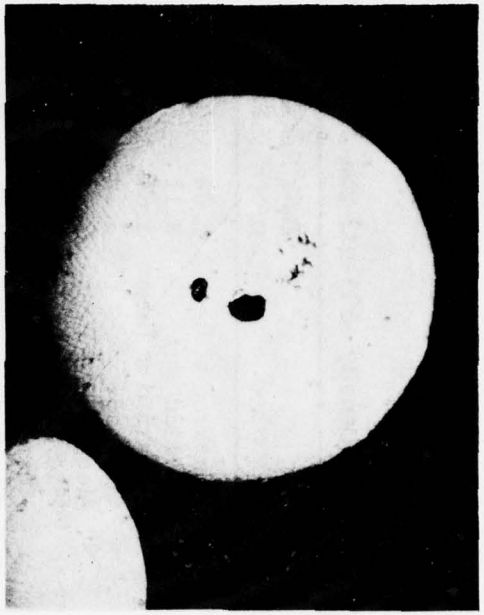
MAX: 250X

Figure 49. Typical "Hollows" Present in Ti-6Al-2Sn-4Zr-6Mo REP Powder

FD 77712

b. Can Preparation

After fabrication, the cans were cleaned and leak-checked. Due to the presence of silicon inclusions noted in Task I material, the standard can cleaning procedure was revised. A chemical cleaning procedure was used in lieu of grit and vapor blasting which could result in silicon particles becoming embedded in the walls of the can and be shaken loose in-transient and mixed with the powder in the can. The principal steps of the revised cleaning process were:

1. Immerse in muriatic acid
2. Electrolytic-alkaline clean
3. Hot-water power spray
4. Immerse in oil
5. Degrease in trichlorethylene.

After leak checking, powder was poured into the cans, and Nicrobraze 10 was placed around the perimeter of the braze cover and on top of the weld ring. Subsequently, the can was placed inside a vacuum-induction melting furnace, and the powder was vacuum-out-gassed about 8 hr at less than 1 μ prior to heating. The can and powder were heated until the braze began to flow (approximately 1650°F); then the cover was lowered into place and brazed onto the weld ring. Following the brazing operation, the sealed can was removed from the vacuum furnace and the head plug welded in place. After leak checking, the space above the brazed cover was evacuated and sealed.

In addition to the three compaction containers filled and sealed at P&WA, Crucible received powder from P&WA to make an additional compaction using their own canning procedures. Crucible loaded the powder into a welded mild steel container through an evacuation stem. The container was then evacuated at room temperature and vacuum outgassed at 500°F. The evacuation stem was then sealed by hot-crimping, shearing, and welding.

c. Extrusions

Task I studies showed that the beta transus was exceeded during extrusion at 1650°F. A lower extrusion temperature should result in a more favorable microstructural response due to a finer grain size than was observed in Phase I, Task I; therefore, lower extrusion temperatures were chosen for Task II.

Three mild steel cans filled with Ti-6Al-2Sn-4Zr-6Mo powder were extruded at RMI, Ashtabula, Ohio. The cans were placed in 1-in. thick graphite containers (to prevent excessive scaling) prior to heatup for extrusion. Furnace time and temperature parameters for the extrusions were as follows:

1. 1500°F (8 hr)
2. 1500°F (7 hr) 1550 (1-1/2 hr)
3. 1500°F (6 hr) 1550 (1-1/2 hr) + 1600°F (1 hr)

The material was extruded from a 6-1/8-in. diameter liner through a 2.4-in. diameter orifice die, with a 60-deg included angle (a reduction ratio of 6.3:1). Average upset pressures of 1248 tons (extrusion constant = 23.1) and average run pressures at 1093 tons (20.2) were required. This compares with a Task I upset pressure of 1054 tons (19.1 tons/in.^{2}) and an average run pressure of 925 tons (16.8 tons/in.^{2}) at 1650°F.

d. *Hot Isostatic Pressing*

Task I studies showed that full consolidation was obtainable at 1650°F. However, the alpha platelets were very large and resulted in elongated alpha in a transformed beta matrix after forging rather than a predominantly equiaxed alpha in a transformed beta matrix. It was felt that lower compaction temperatures would result in a greater amount of stored energy, resulting in more equiaxed alpha after forging. Three sealed cans were sent by Crucible to Industrial Materials Testing Laboratories (IMT) for compaction in their small, internally heated ASEA autoclave at 1500°F (15.3 ksi), 1550°F (14.6 ksi), and 1600°F (14.9 ksi). The minimum time at temperature was 2 hr after the can surface reached the indicated temperature. A concurrent minimum hold at pressure for 3 hr was used. The 1750°F HIP performed by Crucible was held at temperature for 6 hr. The charge was then transferred into the autoclave, pressurized to 14,200 psi, and held for 30 min.

4. Billet and Forging Evaluations

a. Extrusions

(1) Structural Evaluation

Macroetch slices taken near the nose and tail of the extrusions failed to reveal any inclusions (Figure 50). The concentric rings observed in the as-extruded billet were investigated. The most prevalent ring (1500°F extrusion) consisted of elongated and globular alpha at the edge, shorter elongated alpha at the ring, and very short elongated alpha and equiaxed alpha towards the center of the extrusion. Blue etch anodizing of the etch slices failed to reveal any inclusions.

A variation in microstructure and/or grain size from edge to center of the as-extruded material was noted. (See Figure 51.) Primary alpha was present in the rim area of the lower temperature extrusions. Microstructural evidence indicates that adiabatic heating during extrusion was approximately 200°F at the center of the extrusion. The surfaces of the extrusions were probably cooled somewhat by the tooling and could account, in part, for the variation in microstructure observed.

Microstructural analysis of as-extruded and heat-treated material (1670/1/AC+1100/8/AC) revealed only minor structural changes resulting from the heat treatment. (See Figure 52.) Coarsening of the primary alpha present at the lower extrusion temperatures and coarsening of the acicular platelets occurred during the heat treatment. (Pancakes measuring approximately 1/2 in. thick and 5 in. in diameter (88% reduction) were forged from extrusion multiples at 1650°F). The forged and heat-treated material consisted of primary alpha in a transformed beta matrix.

(2) Mechanical Properties

Tensile and room temperature notched-stress-rupture testing was conducted on the as-extruded and heat-treated (1670°F/2/AC+1100°F/8/AC) material. Results are presented in Table XVII. All material extruded above 1550°F exhibited nearly identical mechanical properties. The structure consisted

of fine equiaxed beta grains. Material extruded at 1500°F exhibited slightly higher strengths and better ductility, which was attributed to the greater percentage of alpha and/or finer beta grain size.

A mult from each of the extrusions was forged at 1650°F and given a 1670/1/AC+1100/8/AC heat treatment. Tensile and room temperature notched-stress-rupture testing was performed on the heat-treated material. The strengths followed the same trend observed in the as-extruded and heat-treated material. (See Table XVII.) Low ductilities in the forged material were subsequently found to be attributed to inclusions present on the plane of failure. Several of the inclusions were submitted for microprobe analysis. (See Figure 54.) Two of them were found to consist of nickel and phosphorus. One possible source of these inclusions would be the brazing compound used in the canning procedure. The braze compound is applied in a paste-like condition. It is possible that some braze powder fell into the titanium powder and sifted through during shipping. A new canning procedure was used for the remainder of the program. Another possible source would be the introduction of the inclusions during the powder making process from contamination present in the chamber due to the previous runs. The third inclusion (failure did not originate from this inclusion) consisted of the same base metals as the alloy. High tensile strengths may have also contributed to the low ductilities observed in the forged material. Hence, two additional pancakes were forged at 1650°F and tested in the as-forged condition to determine the effect of high strengths on ductility. Typical microstructures are shown in Figure 55. Tensile results are presented in Table XVII. The enhanced ductility was attributed to the greater amount of primary alpha present in the microstructure.

(3) Chemistry Results

Interstitial chemistry results are presented in Table XVIII. Comparison of Lot 1 powder to the extrusions made from the powder shows a minimal increase of O_2, a slight increase in hydrogen, and a decrease in nitrogen. The nitrogen results on Lot 1 powder, however, appeared to be abnormally high in comparison with the rest of the powder. None of the chemistry variations were deemed significant.

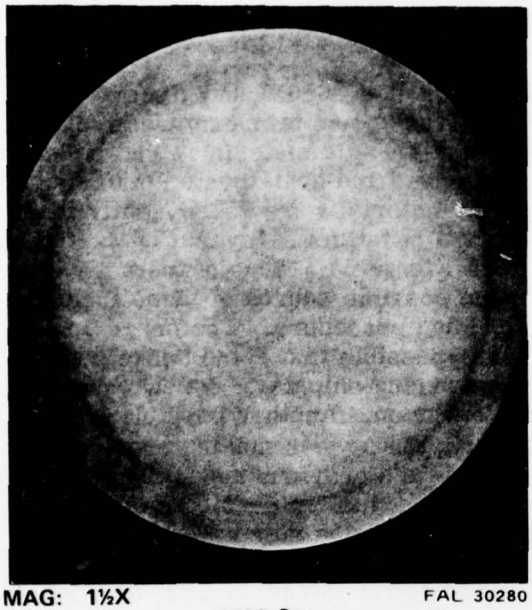

MAG: 1½X FAL 30280

1500 °F

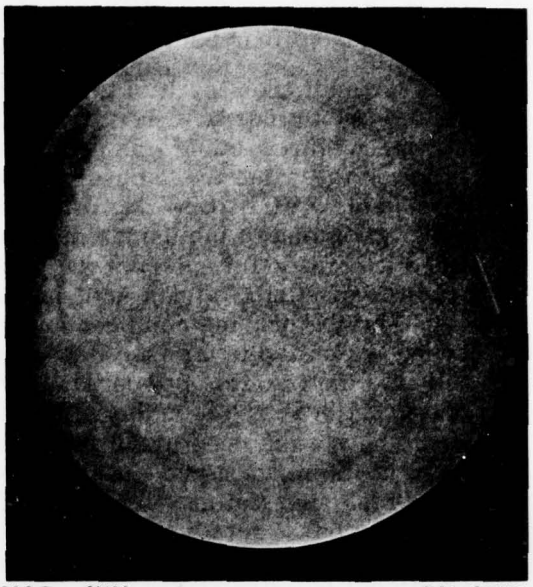

MAG: 1½X FAL 30281

1550 °F

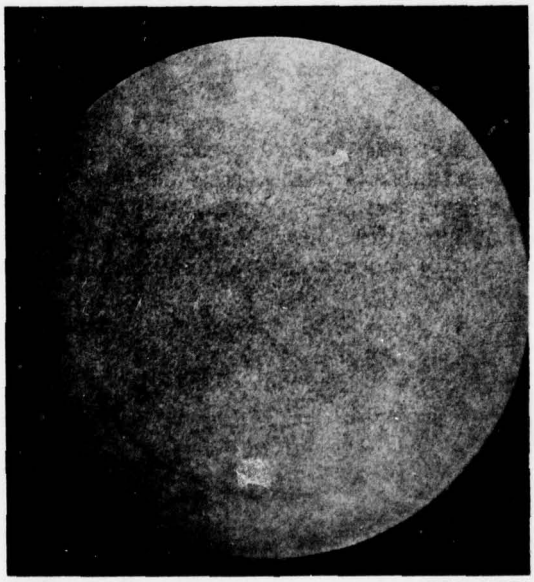

MAG: 1½X FAL 30282

1600 °F

EXTRUSION TEMPERATURE

Figure 50. Macroetched Slices from As-Extruded Ti-6Al-2Sn-4Zr-6Mo Billet FD 77713

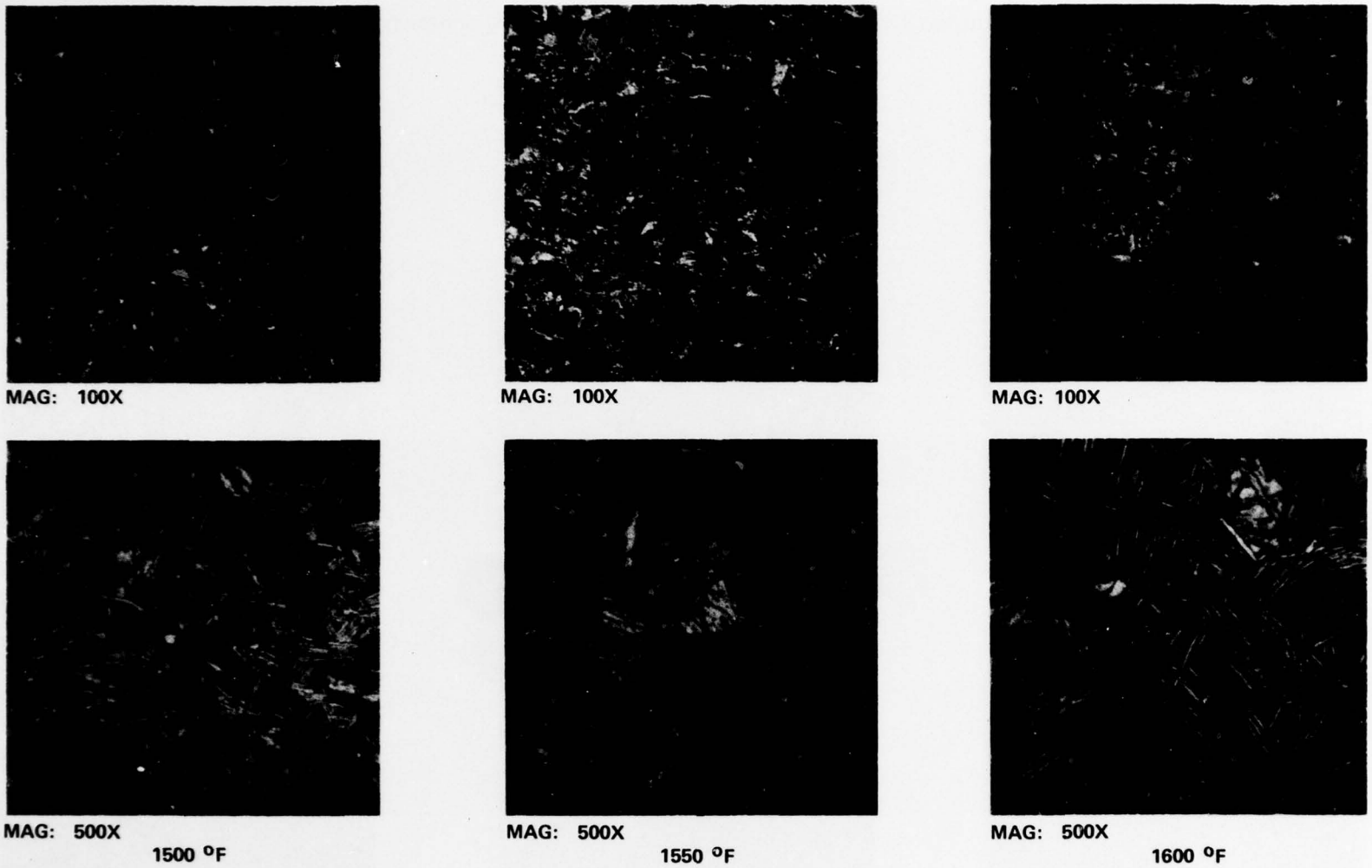

Figure 51. Microstructures of Extrusions Near Edge (Top) and at Center (Bottom)

FD 77716

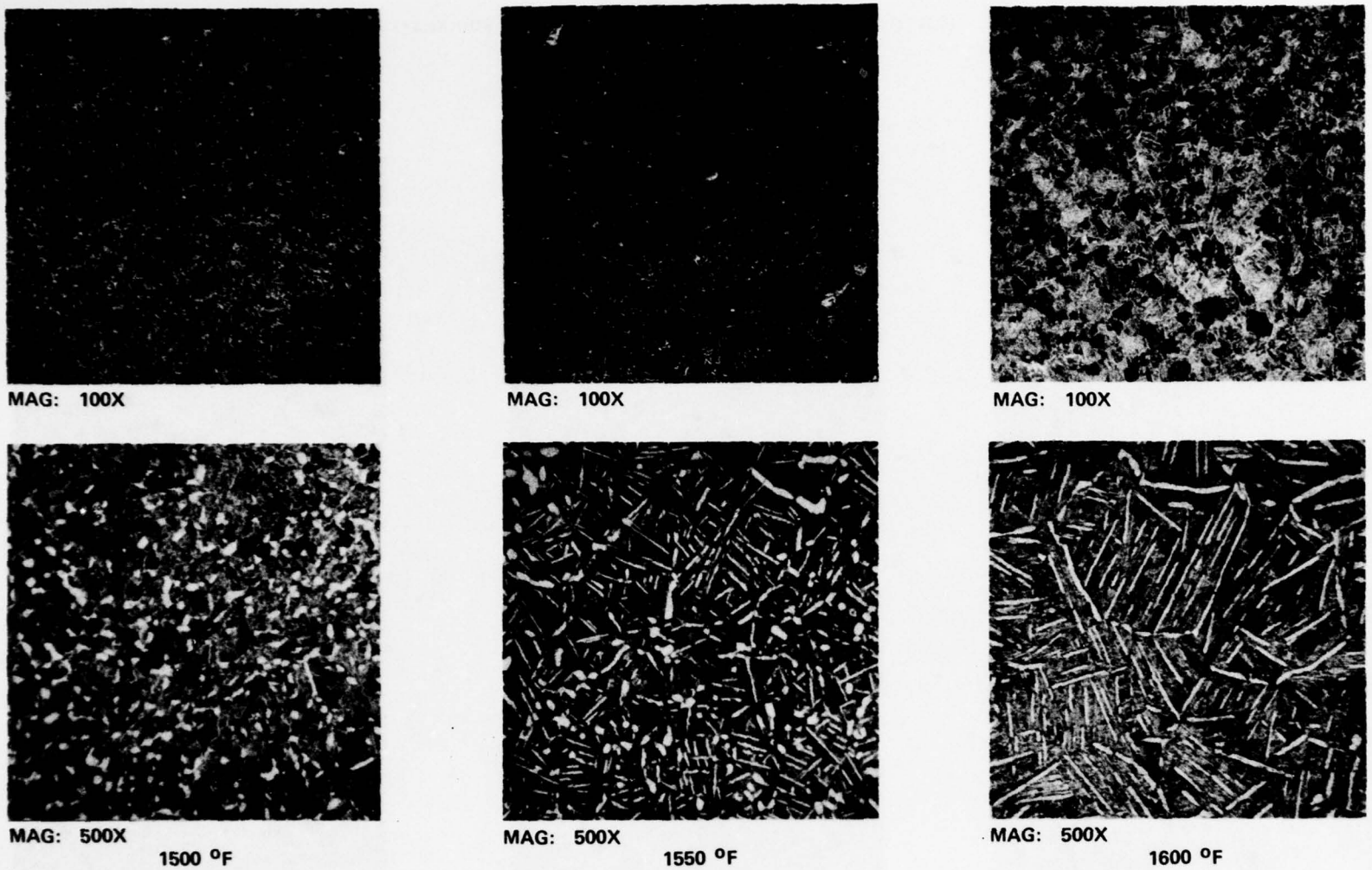

Figure 52. Microstructure of Extrusions After a 1670(1)AC + 1100(8)AC Heat Treatment Near Edge (Top) and Center (Bottom)

FD 77715

Table XVII. Mechanical Properties

Vendor	Material Condition	Compaction Temperature, °F	RT Tensile 0.2% YS	RT Tensile UTS	RT Tensile EL	RT Tensile RA	RT Notched Stress Rupture Failure Stress	RT Notched Stress Rupture Total Time	RT Notched Stress Rupture Time at Failure Load
IMT	HIP	1500	-	55.5	-	-	190	(Failed on Loading)	
			-	56.4	-	-	190	(Failed on Loading)	
IMT	HIP	1550	-	106.8	-	-	190	(Failed on Loading)	
			-	105.5	-	-	190	(Failed on Loading)	
IMT	HIP	1600	-	124.5	-	-	190	(Failed on Loading)	
			134.5	135.7	1.5	1.2	190	(Failed on Loading)	
Crucible*	HIP	1650	157.7	173.0	2.1	2.2	180	30.2	0.2
			159.4	178.0	0.87	2.9	170	21.2	1.2
Crucible	HIP	1750	158.0	177.0	10.0	16.0	210	10.1	0.1
			157.9	177.8	9.5	16.8	210	10.2	0.2
RMI	Extruded	1500	163.1	178.5	14.0	39.6	220	15.1	0.1
			167.3	181.9	15.0	44.0	210	10.1	0.1
RMI	Extruded	1550	158.0	175.1	12.5	32.1	220	15.1	0.1
			158.1	175.2	12.5	33.1	210	10.2	0.2
RMI	Extruded	1600	157.5	174.9	12.0	29.0	220	15.1	0.1
			156.1	173.6	13.0	28.4	200	6.6	1.6
RMI*	Extruded	1650	159.4	177.9	12.8	23.2	225	68.9	-
			157.7	176.3	13.0	20.1	215	68.9	-
IMT	HIP and Forge	1500	-	87.5	-	-	190	(Failed on Loading)	
			-	81.1	-	-	Failed in Machining		
IMT	HIP and Forge	1550	-	8.7	-	-	190	(Failed on Loading)	
			-	106.5	-	-	Failed in Machining		
IMT	HIP and Forge	1600	-	113.0	-	-	170	(Failed on Loading)	
			-	143.0	-	-	190	(Failed on Loading)	
Crucible*	HIP and Forge	1650	-	179.9	-	-	230	30	
			165.0(1)	169.2	1.0	3.5	230	30	
Crucible	HIP and Forge	1750	160.2	176.2	9.0	16.8	210	10.1	0.1
			160.4	176.2	9.0	16.9	210	13.4	3.4
RMI	Extruded and Forge	1500	-	166.1	-	-	190	5.0	5.0
			183.3	188.9	1.5	4.7	200	10.0	5.0
			146.7(2)	151.9	13.5	38.8			
			148.6(2)	154.2	16.5	54.0			
RMI	Extruded and Forge	1550	174.2	183.3	5.6	9.4	210	12.7	2.7
			175.0	176.1	<1.0	1.6	210	15.0	5.0
			151.1(2)	156.1	17.0	55.9			
			146.0(2)	152.8	16.5	52.6			
RMI	Extruded and Forge	1600	170.0	178.0	2.5	5.4	210	12.9	2.9
			170.3	180.6	10.0	27.3	210	15.0	5.0
RMI*	Extruded and Forge	1650	-	49.7	-	-	230	30.0	5.0
			173.0(1)	181.3	11.0	29.3	230	30.0	5.0

*Task I results
(1) 1700 (1) AC + 1100 (8) AC
(2) No heat treatment

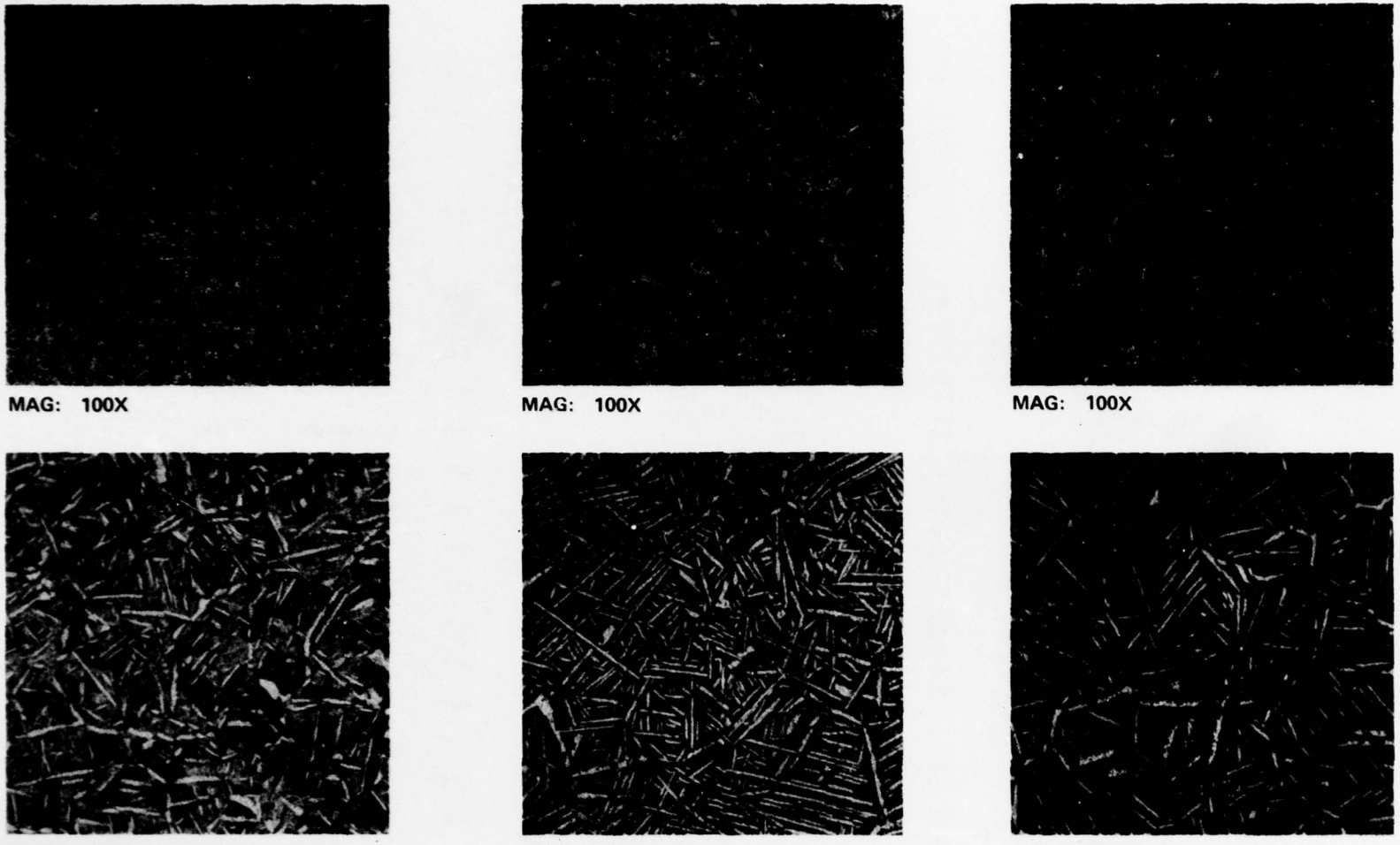

Figure 53. Microstructures of Extrusions After a 1670(1)AC + 1100(8)AC Heat Treatment (Structures Taken at Center)

FD 77717

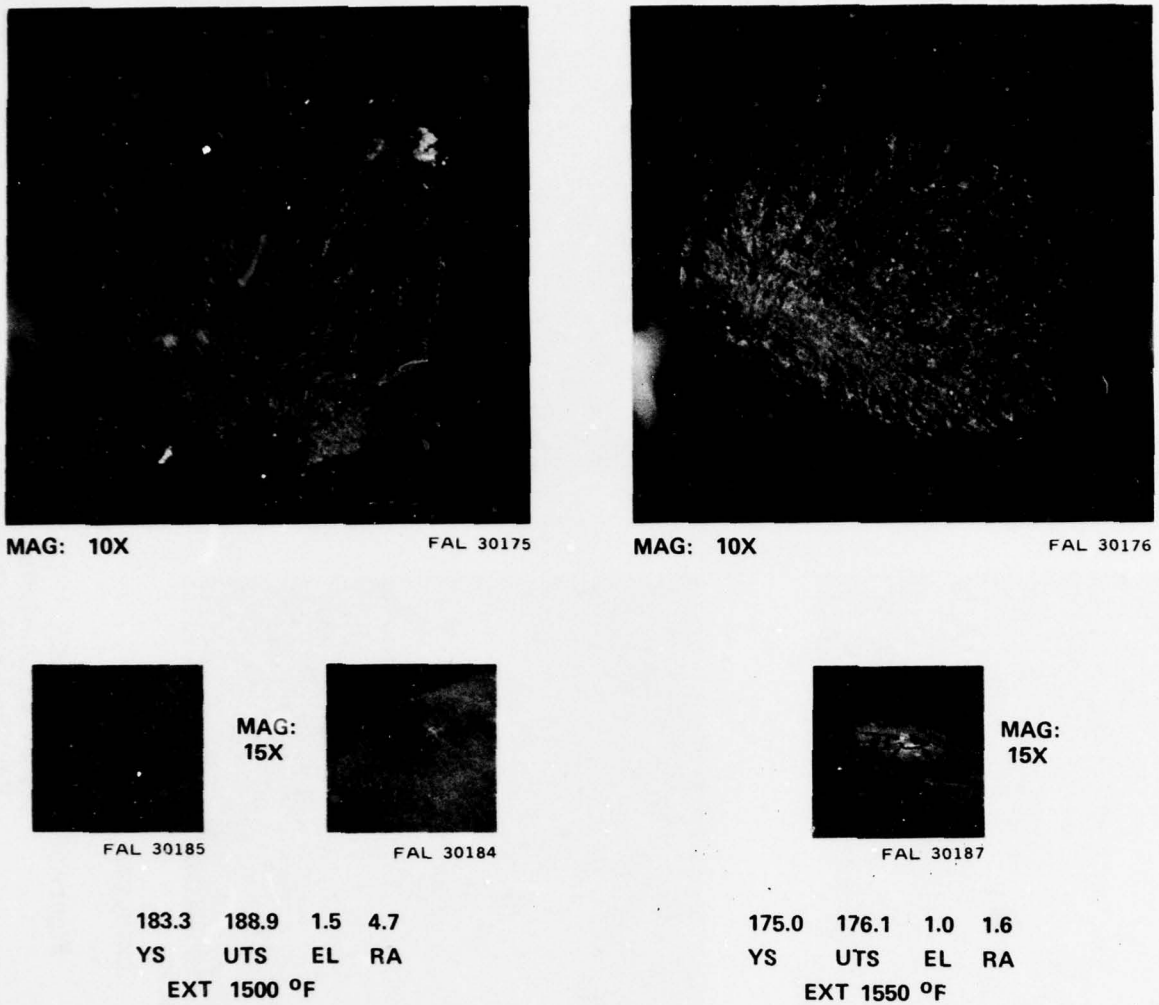

Figure 54. Fracture Surfaces of Tensile Specimens Taken From Extruded (1500 and 1550°F), Forged (1650°F) and Heat-Treated [1670(1)AC + 1000(8)AC] Material

FD 77719

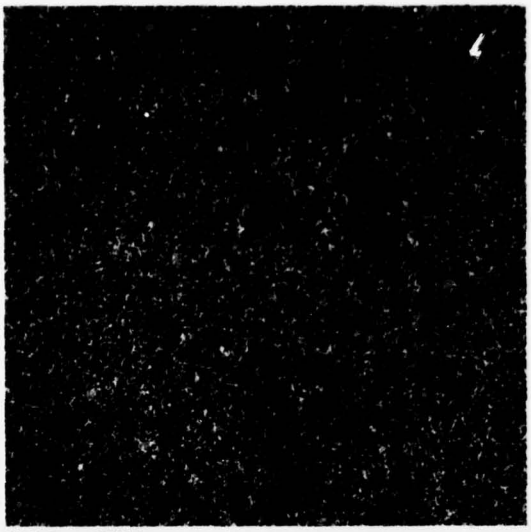

MAG: 100X

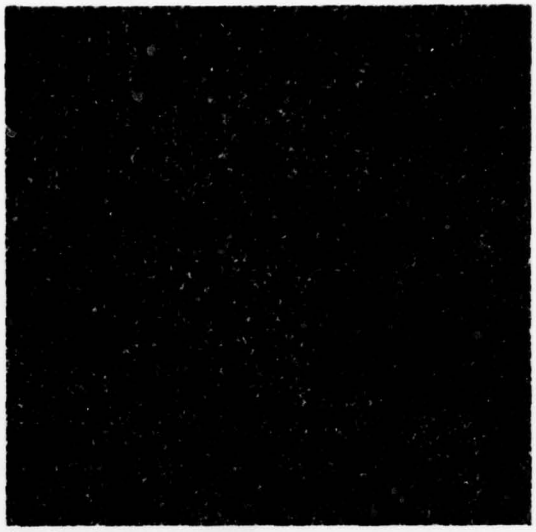

MAG: 100X

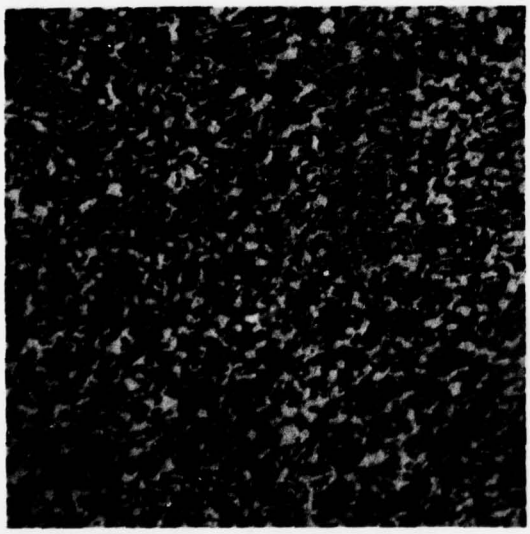

MAG: 500X

EXTRUDED AT 1500°F

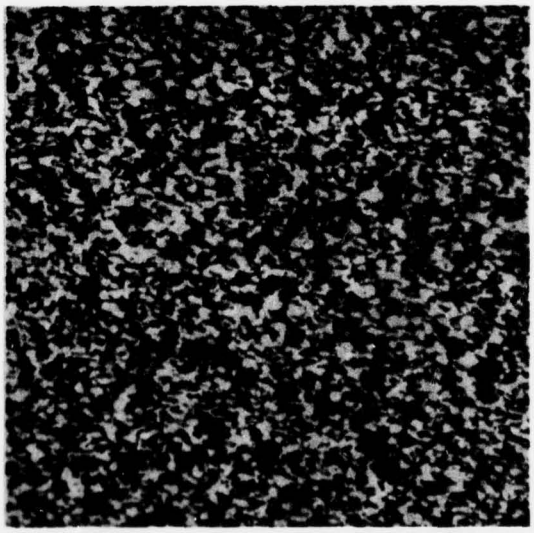

MAG: 500X

EXTRUDED AT 1550°F

Figure 55. Microstructure of As-Forged Pancakes (1650°F) Consisting of Very Fine, Equiaxed Alpha in a Transformed Beta Matrix FD 77720

Table XVIII. Interstitial Chemistry Analysis

Task I	O	H	N
Ingot (Tel-Ti)	0.100	0.0084	0.0110
REP Powder	0.085	0.0046	0.0040
1650°F HIP	0.120	0.0090	0.0010
1650°F Extrusion	0.121	0.0080	0.0080
Task II and III			
Ingot (TMCA)	0.080	0.0090	0.0050
Lot 1	0.077	0.0067	0.0275
Lot 2	0.084	0.0078	0.0060
Lot 3	0.086	0.0098	0.0040
Blended Lots (2 and 3)	0.080	0.0066	0.0032
Lot 1 (1500°F HIP)	0.117	0.0099	0.0126
Lot 1 (1550°F HIP)	0.100	0.0107	0.0364
			0.0407
Lot 1 (1600°F HIP)	0.129	0.0104	0.0058
Lot 1 (1750°F HIP)	0.090	0.0070	0.0092
		0.0072	
Lot 1 (1500°F Extrusion)	0.084	0.0089	0.0119
Lot 1 (1550°F Extrusion)	0.080	0.0078	0.0101
Lot 1 (1600°F Extrusion)	0.078	0.0072	0.0085
Blended Lots (2 and 3) (1550°F Extrusion)	0.084	0.0078	0.0170
Blended Lots (2 and 3) (1675°F HIP)	0.097	0.0076	0.0063
Blended Lots (2 and 3) (1800°F HIP)	0.095	0.0080	0.0075
P&WA Specification	0.15 Maximum	0.015 Maximum	0.04 Maximum

b. Hot-Isostatic Pressings

(1) Structural Evaluation

Macroetch slices taken near the bottom of each hot pressing revealed the presence of porosity in all but the 1750°F compaction. (See Figure 56.) Microstructures of the as-hipped material (Figure 57) showed a large amount of porosity present in the 1500 and 1550°F compaction. Some porosity was also observed in the 1600°F compaction. The 1750°F compaction appeared to be fully dense. The porosity present could result from either absorption of argon during consolidation at IMT due to a can leak or to insufficient pressure and/or temperature during consolidation. Insufficient pressure appears to be the most likely based on micro-structural results, which show fewer pores present as the compaction temperature increased. Heat treatment of the hot isostatically pressed billets resulted in a coarsening of the acicular alpha platelets. (See Figure 58.) Forging at 1650°F did not eliminate all the porosity. In addition to the continued existence of pores in the forged pancakes, primary alpha lean areas were prevalent. (See Figure 59.) These primary alpha lean areas may be related to interstitial contamination and closing of pores.

(2) Mechanical Properties

Tensile and room temperature notch-stress-rupture results are presented in Table XVII. Tensile strengths of the as-hot-isostatically pressed and heat-treated billets increased as compaction temperature increased. The only acceptable results were obtained from material HIP'ed at 1750°F. Properties appeared to be closely related to the degree of porosity present in the material.

A mult from each of the compactions was also forged at 1650°F and given a 1670/1/AC+100/8AC heat treatment. The continued presence of porosity was again, vividly shown in tensile testing. The only acceptable properties were exhibited by the 1750°F pressing. Ductility exhibited by the 1750°F pressing was typical of beta-processed material.

(3) Chemistry Results

Interstitial chemistry results are presented in Table XVIII. Comparison of Lot 1 powder to the hot-isostatic pressings made from the powder reveals an increase in O_2, a slight increase in hydrogen (except for the 1750°F compaction), and an erratic response in nitrogen levels. No explanation is available for the erratic nitrogen results. There was, however, a consistent increase in oxygen content, which was not observed in the extruded material.

5. Additional Consolidation Evaluation

In accordance with the original program plan, a consolidation practice was to be selected and a tentative powder specification prepared at the completion of Task II. However, Task II results were inconclusive due to the presence of contamination. Extrusion results reflected the presence of nickel and phosphorus inclusions and the hot isostatic pressings, except the one produced by Crucible Steel Co. reflected the absence of complete densification and the presence of contamination. An additional extrusion and two hot isostatic pressings using a different canning procedure were fabricated and evaluated because it was thought the canning procedure may have been the cause of the contamination.

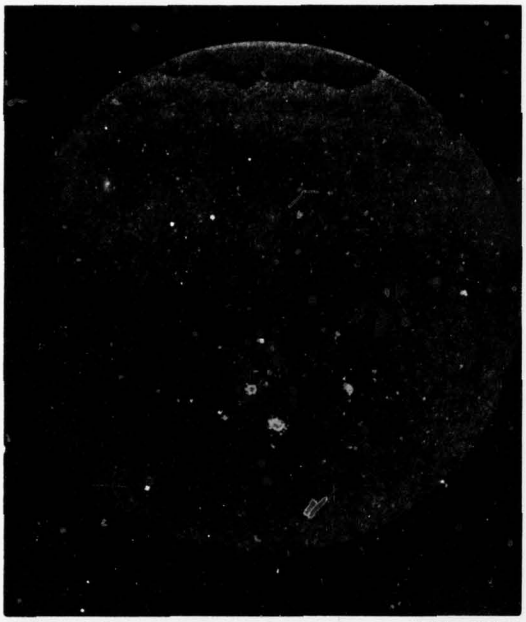

MAG: 1½X FAL 30170

1500 °F

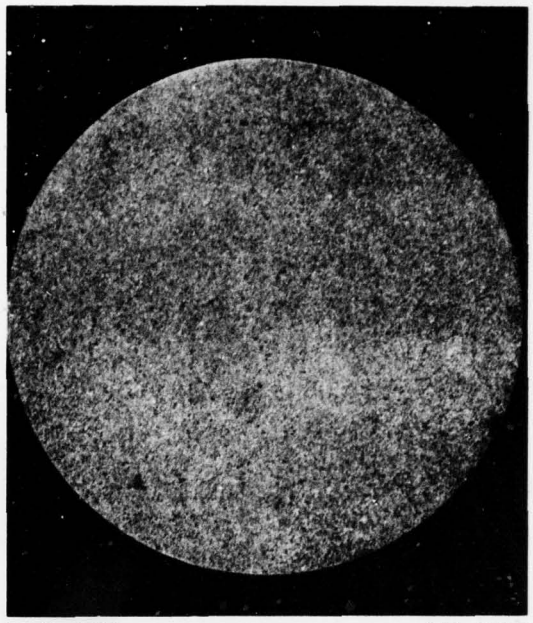

MAG: 1½X FAL 30171

1550 °F

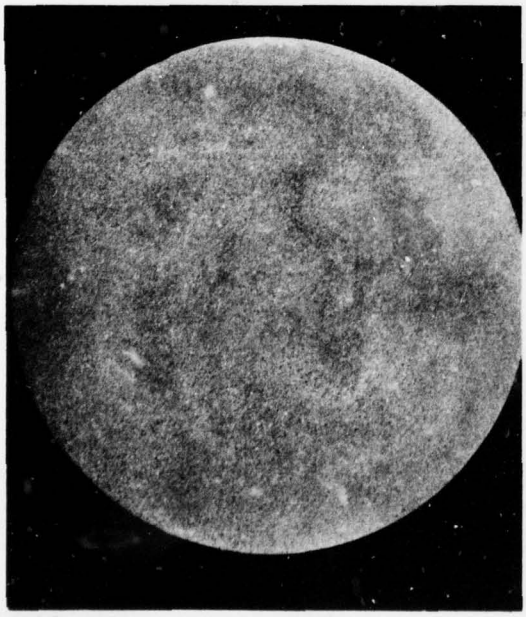

MAG: 1½X FAL 30172

1600 °F

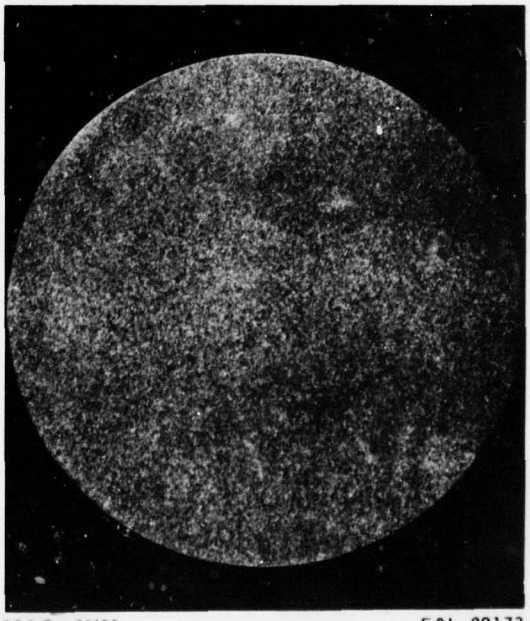

MAG: 1½X FAL 20173

1750 °F

NOTE: POROSITY PRESENT IN 1500, 1550, 1600 °F COMPACTIONS; STAIN IN 1500 °F BILLET INDICATES PRESENCE OF CANNING MATERIAL.

Figure 56. Macrostructure of As-Hipped Billets (Note: Porosity Present in 1500, 1550, and 1600°F Compactions; Stain in 1500°F Billet Indicates Presence of Canning Material) FD 77721

AD-A062 686 PRATT AND WHITNEY AIRCRAFT GROUP WEST PALM BEACH FL G--ETC F/G 11/6
MANUFACTURING METHODS FOR PRODUCTION OF TITANIUM ALLOY COMPRESS--ETC(U)
FEB 77 F33615-72-C-1390

UNCLASSIFIED FR-7778 AFML-TR-77-10 NL

2 OF 2
AD
A062886

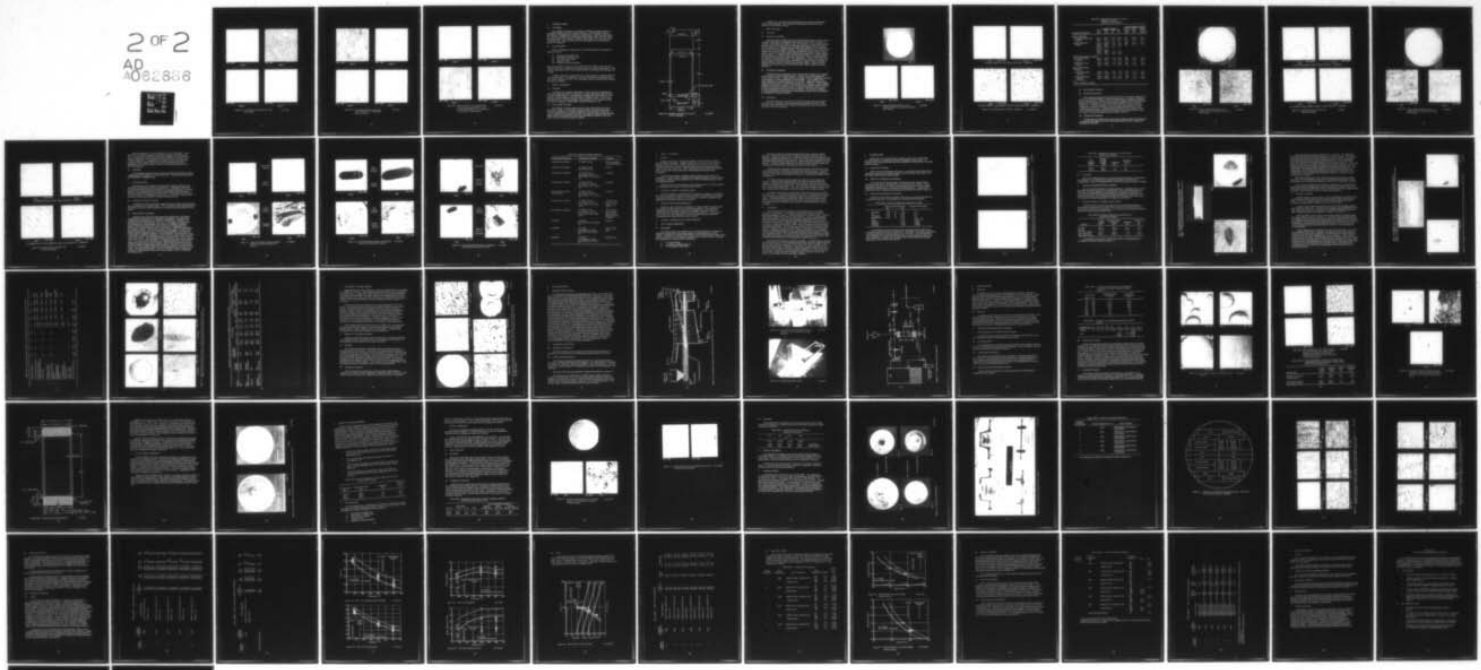

END
DATE
FILMED
3-79
DDC

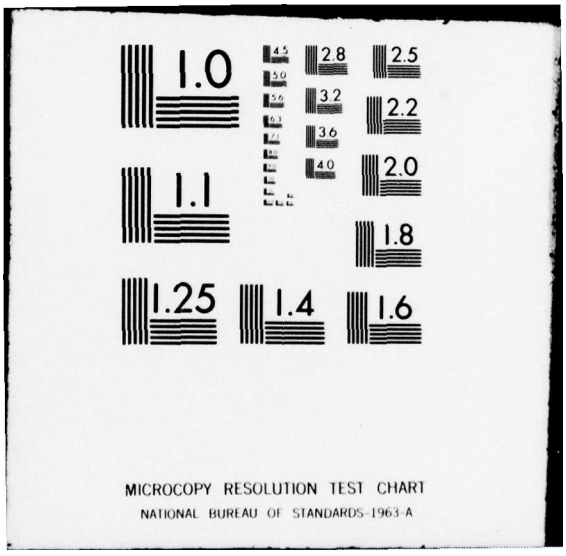
1.0
1.1
1.25
1.4
1.6
1.8
2.0
2.2
2.5
2.8
3.2
3.6
4.0
MICROCOPY RESOLUTION TEST CHART
NATIONAL BUREAU OF STANDARDS-1963-A

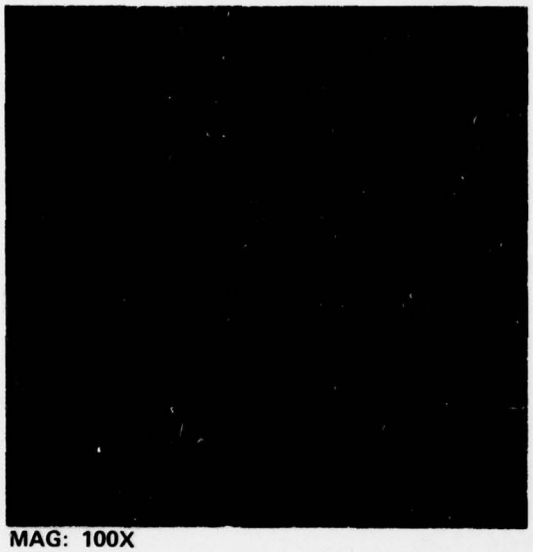

MAG: 100X

1500 °F

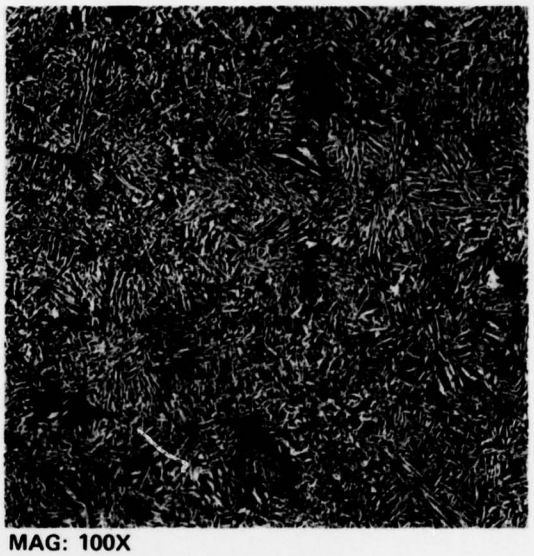

MAG: 100X

1550 °F

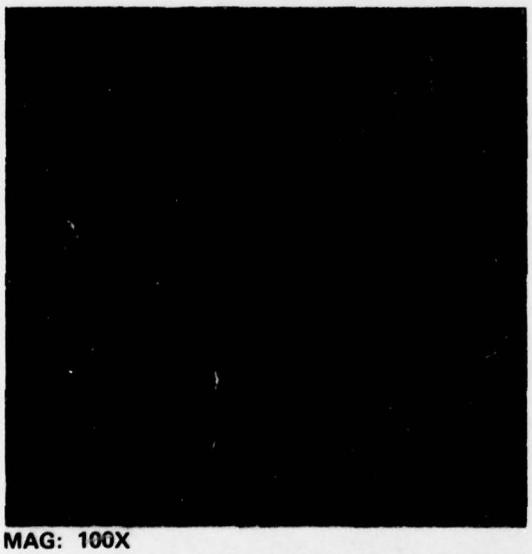

MAG: 100X

1600 °F

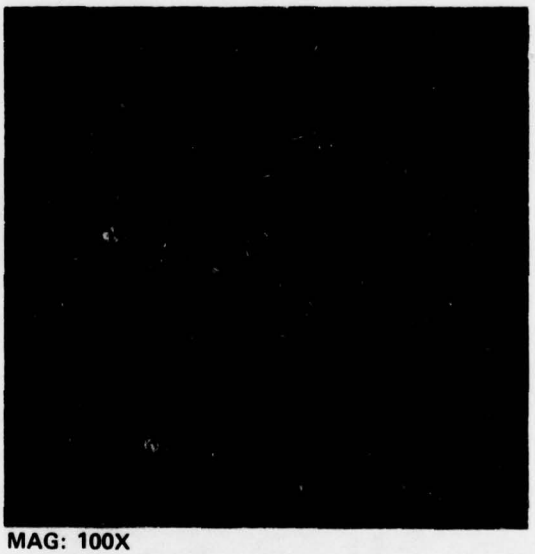

MAG: 100X

1750 °F

Figure 57. As-Hipped Ti-6A1-2Sn-4Zr-6Mo REP Powder FD 77722

MAG: 100X

1500 °F

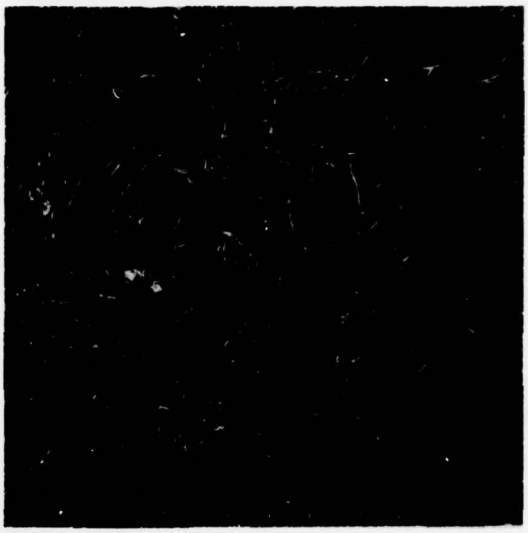

MAG: 100X

1550 °F

MAG: 100X

1600 °F

MAG: 100X

1750 °F

Figure 58. Hot Isostatically Pressed Billet After a 1670/1/AC + 1100/8/AC Heat Treatment

FD 77723

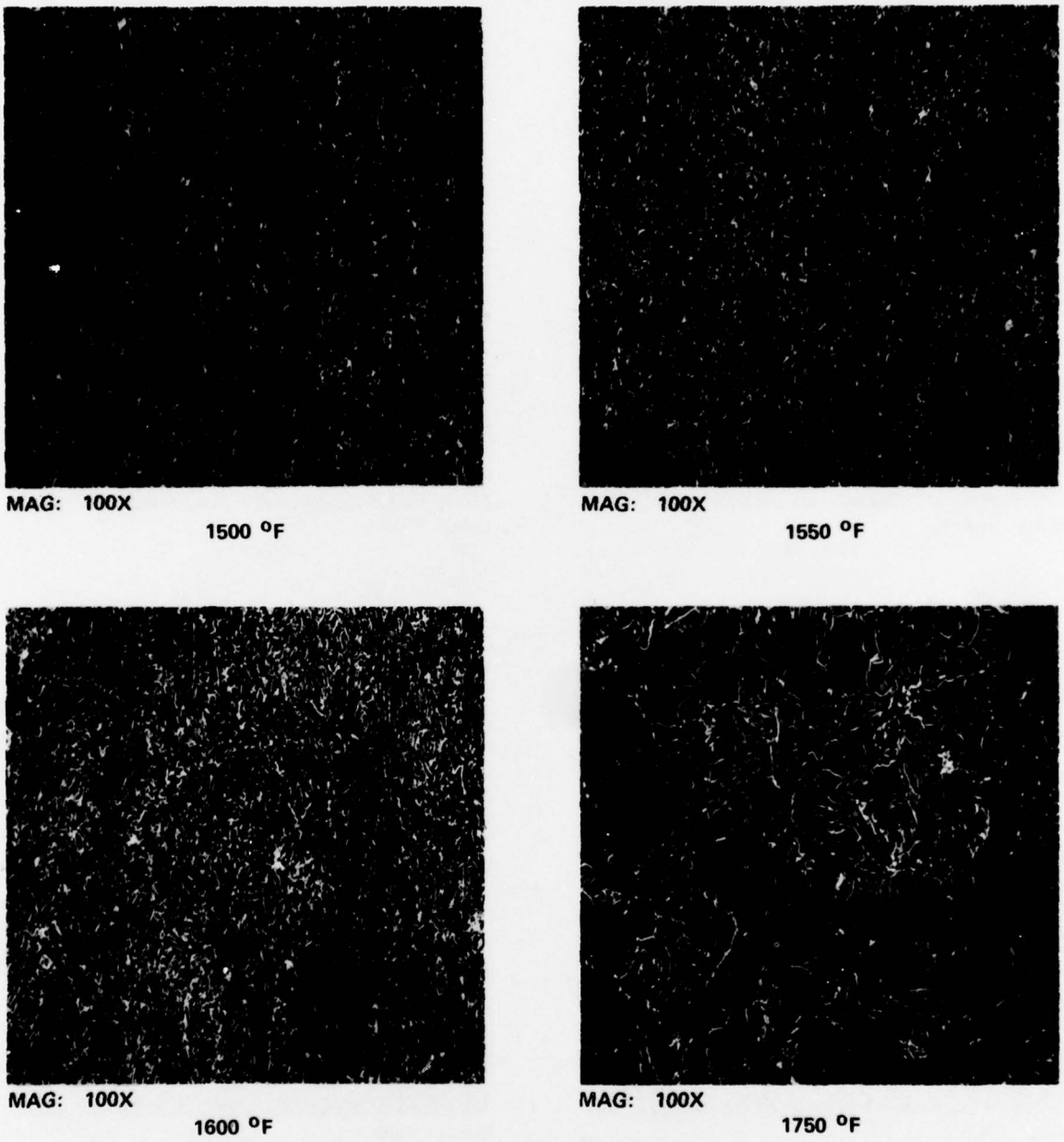

Figure 59. Microstructure of Hot Isostatically Pressed and Forged (1650°F), and Heat-treated (1670/1/AC + 1100/8/AC) Ti-6Al-2Sn-4Zr-6Mo Powder FD 77724

a. Canning Procedure

(1) Can Design

The original can design was modified to eliminate possible powder contamination resulting from the brazing compound. Crucible used a similar can design to encapsulate the powder for consolidation. Extrusion and compaction cans were machined from mild steel tubing, boiler plate, and billet stock. Evacuation tubes were made from stainless steel tubing. No brazing was used to seal the cans. Figure 60 shows the new can design used in preparing the powder for extrusion.

(2) Can Preparation

Prior to welding the extrusion can, the following chemical cleaning procedure was used.

(1) Immerse in muriatic acid
(2) Electrolytic-alkaline clean
(3) Hot water power spray
(4) Immerse in oil
(5) Degrease in trichlorethylene

After the extrusion containers were verified to be leak tight, powder from the blended lots 2 and 3 was poured into the containers in an argon atmosphere. After vacuum outgassing at 500°F, the evacuation stem was sealed by hot crimping and welding.

Crucible similarly loaded powder into welded mild steel containers through an evacuation stem. The containers were then evacuated at room temperature and vacuum outgassed at 500°F. The evacuation stem was sealed by hot crimping, shearing and welding.

b. Powder Consolidation

(1) Extrusion

Previous Task II studies showed that a 1550°F extrusion temperature resulted in a highly desirable "as-extruded" microstructure and a uniform structure after heat treatment. The mild steel can filled with Ti-6Al-2Sn-4Zr-6Mo powder was thus extruded at 1550°F by RMI, Ashtabula, Ohio. The can was extruded from a 6.125-inch diameter liner through a 2.4-in. diameter orifice die, with a 60-degree included angle (a reduction ratio of 6.3:1).

(2) Hot Isostatic Pressing

Hot Isostatic Pressing (HIP) parameters were chosen based on Task I and Task II results. A temperature between 1650°F and 1750°F appeared to offer the best potential for optimum properties and uniformity of structure. A second compaction temperature of 1800°F was chosen to determine the allowable upper limits of hot pressing Ti-6246 while attempting to maintain a fine beta grain size with resulting acceptable ductility.

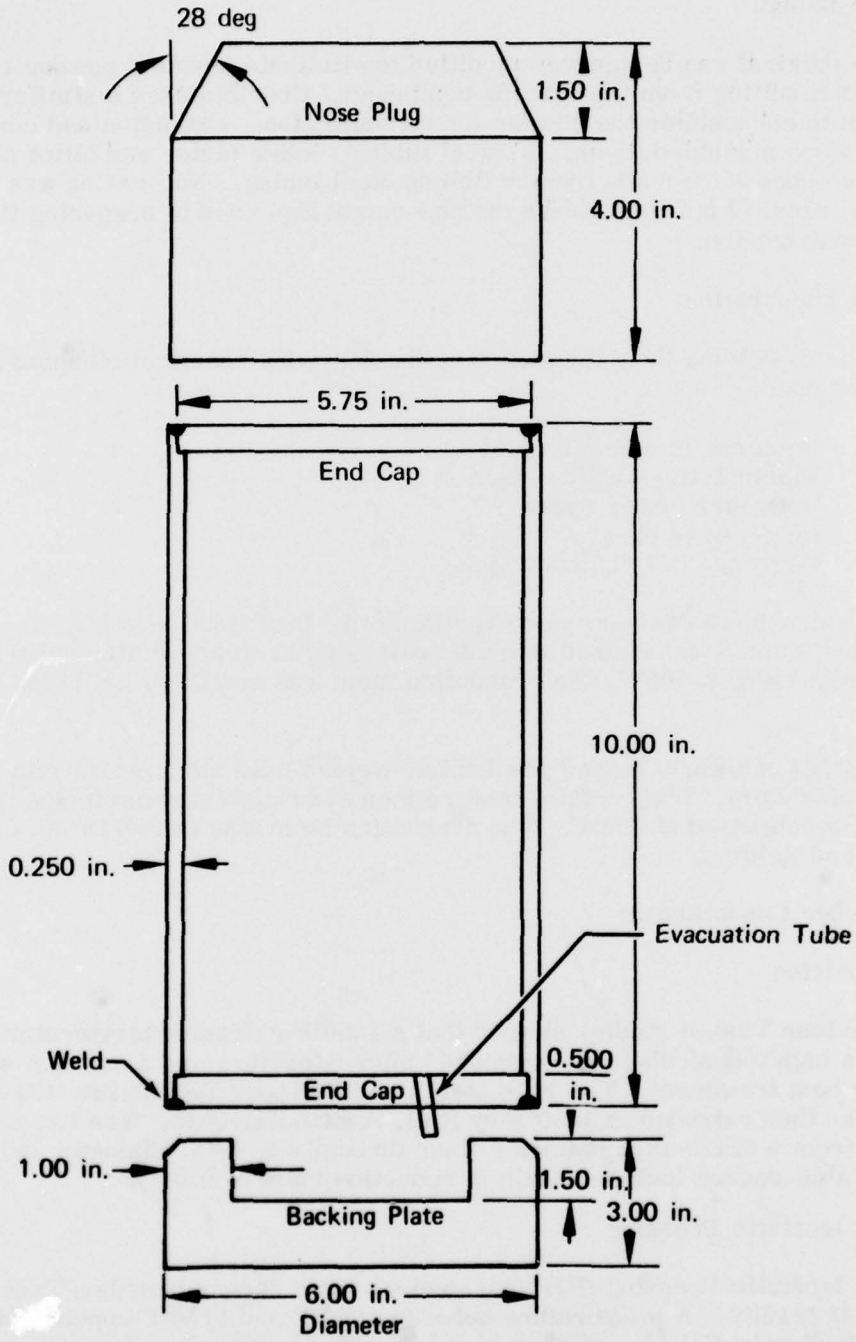

Figure 60. Modified Extrusion Can Used for Task II Extrusions FD 90067

Crucible, Inc. performed the HIP utilizing the procedures established earlier in the program. The consolidation temperatures/pressures were 1675°F/15 ksi and 1800°F/15 ksi.

c. Billet Evaluation

(1) Extrusion

(a) Structural Evaluation

Macroetch slices (Figure 61) from both ends of the extrusion did not show a concentric ring pattern as exhibited in the earlier Task II work. However, a variation of structure from edge to center was observed. A large amount of fine primary alpha was present near the edge with coarser grains near the center. The microstructural variations may be attributed to differences in cooling rate of the material and the adjacent tooling. The extruded and heat-treated material (Figure 62) consisted of short, thick alpha platelets in a fine transformed beta matrix, typical for extruded material that is heat treated with a solution and age heat-treatment. To determine the microstructural effects of a typical forging and heat treatment sequence on the above structure, a mult was machined from the extrusion and forged at 1650°F. The application of a 1670/1/AC+1100/8/AC heat-treatment to the forged material produced a microstructure consisting of equiaxed primary alpha in a fine transformed beta matrix. Experience with this type of structure has been good and generally results in good mechanical properties.

(b) Mechanical Properties

Tensile and room temperature notch stress-rupture testing was conducted on the extruded and heat-treated material. Results were nearly identical to earlier Task II results. Forging and heat-treating resulted in significant increases in strength but a corresponding decrease in ductility. Low ductilities were again attributed to inclusions present in the powder. Additional tensile testing confirmed the presence of contamination in the plane of fracture. Stress-rupture testing was performed as follows: each specimen was initially loaded at 190 ksi. If failure occurred in less than 5 hours, an alternate specimen was loaded at 170 ksi and uploaded 10 ksi every 5 hours to failure. Test results presented in Table XIX indicate that the powder contamination problem was not eliminated by changing the canning procedures.

(c) Chemistry

Interstitial chemistry results for the 1550°F extrusion using the blended lot (2 and 3) are compared with previous interstitial analyses in Table XVIII. Nitrogen content was higher than anticipated but within the range of variations observed in the prior analyses.

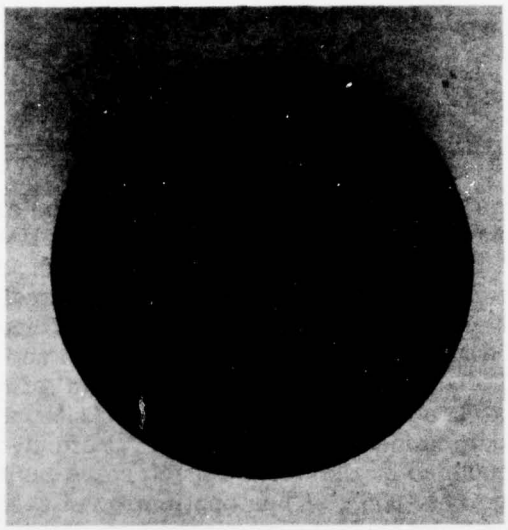

Mag: 1X

Mag: 500X

Edge

Mag: 500X

Center

Figure 61. Macro and Microstructure of As-Extruded (1550°F) Ti-6Al-2Sn-4Zr-6Mo REP Powder

FD 90068

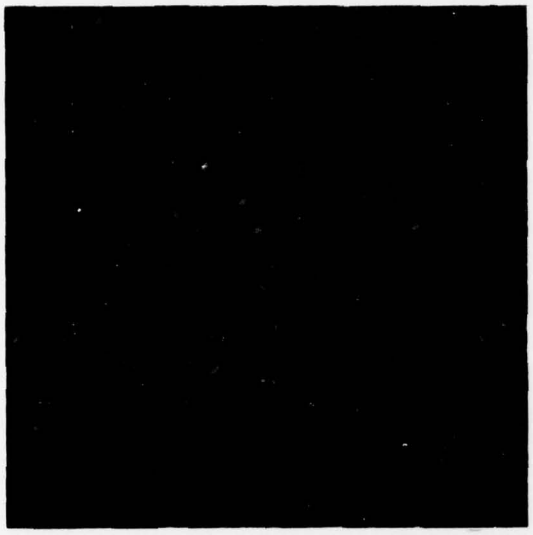

Edge Mag: 500X

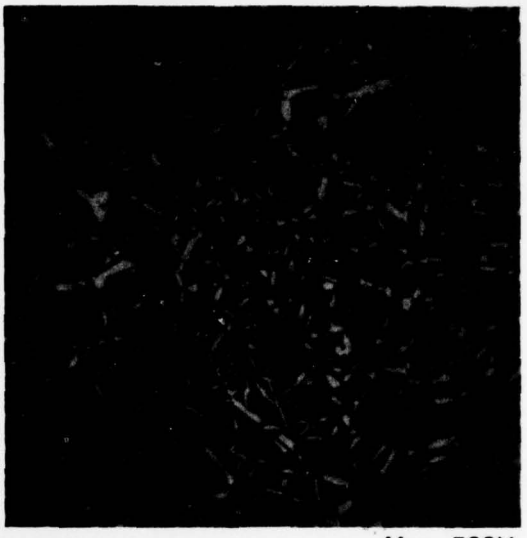

Center Mag: 500X

Extruded (1550°F) and Heat Treated (1670/1/AC + 1100/8/AC)

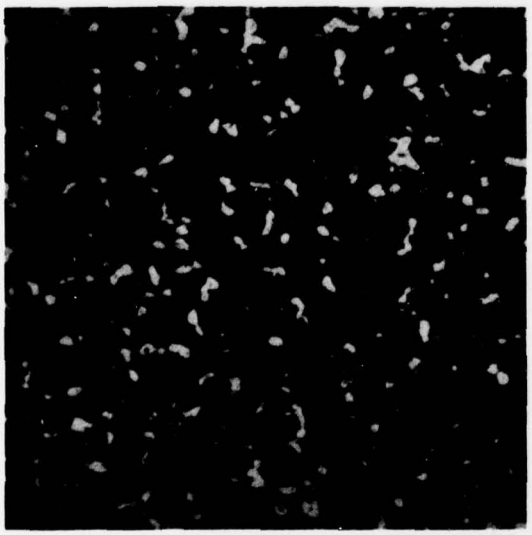

Edge Mag: 500X

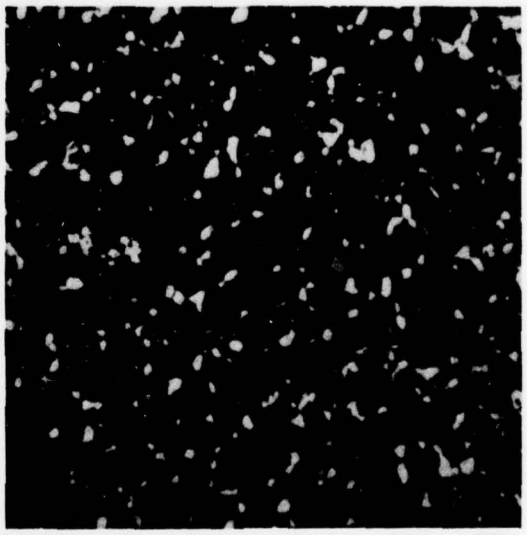

Center Mag: 500X

Extruded (1550°F), Forged (1650°F) and Heat Treated (1670/1/AC + 1100/8/AC)

Figure 62. Microstructures of 1550°F Extrusion FD 90069

Table XIX. Mechanical Properties of Task II
Additional Pancakes
(1670(1)AC plus 1100(8)AC)

Material Description	Tensile Results YS (ksi)	UTS (ksi)	EL (%)	RA (%)	Stress Rupture Results Failure Stress (ksi)	Total Time (hr)	Time at Failure Load (hr)
1550°F Extrusion							
As Extruded Plus Heat	154.3	167.4	15.5	34.0	210	11.5	0.7
Treated	155.6	167.9	13.0	20.0	220	15.0	FOL*
Forged Plus Heat	178.4	188.0	2.0	4.3	190	0.1	0.1
Treated	180.6	185.0	1.5	4.7	220	25.3	0.3
	179.0	188.6	0.7	3.3			
	176.1	-	-	-			
	176.0	181.5	-	-			
	180.7	183.6	1.0	0.8			
	177.5	176.5	11.3	32.4			
1675°F Hot Isostatic Pressing							
As-HIP Plus Heat	153.1	172.9	8.3	14.6	190	0.1	0.1
Treated	154.6	173.9	7.5	10.9	190	10.0	FOL
Forged Plus Heat	177.0	191.0	6.5	13.5	190	0.1	0.1
Treated	188.5	197.0	6.5	19.9	190	10.0	FOL
1800°F Hot Isostatic Pressing							
As-HIP Plus Heat	153.8	173.1	5.0	4.7	190	0.1	0.1
Treated	155.4	174.3	5.5	8.6	190	10.0	FOL
Forged Plus Heat	194.0	203.0	5.0	11.3	190	0.1	0.1
Treated	189.5	200.0	6.0	14.2	190	10.0	FOL

*FOL - Failed On Loading

(2) Hot Isostatic Pressing

(a) Structural Evaluation

Macro and microstructural analyses of the 1675°F and 1800°F (Figures 63, 64, 65, and 66) HIP'ed billets revealed little difference in response to forging and/or heat treatment. Both as - HIP'ed billets consisted of thick acicular alpha platelets and intergranular beta with discontinuous alpha at prior beta grain boundaries. A solution and age (1670°F/1/AC+1100°F/8/AC) heat treatment resulted in a structure consisting of long secondary alpha platelets in a fine transformed beta matrix. A forging operation identical to the one performed on the extruded material resulted in a break-up of the elongated alpha, but did not result in a desirable equiaxed primary alpha structure.

(b) Mechanical Properties

Tensile and room temperature notch stress-rupture testing was performed on specimens machined from the HIP and heat-treated material. Results are presented in Table XIX.

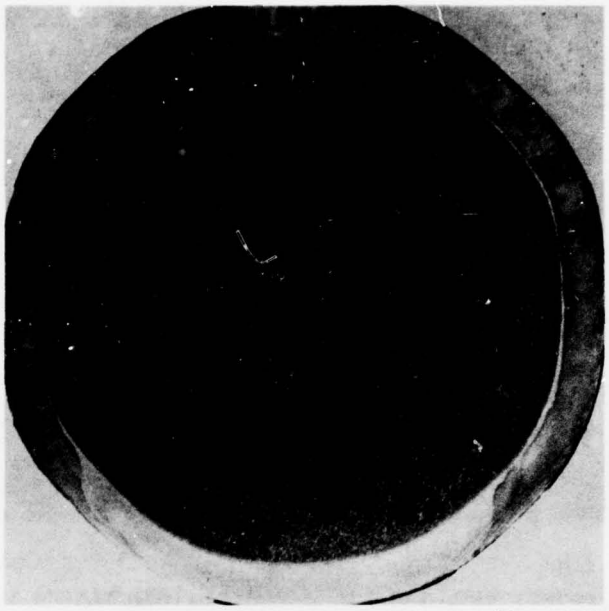

Mag: 1X

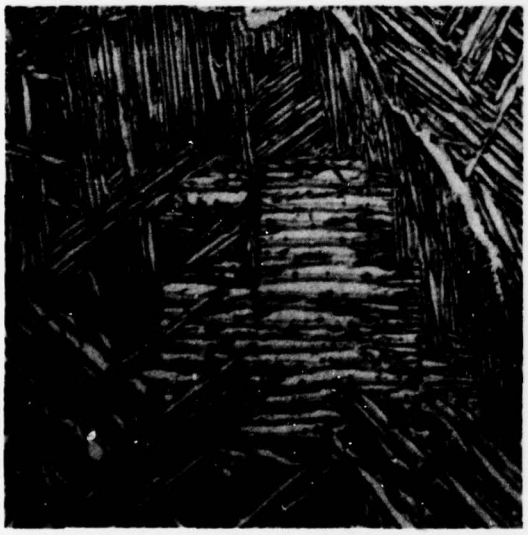

Mag: 500X

Edge

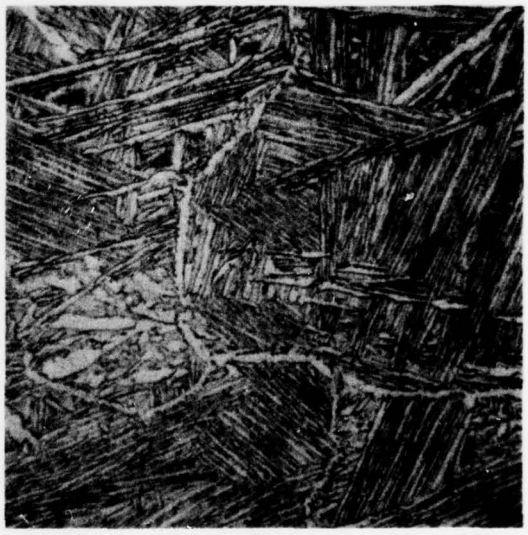

Mag: 500X

Center

Figure 63. Macro and Microstructure of As-Hipped (1675°F) Ti-6Al-2Sn-4Zr-6Mo REP Powder

FD 90070

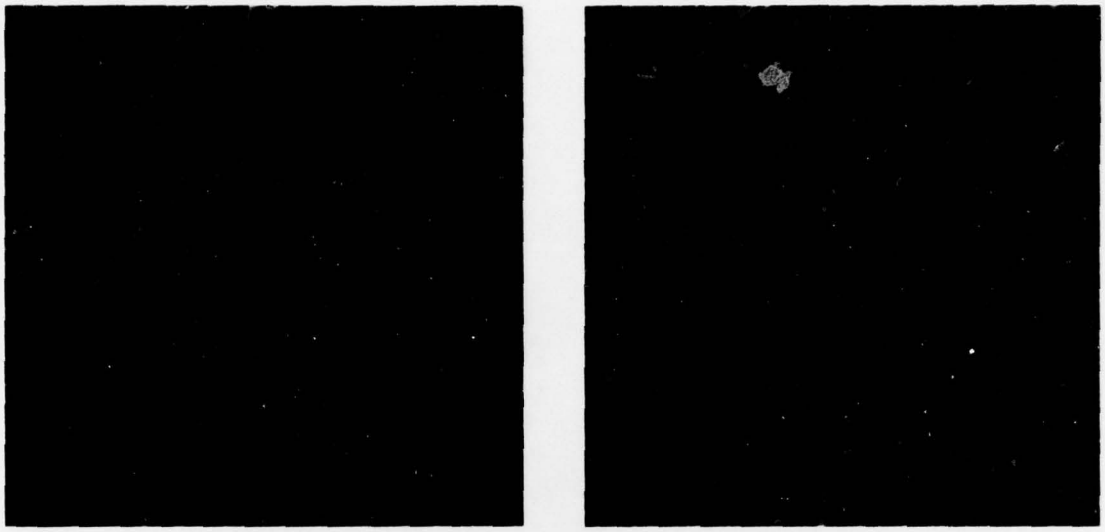

Edge Mag: 500X Center Mag: 500X

HIP (1675°F/15 ksi) and Heat Treated (1670/1/AC + 1100/8/AC)

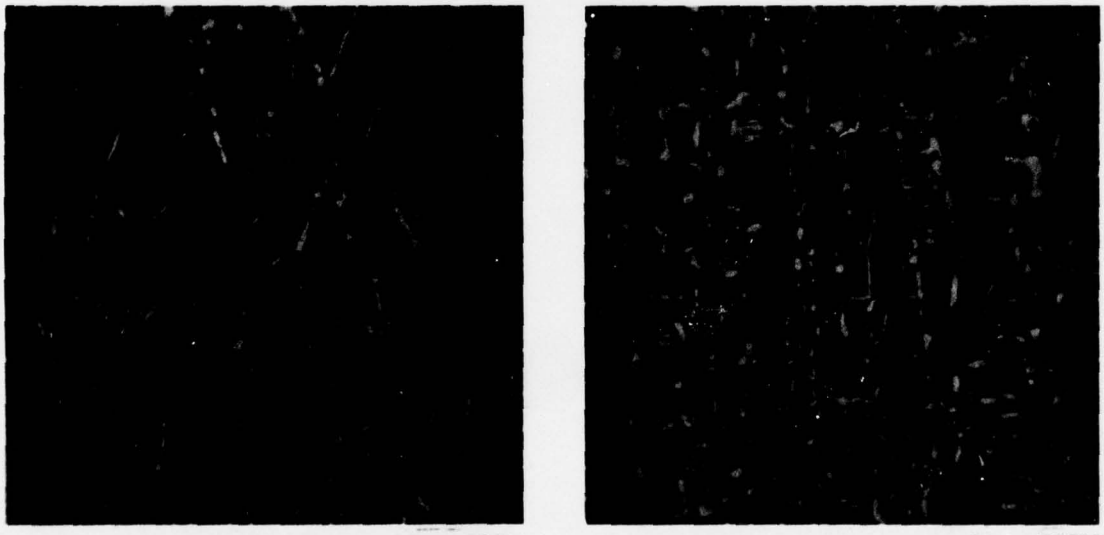

Edge Mag: 500X Center Mag: 500X

HIP (1675°F), Forged (1650°F) and Heat Treated (1670/1/AC + 1100/8/AC)

Figure 64. Microstructures of 1675°F Hot Isostatic Pressing FD 90071

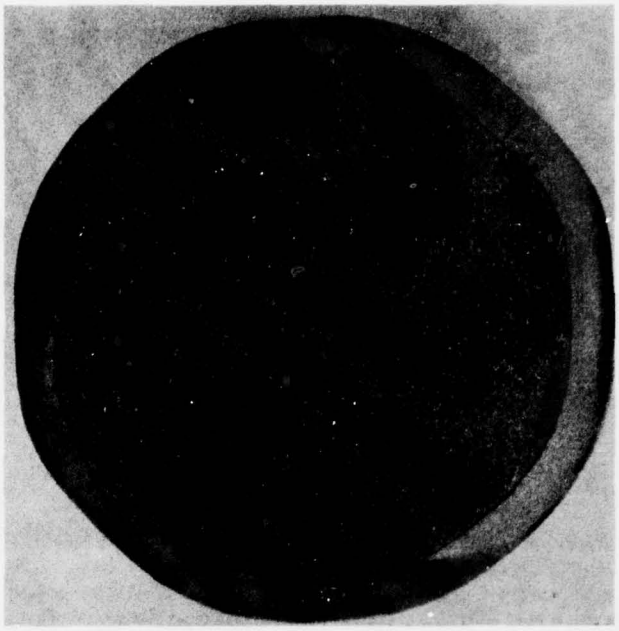

Mag: 1X

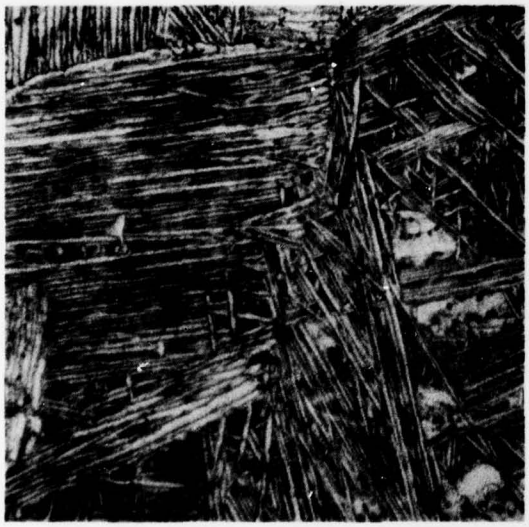

Mag: 500X

Edge

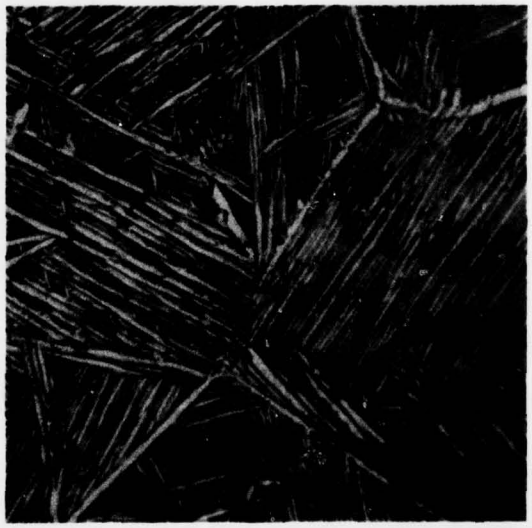

Mag: 500X

Center

Figure 65. Macro and Microstructure of As-Hipped (1800°F) Ti-6Al-2Sn-4Zr-6Mo REP Powder

FD 90062

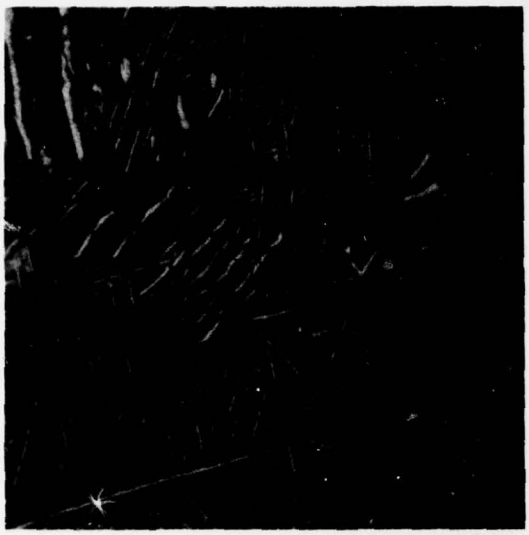

Edge Mag: 500X

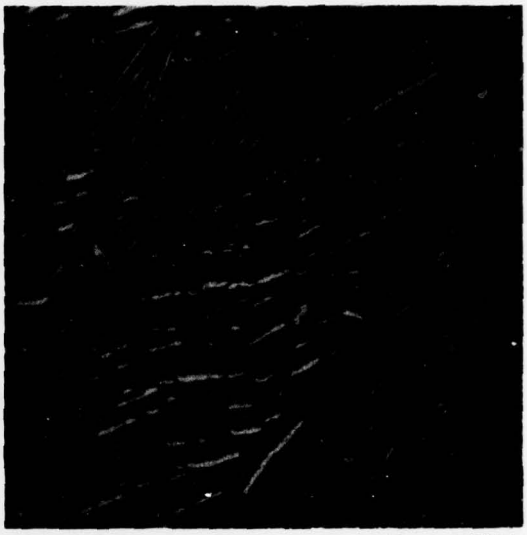

Center Mag: 500X

HIP (1800°F/15 ksi) and Heat Treated (1670/1/AC + 1100/8/AC)

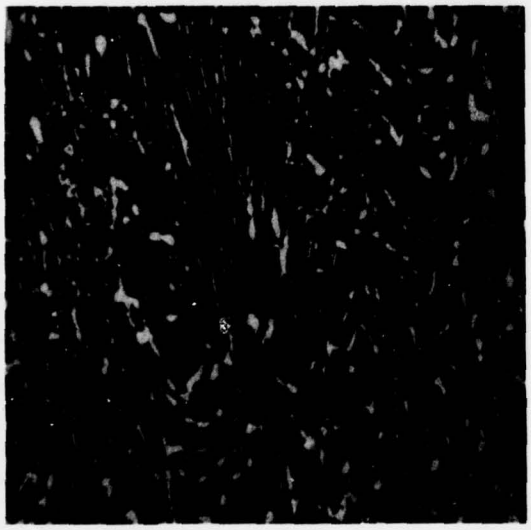

Edge Mag: 500X

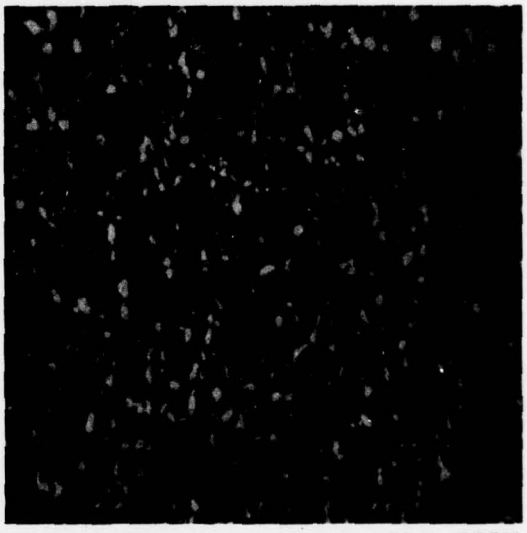

Center Mag: 500X

HIP (1800°F/15 ksi), Forged (1650°F) and Heat Treated (1670/1/AC + 1100/8/AC)

Figure 66. Microstructures of 1800°F Hot Isostatic Pressing FD 90061

Tensile strengths were nearly identical for both compactions. Lower ductility of the 1800°F compaction reflects the presence of a larger grain size. As-compacted and heat-treated tensile strengths and notched stress-rupture properties of the pressings were lower than in the previous Task II 1750°F compaction. Forging and heat-treatment of the hot isostatically pressed material resulted in increased tensile strengths and lowered ductilities. Notch stress-rupture testing revealed marginal properties in both consolidations.

(c) Chemistry

An interstitial analysis of samples taken from the HIP'ed billets revealed a slight increase in oxygen level. See Table XVIII. No increase was observed in the hydrogen or nitrogen levels.

d. Inclusion Analysis

Prior analyses of inclusions present on tensile fracture surfaces were identified by microprobe as nickel and phosphorus. Although the inclusions were not positively identified as coming from the braze compound, the canning procedure was changed to prevent possible contamination from this source. Numerous inclusions found on the surfaces of the failed tensile specimens verified the presence of contamination in the powder. An extensive study was thus initiated to identify the inclusions and their probable sources.

(1) Analytical Technique Selection

A scanning electron microscope equipped with an energy X-ray spectrometer unit was chosen for the inclusion study. The unit enables a rapid identification of inclusions on fracture surfaces without the necessity of special preparation techniques.

(2) Identification of Inclusions

Inclusions were found in all the material irrespective of consolidation method (HIP or extrusion) and consolidation temperature. Ten specimens exhibiting typical inclusions were therefore submitted for evaluation. The inclusions fell into three classes. They were: (1) tungsten, (2) nickel and (3) miscellaneous, including those that could not be positively identified. Figures 67 through 69 show the fracture surfaces and scanning electron micrographs of inclusions from each of these groups. Table XX summarizes the inclusion analysis. Most of the inclusions were tungsten. Erosion of the tungsten stinger electrode on the powder-making apparatus was surmized to be the source of tungsten inclusions. Nickel inclusions may be traced to cross contamination of powders resulting from more than one powder being processed in the same facility. Although rigid cleaning procedures were followed before each powder was run, the probability of removing all the prior powder particles is low. On several of the inclusions, no positive identification could be made using energy dispersive X-ray techniques. Microprobe analysis also failed to result in a positive identification of the inclusions. However, the microprobe analysis did show a slight variation in chemistry between the inclusion and base metal. One plausible explanation for the low ductilities may be localized concentrations of interstitials which would cause premature failures originating from these areas.

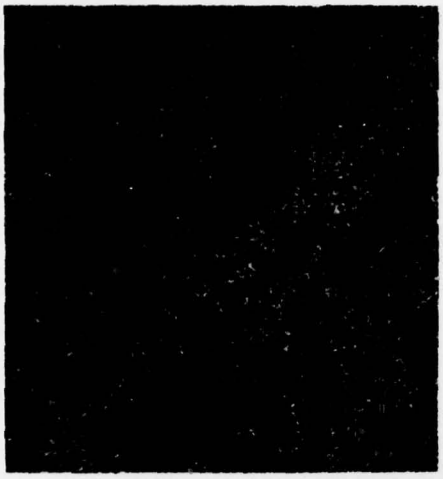

Vacuum Hot Pressing

Nickel Inclusion

Mag: 100X

Macro

Mag: 488X

SEM

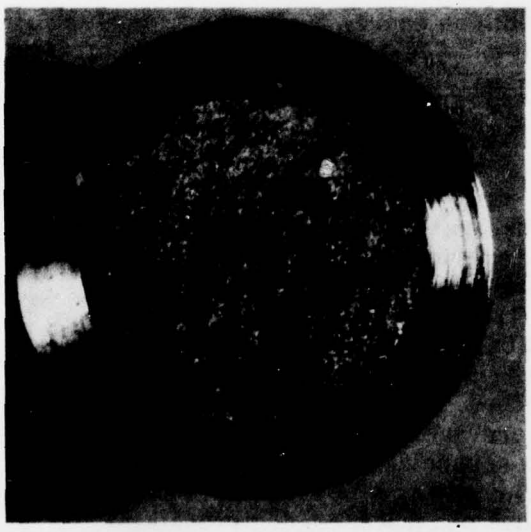

Hot Isostatic Pressing

Tungsten Inclusion

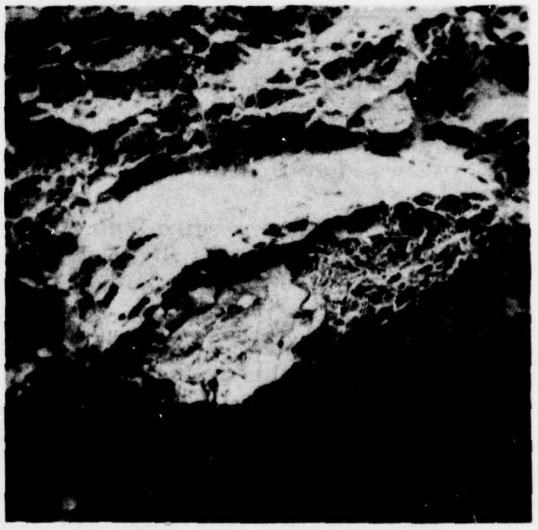

Mag: 10X

Micro

Mag: 262X

SEM

Figure 67. Typical Inclusions Found in Consolidated Ti-6Al-2Sn-4Zr-6Mo REP Powder

FD 90064

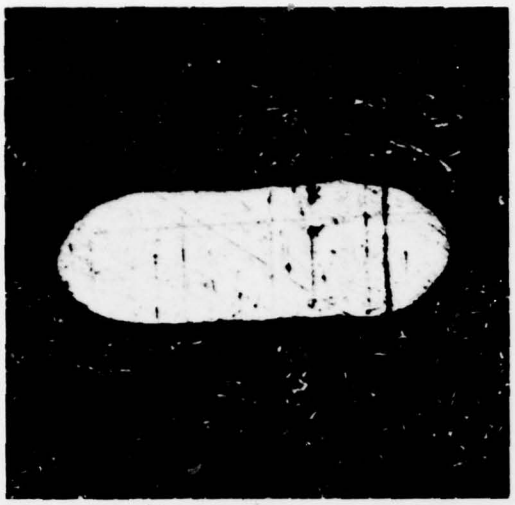

Hot Isostatic Pressing

Tungsten Inclusion

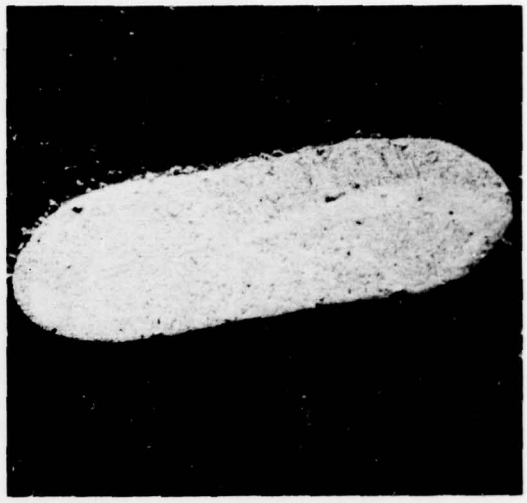

Mag: 200X

Micro

Mag: 260X

SEM

Hot Isostatic Pressing

Possibly an Iron Inclusion

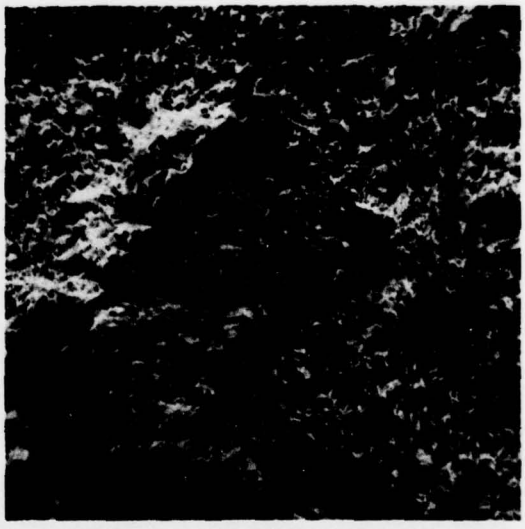

Mag: 10X

Macro

Mag: 204X

SEM

Figure 68. Typical Inclusions Found in Consolidated Ti-6Al-2Sn-4Zr-6Mo REP Powder FD 90063

Extrusion

Possibly an Iron Inclusion

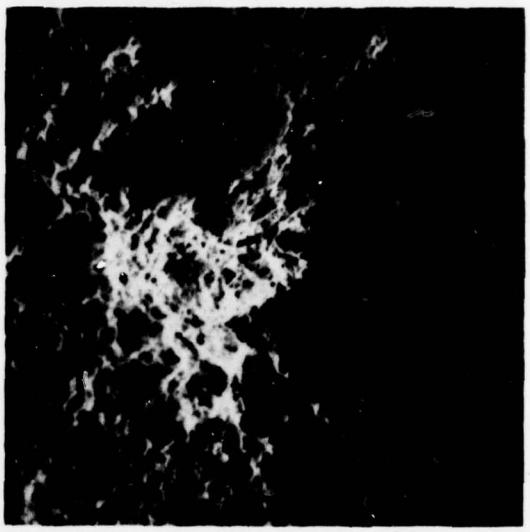

Mag: 10X

Macro

Mag: 102X

SEM

Hot Isostatic Pressing

Inclusion Same as Base Metal

Mag: 10X

Macro

Mag: 220X

SEM

FD 90065

Figure 69. Typical Inclusions Found in Consolidated Ti-6Al-2Sn-4Zr-6Mo REP Powder

Table XX. Inclusion Analysis Summary

Specimen Identification	Materials Processing	Inclusion
Vacuum Hot Pressing	at 1650°F/15 ksi	Nickel; possibly iron and chromium
Vacuum Hot Pressing	at 1650°F/15 ksi plus 1750°F/1/AC	Nickel
Hot Isostatic Pressing	at 1675°F/15 ksi plus forged at 1650°F plus 1670°F/1/AC+1100/8/AC	Tungsten
Hot Isostatic Pressing	at 1675°F/15 ksi plus forged at 1650°F plus 1670°F/1/AC+1100/8/AC	Tungsten
Hot Isostatic Pressing (Gradient Bar)	at 1800°F/15 ksi plus forged at 1650°F plus 1670°F/1/AC+1100/8/AC	Tungsten
Hot Isostatic Pressing	at 1800°F/15 ksi plus forged at 1650°F plus 1670°F/1/AC+1100/8/AC	Possibly iron (appears to be same as base metal)
Hot Isostatic Pressing	at 1800°F/15 ksi plus forged at 1650°F plus 1670°F/1/AC+1100/8/AC	Same as Base Metal (Microprobe showed slight chemistry variation)
Extrusion	at 1550°F plus 1670°F/1/AC+1100/8/AC	Tungsten
Extrusion	at 1550°F plus forged at 1650°F plus 1670/1/AC+1100/8/AC	Same as Base Metal
Extrusion	at 1550°F plus forged at 1650°F plus 1670/1/AC+1100/8/AC	Possibly iron

6. Task II - Conclusions

a. General

Rotating electrode processed (REP) powder has been found to contain several types of inclusions. Tungsten inclusions were traced to the erosion of tungsten stinger electrodes. Nickel inclusions were traced to a cross contamination of powders resulting from more than one type of powder being processed in the same powder rig. Other inclusions may be present due to erosion of the viewing port on the powder rig or mishandling of the powder after production.

Vacuum hot pressing is a reliable method to detect gross powder contamination. However, either radiography or forging and testing a small compact is necessary to determine the presence and/or effect of small inclusions on the consolidated material.

Both HIP and direct extrusion have been demonstrated to be viable methods of consolidating REP powder to full theoretical density.

b. Selection of Powder Consolidation Method

Due to the influence of inclusions on the mechanical properties of both the HIP and the extrusions, a judicious choice of powder consolidation method could not be made at the end of Task II. The choice was, therefore, postponed until additional consolidations were made in Task III.

c. Tentative Powder Billet Specification

Based on Task I and Task II evaluations, a tentative billet specification for Ti-6Al-2Sn-4Zr-6Mo powder was prepared (Appendix B). The composition requirements are the same as those of the wrought Ti-6246 alloy and are required to insure desirable properties in the finished product. Other acceptance criteria are only temporary and cannot be determined until sufficient contamination-free billet stock has been evaluated.

C. TASK III - FERROFLUID CLEANING PROCESS

1. First Program Modification

a. Background

The initial program was negotiated as a 19-month technical effort plus an additional 3-month effort for writing, approval, and publication of a final report. Contamination problems necessitated a hold on the program in March 1974. Possible solutions to the contamination problem were reviewed with the following three suggestions meriting further investigation:

1. Air classification
2. Leaching out tungsten and iron
3. Ferro-magnetic separation.

Several air particle classifier manufacturers were contacted, and the general consensus was that the air classification method would not solve our problem. Tungsten inclusions have a range of particle sizes and for good separation the particles should be the same size. Many of the particle classifiers cannot efficiently handle particles larger than 325-mesh because they depend on air suspension. A special system would have to be built to handle titanium powder and no guarantee could be made concerning the success of the system.

Discussions with chemists concerning the possibility of leaching out some of the contamination revealed the impracticability of this technique. Due to the wide variance in types of inclusions present, several wash solutions would be required. With such a large number of solutions, contamination problems would be imminent.

Ferrofluid cleaning techniques appeared to offer the best potential for success. The basic operating principle is that when two objects of different density are immersed in a fluid of intermediate density, the less dense object will float and the denser one will sink. The system has already proved successful in several other applications. The range of inclusion densities would necessitate a system such as ferrofluid cleaning to separate the various inclusions.

A program modification was submitted in July 1974 with work to resume in October 1974. The modified program consisted of a 12-month technical effort with an additional 3 months for submission, approval and publication of a final report. The modified program deleted the Phase II effort and substituted the effort required to clean approximately 250 pounds of titanium powder, using ferrofluid separation techniques, and perform an additional extrusion and HIP evaluation.

b. Ferrofluids

The ferrofluid levitation technique was developed by AVCO Systems Division, Lowell, Mass. A ferrofluid consists of tiny magnetic particles, generally magnetite, put into a colloidal suspension in a liquid carrier. Typical liquid bases would be hydrocarbons, fluorocarbons, esters, organometallics and polyphenylethers. The size of the particles (approximately 100 Å) allows Brownian motion to keep the particles suspended indefinitely, so there is no settling out in a gravity or magnetic field. The small concentration of particles (3 to 10% by volume) means there is little effect on physical and chemical characteristics of the liquid. The particles are stabilized with an absorbent coating (about 25 Å thick) to prevent particle sticking. Coating serves a dual purpose, namely, solvating in the liquid carrier, coupling each particle to a substantial volume of surrounding liquid and "bumping" particles before magnetic or molecular attractions occur. The particles respond quickly when subjected to a magnetic field and transfer by solvation the force they experience to the liquid phase so that the whole liquid acts as a homogeneous magnetic material.

The sink/float technique is simple in principle. A simple change in current flow through the coils of an energizing electromagnet changes the apparent specific gravities from less than 1 gm/cm^3 to over 20 gm/cm^3 in the ferrofluid. If the object submerged in the ferrofluid is denser than the apparent specific gravity, it will sink; if it is lighter, it will float. Present capabilities of the system allow any two nonferrous metals or alloys differing in density by 5 to 10% or more to be separated. Tungsten inclusions would be easily separated from the less dense Ti-6246 powder using the sink/float technique.

c. Feasibility Study

AVCO used their small laboratory facility to clean 1 lb of Ti-6Al-2Sn-4Zr-6Mo powder for evaluation to prove the feasibility of the process. An evaluation was conducted to determine the adaptability of the process for cleaning titanium powders.

(1) Vacuum Hot Pressings

Three vacuum hot pressings were made: two from the ferro-fluid "sinks" (material heavier than the apparent density of the ferrofluid) and the other from the "floats" (the cleaned Ti-6246 powder).

(2) Analytical and Structural Evaluations

X-ray analysis of both pressings revealed the presence of high density inclusions in the "sinks" and the absence of inclusions in the "floats." X-ray spectograph analysis of the "sinks" revealed the presence of iron and tungsten inclusions, probably due to an inadequate washing procedure. Typical microstructures of the ferrofluid cleaned vacuum hot pressing are shown in Figure 70.

(3) Chemistry and Mechanical Properties

Results from the chemical analysis of the "float" vacuum hot pressing are presented in Table XXI. All elements were within specification limits.

Table XXI. Chemical Analysis of Vacuum Hot Pressing

	P&WA 1216 Specification Min		Max	Vacuum Hot Pressing
Aluminum	5.50	to	6.50	6.0
Tin	1.75	to	2.25	1.9
Zirconium	3.50	to	4.50	4.1
Molybdenum	5.50	to	6.50	6.0
Iron			0.15	0.03, 0.06
Oxygen			0.15	0.083
Nitrogen			0.04	0.0093
Hydrogen			0.015	0.0062

Two substandard tensile specimens were machined from the heat treated vacuum hot pressing as shown in Table XXII. Although the test results were somewhat disappointing, the fracture surfaces were very clean. The low ductilities were attributed to the coarse beta grain structure and discontinuous alpha at the grain boundaries, resulting from the higher than normal vacuum hot pressing temperature (1700°F rather than 1650°F).

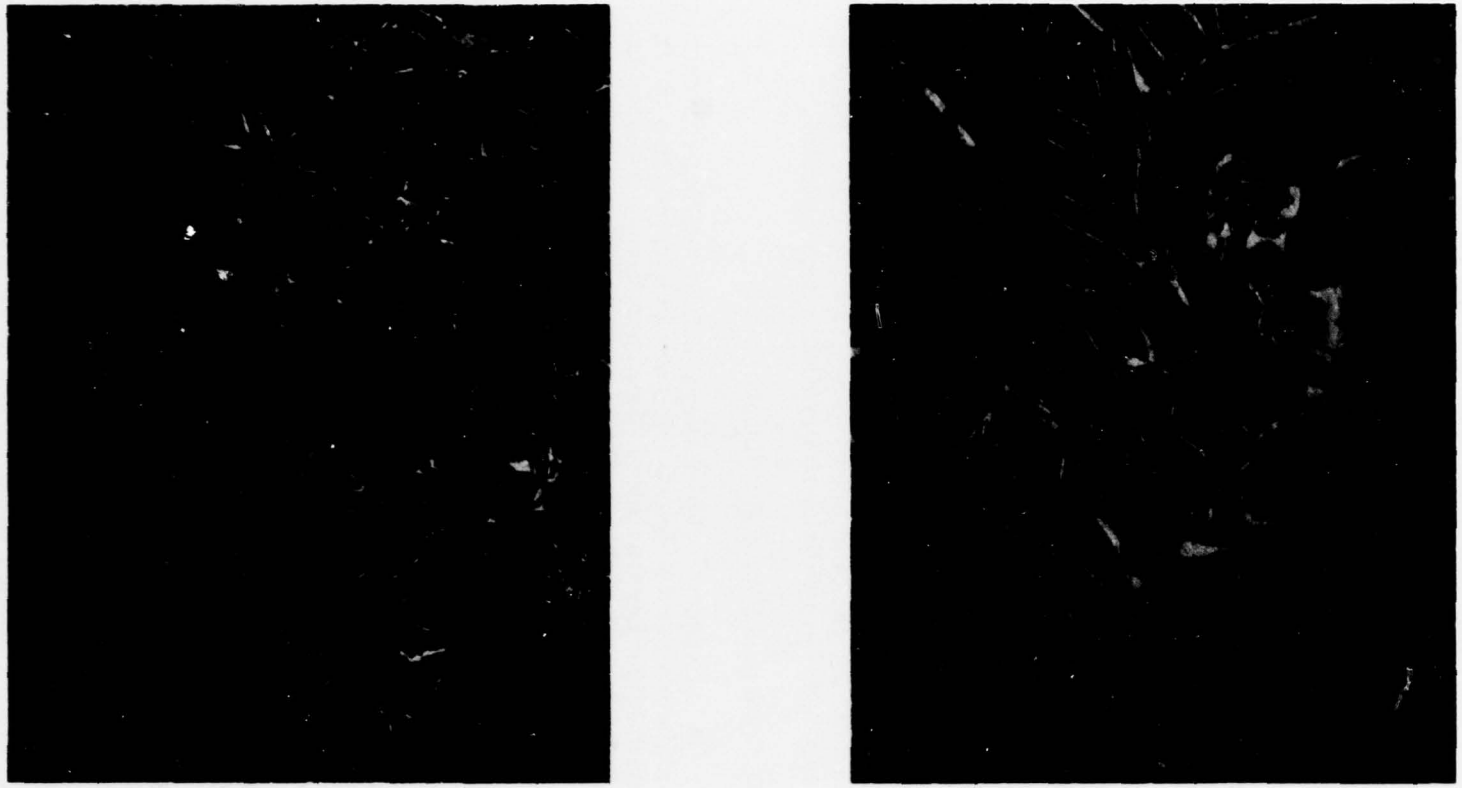

Mag: 100X

Mag: 500X

Figure 70. Typical Microstructure of Ferro-Fluid Cleaned Ti 6246 Powder Vacuum Hot Pressed at 1700°F/15 ksi and Heat Treated 1670/1/AC + 1100/8/AC

FD 90066

Table XXII. Mechanical Properties of 1700°F/15 ksi Vacuum Hot Pressing

Yield Strength (ksi)	Ultimate Tensile Strength (ksi)	Elongation (%)	Reduction of Area (%)
173.8	197.5	1.3	3.3
173.0	194.6	1.3	5.5

(4) Conclusion

Based on the feasibility study, a decision was made to submit a modification of the program. The modification included a subcontract effort by AVCO Corporation to "clean" the contaminated Ti-6246 powder using ferrofluid techniques.

2. Laboratory Processed Powder Evaluation

In order to provide samples of purified powder for evaluation before AVCO's pilot plant separation chamber was constructed, AVCO's laboratory scale sink/float separator was modified to accommodate the cleaning of Ti-6246 powder. Due to the similarity of procedures and techniques between the laboratory scale sink/float separator and the pilot plant facility, the laboratory-processed powder was used for our initial evaluations of ferrofluid cleaned powder.

a. Characterization of Ferrofluid Cleaned Powder

A 1650°F/15 ksi vacuum hot pressing (VHP) measuring approximately three inches in diameter and 3/4-inch thick was fabricated from the first lot of powder processed in the lab separator. Two specimens were machined and tested from the as-VHP material (Table XXIII).

Table XXIII. Mechanical Properties of 1650°F/15 ksi Vacuum Hot Pressing

Condition	Yield Strength (ksi)	Ultimate Tensile Strength (ksi)	Elongation (%)	Reduction of Area (%)
As-VHP	137.0	149.2	15.3	40.0
As-VHP	138.0	148.8	10.7	15.3
VHP Plus Forged Plus 1670/1/AC	184.0	198.5	6.7	18.3
Plus 1100°F/8/AC	186.1	200.4	7.3	22.3

Metallographic examination revealed the presence of foreign particles throughout the matrix as shown in Figure 71.

TOP: AS VACUUM HOT PRESSED FERRO-FLUID CLEANED POWDER
LEFT: MICROSTRUCTURE SHOWING FOREIGN PARTICLE
RIGHT: TYPICAL FRACTURE SURFACE SHOWING GOOD DUCTILITY

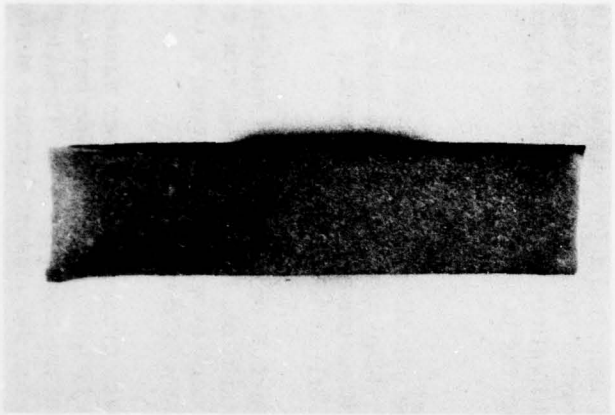

Mag: 1X

Mag: 100X

Mag: 10X

Figure 71. Vacuum Hot Pressing of Lab-Processed Ferro-Fluid Cleaned Ti 6246 Powder FD 90072

Analyses indicated that these particles were Ti 6Al-4V. The laboratory facility had previously been used to clean some Ti 6Al-4V powder. The presence of foreign particles in the as-vacuum hot pressed (no heat treatment) material did not have any deleterious effects on tensile properties. The remaining half of the VHP was forged down approximately 35% as shown in Figure 72. Two tensile specimens were machined and tested from the forged material. The tensile ductilities of the forged material were good considering the strength levels and compared favorably with wrought material of the equivalent strength level. (See Table XXIII.) No inclusions were found on the fracture surfaces. However, radiographs of the failed specimens showed the presence of inclusions. These results indicate that methods other than tensile testing are required to insure the absence of inclusions.

Radiographs taken of the "sink" material indicated the presence of many inclusions. X-ray diffraction chart traces and film patterns indicated the possible presence of iron oxide but could not be verified by metallographic analysis.

Wet chemistry analysis of the VHP powder indicated a Fe content of 0.19% (Table XXIV) which is roughly three times the normal iron content. AVCO was informed of the findings and instituted some modifications to the cleaning procedure to ensure complete removal of the ferrofluid from the powder.

b. Extrusion Evaluation

Canning procedures were identical to those established in the Task II work. A mild steel can filled with ferrofluid cleaned Ti-6246 powder was extruded at RMI. The can was extruded from a 6-1/8 inch diameter orifice die, with a 60-degree included angle (a reduction ratio of 6.3:1) at 1550°F.

A summary of the chemistry analysis performed on the extruded material is presented in Table XXIV. Difficulty was encountered in determining iron content. Apparently, there was a variation in iron content within the extrusion because repeated measurements ranged from 0.079 w/o to 0.19 w/o.

Structural studies on etch slices revealed the presence of a large number of foreign particles as shown in Figure 73. The lack of any interaction between the foreign particles and the matrix indicated that the particles were Ti-6Al-4V. The presence of these particles was responsible for the unusual fracture surfaces. Forgings from the extrusions indicated the inclusions were ductile and did not react excessively with the matrix in either the forged or the forged and heat-treated condition.

Tensile properties on the extruded and heat-treated material were acceptable as shown in Table XXV. However, the forged and heat-treated material exhibited lower than expected ductilities. The presence of the large quantity of Ti-6Al-4V may have been responsible for the low ductilities. Stress rupture properties were excellent. Electron spectroscopy was performed on the fracture surfaces of the tensile specimens. Nickel and iron indications were found on the surfaces but their concentrations were not significant. No inclusions other than Ti-6Al-4V were observed in any of the extruded material indicating that the ferrofluid process was effective in removing high density inclusions such as tungsten and nickel.

TOP: VHP (1650°F/15 ksi) AND FORGED (35%) FERRO-FLUID CLEANED POWDER
LEFT: HT 1670°F/1/AC + 1100°F/8/AC MICROSTRUCTURE SHOWING FOREIGN PARTICLES
RIGHT: TYPICAL FRACTURE SURFACE

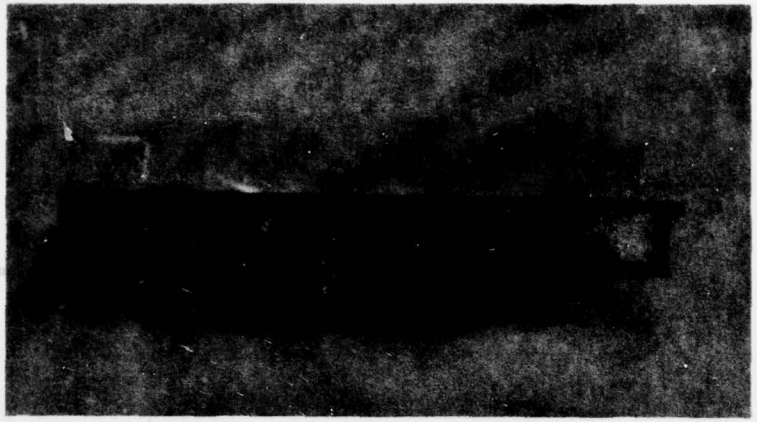

Mag: 1X

Mag: 100X

Mag: 10X

Figure 72. Forged Vacuum Hot Pressing of Lab-Processed Ferrofluid Cleaned Ti 6246 Powder FD 90073

Table XXIV. Task III Chemistry Analysis of Ferrofluid Cleaned Powder (Ti-6Al-2Sn-4Zr-6Mo)

Material Condition	Al	Sn	Zr	Mo	Fe	O_2	N_2	H_2	C
As-Vacuum Hot Pressed	6.2	2.0	4.3	6.0	0.19	0.09	0.006	0.005	0.026
Vacuum Hot Pressed, Forged and Heat-Treated	-	-	-	-	0.089 0.095	0.088	0.007	0.0029	0.028
As-Extruded	6.1	2.1	4.0	6.6	0.19/ 0.18	0.10	0.008	0.007	0.024
Extruded, Forged and Heat-Treated	-	-	-	-	0.084 0.079	0.094	0.014	0.014	Less than 0.010
As-Hot Isostatically Pressed	6.2	2.2	3.9	6.5	0.083/ 0.12	0.09	0.034	0.015	0.023
Hot Isostatically Pressed and Heat-Treated	-	-	-	-	0.196 0.080	0.095	0.008	0.0076	Less than 0.010
Hot Isostatically Pressed, Forged and Heat-Treated	-	-	-	-	0.065 0.072	0.091	0.006	0.012	0.019
Triple Cleaned Powder Sample	-	-	-	-	0.075	-	-	-	-
PWA 1216 Specification	5.30-6.50	1.75-2.25	3.50-4.50	5.50-6.50	0.15 Max	0.15 Max	0.04 Max	0.015 Max	-

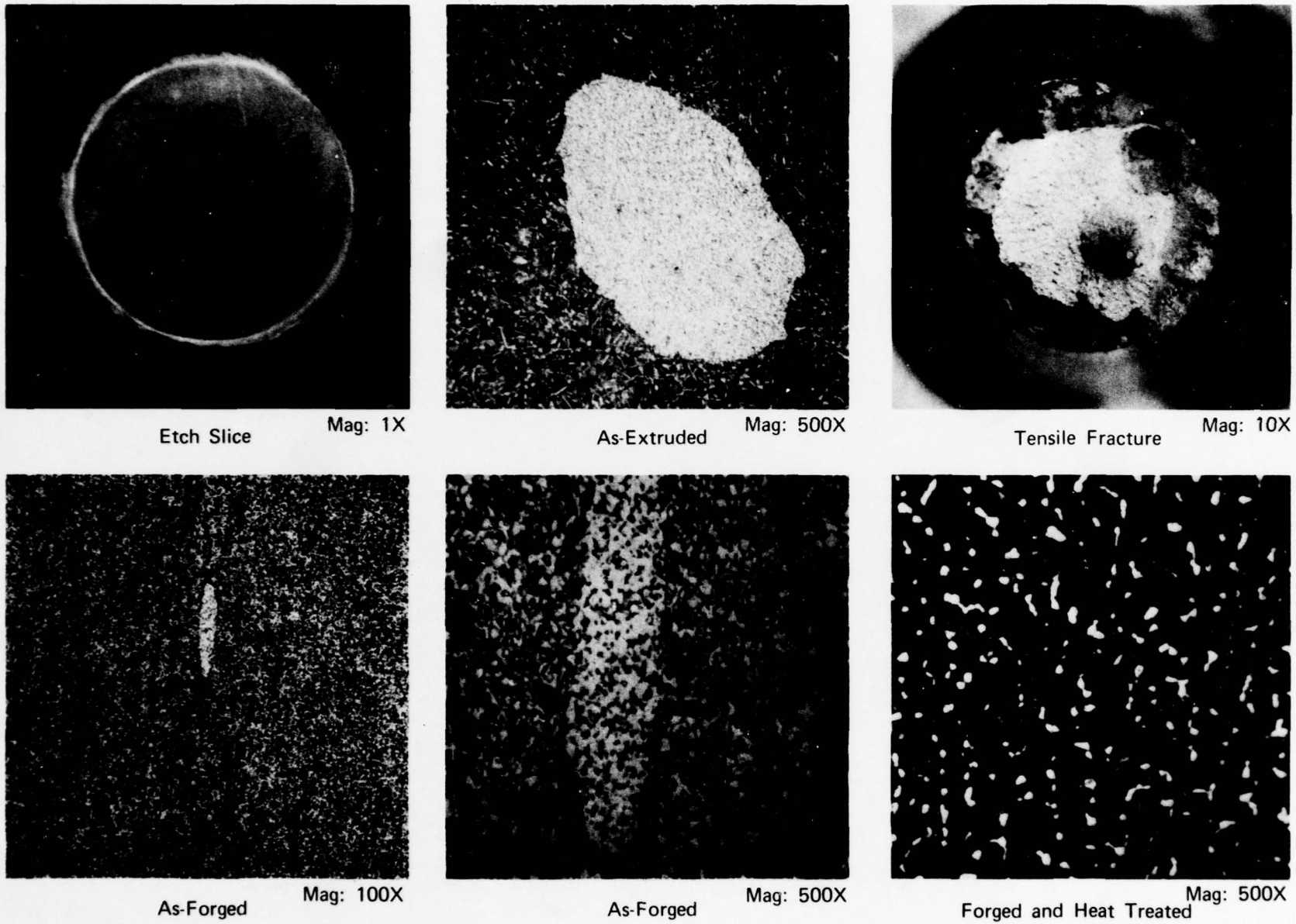

Figure 73. Microstructural Review of Extruded (1500°F); Forged (1650°F) and Heat Treated (1670°F/1 hr/AC + 1100°F/8 hr/AC) Ferrofluid Cleaned Ti-6Al-2Sn-4Zr-6Mo Powder

FD 90074

Table XXV. Mechanical Properties of Ferrofluid Cleaned Ti-6246 Powder

Vendor	Material Condition	Compaction Temperature (°F)	RT Tensile				RT Notched Stress Rupture		
			0.2% YS	UTS	%EL	%RA	Failure Stress (ksi)	Total Time (hr)	Time at Failure Load (hr)
RMI	Extruded	1550	175.5	187.1	7.0	10.9	220	15.2	0.2
			170.8	187.8	13.5	31.4	220	15.8	0.8
RMI/ P&WA-Florida	Extruded and Forged	1550	175.3	186.4	4.0	7.0	230	24.5	4.2
		1650	180.0	190.6	2.0	4.7	230	20.2	0.1
Crucible	HIP	1675	155.7	172.2	11.5	17.8	200	7.7	2.7
			155.8	171.8	4.0	7.0	200	5.1	0.1
Crucible/ P&WA-Florida	HIP and Forged	1675	183.4	195.9	9.5	22.3	230	20.1	0.1
		1650	188.3	202.0	4.5	6.3	230	0.1	20.1

c. Hot Isostatic Pressing Evaluation

Approximately 15 lb of the laboratory cleaned ferrofluid powder was shipped to Crucible, Inc. for HIP. After double canning, the material was compacted at 1675°F and 15 ksi. A chemistry analysis performed on the compacted material is presented in Table XXIV. The same range of iron contents observed in the extruded material was observed in the HIP material. One high nitrogen reading (0.034 w/o) was discounted upon rechecking additional material (0.006 w/o, 0.008 w/o).

The microstructure was typical for material processed at 1675°F and 15 ksi. The fracture surface of the HIP and forged and heat-treated material exhibited a surface typical for low ductility material. Fracture surfaces similar to Figure 74, have been examined with no success in determining the reason for the low ductility. The HIP'ed billet was made using the powder processed through the ferrofluid after the lot used in the extrusion evaluation and contained no Ti-6Al-4V powder. The powder used, as previously mentioned, for the extrusion probably contained the majority of any Ti-6Al-4V present in the laboratory separator. The low ductility was therefore attributed to the microstructure and not to the presence of foreign particles.

Tensile properties were erratic as shown in Table XXV. One specimen from the as-HIP'ed billet and one from the forged material exhibited good ductility while the other exhibited a much lower ductility. No high density inclusions were found in the compacted or forged material.

d. Selection of Consolidation Method

Based on evaluations of numerous extrusions and hot isostatic pressings, the extrusion process was chosen for use in the remainder of the program. A brief summary of the reasons for the selection follows.

(1) Structure

The extruded material has consistently shown a favorable response to processing and heat-treatment. A desirable fine equiaxed primary alpha in a transformed beta matrix structure has been obtainable in all the extrusions subsequent to forging and heat-treating. The HIP material exhibited a coarse structure consisting of thick acicular alpha platelets and intergranular beta. The platelets were not sufficiently broken up by a heat-treatment. Heat treated forgings of the hot pressed material often exhibited areas of segregation and/or both equiaxed and elongated alpha. A more consistent, and, consequently, more predictable structure was obtained in the directly extruded powder.

(2) Mechanical Properties

Due to the presence of inclusions in all the powder consolidations, a selection on the basis of tensile properties is difficult to make. However, better stress-rupture properties were obtained in material that had been extruded.

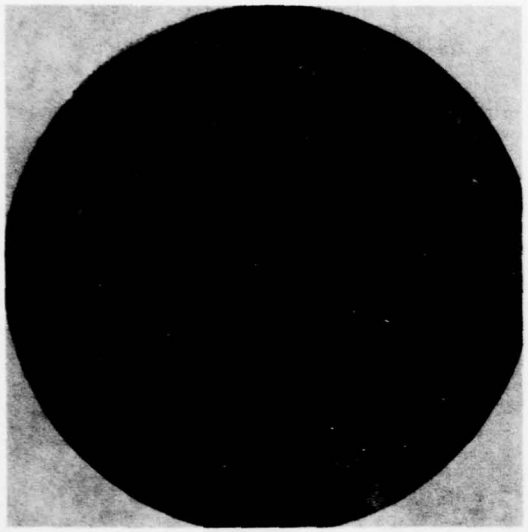

Etch Slice Mag: ¾X

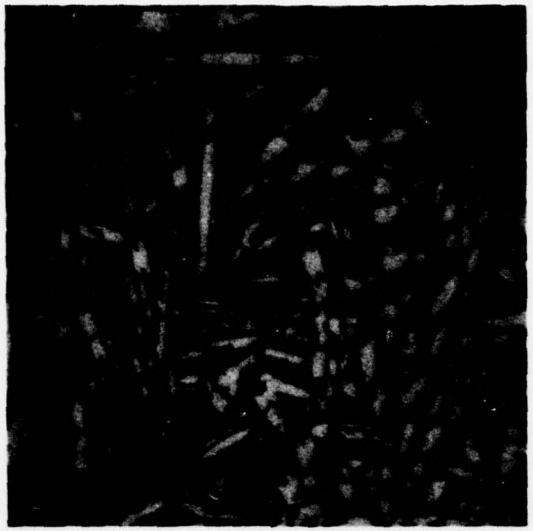

AS-HIPPED Mag: 500X

HIP + Forged

AS-HIPPED Mag: 500X

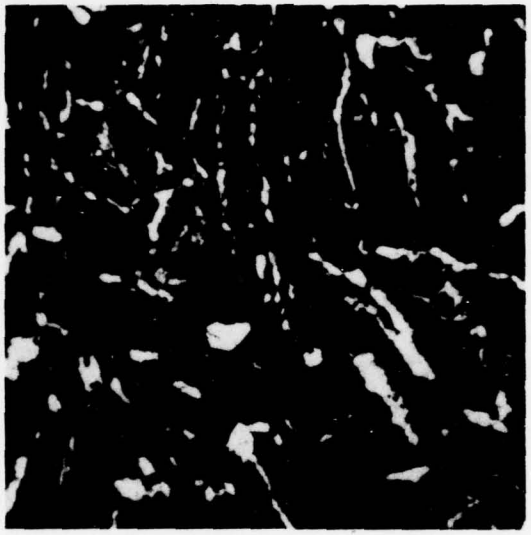

HIP + Forged Mag: 500X

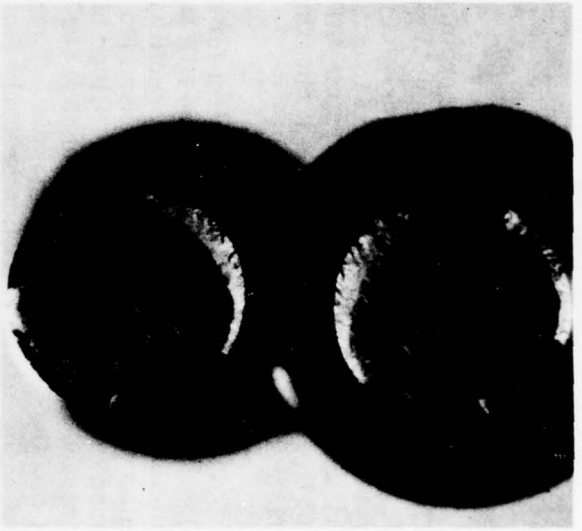

Tensile Fracture Mag: 5X

Figure 74. Microstructural Review of Hot Isostatically Pressed (1675°F/15 ksi); Forged (1650°F) and Heat Treated (1670°F/1 hr/AC + 1100°F/8 hr/AC) Ferrofluid Cleaned Ti-6Al-2Sn-4Zr-6Mo Powder

FD 90075

3. AVCO's Pilot Plant

a. Separation System Design

To complete the program in the allocated time frame, AVCO made available to P&WA their Ferrofluid Separation Pilot Plant. However, to have good separation and to ensure against any possible cross-contamination due to other scrap metals being separated in the facility, it was necessary to build a separation chamber specifically designed to separate the powdered titanium feed. A conceptual diagram of the separation vessel is shown in figure 75. It consists of a chamber that fits in the gap of the ferrofluid scrap separation electromagnet in AVCO's Pilot Plant (figure 76). In operation, the chamber is filled with ferrofluid and the powder to be purified is introduced into the chamber by a screw conveyor. The current to the electromagnet is set so that the density of the ferrofluid in the chamber is higher than the density of the titanium particles to be separated, but lower than the densities of the impurities to be removed. The less dense titanium particles will float to the top surface of the ferrofluid pool from which they are removed continuously by a flight conveyor. The dense contaminants sink and accumulate at the bottom of the chamber, from which they are periodically withdrawn. The upper half of the screw conveyor was shrouded in the entrance region of the ferrofluid pool to minimize the probability that an unwanted dense particle is misclassified and remains in the titanium fraction. The separation is operated at ferrofluid density only slightly higher than the density of the titanium particles. While this results in some misclassification and loss of titanium particles, this procedure maximizes the driving force for sinking the dense inclusions, thus minimizing the probability of their being carried over with the titanium particles. To ensure complete separation of the inclusions, the powder was passed through the separator and the floats were then passed through a second time. The actual separation vessel before installation in the magnet is shown in figure 77.

b. Preparation of Pilot Plant

(1) Installation of Separator

Several modifications were made to AVCO's Pilot Plant to prevent contamination of the powders by scrap metals normally processed in the plant.

(2) Product Cleaning Systems

The products leaving the separation chamber are coated with ferrofluid and require cleaning and drying before shipment. The initial powder was cleaned in a batch vapor degreaser using trichloroethane as the cleaning agent. Unfortunately, this process resulted in contamination problems which necessitated a new approach.

The wash column cleaning approach is shown schematically in figure 78.

The washing vessel consisted of a Pyrex® column capable of handling batches of approximately 12 lb. New solvent piping and additional filters were installed to prevent any recurrence of the iron oxide contamination experienced with the initial cleaning procedure. However, for a production process, a continuous counter-current washing technique would be required.

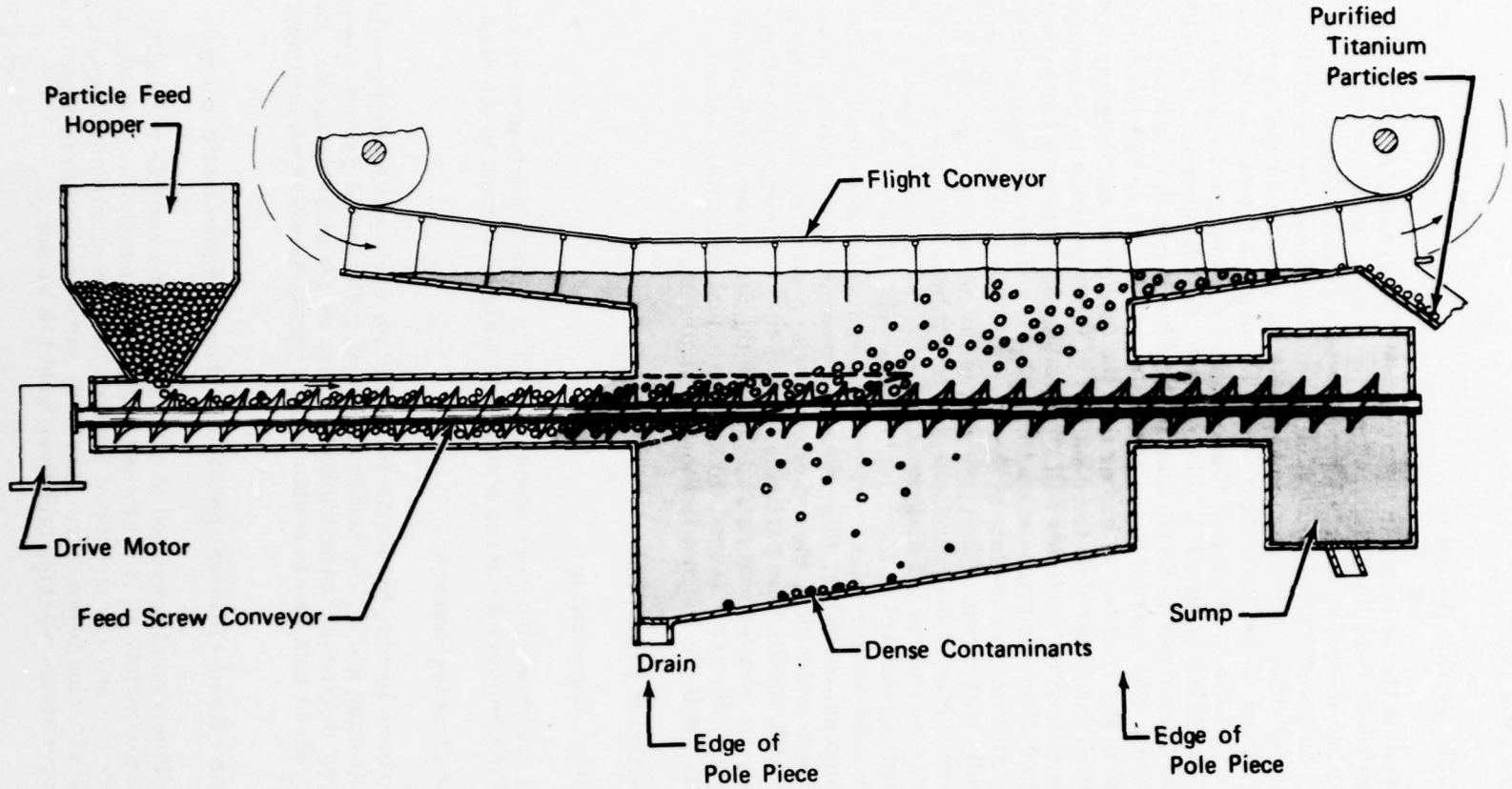

Figure 75. Conceptual Design Ferrofluid Particle Separation Vessel for AVCO Pilot Plant

FD 90078

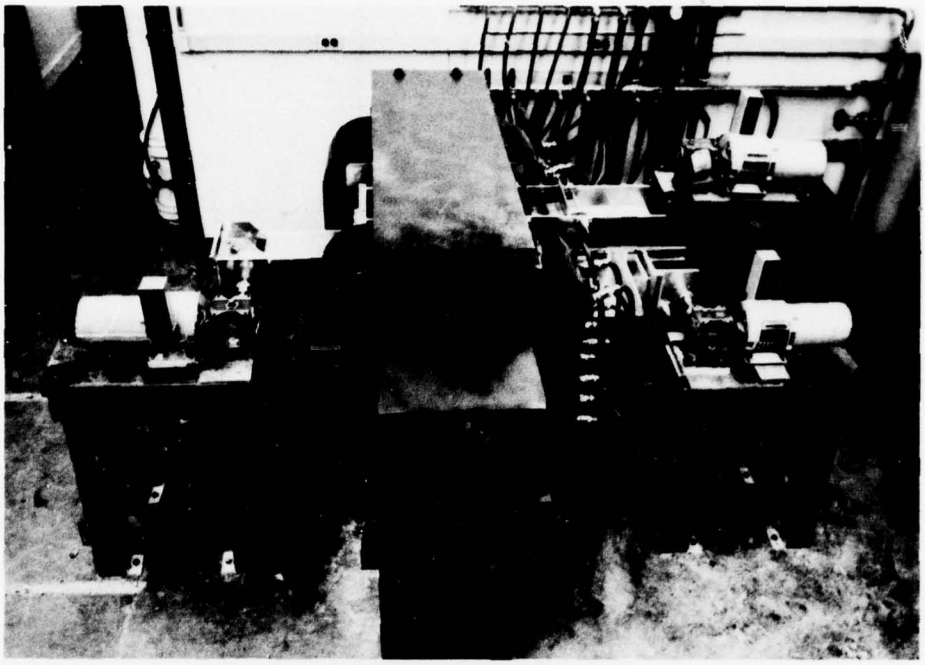

Figure 76. Ferrofluid Density Separation Electromagnet in AVCO Pilot Plant, During Assembly FD 90077

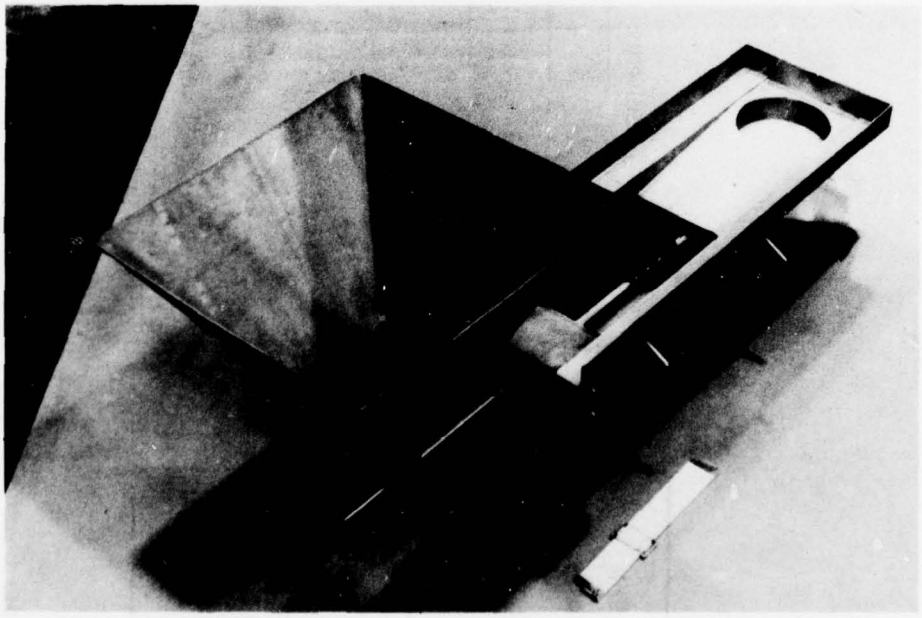

Figure 77. Particle Separation Vessel FD 90076

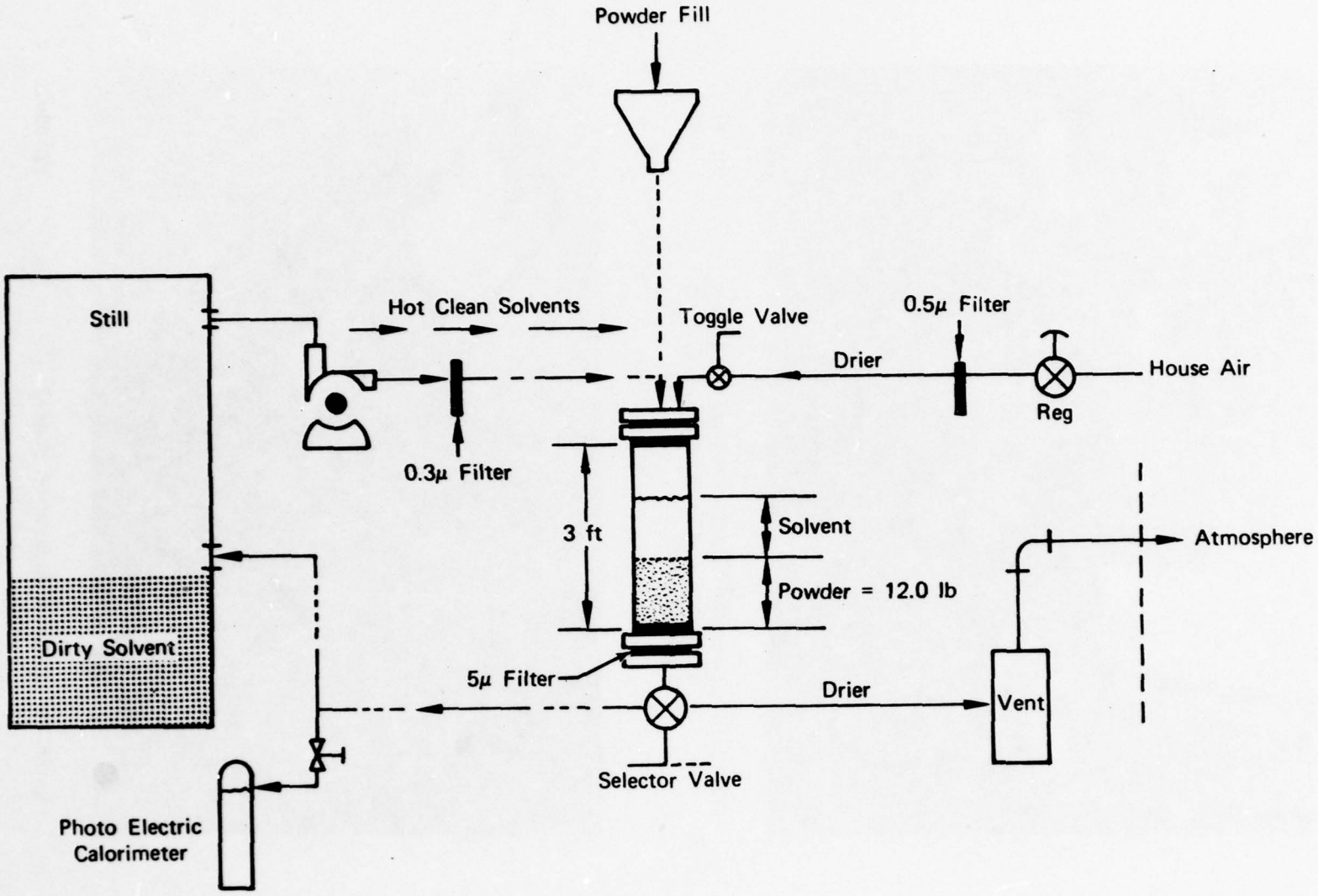

FD 98374

Figure 78. Wash Column Cleaning Approach

c. Purification Runs

(1) Initial Run

The first 270 lb of -35 mesh Ti-6246 powder, Lot 6852-C, was run in AVCO's modified separation vessel. The material was run in two passes. Sinks (material denser than ferrofluid density) amounted to 2.1% of the input weight during the first pass and 1.9% by weight in the second pass for a material loss of 3.9% (yield of 96.1%). However, a final inspection prior to shipment resulted in the discovery of caking and the presence of very small particles of iron oxide. Both of these contaminants were traced to the cleaning procedure. After several unsuccessful attempts to clean several samples the remaining contaminated powder was sent to P&WA.

(2) Final Run

An additional batch of 205 lb of -35 mesh Ti-6246 powder, Lot 6852-C, was processed under similar conditions to the first batch except that the revised cleaning method was used. The material was given two passes, with cleaning (washing) performed after each pass. The yield was 90% due to the lower actual apparent density of the ferrofluid, allowing more titanium to sink but giving even less chance for any heavy contaminants to float with the good material.

4. Pilot Plant Processed Powder Evaluation

a. Characterization of Ferrofluid Cleaned Powder

A characterization of the second batch of ferrofluid cleaned powder run at AVCO using the revised cleaning method was performed.

(1) X-Ray Evaluation

Prior problems and inconclusive results using blue etch anodizing required the use of radiography to evaluate powder cleanliness. Several samples were run with no indications of high density inclusions.

(2) Particle Size Distribution

The particle size distribution was conducted in accordance with ASTM B-214-64, viz., by screening a 100 gram sample on a vibrating platform in an 8-in. diameter US Standard Series Screen for 15 min. Results as shown in Table XXVI were nearly identical to the particle size distribution run on the as-received powder from Nuclear Metals, Inc.

(3) Bulk and Interstitial Chemistry Analysis

Results of bulk and interstitial analyses performed on the powder are tabulated in Table XXVII.

Table XXVI. Particle Size Distributions of 35 Mesh REP Ti-6Al-2Sn-4Zr-6Mo Ferrofluid Cleaned Powder

Screen Size Mesh	Screen Size μin.	Weight Retained on Screen, %	Less Than Cumulative, %
45	354	5.8	99.9
60	250	25.5	94.1
80	177	41.6	68.6
120	125	18.2	27.0
170	88	6.6	8.8
230	62	2.1	2.2
325	44	0.1	0.1
400	37	0.0	0

Table XXVII. Chemistry of Ferrofluid Cleaned REP Ti-6246 Powder

Identification	Al	Sn	Zr	Mo	Fe	H	N	O	C
Powder	6.1	2.0	4.1	6.0	0.060	0.0023	0.001	0.083 0.094	0.005
VHP						0.004 0.003	0.005	0.088 0.102	

(4) Vacuum Hot Pressing

Typical SEM photomicrographs of the ferrofluid cleaned powder are shown in Figure 79. The flat spots on the particles apparently result from the particles scraping on either the feed screw, the sides of the separator or against each other. A three inch diameter VHP (1650°F/15 psi) was fabricated from the cleaned powder. Half the VHP was forged down 50% and 2 tensile specimens were machined from both the as-VHP and the VHP and forged material shown in Figure 80. Tensile results are tabulated in Table XXVIII. The ductilities were lower than anticipated. Although no obvious inclusions were observed on the fracture surfaces, X-rays were taken on all four specimens and small high density inclusion indications were found in all the specimens. Apparently the smaller high density inclusions were not entirely removed by the ferrofluid cleaning process. A microprobe analysis of several of the fracture surfaces showed the presence of nickel, iron and silicon inclusions (Figure 81).

b. Full-Scale Extrusion

In accordance with the modified work statement, an extrusion can was designed to yield approximately 80 inches of 4-inch diameter stock. A drawing of the Task III extrusion can is presented in Figure 82. The can was filled with the batch of ferrofluid cleaned powder washed by the revised cleaning technique.

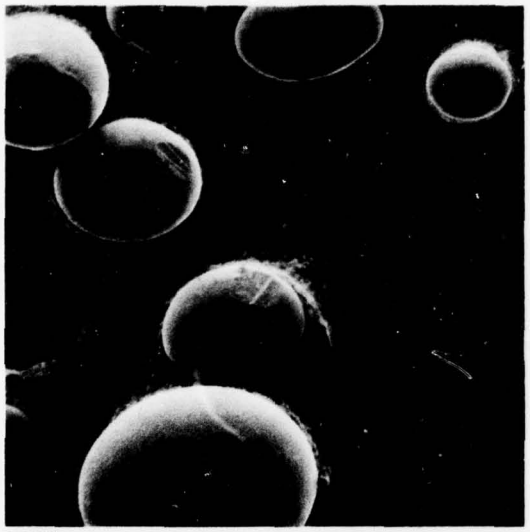

SEM Mag: 80X

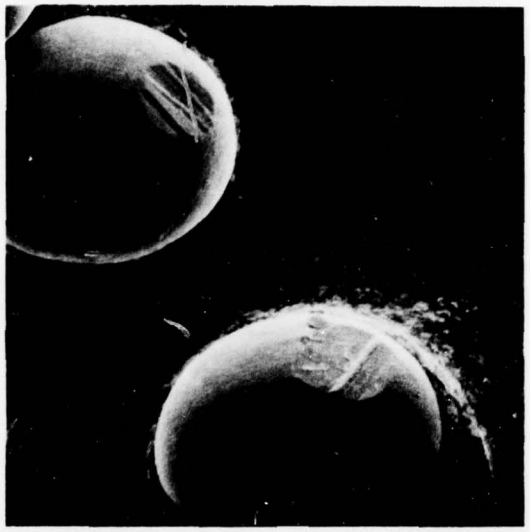

SEM Mag: 160X

SEM Mag: 300X

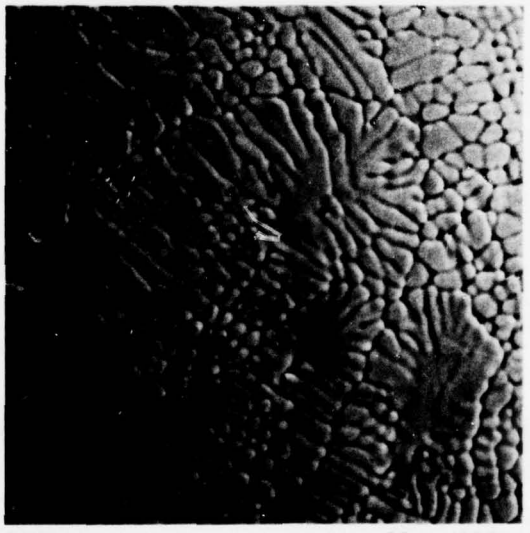

SEM Mag: 720X

Figure 79. Ferrofluid-Cleaned Ti-6246 REP Powder FD 98373
Task III

Mag: 100X

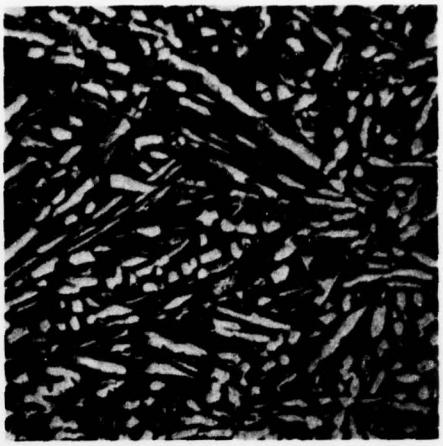

Mag: 500X

Mag: 100X

Mag: 500X

Figure 80. Microstructure of VHP (1650°F/15 ksi - Top) and VHP Plus 50% Forged (1650°F - Bottom) Ferrofluid Cleaned Ti 6246 Powder After a 1670°F/1/AC and 1100°F/8/AC Heat Treatment FD 98369

Table XXVIII. Room Temperature Tensile Test Results From Consolidated Ferrofluid Cleaned Ti 6246 Powder (1670°F/1/AC+1100°F/8/AC)

Identification	Yield Strength (ksi)	Ultimate Strength (ksi)	Elongation (%)	Reduction of Area (%)
Vacuum Hot Pressed (1650°F/15 ksi)	176.4	186.6	2.0	4.9
	177.8	188.6	5.3	19.9
Vacuum Hot Pressed and Forged (1650°F)	190.2	201.0	2.0	3.3
	192.9	202.0	4.7	15.5

Mag: 200X

Nickel

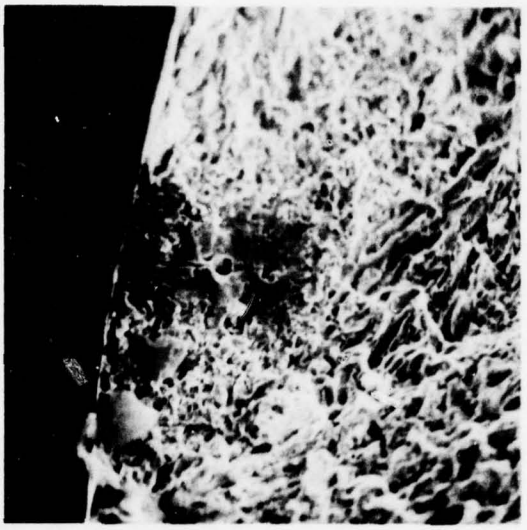

Mag: 400X

Iron

Mag: 100X

Silicon

Figure 81. Inclusions Found on Tensile Fracture Surfaces of VHP and Forged Ferrofluid Cleaned Ti 6246 Powder Tensile Specimens

FD 98368

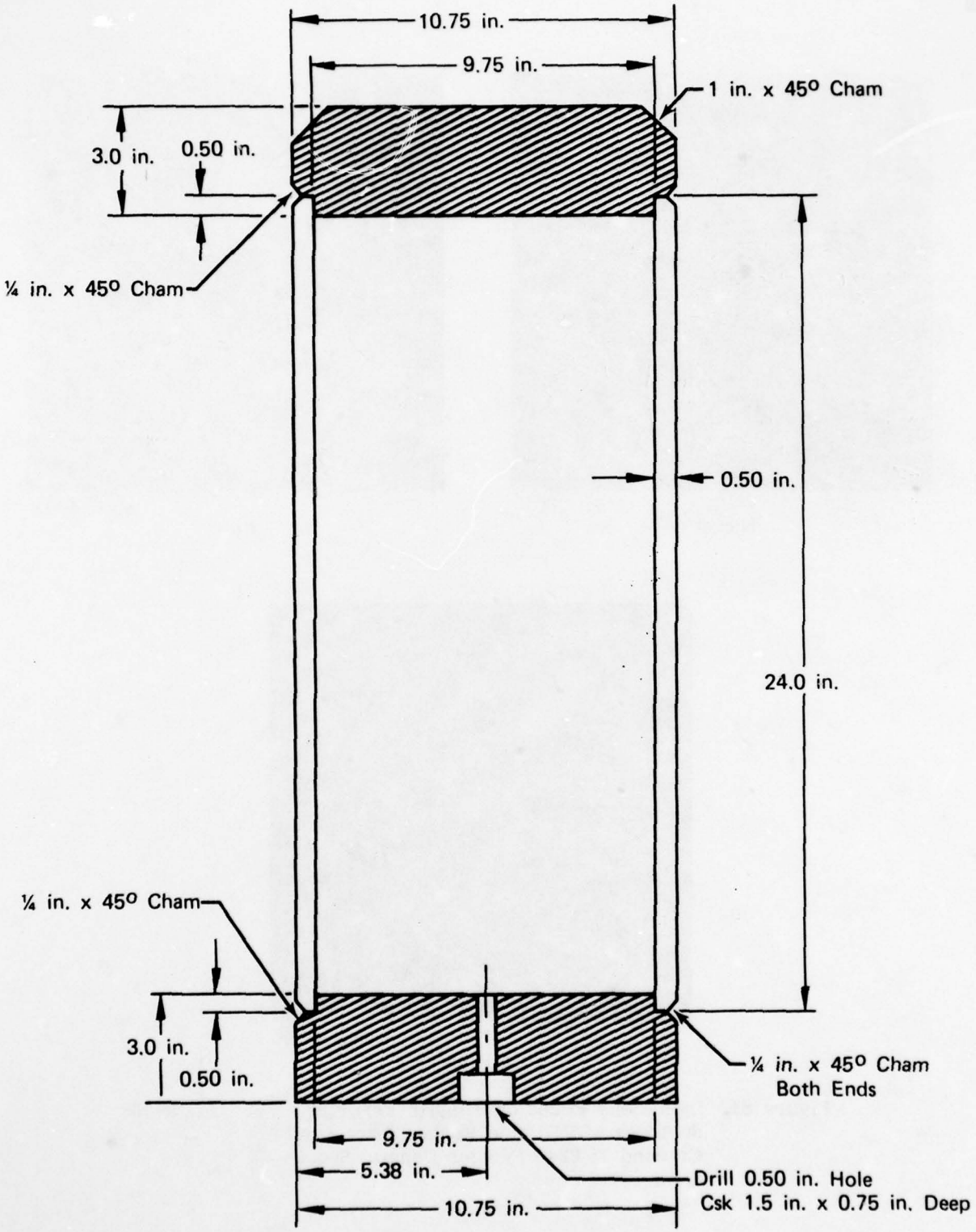

Figure 82. Full Scale Task III Extrusion Can FD 98366

Based on prior subscale extrusion work, the press had the capability of extruding the can at 1550°F after a 4-hr soak in a salt bath. Unfortunately, the extrusion stalled the press. After cooling, the extruded material (consisting of the nose plug and about 4 inches of partially consolidated powder) was cut off. The extrusion can was turned down approximately 1/4 inch in outside diameter and a new carbon steel plate welded to the nose of the extrusion can. To insure a successful extrusion, the salt bath was raised to 1625°F and the can soaked for 2-1/2 hours prior to extrusion. Upon examination of the extruded bar, evidence of salt contamination was observed.

Microstructural evaluation of slices revealed salt contamination throughout the extrusion. Microprobe analyses of the contaminated material indicated salt contamination throughout the material. Apparently, the weld leaked during the salt bath soak. In addition, porosity present at the center of the extruded material indicated an insufficient time was spent in the salt bath. Fine cracks were also observed in some of the etch slices (Figure 83). The material was found to be unsuitable for further evaluation.

5. Second Program Modification

After evaluation of the salt contaminated extrusion, discussions were held with the AFML technical monitor. Because the ferrofluid cleaning process had been determined effective in removing high density inclusions, a decision was made to attempt to clean the initial lot of ferrofluid processed powder that had been inadequately cleaned and therefore contaminated with iron oxide and acrylic resin binder. A comprehensive study involving several chemical solutions was performed on samples of the contaminated powder. A chemical cleaning technique was evaluated and found to be effective in removing iron. A modification to the program was suggested and approved.

Basically, the modified program consisted of cleaning a sufficient quantity of contaminated ferrofluid cleaned Ti 6264 powder to yield approximately 55 inches of 3-in. diameter extruded stock. The billet underwent an evaluation similar to Task II evaluations prior to being forged into six flat pancakes. The pancakes were heat-treated and cut up for a detailed structural and mechanical property evaluation.

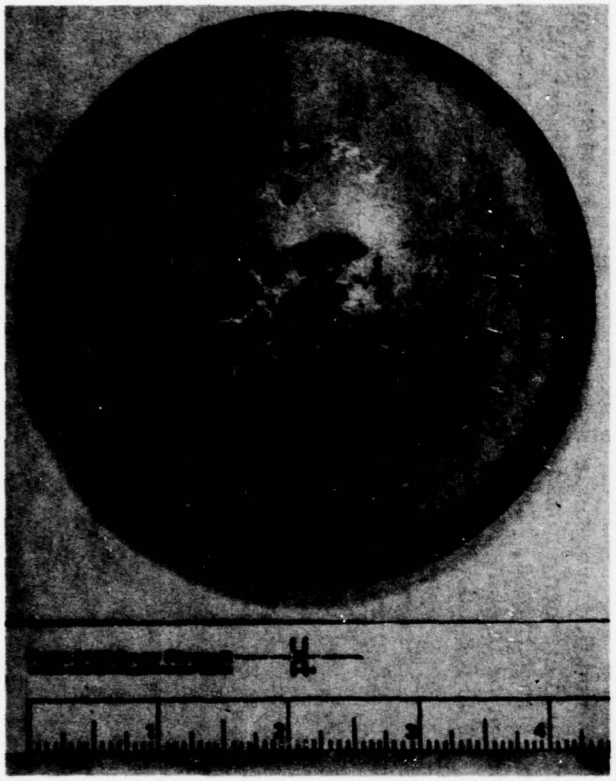

Mag: ¾X

Porosity

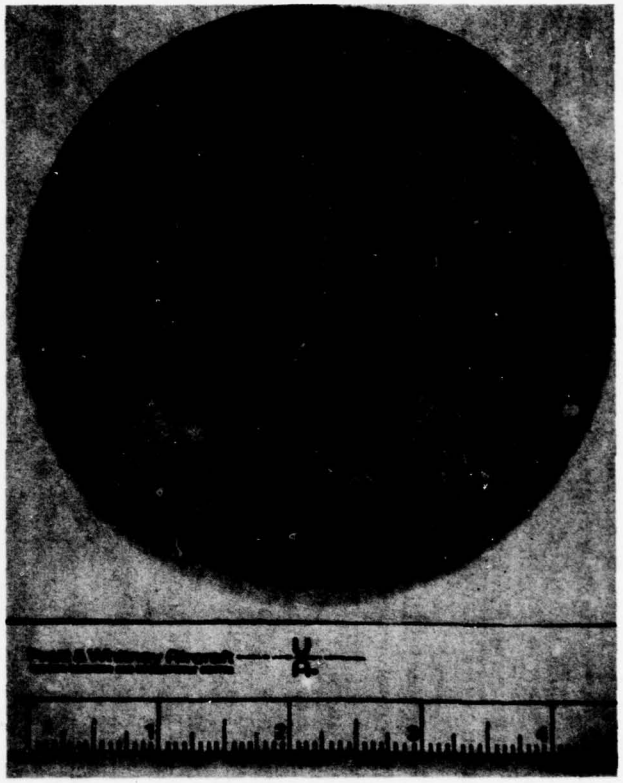

Mag: ¾X

Cracks

Figure 83. Macroslices of Full-Scale Extrusion Showing Porosity and Small Cracks

FD 98367

a. Selection of Cleaning Technique

Several chemical solutions were used in an attempt to remove the iron contamination. Atomic absorption analysis for iron was used before and after each cleaning technique to determine the effectiveness of each solution in removing the iron. The most effective cleaning technique utilized a PS 140 solution which is a neutral cleaning and descaling solution containing a minimum 36% by weight chelating agent. Based on this information, a larger sample of powder was cleaned and a vacuum hot pressing (VHP) fabricated (1650°F/15 ksi). The VHP was subsequently forged at 1650°F and heat-treated (1670°F/1/AC+1100/8/AC). The tensile test results of the forged and heat-treated VHP are presented in Table XXIX. The material exhibited good ductility for the high tensile strengths resulting from this heat treatment and additional powder was therefore cleaned using the following procedures:

1. Powder was cleaned using a batch process consisting of 2000 grams of powder mixed with 15 grams of PS 140 and 1700 ml of deionized water
2. The metal was heated to approximately 212°F and stirred frequently for 1 hr
3. After one hour, the powder was washed under a stream of tap water, stirring constantly and thereby removing lint, plastic, paper, etc.
4. The batch of powder was rinsed three times with deionized water and subsequently dried in flat baking dishes in an oven at 212°F.

Table XXIX. Room Temperature Tensile Properties of PS 140 Cleaned Ti 6246 Powder

Yield Strength (ksi)	Ultimate Strength (ksi)	Elongation (%)	Reduction of Area (%)
190.0	200.5	6.7	15.5
186.5	198.5	8.0	17.5
185.0	197.8	5.3	9.4

b. Can Preparation

The can design for the extrusion was the same as the full-scale extrusion can except the outside diameter was reduced from 10.75 in. to 8.00 in. Prior to welding, the can was chemically cleaned as follows:

1. Immerse in muriatic acid
2. Electrolytic - alkaline clean
3. Hot water power spray
4. Immerse in oil
5. Degrease in trichlorethylene

After the container was verified to be leak tight, powder was poured into the can under an argon atmosphere. After vacuum outgassing at 750°F for approximately 30 hours the evacuation stem was sealed by hot-crimping and welding.

c. Powder Consolidation

The size of the extrusion can was reduced to 8.0-in. OD due to the amount of powder available. A sufficient amount of powder was available to complete all of the forging and testing requirements.

Prior to extrusion the can was heated for 12 hr at 1600°F. The material was extruded from an 8-in. diameter liner through a 3.140-in. diameter orifice die, with a 60-deg included angle (a reduction ratio of 6.5 to 1). Average upset pressures of 1987 tons (extrusion constant equals 22.0 tons/in^2) and average run pressures of 1513 tons (extrusion constant equals 16.7 tons/in^2) were required. Approximately 55% of the maximum press capacity was used.

d. Billet Evaluation

(1) Structural

Macroetch slices taken near the nose and tail of the extrusion indicated full consolidation and no detectable contamination. However, X-ray analysis revealed small high density indications which could not be verified by subsequent metallographic techniques. A variation in grain size from edge to center was noted (Figure 84). A large amount of fine primary alpha was present near the edge with coarser grains near the center. *Differences in cooling rate of the* material and the adjacent tooling probably accounted for the variation in structure. The structure of the extrusion after a 1670°F/1/AC+1100°F/8/AC heat-treatment consisted of elongated primary alpha in a fine transformed beta matrix (Figure 85) identical to material extruded and heat-treated in a like manner in Task II. (See Figure 52).

(2) Mechanical Properties

Tensile and room temperature stress-rupture testing was performed on the extruded and heat-treated material. Results were nearly identical to the Task II 1600°F extrusion except for the low elongation and reduction of area on one of the specimens (as shown in Table XXX). An electron microprobe analysis of the low ductility specimen's fracture surface revealed the inclusion to be similar to the base metal. Stress-rupture properties were typical of similarly processed material.

Table XXX. Mechanical Properties of Task III Extrusion (1600°F) [1670°F(1)AC plus 1100°F/8/AC]

RT Tensile				RT Notched Stress Rupture		
0.2% YS	UTS	% EL	% RA	Failure Stress (ksi)	Total Time (hr)	Time at Failure Load (hr)
160.1	172.4	2.5	7.1	220	17.8	FOL
158.3	175.6	13.0	30.1	220	15.5	0.5

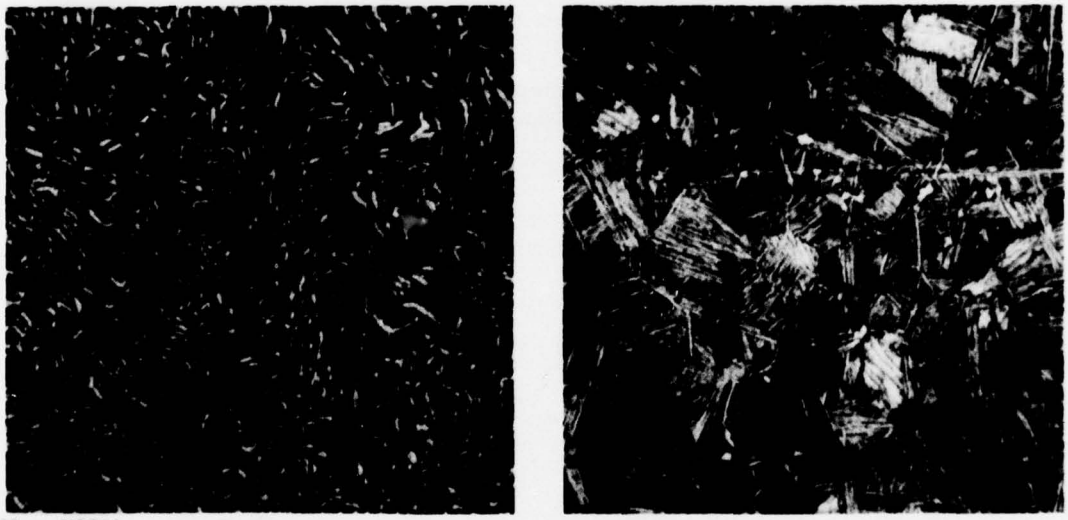

Mag: 500X Edge

Mag: 500X Center

Figure 84. Macro and Microstructure of Extruded (1600°F) Ti-6Al-2Sn-4Zr-6Mo REP Cleaned Powder FD 101155

Mag: 100X Mag: 500X

Figure 85. Microstructure of Heat Treated (1670°F/1/AC +1100°F/8/AC) Extrusion FD 101156

(3) Chemistry

An interstitial and iron analysis of the extruded material (Table XXXI) revealed the material to be within specification limits and compared favorably with previous analyses.

Table XXXI. Interstitial and Iron Analysis of Large-Scale Extrusion

Fe	O_2	N_2	H_2	
	w/o			
<0.15	0.080	0.013	0.0037	
0.15 Max	0.15 Max	0.04 Max	0.015 Max	PWA 1216 Specification

e. Subscale Disk Shapes

Four subscale disk shapes were produced using existing tooling for structural evaluation. No difficulty was encountered in forging (1650°F) any of the disks. Different configurations were used to show the ability of the powder billet to fully utilize the potential of the GATORIZING™ process.

The preforms and cross-sections of the disks are shown in Figures 86 and 87. Structural evaluation revealed a uniform microstructure with good grain flow and no structural abnormalities.

f. Forging Evaluation

Six pancakes were forged from the extruded billet. The forging temperatures were chosen to cover the range of temperatures normally used on Ti-6Al-2Sn-4Zr-6Mo. The forging mults received an 88% reduction. The pancakes measured approximately 8 in. in diameter by 3/4-in. thick. A single step forging reduction was used. Two pancakes were forged at each of the three selected forging temperatures (Table XXXII). Three of the pancakes, one representing each of the forging temperatures, were heat-treated per the PWA 1220 specification. The remaining three pancakes were heat-treated to optimize fracture toughness properties. The heat treatment was based on previous results obtained from conventionally processed material.

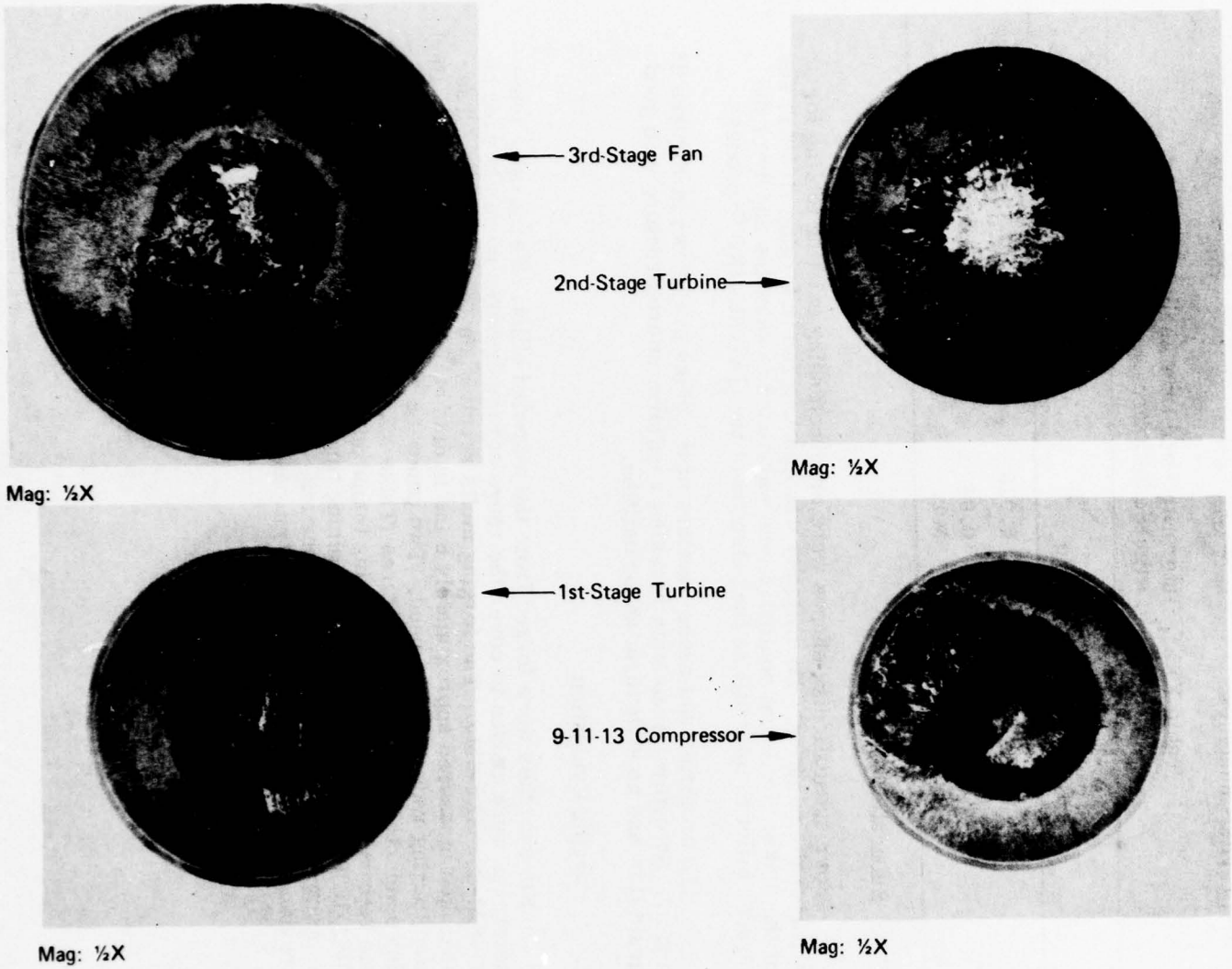

FD 101157

Figure 86. Subscale Disk Preforms

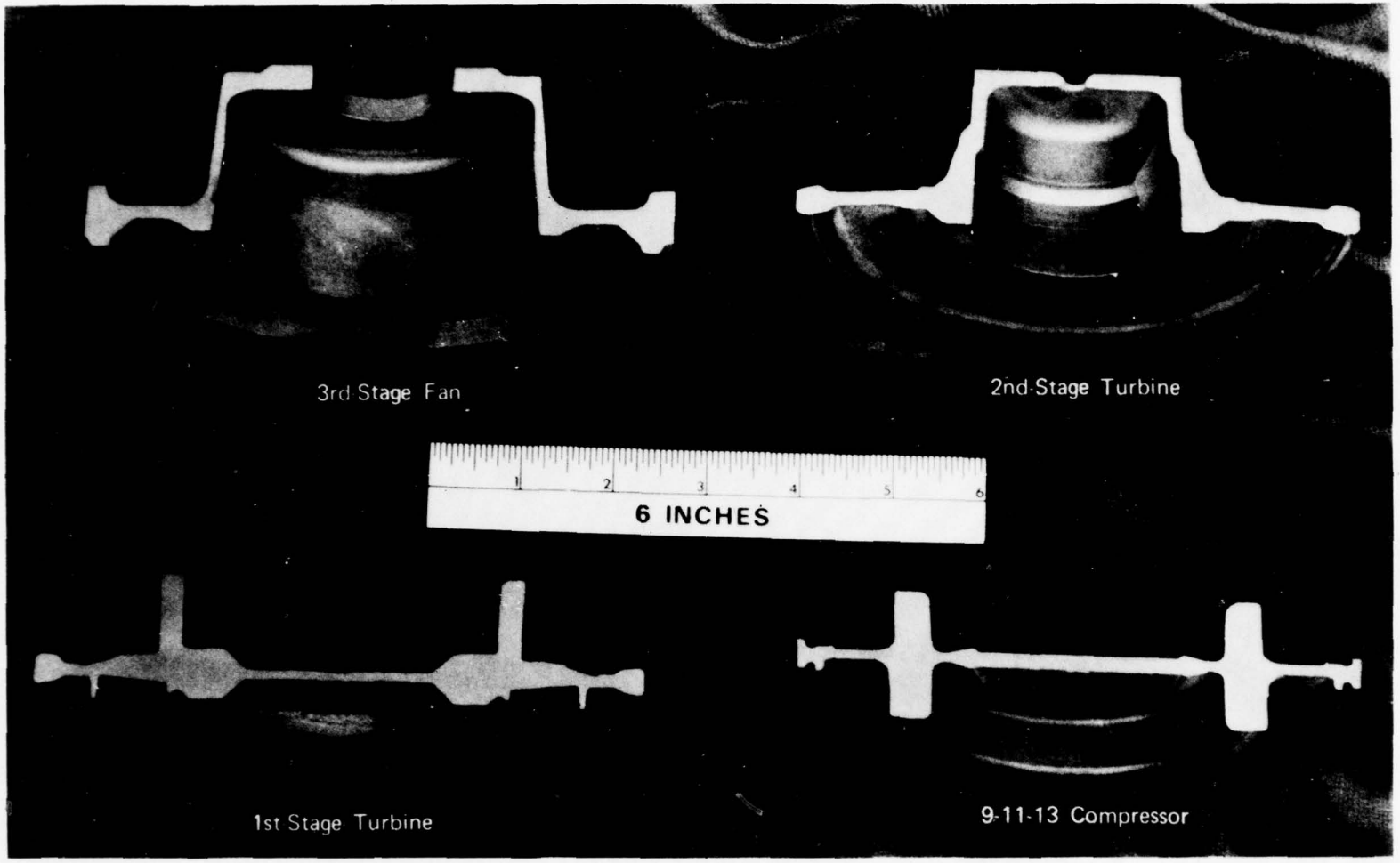

Figure 87. Cross Sections of Subscale Disk Forging

FD 101159

Table XXXII. Pancake Processing Parameters

Pancake Identification	Forge Temperature (°F)	Heat Treatment
1	1600	1690°F(2)RAC+1525°F(2)AC +1100°F(8)AC
2	1600	1720°F(2)FC to 1500°F(2)AC +1100°F(8)AC
3	1650	1690°F(2)RAC+1525°F(2)AC +1100°F(8)AC
4	1650	1720°F(2)FC to 1500°F(2)AC +1100°F(8)AC
5	1700	1690°F(2)RAC+1525°F(2)AC +1100°F(8)AC
6	1700	1720°F(2)FC to 1500°F(2)AC +1100°F(8)AC

The cutup plan for each of the pancakes is shown in Figure 88.

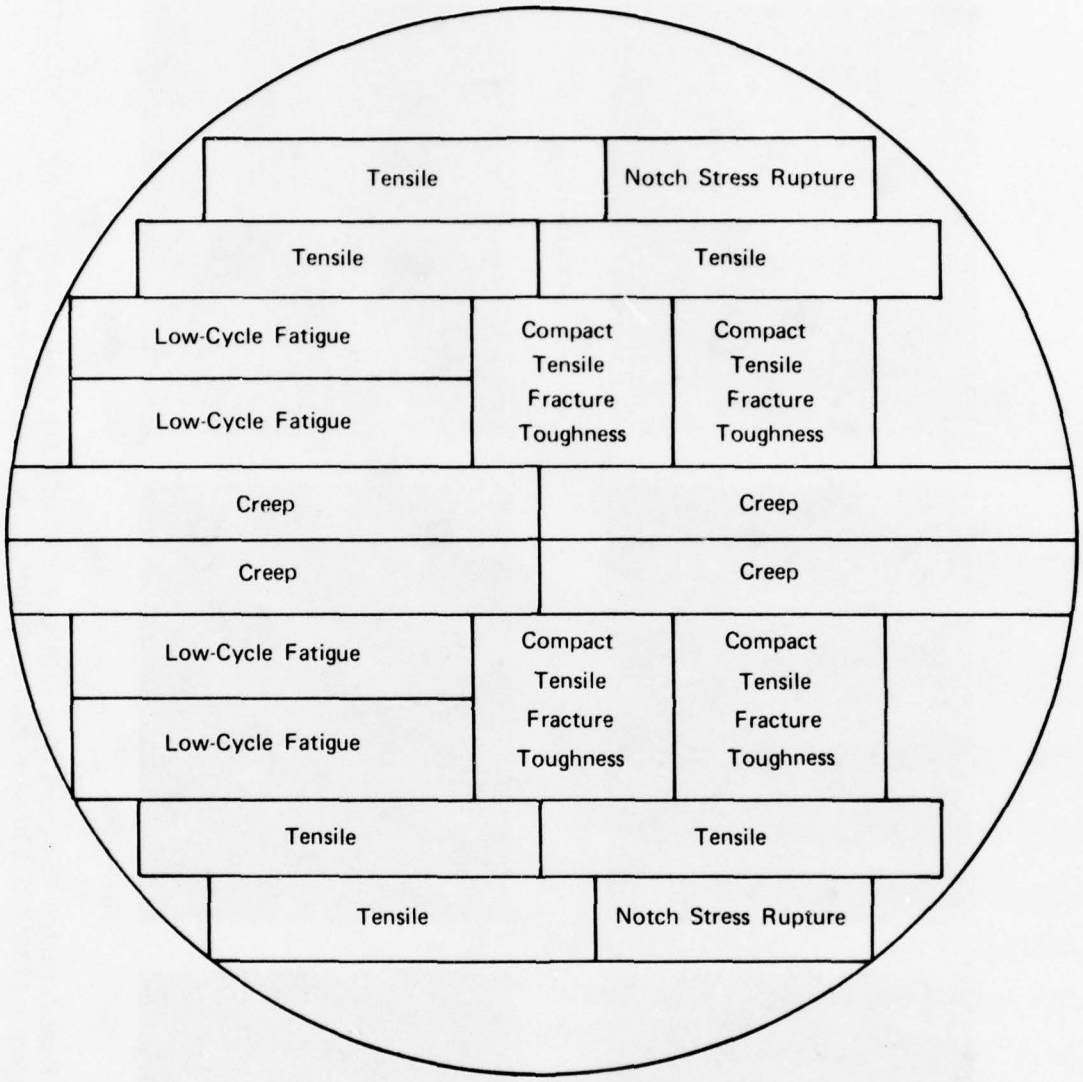

Figure 88. Diagram for Test Specimens Machined from FD 101160 8-in. Diameter Pancake Forgings

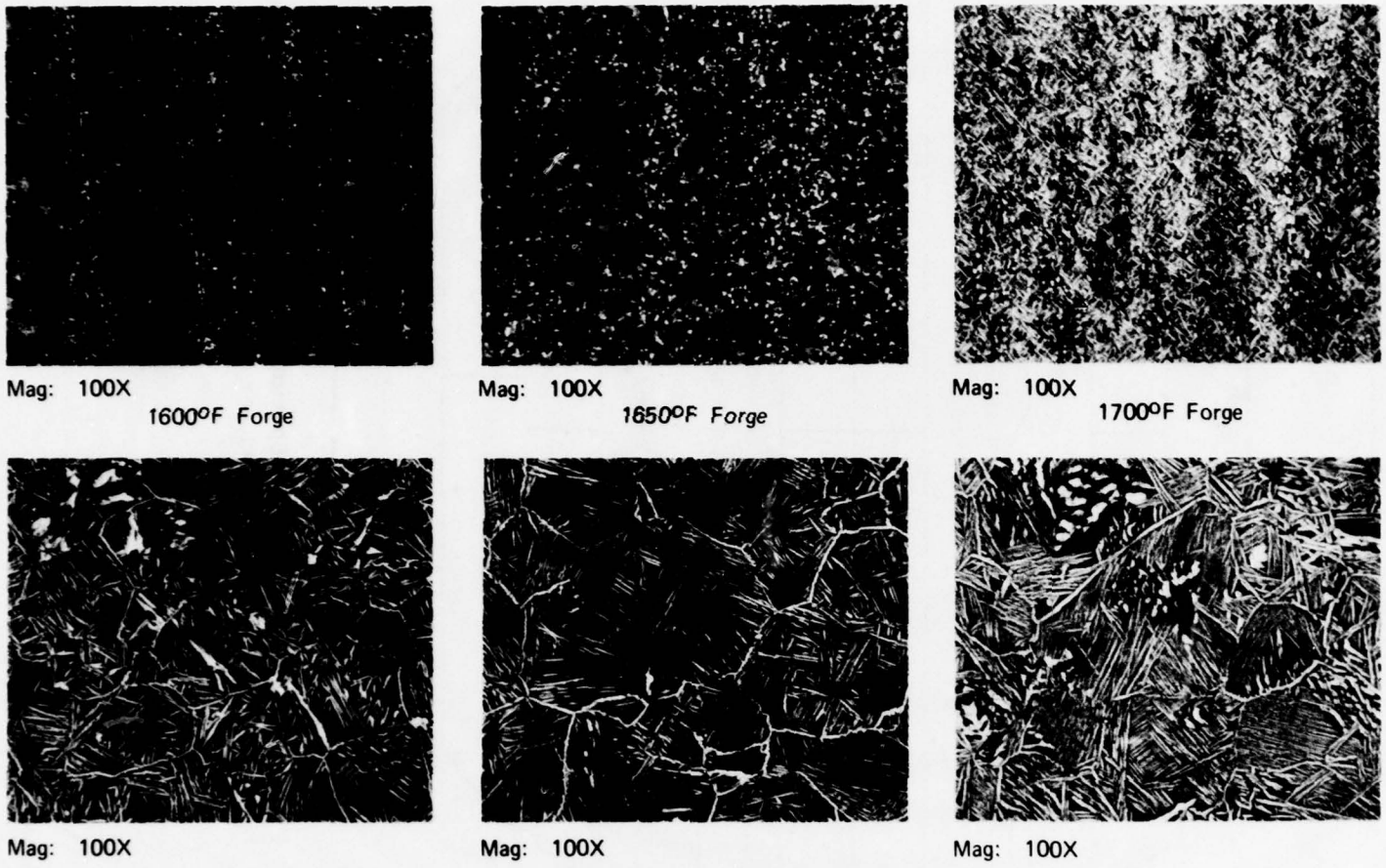

Figure 89. Microstructures of Heat-Treated Forgings (Top - 1690°F/2/Rapid Air Cool +1525°F/2/AC +1100°F/8/AC) (Bottom - 1720°F/2/Furnace Cool to 1500°F/2/AC +1100°F/8/AC) FD 101161

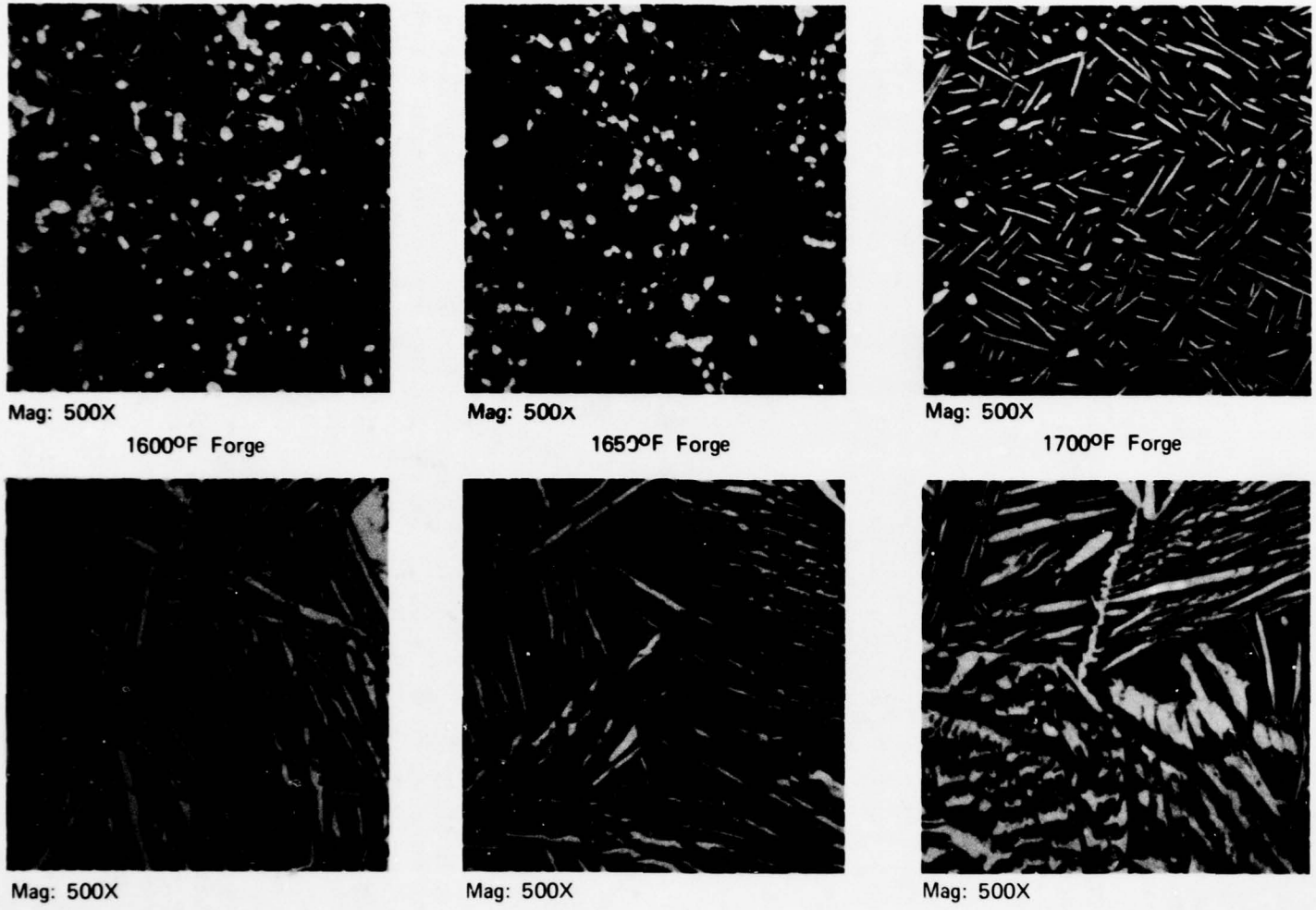

Figure 90. Microstructures of Heat-Treated Forgings (Top – 1690°F/2/Rapid Air Cool +1525°F/2/AC +1100°F/8/AC) (Bottom - 1720°F/2/Furnace Cool to 1500°F/2/AC+1100°F/8/AC FD 101158

(1) Structural Evaluation

A microstructure evaluation was performed on the forged and heat-treated pancakes. The only discernible effect of forge temperature was observed on the 1700°F forged pancake that received the standard PWA 1220 heat-treatment (Figures 89 and 90). The alpha was in the form of elongated platelets with very little equiaxed alpha. The material receiving the standard PWA 1220 heat-treatement had less primary alpha present due to a slightly lower than normal beta transus.

The beta transus was found to be about 1700°F, which is slightly lower than normally observed for this alloy (1720°F).

The special heat-treatment given to the other pancake from each forging temperature resulted in a beta structure. Although the desired fine beta grain size microstructure was not obtained in the pancakes, this type of structure has resulted in excellent fracture toughness on conventionally processed material. The high solution heat-treatment resulted in identical microstructures, namely beta grains consisting of coarse acicular alpha platelets. Apparently there is a critical temperature/forging range to optimize Ti 6246's response to this type of heat-treatment.

(2) Mechanical Properties

(a) Tensile

Room temperature tensile strengths were sensitive to the amount of primary alpha present in the microstructure. The best strengths were obtained in pancakes No. 1 and No. 3 which contained the largest amount of primary alpha. The failure of all the specimens to meet PWA 1220 specification can be attributed to the lower than usual amount of primary alpha and the presence of inclusions. The lower strengths and ductilities of the high alpha/low beta heat-treated material (pancakes No. 2, 4, and 6) was attributed to the beta microstructure. A comparison of the tensile results and the PWA 1220 design curve is shown in Figures 91 through 94. The most obvious differences were noted in elongation and reduction in areas. Lower elongations were most notable at room temperature. Elevated temperature testing revealed elongations equivalent to or slightly below conventionally processed material. The most significant differences were noticed in reduction in areas. The structures containing primary alpha exhibited the best reduction in areas. Pancake No. 6 (1700°F forge, 1720°F solution) exhibited the lowest reduction in area (Table XXXIII).

In conclusion, tensile properties (particularly ductility) reflect microstructural differences as well as contamination present in the material. Tensile strengths (yield and ultimate) are not significantly affected by either forge temperature or inclusion level. The low reduction in areas were exhibited primarily by the pancakes exhibiting a beta structure.

Table XXXIII. Task III Tensile Properties

Pancake Serial No.	Forging Temperature (°F)	Heat Treatment	Test Temperature (°F)	YS (ksi)	UTS (ksi)	EL (%)	RA (%)
1	1600	1690°F/2/RAC+1525/2/AC	RT	157.2	174.6	11	24
			RT	163.0	167.9	2.0	9.4
		+1100°F/8/AC	400	127.7	152.1	16	36
			400	126.1	151.1	15	33
			600	117.1	144.7	14	36
			600	116.6	143.5	12	20
2	1600	1720°F/2/FC to 1500°F/2/AC	RT	149.7	170.7	13	25
			RT	154.1	170.9	12	25
		°1100°F/8/AC	400	120.1	147.3	14	35
			400	122.9	148.2	13	21
			600	107.2	139.7	14	29
			600	106.2	139.0	13	23
3	1650	1690°F/2/RAC+1525°F/2/AC	RT	153.6	169.2	9.6	18
			RT	161.4	171.9	2.0	0.3
		+1100°F/8/AC	400	124.7	147.1	17	50
			400	125.7	150.4	13	21
			600	115.1	138.3	14	33
			600	119.9	140.6	17	49
4	1650	1720°F/2/FC to 1500°F/2/AC	RT	152.8	172.6	8.4	11
			RT	153.8	172.5	7.7	11
		+1100°F/8/AC	400	125.5	152.0	12	17
			400	124.1	150.4	11	16
			600	97.4	139.6	11	18
			600	110.8	145.3	13	19
5	1700	1690°F/2/RAC+1525°F/2/AC	RT	150.1	167.7	13	22
			RT	155.4	171.1	12	18
		+1100°F/8/AC	400	121.9	145.9	15	27
			400	119.4	144.9	16	35
			600	109.1	137.0	14	32
			600	111.2	134.4	15	34

Table XXXIII. Task III Tensile Properties (Continued)

Pancake Serial No.	Forging Temperature (°F)	Heat Treatment	Test Temperature (°F)	YS (ksi)	UTS (ksi)	EL (%)	RA (%)
6	1700	1720°F/2/FC to 1500°F/2/AC	RT	152.4	168.8	3.9	6.0
			RT	151.7	169.9	4.6	6.4
		+1100°F/8/AC	400	119.0	147.1	12	13
			400	118.9	147.2	10	15
			600	106.5	138.6	11	17
			600	108.7	142.9	10	14
PWA 1220 Specification			RT	155	170	10	20
			400	124	147	12	30

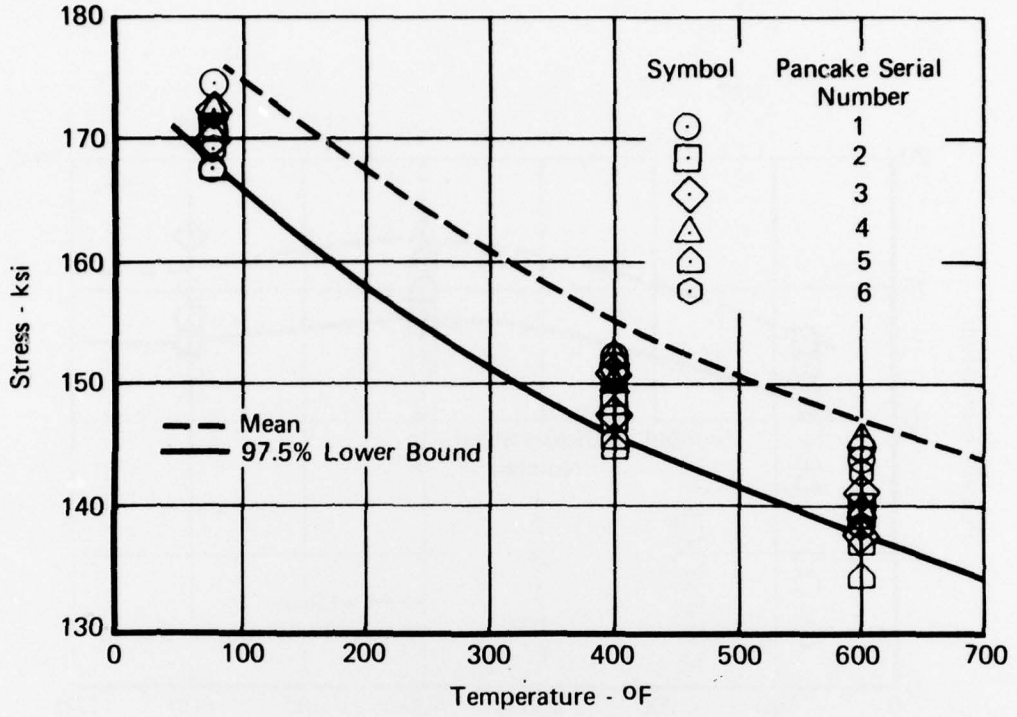

Figure 91. PWA 1220 Ultimate Tensile Strength FD 101702

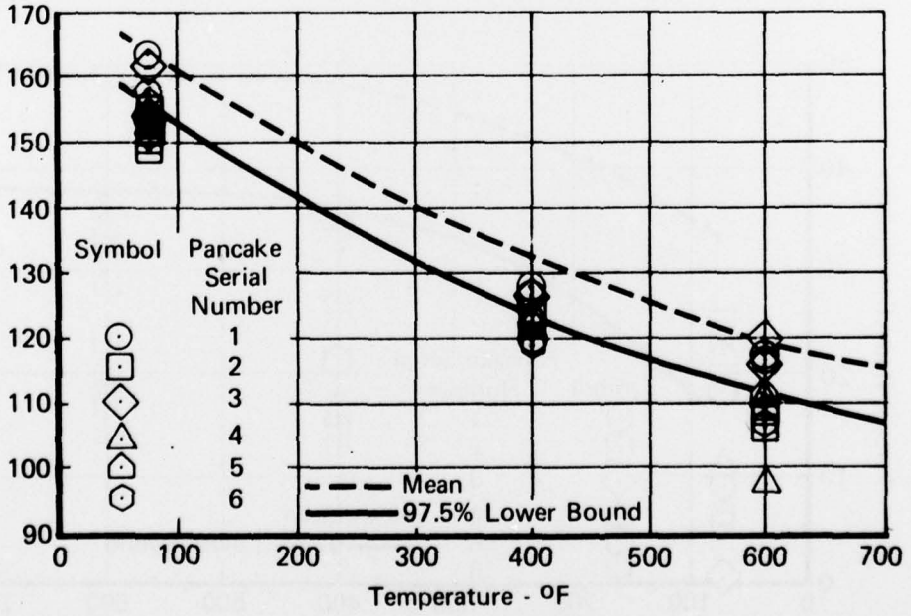

Figure 92. PWA 1220 Yield Strength FD 101703

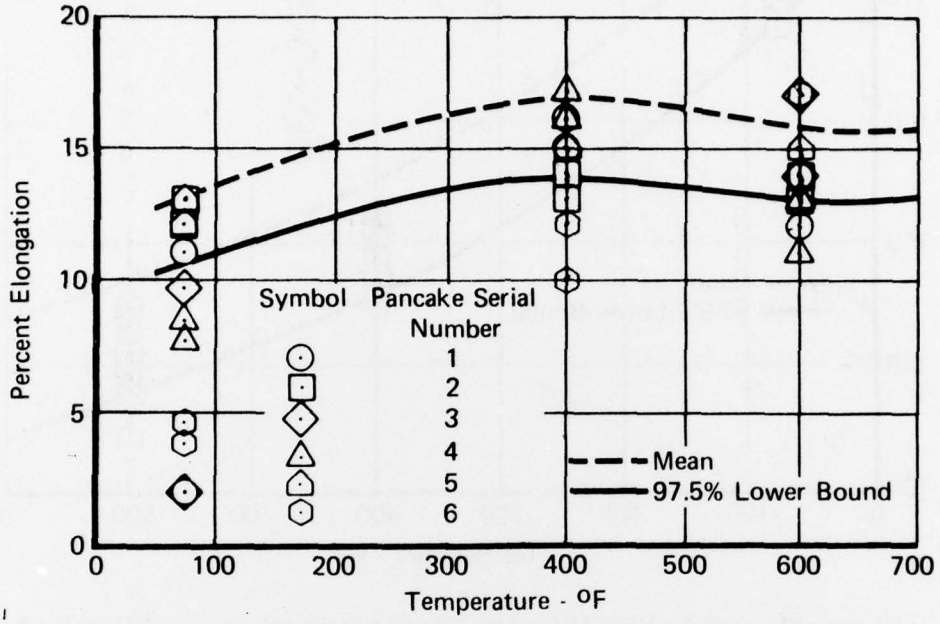

Figure 93. PWA 1220 Elongation FD 101704

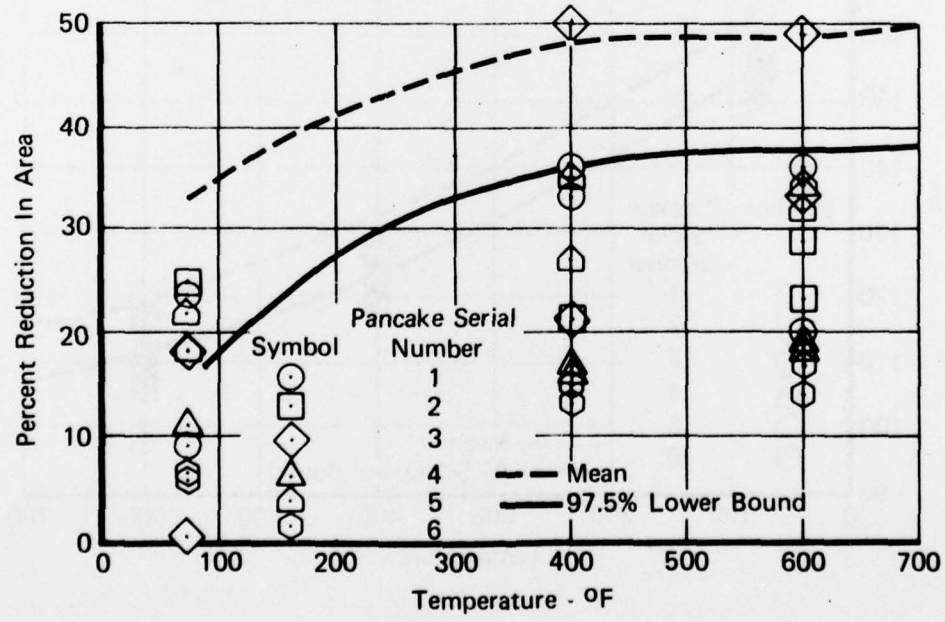

Figure 94. PWA 1220 Reduction in Area FD 101705

(b) Creep

A Larson/Miller curve comparing the pancake forging properties with PWA 1220 is shown in Figure 95. Due to the high solution temperatures, the grain sizes were slightly larger than normal. The creep results, shown in Table XXXIV, reflect this fact. Properties, in general, exceeded those of conventionally processed Ti-6246 at and above 800°F.

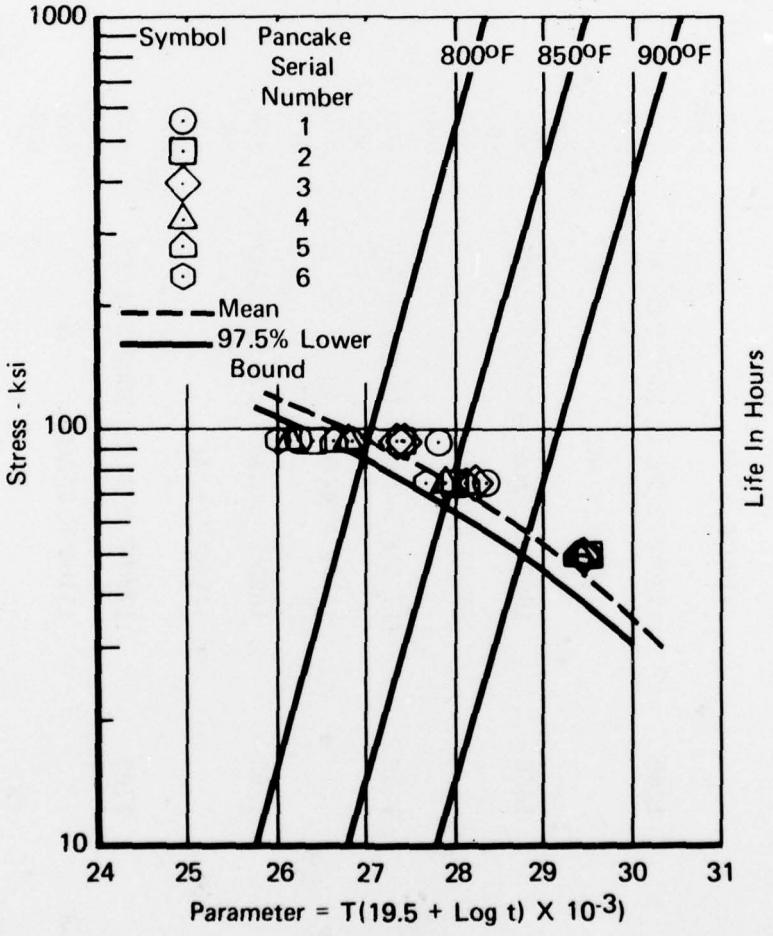

Figure 95. PWA 1220 0.2 Percent Creep FD 101706

Table XXXIV. Task III Creep Properties

Pancake Serial No.	Forging Temperature (°F)	Heat Treatment	Test Temperature (°F)	Stress (ksi)	Creep (hr) 0.1%	Creep (hr) 0.2%
1	1600	1690°F/2/RAC+1525°F/2/AC	800	95	55.3	362.5
			800	95	0.4	23.9
		+1100°F/8/AC	850	75	31.2	139.2
			900	50	23.3	161.3
2	1600	1720°F/2/FC to 1500°F/2/AC	800	95	0.4	27.1
			800	95	41.7	191.7
		+1100°F/8/AC	850	75	15.4	80.1
			900	50	28.4	178.1
3	1650	1690°F/2/RAC+1525°F/2/AC	800	95	33.3	175.3
			800	95	73.7	189.5
		+1100°F/8/AC	850	75	31.5	123.5
			900	50	29.3	163.3
4	1650	1720°F/2/FC to 1500°F/2/AC	800	95	2.6	61.4
			800	95	0.4	21.1
		+1100°F/8/AC	850	75	14.6	62.9
			900	50	20.0	136.0
5	1700	1690°F/2/RAC+1525°F/2/AC	800	95	0.8	48.3
			800	95	4.1	63.3
		+1100°F/8/AC	850	75	27.5	97.5
			900	50	22.5	123.5
6	1700	1720°F/2/FC to 1500°F/2/AC	800	95	0.2	14.3
			800	95	1.7	3.2
		+1100°F/8/AC	850	75	7.6	48.0
			900	50	33.4	154.5

(c) Low-Cycle Fatigue

The constant strain low-cycle fatigue results are presented in Table XXXV and plotted in Figures 96 and 97. Both room temperature and 500°F results compare favorably with PWA 1220 data. The effect of grain size was evidenced at both temperatures with the finer grain sizes exhibiting better LCF life. The presence of small inclusions does not appear to affect LCF properties at room temperature or 500°F.

Table XXXV. Task III LCF Properties

Pancake Serial No.	Forge Temperature	Heat Treatment	Test Temperature	Strain	Cycles to Fail
			RT	1.0	7,870
1	1600	1690°F/2/RAC + 1525°F/2/AC	RT	1.5	3,200
			500	1.0	12,846
		+1100°F/8/AC	500	1.0	10,865
			RT	1.0	No test
2	1600	1720°F/2/FC to 1500°F/2/AC	RT	1.5	2,025
			500	1.0	8,497
		+1100°F/8/AC	500	1.5	3,892
			RT	1.0	5,417
3	1650	1690°F/2/RAC + 1525°F/2/AC	RT	1.25	2,938
			500	1.0	7,947
		+1100°F/8/AC	500	1.5	3,869
			RT	1.25	2,062
4	1650	1720°F/2/FC to 1500°F/2/AC	RT	1.5	885
			500	1.0	10,120
		+1100°F/8/AC	500	1.5	4,108
			RT	1.0	6,840
5	1700	1690°F/2/RAC + 1525°F/2/AC	RT	1.5	618
			500	1.0	11,860
		+1100°F/8/AC	500	1.5	1,922
			RT	1.0	6,726
6	1700	1720°F/2/RC to 1500°F/2/AC	RT	1.5	1.196
			500	1.0	8,377
		+1100°F/8/AC	500	1.5	2,490

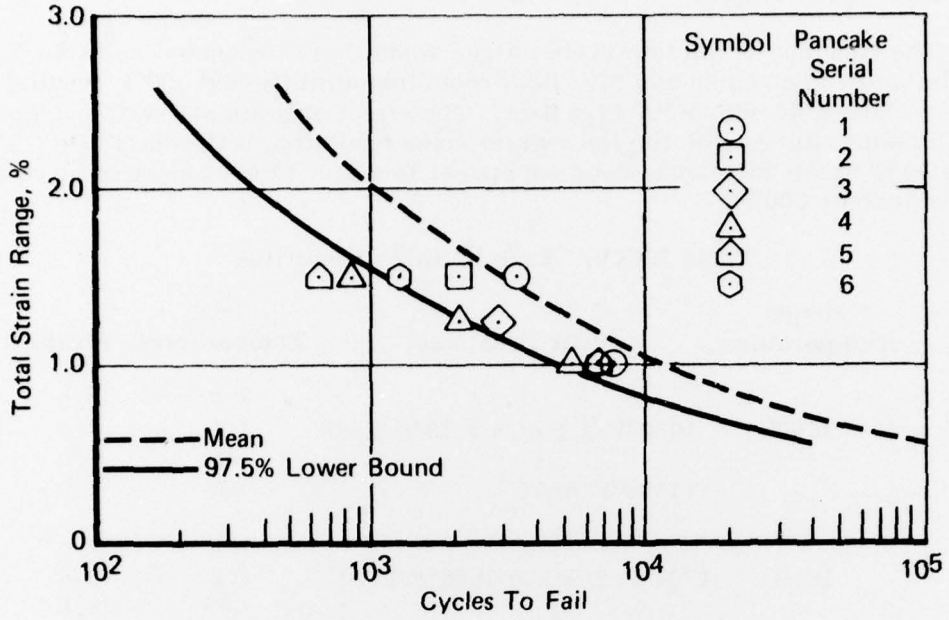

Figure 96. PWA 1220 RT Low-Cycle Fatigue (Strain Control) FD 101707

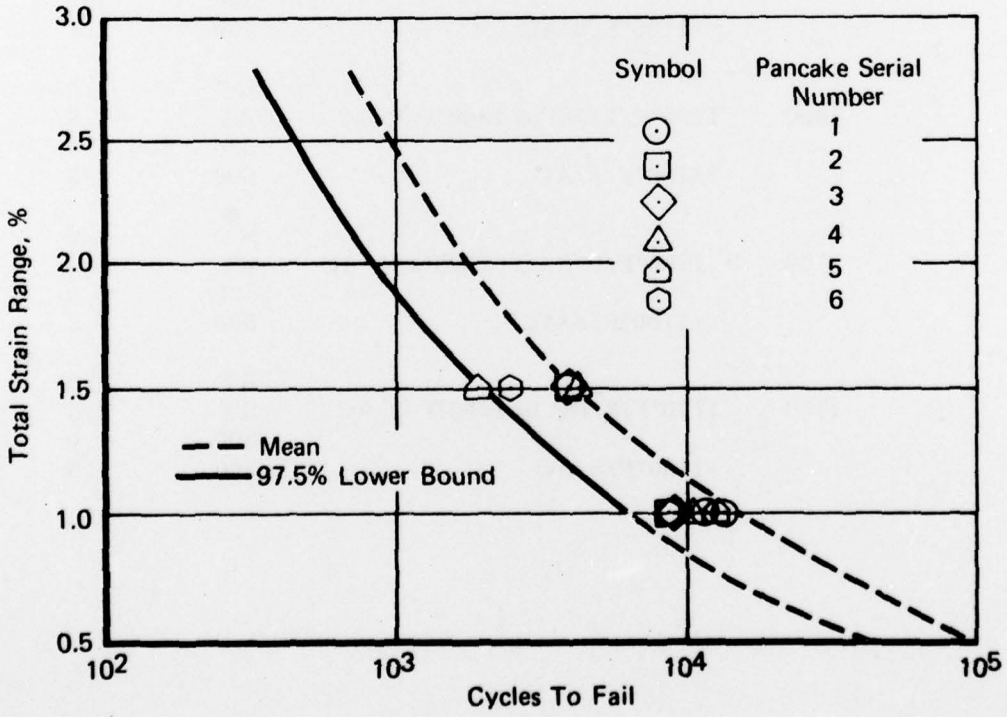

Figure 97. PWA 1220 500°F Low-Cycle Fatigue (Strain Control) FD 101708

(d) Fracture Toughness

Room temperature fracture toughness values were substantially above the PWA 1220 specification minimum of 20 ksi $\sqrt{in.}$ (Table XXXVI). Although the pancakes received the PWA 1220 heat treatment, the amount of primary alpha was less than anticipated and resulted in fracture toughness numbers approximately 10 ksi $\sqrt{in.}$ higher than conventionally processed and heat treated PWA 1220. Previous heat treatment studies on conventionally processed Ti-6246 have shown that a fracture toughness of 40 ksi $\sqrt{in.}$ can be obtained with a yield strength of 150-160 ksi. The 400°F fracture toughness values are comparable to conventionally processed material of the same strength level.

The remaining pancakes (2, 4 and 6) exhibited toughness values typical for beta-heat treated Ti-6246.

(e) Notch Stress Rupture

Stress rupture testing was performed as follows: each specimen was initially loaded at 190 ksi and uploaded 10 ksi every 5 hours to failure. Test results are presented in Table XXXVII. The best notch stress rupture life was observed on the pancakes consisting of some primary alpha in a transformed beta matrix. Results were lower than previously tested material. The presence of a beta grain structure appears to affect the notch stress rupture strength. All the stress rupture testing was performed at AFML. Use of different testing rigs and procedures may also account for the lower than anticipated results.

(f) Failed Specimen Evaluations

AFML and P&WA/Florida performed several analyses on failed specimens. Inclusions identified by AFML were similar to those found in earlier work done at P&WA/Florida. Although fewer inclusions were present in the cleaned powder consolidations, the number present was still unacceptable. Ferrofluid and/or chemical cleaning of contaminated powders does not appear to offer a solution to the powder contamination problem. A clean powder product must be developed before a production forging process can be optimized.

Table XXXVI. Task III Fracture Toughness

Pancake Serial No.	Forge Temperature (°F)		Test Temperature (°F)	K'_{1E}	K_{IC}
1	1600	1690°F/2/RAC+1525°F/2/AC	RT		36.7*
			RT		39.4
		+1100°F/8/AC	RT		40.7*
			400	-	
2	1600	1720°F/2/FC to 1500°F/2/AC	RT		33.7*
			RT		33.8*
		+1100°F/8/AC	RT		45.0
			400	-	
3	1650	1690°F/2/RAC+1525°F/2/AC	RT		36.5
			RT		-
		+1100°F/8/AC	400	-	
			400	-	
4	1650	1720°F/2/FC to 1500°F/2/AC	RT		35.2*
			400	58.9	
		1100°F/8/AC	400	54.6	
			400	63.7	
5	1700	1690°F/2/RAC +2525°F/2/AC	RT		49.5
			RT		45.0
		+1100°F/8/AC	400	61.6	
			400	62.3	
6	1700	1720°F/2/FC to 1500°F/2/AC	RT		47.4
			RT		50.1
		+1100°F/8/AC	400	58.1	
			400	62.0	
	PWA 1220 Specification		RT		20.0

' Does not meet all ASTM E399 requirements.
* Equipment malfunction - actual fracture toughness equal to or greater than this value.
- Specimen failed in precracking.

Table XXXVII. Task III RT Notch Stress Rupture

Pancake Serial No.	Forge Temperature (°F)	Heat Treatment	Failure Stress (ksi)	Total Time (hr)	Time at Failure Load (hr)
1	1600	1690°F/2/RAC+ 1525°F/2/AC+ 1100°F/8/AC	220	16.5	1.50
			190	0.25	0.25
2	1600	1720°F/2/FC to 1500°F/2/AC+ 1100°F/8/AC	190	0.55	0.55
			190	1.30	1.03
3	1650	1690°F/2/RAC+ 1525°F/2/AC+ 1100°F/8/AC	220	20.0	5.00*
			210	11.65	1.65
4	1650	1720°F/2/FC to 1500°F/2/AC+ 1100°F/8/AC	190	0.37	0.37
			190	0.39	0.39
5	1700	1690°F/2/RAC+ 1525°F/2/AC+ 1100°F/8/AC	190	0.42	0.42**
			190	1.88	1.88
6	1700	1720°F/2/FC to 1500°F/2/AC+ 1100°F/8/AC	190	0.23	0.23
			190	0.05	0.05

*Failed during load implementation and load was removed from the specimen at the beginning of the third load level.

**Load spike caused premature failure.

6. Task III Conclusions

a. General

The Ferrofluid cleaning process is effective in removing large numbers of inclusions. However, complete removal of all inclusions present in the powder is not currently possible.

The PS140 cleaning technique was effective in removing iron from contaminated powder but not effective in removing other types of contamination.

b. Selection of Powder Consolidation Method

Direct extrusion of powder resulted in a more uniform structural response than HIP. However, both precesses resulted in fully compacted material.

c. Mechanical Properties

Mechanical properties of directly extruded and GATORIZED forged material compares favorably with conventionally processed Ti-6Al-2Sn-4Zr-6Mo except for low tensile ductility attributed to the presence of inclusions in the powder.

d. Specifications

Based on the work performed on this contract, finalization of the Ti-6Al-2Sn-4Zr-6Mo powder and powder billet specification would be premature. A method for the production of clean titanium powder remains to be developed. Mechanical property requirements cannot be established until the inclusions causing low ductility are eliminated or minimized.

e. Inclusion Detection

Throughout the conduct of the program, difficulty has been encountered in detecting small inclusions. Inclusions smaller than a number two flat bottom hole (0.03125 in) were not detectable by existing techniques. Recent progress in ultrasonic techniques now enable a number one (0.015625 in) flat bottom hole to be detected in Ti-6Al-2Sn-4Zr-6Mo production disks. Additional studies, however, are required to correlate flat bottom hole reflections with actual inclusions. Unfortunately, many inclusions are smaller than 0.015 in and cannot be detected by either ultrasonic or radiographic techniques. Any future titanium program should concentrate on developing techniques capable of detecting inclusions smaller than 0.025 in.

SECTION III
CONCLUSIONS AND RECOMMENDATIONS

This program was aimed at selecting powder production and consolidation methods. Forging parameter selection and methods of cleaning contaminated powder were also investigated. Conclusions were presented at the end of each task and primarily dealt with the specifics in each task, such as powder selection and specifications. The following conclusions and recommendations present an overview of the entire program.

A. CONCLUSIONS

1. Clean Ti-6Al-2Sn-4Zr-6Mo powder is not currently available

2. Methods capable of cleaning contaminated powder are available but not fully effective

3. Cleaning procedures are at best only a crutch and not a cure and may introduce additional contamination into the powder.

4. The use of the GATORIZING forging process allows the forging of powder billet to obtain structurally uniform complex shapes

5. Mechanical properties of extruded and forged Ti-6Al-2Sn-4Zr-6Mo powder billet compares favorably with conventially processed billet receiving similar heat-treatments except for tensile ductility.

B. RECOMMENDATIONS

1. Methods of producing clean titanium powder should be pursued

2. Ferrofluid cleaning techniques should be used only as a remedial procedure and not as an integral part of a process for making clean powder

3. A clean powder product must be developed before a production forging process can be optimized or parts tested in an engine.

4. Methods capable of detecting inclusions smaller than 0.025 inch should be developed for titanium powder alloys.

APPENDIX A
TENTATIVE Ti-6Al-2Sn-4Zr-6Mo POWDER SPECIFICATION

1. COMPOSITION REQUIREMENTS

Element	Minimum	Maximum
Aluminum	5.50	6.50
Zirconium	3.50	4.50
Tin	1.75	2.25
Molybdenum	5.50	6.50
Iron		0.15
Carbon		0.04
Oxygen		0.15
Nitrogen		0.03
Hydrogen		0.015
Boron		0.003
Other Elements, Total*		0.40
Titanium	Remainder	

*If Determined.

2. PARTICLE SIZE DISTRIBUTION

A Sieve Analysis, using standard ASTM or Tyler standard sieves, shall be run per ASTM B214-64-35+325 mesh powder with a maximum of 5% fines outside of range.

3. DENSITY MEASUREMENTS

3.1 Apparent density shall be measured per ASTM B212-48.

3.2 Particle density shall be measured per ASTM B328-60.

4. INCLUSION COUNT AND CHARACTERIZATION

4.1 A sample of powder shall be vacuum hot pressed or sheet rolled so that an inclusion count per square inch can be determined.

4.2 Inclusions to be classified into groups:

a. Nonmetallic
b. Nontitanium
c. Anomalous Titanium Areas.

PRECEDING PAGE NOT FILMED
BLANK

APPENDIX B
TENTATIVE Ti-6Al-2Sn-4Zr-6Mo POWDER BILLET SPECIFICATION

1. COMPOSITION REQUIREMENTS

Element	Minimum	Maximum
Aluminum	5.50	6.50
Zirconium	3.50	4.50
Tin	1.75	2.25
Molybdenum	5.50	6.50
Iron		0.15
Carbon		0.04
Oxygen		0.15
Nitrogen		0.03
Hydrogen		0.015
Boron		0.003
Other Elements, Total*		0.40
Titanium	Remainder	

*If determined

2. TECHNICAL REQUIREMENTS

2.1 Condition: Material shall be supplied as extruded billet.

2.2 Properties as Extruded

2.2.1 *Micro/Macrostructure:* Nominal 1 in. slices shall be taken from each end of each billet, etched, and evaluated for uniformity in the longitudinal direction. Standards for acceptance or rejection will be established at a later date.

2.2.2 Inclusions: Inclusion content shall be determined and identified as to type and elements present.

2.3 Ultrasonic Inspection: Each billet shall be ultrasonically inspected in accordance with standards to be established.

2.4 Quality: Billet or bar shall be extruded from powder or a powder product. Powder shall be produced from material which has been melted by vacuum induction, or vacuum induction plus the vacuum consumable process.

2.4.1 Billets shall be uniform in quality and condition, clean, sound, and free from foreign materials and from surface and internal imperfections detrimental to fabrication or to performance of parts.

2.5 Tolerance: Shall be as specified on the purchase order.

PRECEDING PAGE NOT FILMED BLANK